Unraveling variations in ribosome biogenesis activity in the mouse hematopoietic system at homeostasis in vivo

Léonard Jarzebowski

THÈSE DE DOCTORAT DE L'UNIVERSITÉ PIERRE ET MARIE CURIE

École Doctorale: Complexité du Vivant

Spécialité: Biologie du Développement

Présentée par

Léonard JARZEBOWSKI

Pour obtenir le grade de

DOCTEUR DE L'UNIVERSITÉ PIERRE ET MARIE CURIE

Unraveling variations in ribosome biogenesis activity in the mouse hematopoietic system at homeostasis *in vivo*.

Sous la direction de

Michel COHEN-TANNOUDJI

Soutenue le 11 octobre 2016, devant le jury composé de:

Dr Thierry JAFFREDO	Président du jury
Dr Evelyne LAURET	Rapportrice
Pr Sébastien BLOYER	Rapporteur
Dr Alexandre DAVID	Examinateur
Dr Michel COHEN-TANNOUDJI	Directeur de thèse

Unraveling variations in ribosome biogenesis in the mouse hematopoietic system at homeostasis in vivo

Stem cells differ from progenitor and differentiated cells on many aspects. Notably, stem cells display particular characteristics in fundamental cellular processes such as cell cycle control, energetic metabolism or DNA damage stress response. Over the past decade, another fundamental process, ribosome biogenesis, has been proposed to play an important role in the regulation of stem cells. Indeed, beyond their universal role in protein synthesis, ribosomes also regulate developmental processes, through modulation of the ribosome biogenesis pathway and its activity. Several studies have shown that genes involved in ribosome biogenesis are essential for the maintenance or differentiation of stem cells, suggesting that regulation of the ribosome biogenesis pathway can influence the fate of stem cells. Furthermore, in addition to increasing risks of tumorigenesis, the deregulation of ribosome biogenesis is responsible for human pathologies termed ribosomopathies that preferentially affect the hematopoietic system. The fact that defects in ribosome biogenesis can affect differently and specifically different cell types is surprising and underlines our lack of knowledge on the regulation of this process in vivo in higher eukaryotes.

During my thesis, I have used different approaches to study the role and regulation of ribosome biogenesis in stem cell populations, in vivo and ex vivo using murine models. Using genetic inactivation of a gene involved in ribosome biogenesis, I have participated to the analysis of its role in the adult hematopoietic system, as well as in the establishment of the first cell lineages during early embryogenesis and showed that embryonic stem cells activate the ribosomal stress pathway in response to defective ribosome biogenesis. I have also dedicated an important part of my thesis to the development of approaches to investigate the regulation of ribosome biogenesis activity in hematopoietic stem and progenitor cells at homeostasis, in vivo in the adult mouse. I have unraveled differences in the activity and progression of ribosome biogenesis in these populations, and have discovered unsuspected ribosome biogenesis activity in hematopoietic stem cells despite their quiescent state. Finally, I also had the opportunity to investigate ribosome biogenesis activity in human bone marrow samples, revealing similarities between mouse and Human.

Altogether, the work I performed during my thesis strengthens the hypothesis of a role for ribosome biogenesis in the regulation of stem cells, and provides a better understanding of the activity of this process during hematopoietic differentiation.

Keywords: hematopoiesis, hematopoietic stem cell, ribosome biogenesis, mouse.

Mise en évidence de variations de l'activité de biogenèse des ribosomes dans le lignage hématopoïétique murin *in vivo* à l'homéostasie.

Les cellules souches se distinguent des progéniteurs et cellules différenciées à de nombreux égards. Notamment, les cellules souches présentent des caractéristiques particulières dans des processus cellulaires fondamentaux tels que le contrôle du cycle cellulaire, la gestion du métabolisme ou la réponse à des stress génotoxiques. Au cours des dernières années, un autre processus fondamental a été proposé comme ayant un rôle important dans la régulation des cellules souches : la biogenèse des ribosomes. En effet, au-delà de leur rôle universel dans la synthèse des protéines, les ribosomes régulent également des processus développementaux, via la modulation de la voie de biogenèse des ribosomes. Plusieurs études ont montré que des gènes impliqués dans la biogenèse des ribosomes sont nécessaires au maintien ou à la différentiation de cellules souches, suggérant ainsi que la régulation de la biogenèse des ribosomes peut influencer le destin cellulaire des cellules souches. Aussi, en plus d'augmenter les risques de tumorigénèse, la dérégulation de la biogenèse des ribosomes est responsable chez l'Homme de pathologies appelées ribosomopathies qui affectent souvent le système hématopoïétique. Le fait que des défauts de biogenèse des ribosomes puissent affecter différentiellement et spécifiquement différents types cellulaires est surprenant et souligne notre manque de connaissances sur la régulation de ce processus *in vivo* chez les eucaryotes supérieurs.

Au cours de ma thèse, j'ai utilisé différentes approches pour étudier le rôle et la régulation de la biogenèse des ribosomes dans des populations de cellules souches, *in vivo* et *ex vivo* dans des modèles murins. En utilisant un modèle d'inactivation génétique d'un gène impliqué dans la biogenèse des ribosomes, j'ai participé à l'analyse de son rôle dans le lignage hématopoïétique adulte ainsi que dans l'établissement des premiers lignages cellulaires au cours du développement embryonnaire précoce, et j'ai montré que les cellules souches embryonnaires déclenchent la voie de stress ribosomique en réponse à des défauts de biogenèse des ribosomes. J'ai également dédié une grande partie de ma thèse au développement d'approches pour examiner la régulation de l'activité de biogenèse des ribosomes dans les cellules souches et progéniteurs hématopoïétiques, chez la souris adulte. Ainsi, j'ai mis en évidence des différences dans l'activité et la progression du processus de biogenèse des ribosomes dans ces populations, et j'ai montré que les cellules souches hématopoïétiques ont une activité de biogenèse des ribosomes inattendue au vu de leur état quiescent. Enfin, j'ai aussi eu l'occasion d'étudier l'activité de biogenèse des ribosomes dans des échantillons de moelle osseuse humaine, montrant des similarités entre l'Homme et la souris.

Dans son ensemble, mon travail de thèse renforce l'idée que la biogenèse des ribosomes a un rôle dans la régulation des cellules souches, et apporte une meilleure compréhension de la régulation de ce processus au cours de la différentiation du lignage hématopoïétique.

Mots-clés : hématopoïèse, cellule souche hématopoïétique, biogenèse des ribosomes, souris.

Table of Contents

List of Figures

Introduction Figures

Introduction Tables

Results

List of abbreviations (in alphabetical order):

BM:	bone marrow
CDK:	cyclin-dependent kinase
CKI:	CDK inhibitor
cKO:	conditional knockout
CMP:	common myeloid progenitor
DDR:	DNA damage response
DSB:	DNA double-strand break
EPI:	epiblast
ES cell:	embryonic stem cell
FACS:	fluorescence automated cell sorting
FISH:	fluorescent in situ hybridization
GMP:	granulocyte-monocyte progenitor
HR:	homologous recombination
HSC:	hematopoietic stem cell
HSPC:	hematopoietic stem and progenitor cell
ICM:	inner cell mass
IR:	ionizing radiation
ISC:	intestinal stem cell
ISPC:	intestinal stem and progenitor cell
KO:	knockout
Lin+/–:	bone marrow cells positive/negative for lineage-specific cell surface markers
LSK:	bone marrow cells bearing Lin– Sca-1+ cKit+ markers (HSCs and MPPs)
MEP:	megakaryocyte-erythroid progenitor
MPP:	multipotent progenitor
MSC:	melanocyte stem cell
NHEJ:	non-homologous end joining
Nle:	Notchless
OHT:	4-hydroxytamoxifen
pre-rRNA:	rRNA precursor
PrE:	primitive endoderm
RiBi:	ribosome biogenesis
RNA Pol:	RNA polymerase
RNP:	ribonucleoprotein
ROS:	reactive oxygen species
RP:	ribosomal protein
rRNA:	ribosomal RNA
TE:	trophectoderm

Introduction

Part 1 Hematopoietic stem cells

I. Hematopoietic stem cells, a privileged model to study stem cell maintenance and differentiation

In this first part, I would like to give you an overview of the hematopoietic system and how our knowledge on hematopoietic stem cells (HSCs) has evolved in the past decades. Research in this field has lead to pioneer advances in the understanding of stem cell biology, from the discovery of the very concept of stem cells to the development of phenotypical and functional approaches for the identification of stem cells. We will see how these advances position HSCs as a model of study for stem cell biology.

1. Introduction: HSCs and hematopoiesis

1.1 A bit of history: discovery of HSCs, and birth of the concept of stem cell

Hematopoietic stem cells (HSCs) were the first tissue-specific stem cells identified, thanks to the pioneer work of J.E.Till and E.A.McCulloch. Performing transplantation of bone marrow in lethally irradiated mice, they observed the development of nodules in the spleen of these animals and hypothesized that the nodules had derived from stem cells present in the engrafted bone marrow (Till and McCulloch, 1961). They validated the existence of cells capable of reconstituting all blood cell types in the host, and that such cells were able to self-renew (Wu et al., 1968). This work, in addition to being the first evidence of the HSCs existence, also established the first functional definition of stem cells: the ability to generate all cells of a tissue and to self-renew.

In 1988, G.Spangrude, S.Heimfeld and I.Weissman publish for the first time how to isolate bone marrow (BM) cells enriched in HSCs (Spangrude et al., 1988). Thanks to the development of flow cytometry technology and monoclonal antibodies, they are able to isolate Lin^{-} $Sca1^{+}$ $Thy1^{low}$ cells (approx. 0.05% of adult BM). They showed that some of these cells, and no others, are able to repopulate the bone marrow of lethally irradiated hosts and reconstitute all blood cell types in these animals, thus validating the concept of stem cell, and leading the way towards phenotypical characterization of HSCs.

1.2 Hematopoiesis: a highly hierarchized system

Etymologically, hematopoiesis comes from ancient greek *αἷματος* (haimatos = blood) and *ποιέω* (poiéō = to make), meaning “production of blood cells”. In human adults, this process is responsible for the production of over 10^{11} cells per day, or approximately 10^{6} per second!! The hematopoietic system comprises over 10 different mature cell types, including erythrocytes, platelets, myeloid cells (granulocytes and monocytes/macrophages) and lymphoid cells (B and T lymphocytes, dendritic and natural killer cells). The fact that HSCs can generate such an important amount of cells with such diverse functions is baffling, and underlines an amazing differentiation

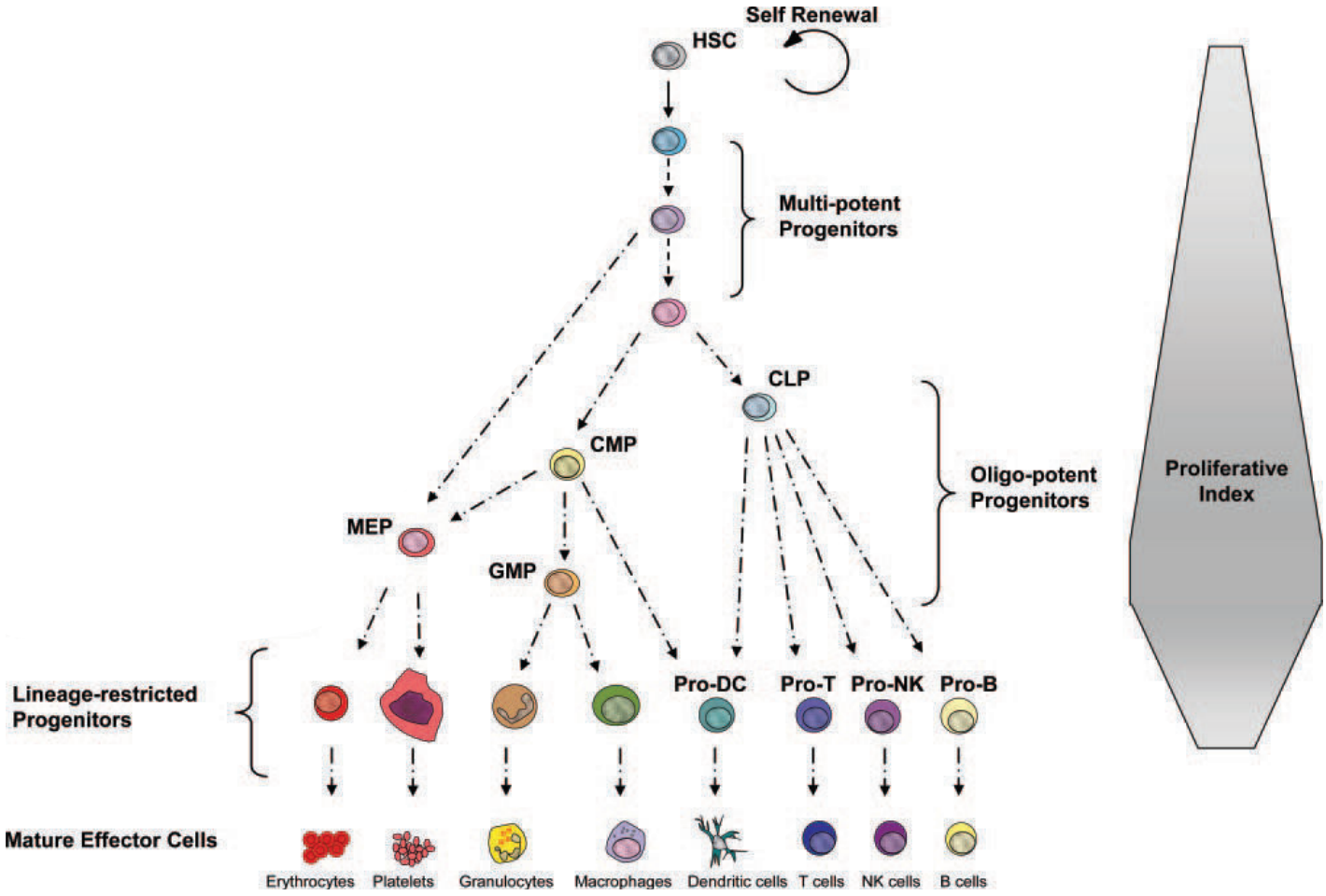

Figure 1. Simplified hierarchized model of the hematopoietic system

HSCs, which can self-renew, are at the top of the hierarchy in the hematopoietic system. They can generate multipotent progenitors (MPP), which in turn give rise to oligopotent progenitors. Common Lymphoid Progenitors (CLP) give rise to both B ant T lymphoid lineages and to Natural Killer (NK) cells. Common Myeloid Progenitors (CMP) give rise to Granulocyte and Macrophage progenitors (GMP), which differentiate into monocytes/macrophages and granulocytes, and to Megakaryocyte and Erythrocyte Progenitors (MEP), which differentiate into megakaryocytes/platelets and erythrocytes. CLP and CMP can both give rise to dendritic cells. MEP and GMP could also be generated directly from MPP without passing through the CMP stage. This differentiation process is generally associated with increased proliferative capacity, although this is not always the case or has not yet been shown for all differentiation steps.

Adapted from Bryder et al., 2006

potential of HSCs. As I will discuss later most HSCs are in a quiescent state, which might seem surprising given the enormous amount of cell production demanded by the hematopoietic system.

Over the years, many teams have pursued the phenotypical characterization of HSCs started by Spangrude *et al.* in 1988, to isolate distinct hematopoietic populations, test their differentiation potential, and identify specific markers of HSCs. This titanic work has lead to the establishment of a model for this complex, highly hierarchized hematopoietic system, as depicted in Figure 1 (Bryder et al., 2006). Self-renewing, rarely-dividing multi-potent HSCs give rise to transient amplifying, multi-potent progenitors (MPPs) which in turn give rise to oligopotent progenitors (OPPs) that are already committed towards lymphoid, myeloid, erythroid or megakaryocytic lineages. OPPs then further differentiate into even more lineage-restricted, unipotent cells, and eventually terminally differentiated effector cells. Collectively, HSCs, MPPs and OPPs can be regrouped under the appellation HSPCs, for hematopoietic stem and progenitor cells.

This multi-tiered strategy allows for the production of a tremendous amount of mature cells from a single HSC, with fine-tuning at each differentiation step to meet the homeostatic needs for each mature cell type depending on their turnover. Furthermore, the amplification by progenitor cells alleviates proliferative pressure on HSCs, thus preventing their exposition to potential mutations due to DNA replication, cell divisions or damage-inducing metabolic side-products such as reactive oxygen species (ROS), all of which I will discuss later. This strategy also requires a fine balance between HSCs, progenitors and differentiated cells, and aberrant homeostasis can be highly deleterious. For instance, defective differentiation or acquisition of proliferative abilities can lead to immunodeficiency or cancer, respectively.

The model proposed in Figure 1 is based mostly on functional and phenotypical characterization of the different stem and progenitor cell populations. This is a simplified view of the hematopoietic system, and displays differentiation as a linear, irreversible process with distinct cell populations. Although it does underline some of the complexity of this system, it does not reflect the heterogeneity within the different populations. Notably, we will see that the HSC population is actually a heterogeneous population composed of quiescent (or dormant) HSCs and activated HSCs, with potentially different reconstituting capabilities in transplantation experiments.

1.3 The environment of HSCs: the niche

The concept of “niche”, defined as an organized micro-environment that controls HSC homeostasis, was proposed by R.Schofield in 1978 (Schofield, 1978). This concept was adopted after the study of two mutant mouse strains termed W and Sl, which exhibit similar phenotypes with defective maintenance of hematopoietic homeostasis (see (Seita and Weissman, 2010) for review) First BM transplant experiments revealed the existence of effects extrinsic to hematopoietic cells, suggesting that environmental cues were required for the maintenance of HSCs. It is only in the 1990s that the molecular signal pathway involved in the W and Sl phenotypes was identified: the receptor tyrosine kinase cKit encoded by the W locus, and its ligand SCF (stem cell factor) encoded by the Sl locus. Since the birth of the concept of niche, many studies have been conducted in invertebrates that show the importance of the niche in the maintenance of stem cell populations in different organs, bringing the first molecular and cellular information of how the niche operates.

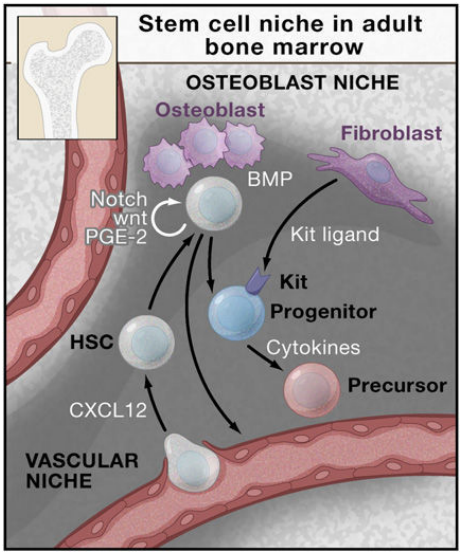

Figure 2. The hematopoietic niches in the adult bone marrow (1)

HSCs are found adjacent to osteoblasts that are under the regulation of bone morphogenetic protein (BMP) (the osteoblast niche). HSCs are also found near blood vessels (the vascular niche). The chemokine CXCL12 regulates HSC migration from the circulation to the bone marrow. The osteoblast and vascular niches *in vivo* lie in close proximity or may be intermingled. The marrow space also contains stromal cells that support hematopoiesis, including the production of cytokines, such as c-Kit ligand, that stimulate stem cells and progenitors. Cytokines, including interleukins, thrombopoietin (Tpo), and erythropoietin (Epo), also influence progenitor function and survival.

Adapted from Orkin and Zon, 2008

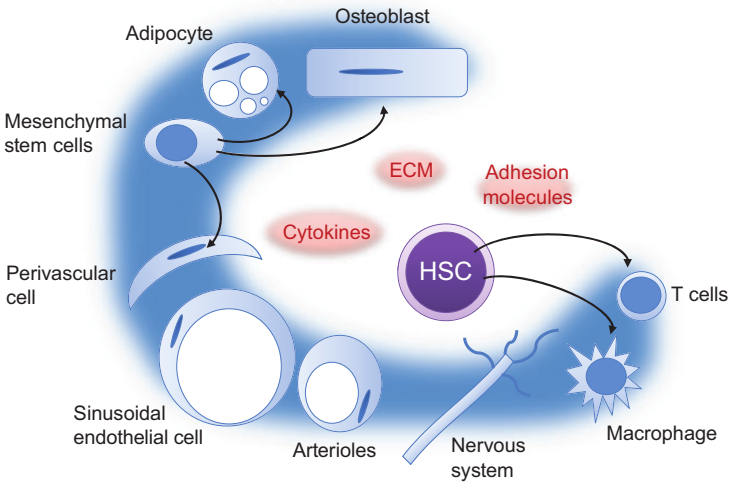

Figure 3. The hematopoietic niches in the adult bone marrow (2)

Several studies have proposed that the HSC niche is composed of many different cell types, both hematopoietic and non-hematopoietic, highlighting the complexity of the niche organization, composition and regulation. Niche cells regulate HSCs through the production of cytokines, growth factors, extracellular matrix proteins (ECM) and adhesion molecules.

Adapted from Nakamura-Ishizu et al., 2014

In the hematopoietic system, two main niches have been proposed and are supported by *in vitro* and *in vivo* studies: the endosteal and the vascular niches, which I will briefly describe here.

The endosteal niche: First experiments showed that the only cells capable of forming hematopoietic colonies localized to the surface of the endosteum, the conjunctive tissue of the medullar cavity of bones (Lord et al., 1975). Several *in vitro* studies then showed that the osteoblasts located in this region produce cytokines that can promote the expansion of myeloid progenitors in culture (Taichman et al., 1996), and *in vivo* studies have later shown interactions between osteoblasts and HSCs (Wilson et al., 2008; Zhang et al., 2003).

The vascular niche: In 2005, the team of S.Morrison showed that HSCs are associated with endothelial cells of the sinusoids, specialized blood vessels with a thin wall that allows hematopoietic cell migration into the bloodstream (Kiel et al., 2005). *In vivo* experiments have further supported these results, highlighting the importance of endothelial cells for the control of hematopoiesis. HSCs have been localized in contact with reticular cells secreting important levels of CXCL12 (=SDF-1) that have been identified around sinusoids(Sugiyama et al., 2006).

In a review published in 2010, Li and Clevers propose the coexistence of quiescent and active adult stem cells that are maintained by distinct niches (Li and Clevers, 2010). In this model, the endosteal niche provides a suitable environment for quiescent HSCs, keeping them in hypoxic conditions (which we will see later is crucial for HSC homeostasis) while promoting self-renewal through the secretion of cytokines. The vascular niche, on the other hand, ensures maintenance of activated HSCs that are actively dividing or participating in tissue regeneration. Actually, both niches may very well be part of a single niche divided into two communicating compartments (Figure 2). More recently, Wang *et al.* identified BM compartments around distal sinusoidal vessels, composed of endothelial, mesenchymal and hematopoietic cells ((Wang et al., 2013)). These hemospheres, as the authors call these compartments, display a distinct morphology and features that differ from the rest of the BM cavity and are enriched in rapidly amplifying Lin^- $CD150^+$ $CD48^-$ hematopoietic cells. Upon intra-femoral injection of BM cells into irradiated hosts, clusters of transplanted cells appear rapidly in hemospheres and only later in the rest of the BM cavity, suggesting that repopulation of the BM first occurs in these hemospheres.

Finally, other studies have suggested that the nervous and immune systems could also play a role in the niche of HSCs (Figure 3). More detailed analysis and the development of new tools are required to understand more of the nature, composition and regulation of the niche(s). One thing is certain: the niche is crucial for HSC maintenance and participates in the regulation of their behavior both at homeostasis and in stress conditions.

2. Phenotypical and functional characterization of HSCs

2.1 Identification of HSCs

2.1.1 Phenotypical identification of HSCs (1): membrane markers and flow cytometry

The development of flow cytometry technologies, with the use of monoclonal antibodies directed against surface membrane markers have brought a revolution in the identification of combinations of markers expressed by HSCs, progenitors and other hematopoietic populations

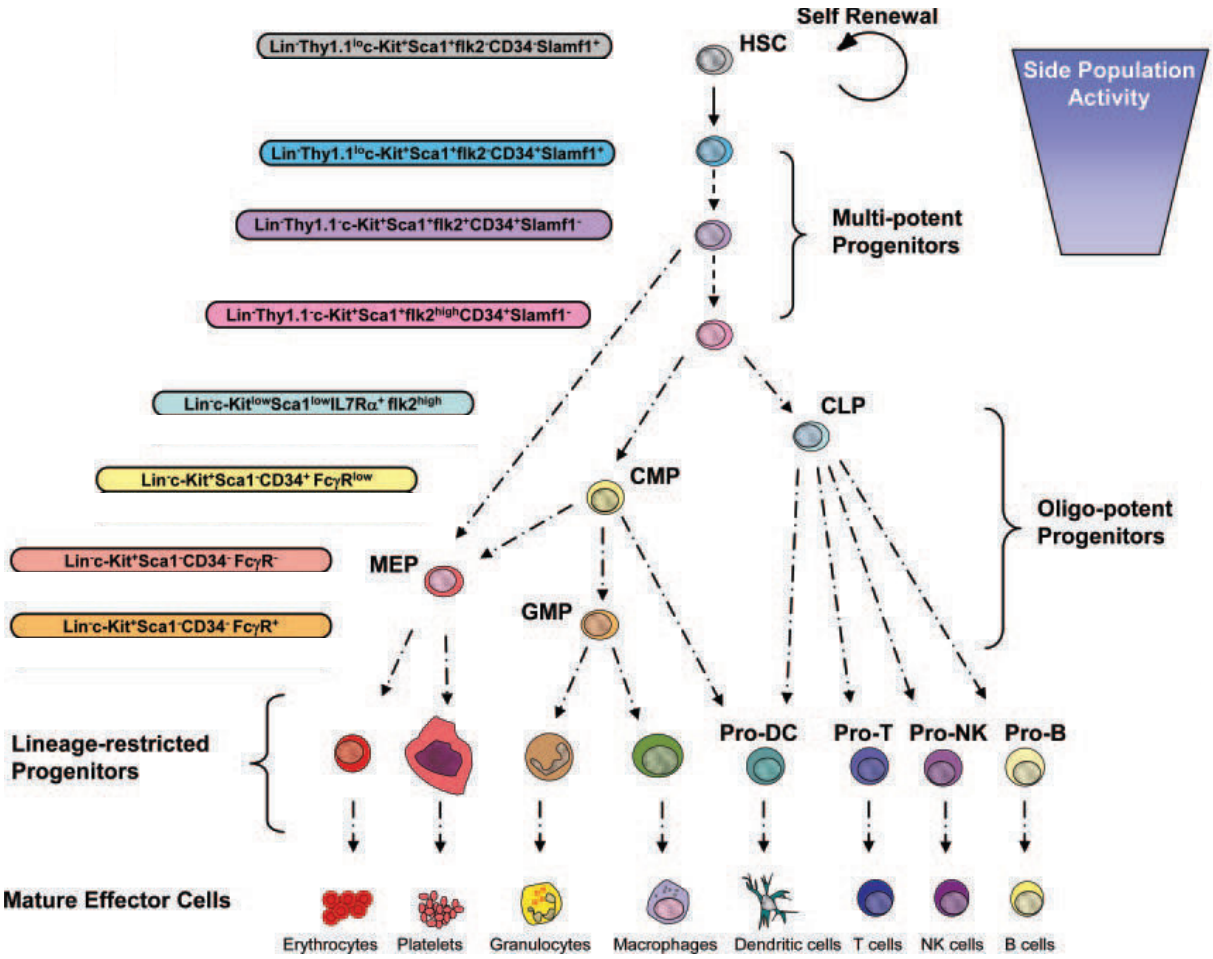

Figure 4. Combinations of cell surface markers allow phenotypical definition of mouse HSCs and immature progenitors

The expression of the different cell surface markers in mouse is indicated left of each population. Since only HSCs can self-renew and MPP have transient amplifying potential, the Side Population activity is restricted to these populations

Adapted from Bryder et al., 2006

a

Fraction	Surface marker expression
HSC-1	$CD150^{+}CD48^{-/low}CD229^{-/low}CD244^{-}Lineage^{-/low}Sca\text{-}1^{+}c\text{-}Kit^{+}$
HSC-2	$CD150^{+}CD48^{-/low}CD229^{+}CD244^{-}Lineage^{-/low}Sca\text{-}1^{+}c\text{-}Kit^{+}$
MPP-1	$CD150^{-}CD48^{-/low}CD229^{-/low}CD244^{-}Lineage^{-/low}Sca\text{-}1^{+}c\text{-}Kit^{+}$
MPP-2	$CD150^{-}CD48^{-/low}CD229^{+}CD244^{-}Lineage^{-/low}Sca\text{-}1^{+}c\text{-}Kit^{+}$
MPP-3	$CD150^{-}CD48^{-/low}CD229^{+}CD244^{+}Lineage^{-/low}Sca\text{-}1^{+}c\text{-}Kit^{+}$
HPC-1	$CD150^{-}CD48^{+}Lineage^{-/low}Sca\text{-}1^{+}c\text{-}Kit^{+}$
HPC-2	$CD150^{+}CD48^{+}Lineage^{-/low}Sca\text{-}1^{+}c\text{-}Kit^{+}$

b

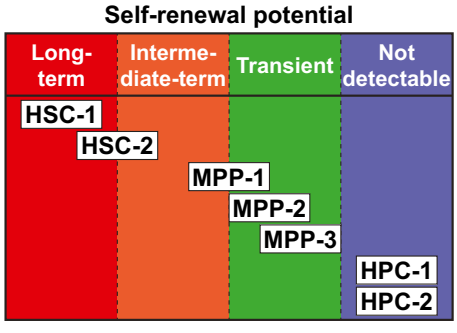

Figure 5. Self-renewal potential of phenotypically defined subsets of HSCs and MPPs

Here, the authors used isolated subsets of HSCs, MPPs and hematopoietic progenitor cells (HPC) defined on their expression of SLAM markers (**a**), and investigated their respective self-renewal potential upon transplantation into irradiated host (**b**), thus highlighting heterogeneity in the self-renewal potential of HSC subsets.

Adapted from Oguro et al., 2013

(Figure 4). First of all, identification of markers for terminally differentiated cells and lineage-restricted progenitors allowed the analysis of more immature hematopoietic populations negative for these lineage markers (Lin^-), which displayed higher differentiation potential. Within this Lin^- population, cells expressing the cKit and Sca1 markers (termed LSK cells for Lin^- $Sca1^+$ $cKit^+$) comprise multi-potent cells, i.e. MPPs and HSCs. LSK cells can be further refined using other markers to obtain higher purity in HSCs, such as CD34 or SLAM family markers CD150 and CD48: 24% of LSK $CD34^-$ cells, or 47% of LSK $CD150^+$ $CD48^-$ cells exhibit strong, long-term stem cell activity (Kiel et al., 2005; Osawa et al., 1996). Other markers such as CD49b, EPCR or Flk2 are also used to identify HSCs. However, HSC populations identified with these markers are still heterogeneous, at different levels: long-/short-term repopulation capability, activation/quiescence, lineage-biased repopulation capacity upon transplantation... which I will describe more later.

To resolve some of this heterogeneity, the team of Sean Morrison used SLAM family markers CD299 and CD244 in addition to the aforementioned markers, and were able to subdivide HSC and MPP populations into a hierarchy of functionally distinct subsets in regard with cell-cycle status, self-renewal and reconstitution potentials (Oguro et al., 2013). They showed that LSK $CD150^+$ $CD48^-$ HSCs could be separated into $CD299^-$ $CD244^-$ and $CD299^+$ $CD244^-$ subsets, the former containing more primitive HSCs. LSK $CD150^-$ $CD48^-$ cells, which they consider as MPPs, could also be subdivided into $CD299^-$ $CD244^-$ (MPP-1), $CD299^+$ $CD244^-$ (MPP-2) and $CD299^+$ $CD244^+$ (MPP-3) subsets with MPP-1 being the most primitive and MPP-3 the least primitive (Figure 5).

Altogether, finding better markers for each population will lead to better phenotypical definition of hematopoietic stem cells, and better understanding of the steps of hematopoietic differentiation. I would like to stress here that the identification of such markers could not be done without performing functional tests together with phenotypical characterization to assess the properties of each subset of cells, as I will discuss in *I.2.2*.

2.1.2 Phenotypical identification of HSCs (2): metabolic labeling

Although membrane markers are the most abundantly used to identify hematopoietic populations, other methods can be used to identify and purify HSCs, taking advantage of the metabolic properties of HSCs.

While staining live BM cells with the vital dyes Hoechst 33342 and Rhodamine 123, Goodell *et al.* have made a very interesting discovery: HSCs were found in a distinct subset of whole BM cells regarding their position on a FACS (Fluorescence Automated Cell Sorting) profile, where they appeared as a "Side Population" (Figure 6), hence their appellation as SP cells (Goodell et al., 1996). These SP cells display low cell cycling activity and high enrichment in HSCs. It was later shown that the efflux of these dyes by SP cells is due to the expression of ATP-dependent transporter molecules such as *Mdr1* and *Bcrp1* (Challen and Little, 2006). This property of SP cells allows them to avoid accumulation of toxic compounds, hence protecting HSCs.

As I mentioned earlier, HSCs have another interesting property: quiescence, which I will describe in more details in *II.1*. In a nutshell, quiescence is a resting state associated with reversible cell cycle arrest in an extended G_1 phase termed G_0 phase. Most HSCs are in such a quiescent state,

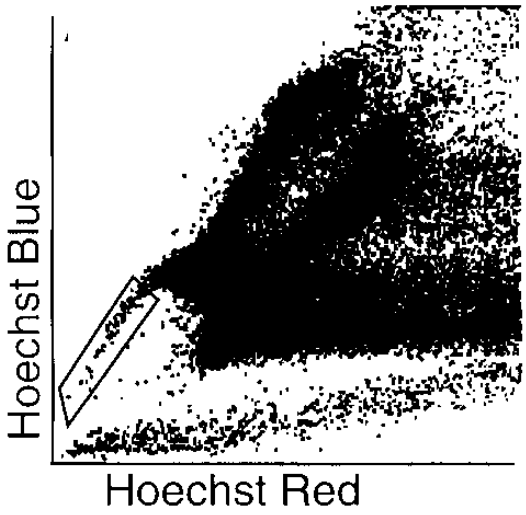

Figure 6. Identification of a "Side Population" within whole bone marrow cells

Adapted from Challen et al., 1996

and rarely enter the cell cycle, hence dividing rarely. This can be used to identify them using DNA or chromatin markers such as BrdU or H2B-GFP, respectively. Thanks to their low rate of division, HSCs are able to retain such labels for a long time. This property of label retaining cells (LRC), together with the use of membrane markers, appears as the only way to phenotypically identify dormant HSCs today.

2.2 Functional characterization of HSCs

The phenotypical characterization of HSCs and other hematopoietic populations mentioned above has lead to tremendous progress in the understanding of hematopoiesis and in clinical uses. However, such findings would not have been possible without rigorously testing the properties of these cells, and functional tests remain the most relevant approach to assess the presence of HSCs. Numerous studies have proposed ways of testing the properties of HSCs, some examples of which I will describe here.

2.2.1 *Ex vivo* culture of HSCs

In their pioneer work on the identification of hematopoietic stem cells, McCulloch and Till demonstrated the formation of colonies in the spleen of lethally irradiated mice transplanted with healthy BM cells, proving the existence of cells with Colony Forming Units (CFU; CFU-S for colonies formed in the spleen) potential. This work inspired the development of assays to similarly identify clonogenic hematopoietic progenitors *ex vivo* in culture (CFU-C). Low-density seeding of BM cells in semi-solid medium and in the presence of cytokines allows formation of colonies from progenitors. Such assays can bring some understanding to the differentiation potential of the cultured cells and allow to test the presence of HSCs in the seeded populations (Miller et al., 2008), however no conditions that reliably induce important expansion of HSCs have been discovered yet (Walasek et al., 2012).

The main limitation to *ex vivo* HSC expansion is the lack of understanding of the extrinsic regulators of HSC fate, many of which are present and/or produced in the *in vivo* micro-environment (the niche) of HSCs. This is also a major drawback to the identification of human HSCs and their use for therapeutic purposes.

2.2.2 Transplantation, the ultimate functional test for stem cell potential

By definition, a hematopoietic stem cell is considered as such based on its ability to repopulate the hematopoietic tissue of irradiated hosts in the long term. This is by far the best way to test the functionality of a stem cell, since it requires for the cell to be able to self-renew and differentiate into all lineages of the tissue. Engraftment is particularly convenient for HSCs, since they can be easily isolated as single cells from the bone marrow of a donor individual, and simply injected into the blood stream of a recipient host. Their ability to then migrate to the niche of the host where they can integrate, while keeping all of their stem cell potential is quite extraordinary, and actually reflects the fact that some HSCs already do migrate at homeostasis, leaving and coming back to their niche. Engrafting cells with different markers is actually how most of the

phenotypical characterizations of HSCs were validated, and helped consolidating the concept of stem cell(Ema et al., 2005; Oguro et al., 2013; Osawa et al., 1996; Wagers et al., 2002).

Experimentally, the gold-standard to define a hematopoietic stem cell as such, is that upon transplantation into an irradiated host it gives rise to both lymphoid and myeloid lineages and reconstitutes >1% of peripheral blood mononuclear cells (PBMCs), and this beyond 16 weeks after transplantation. Such timing enables the distinction between HSCs with only short-term repopulation capacity (around 2 months; ST-HSCs) from HSCs with long-term repopulation potential (> 3-4 months; LT-HSCs), while remaining a reasonable period of experimentation. Since the repopulation capacity is evaluated by the number of graft-derived cells of the lymphoid and myeloid lineages in PBMCs, it has to take into account the half-life of each population. Indeed, some mature lymphoid cells can persist for a long time after exhaustion of the stem or progenitor cell they originate from. Hence, lymphoid cells may not reflect the presence of functional HSCs at a given time, and it has been proposed that following the myeloid content of circulating blood would be more pertinent (Dykstra et al., 2007). As I will discuss later, the definition of HSC subsets is very variable and can be confusing, with different teams using different parameters to distinguish different HSC populations, suggesting the need of a new standard for the detection of HSCs (see part *I.3.4*).

Transplant experiments are also largely used to test the properties of HSCs bearing mutations. Such cells can be injected either alone or together with competitor cells to assess their absolute or relative repopulating capacity, respectively. Adding wild-type competitor cells can also help reaching homeostasis of the hematopoietic tissue by alleviating some of the pressure due to the hematopoietic failure induced by irradiation of the host prior to transplantation. Using limiting-dilution analyses together with mathematical modelization, one can evaluate the properties of HSCs such as their self-renewal capacity, short/long-term reconstitution potential and possible biases in their differentiation(Benveniste et al., 2010; Busch et al., 2015; Sieburg et al., 2002; 2006).

2.2.3 Humanized mice: xenograft models of human hematopoiesis

For obvious reasons, studying hematopoiesis in human is much more complex, making the mouse an indispensable model. However, despite the advances in mouse hematopoiesis, the need to complement mouse studies with human studies has been driven by increasing evidence of species-specific differences in basic biology and the will to develop HSC-based therapy. Inspired by the CFU-C assays developed in mouse, first investigations of human hematopoiesis focused on *ex vivo* culture of human BM cells. Although this allowed the identification of long-term culture-initiating cells (Gartner and Kaplan, 1980), this approach faced the same limitations as in mouse due to the complexity of hematopoietic cell regulation by extrinsic factors.

A breakthrough for the study of human hematopoiesis is the use of humanized mice. In 1988, the team of I.Weissman transplanted human fetal liver hematopoietic cells into sever combined immunodeficient mice lacking lymphoid lineage, which resulted in sustained production of human B and T cells (McCune et al., 1988). Such xenograft models –notably using SCID and NOD/SCID mouse strains– have lead to tremendous progress in the phenotypical identification of human HSCs and their isolation, and better comprehension of human hematopoiesis. I will not go into the details

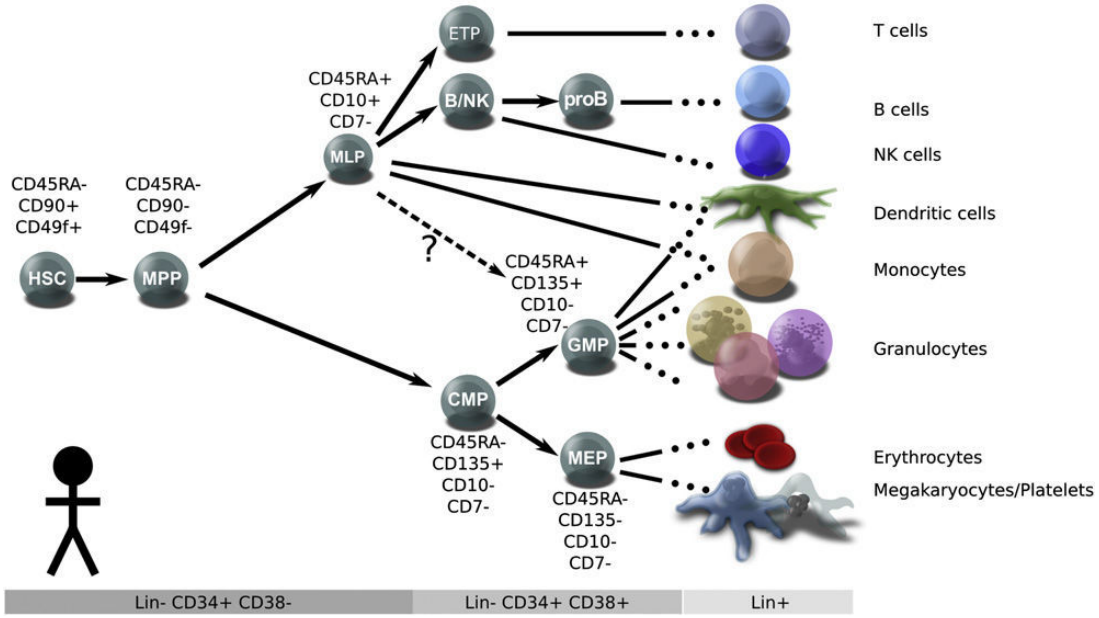

Figure 7. Phenotypical identification of human immature hematopoietic populations using combinations of surface markers

Adapted from Doulatov et al., 2012

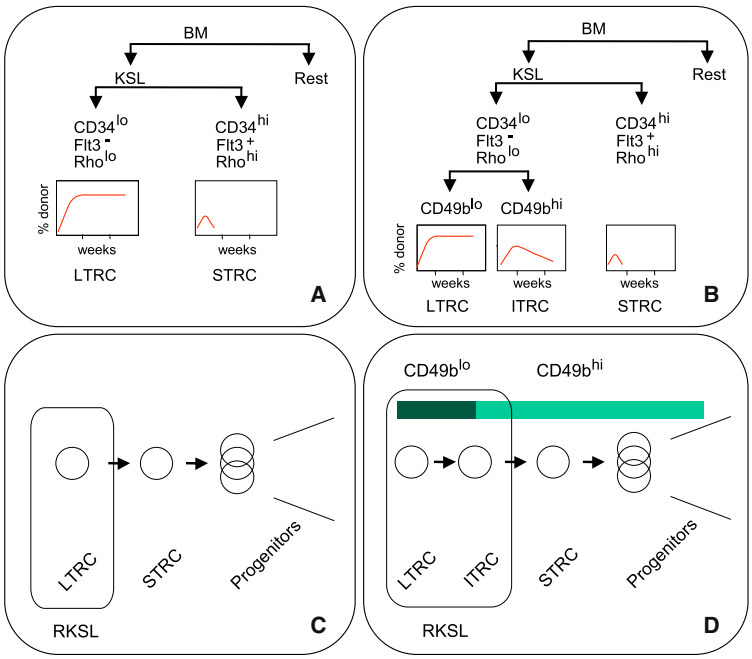

Figure 8. Hierarchization of immature hematopoietic populations based on their self-renewal capacity

As illustrated in A (purification scheme) and C (lineage hierarchy), the classical model proposes that the LSK can be subdivided into long-term and short-term reconstituting cells (LTRC and STRC, respectively) based on their expression of CD34 and Flt3 surface markers, and exclusion of Rhodamin123 (Side Population activity). Here, the authors propose an additional subset of intermediate-term reconstituting cells that can be separated from LTRC based on the expression of CD49b (see B and C for purification scheme and lineage hierarchy, respectively).

Adapted from Beneviste et al., 2010

of human hematopoiesis here, especially since it is well reviewed in (Doulatov et al., 2012) from which Figure 7 is adapted.

3. Heterogeneity within the HSC compartment

The model for hematopoiesis proposed by the team of I.Weissman (presented in Figure 1) has been established a decade ago. Since then, extensive analyses of reconstitution kinetics after transplantation have brought light on the unexpectedly important heterogeneity of HSCs, thus challenging this model. Here, I will present studies from the literature showing that the HSC compartment exhibits heterogeneity at different levels: self-renewal activity, lineage reconstitution potential and quiescence properties.

3.1 Heterogeneous self-renewal capacity among HSCs

The existence of HSC subsets with short- and long-term repopulating potential has been recognized for a long time in the field. The team of N.Iscove has analyzed this heterogeneity through transplantation experiments in limiting-dilution conditions, in which single donor HSCs were engrafted in different recipient hosts. Among HSCs with repopulating potential of over 16 weeks (the prevailing criterion for long-term repopulation), although some gave rise to maintained progeny beyond 32 weeks, others were exhausted more rapidly (Benveniste et al., 2010). Thus, they uncovered the existence of a subset of HSCs with an intermediate self-renewal potential between ST-HSCs and LT-HSCs, hence their appellation as intermediate-term HSCs (IT-HSCs, Figure 8): myeloid progeny from these IT-HSCs was present at 16 weeks post-transplant but disappeared between 16 and 32 weeks. Benveniste *et al.* were able to isolate these IT-HSCs using the Lin^{-} $Sca1^{+}$ $cKit^{+}$ $Rho123^{low}$ $CD49b^{high}$ markers, thus demonstrating that this intermediate self-renewal potential is indeed intrinsic to these cells at the moment of transplantation.

These results challenge the classical criterion of 16 weeks in the definition of long-term repopulation potential. Moreover, one could argue that “short-term” or “long-term” are not really suitable designations for HSCs, since by definition a stem cell is capable of long-term maintenance: strictly speaking, ST-HSCs are thus not so much HSCs but rather progenitor cells. In fact, these appellations allow artificial ranking of the most immature cell population of the hematopoietic system. The identification of IT-HSCs brings an additional step in the differentiation process, and supports the idea that immature hematopoietic cells would consist of a continuum of cells with decreasing self-renewal potential. Finding precise criteria for the definition of HSCs would therefore become complicated, and the classification as ST-, IT- and LT-HSCs could help resolving this problem.

3.2 Lineage-biased HSC subsets

When performing limiting-dilution analyses, several studies have observed that different subsets of HSCs displayed heterogeneous mature lineage output. The prevailing view was that this heterogeneity originated from the combination of extrinsic factors from heterogeneous stromal niches, and random decisions by HSCs at each division (Enver et al., 1998). However, in 2002

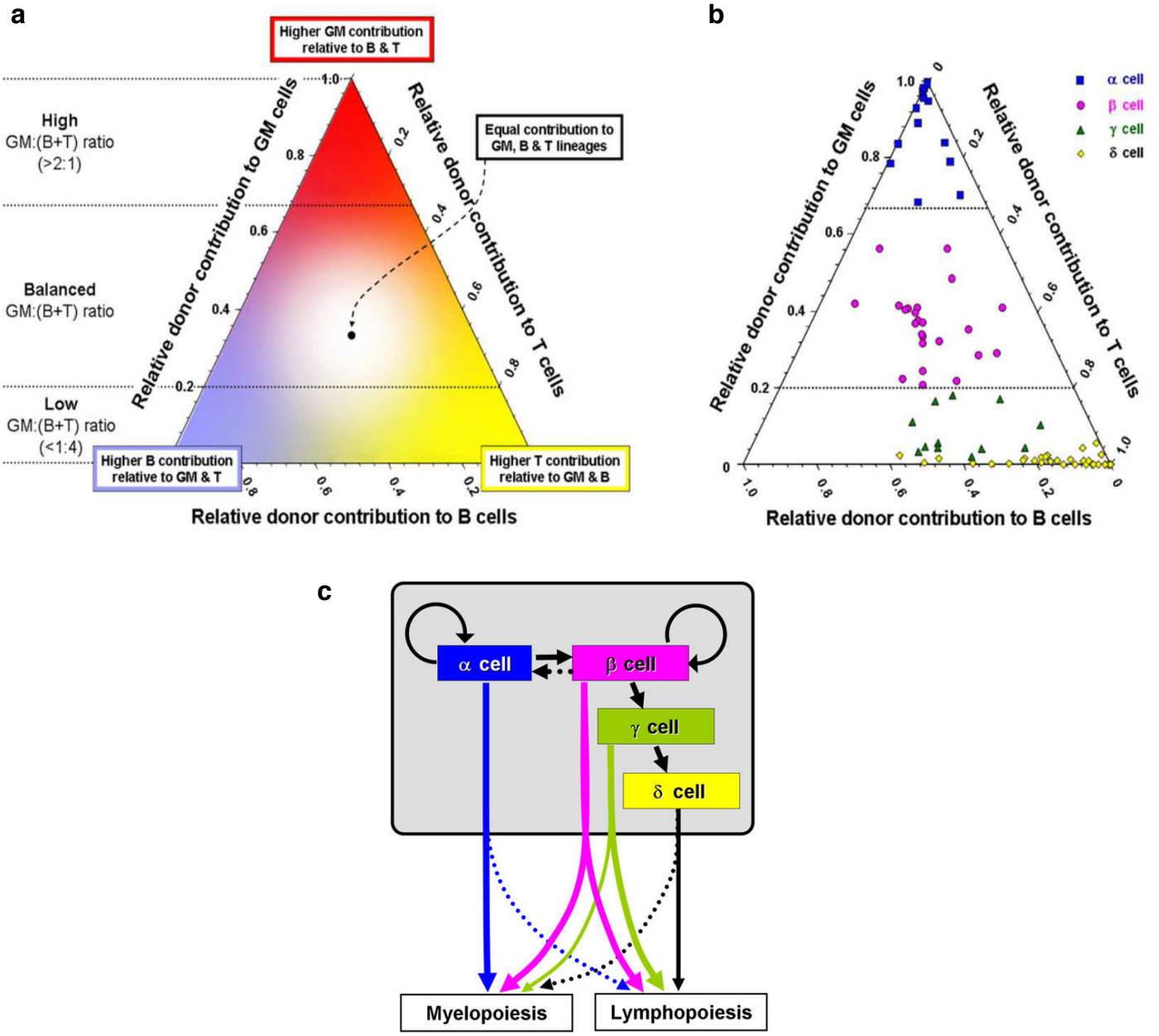

Figure 9. HSC subsets can be identified based on their differentiation potential

a. Comparison of the ratio of donor clone contribution to the myeloid (GM for granulocyte-macrophage), B and T lineages. If a clone only contributes to one of these lineages, it will be represented at the corresponding corner: GM lineage, top corner; B lineage, lower left corner; T lineage, lower right corner. A clone contributing equally to all lineages will be placed in the center of the triangle. Greater relative contribution to GM, B or T lineage will shift the clone's position towards the top, lower left or lower right corner, respectively. **b.** Contribution of HSCs to the different lineages was assessed in transplanted mice 16 weeks after transplant. Subdivision into 4 HSC subsets is proposed based on their differentiation potential. **c.** Schematic representation of the relationships between the different HSC subsets. Cells within the grey box display repopulation potential of >16 weeks. Serial transplant and *in vitro* culture suggest that HSCs are organized in a hierarchical manner, where the myeloid differentiation potential progressively diminishes, before long-term reconstituting potential is lost. α-HSCs exhibit strong myeloid bias, can be maintained in serial transplants and can give rise to cells with lymphoid differentiation potential.

Adapted from Dykstra et al., 2007

C.Müller-Sieburg and H.Sieburg demonstrated for the first time the existence of lineage-biased HSC clones in the BM with predetermined behaviors (Muller-Sieburg et al., 2002). They performed serial transplantation experiments in limiting-dilution conditions, and analyzed the myeloid (granulocytes and monocytes) and lymphoid (B and T lymphocytes) outputs of HSCs derived from the same or multiple clones. Thus, they were able to subdivide HSCs into 3 classes: HSCs with balanced output ("Bala HSCs", giving rise to physiological levels of both lineages), myeloid-biased HSCs ("My-bi HSCs", with reduced lymphoid differentiation potential) and lymphoid-biased HSCs ("Ly-bi HSCs", with reduced myeloid lineage repopulation capacity). Unexpectedly, they observed unsuspected similarity in the behavior of clonally derived HSCs, suggesting that HSCs behavior in the BM is largely predetermined and that heterogeneity within the HSC compartment would result from the presence in the BM of a limited number of discrete HSC clonotypes with predictable behaviors (Muller-Sieburg et al., 2002; Müller-Sieburg et al., 2004; Sieburg et al., 2006). However, they were not able at the time to identify phenotypical markers for these different subsets.

The team of C.Eaves has later confirmed the existence of such lineage-biased HSCs, although using a different classification. Through the analysis of multiple serial transplants, they also showed that the HSC compartment was composed of heterogeneous HSCs with different self-renewal and differentiation potentials: α HSCs display myeloid-biased repopulation potential, β HSCs give rise to balanced levels of both myeloid and lymphoid lineages, and γ/δ HSCs have lymphoid-biased differentiation potential (Figure 9). Furthermore, although γ and δ HSCs can reconstitute >1% of mature lineages for at least 16 weeks upon primary transplant, they are not able to recolonize a host upon secondary transplant and are exhausted in primary transplants after 6-7 months, indicative of limited self-renewal activity. Conversely, α and β HSC display long-term reconstitution potential in both primary and secondary transplants, indicative of robust self-renewal activity (Dykstra et al., 2007). The team of C.Eaves later showed that all four HSC subsets were found at different stages of development and post-natal ages, although in different proportions: α HSCs are initially in minority and increase in proportion in the aging adult mouse, whereas β HSCs are in majority from the developing fetus to the young adult (Figure 10)(Benz et al., 2012). Interestingly, they showed that α and β HSCs could interconvert, although they predominantly give rise to daughter HSCs with the parental differentiation program. Finally, another team showed that in the LSK $CD34^{-}$ compartment, $CD150^{high}$ cells –which are highly enriched in LT-HSCs– display myeloid-biased differentiation, whereas $CD150^{med}$ cells were balanced and $CD150^{neg}$ cells gave lymphoid-biased progeny (Morita et al., 2010).

Altogether, these studies suggest a model where the HSC compartment is composed of different subsets of HSCs with predictable differentiation programs and self-renewal activity. Importantly, this differentiation potential is conserved upon transplantation and is transmitted to the daughter cells in a clonal manner. The clonality of this predetermination is quite surprising, and suggests that it could be due to an intrinsic programming of HSCs such as epigenetic marks set during development. This heterogeneity could be useful in case of lineage-specific cytopenia: the associated HSC clones would be recruited. Furthermore, it could explain the heterogeneity found in genetically similar leukemias, and may have an impact on clinical uses of HSC transplantation therapy in human.

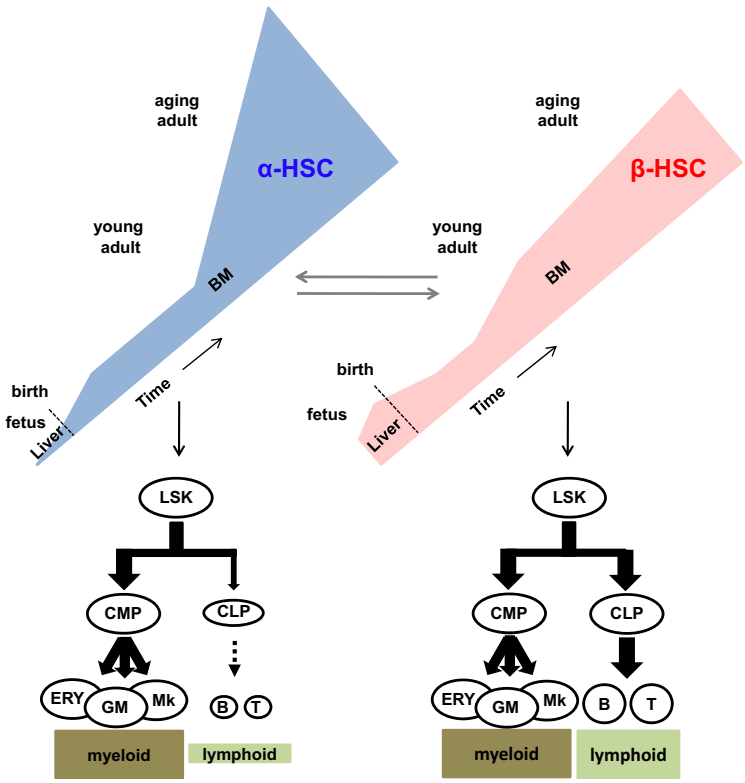

Figure 10. Progressive switch from balanced to myeloid-biased differentiation during development and aging

Adapted from Benz et al., 2012

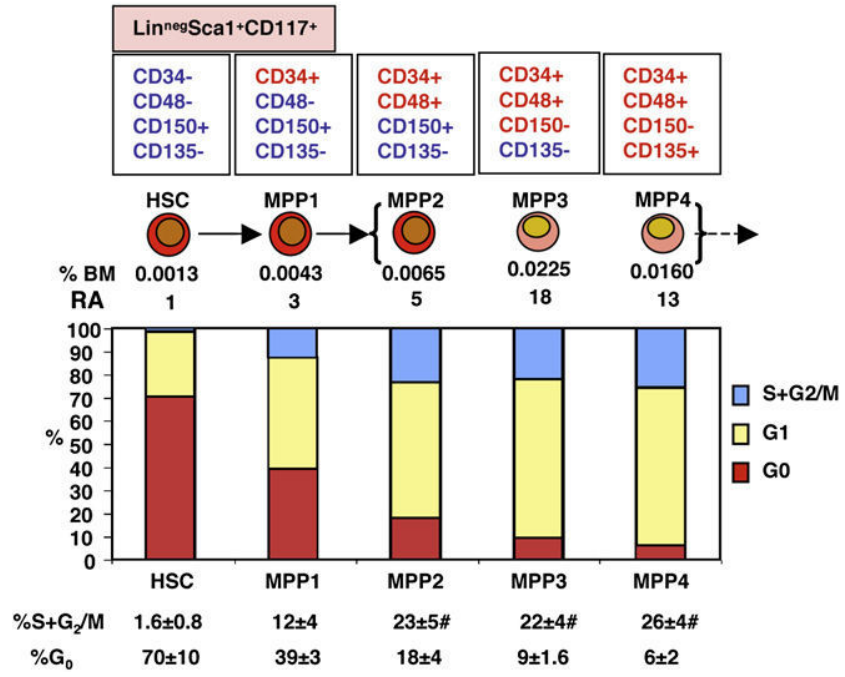

Figure 11. HSCs are mostly quiescent

Here, authors subdivided LSK cells in 5 subsets. Based on the surface markers, relative abundance, cell cycle status and long-term reconstitution potential of these subsets, they were hierarchized into HSC, MPP1, MPP2, MPP3 and MPP4 populations. HSCs are the most quiescent LSK cells, with 70% of cells in G_0 (Ki67-negative and 2N DNA content) and 1.6% in $S/G_2/M$ (Ki67-positive and DNA content >2N).

Adapted from Wilson et al., 2008

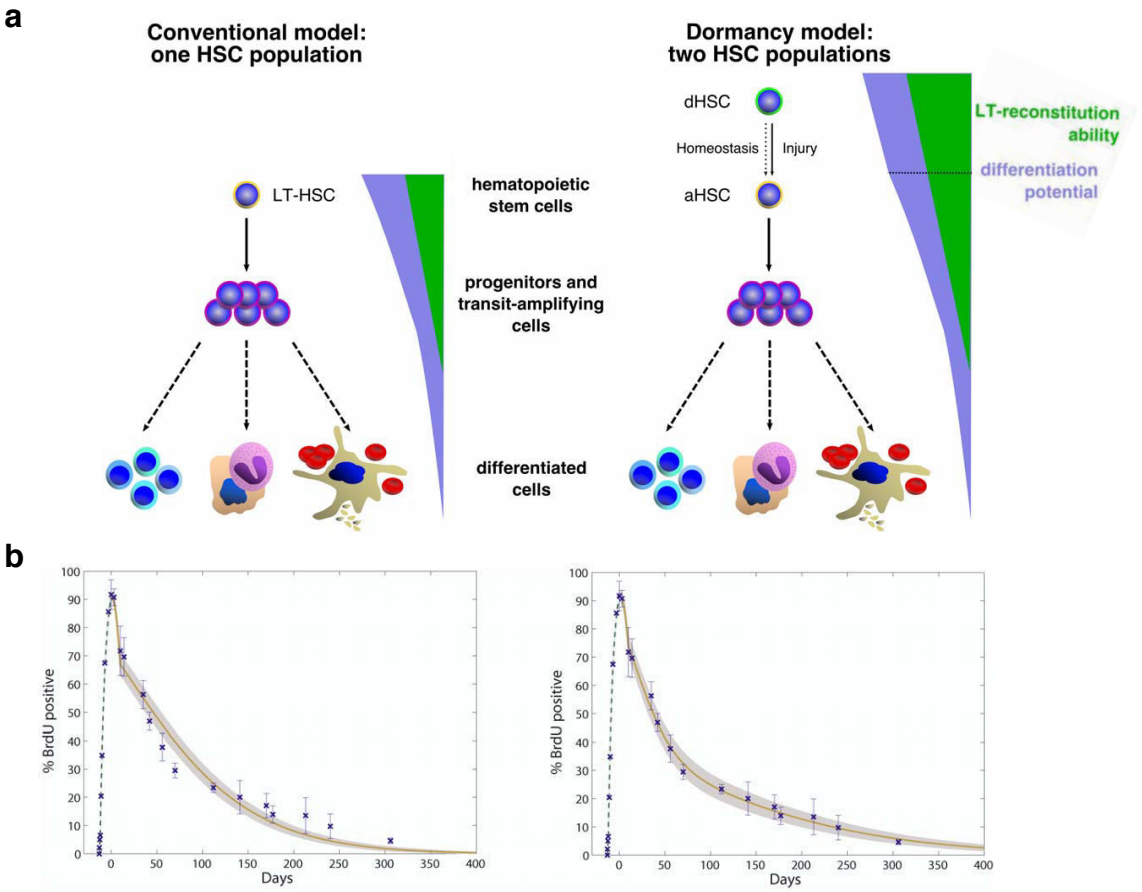

Figure 12. Conventional model of one HSC population vs. model with active and dormant HSCs

Two models have been proposed for the composition of the HSC pool. **a.** The "conventional" model (left) suggests that HSCs are a homogeneous population of cells that rarely but regularly undergo cell division. In contrast, the "dormancy" model (right) suggests the existence of dormant and activated HSCs (dHSCs and aHSCs, respectively). In this model, aHSCs ensure the maintenance of homeostasis, whereas dHSCs undergo very few cell divisions throughout the mouse's life (dotted line between dHSC and aHSC) but can be activated upon injury and actively participate to tissue regeneration (full-line). **b.** Mathematical modeling predicting the loss of BrdU retaining cells for either model (left: conventional model; right: dormancy model). Red lines and grey areas represent predictions and their estimated variance, and experimental data are represented as blue dots. For both predictions, loss of BrdU labeling was estimated to occur after 6-7 divisions. For the dormancy model predictions, dHSCs were estimated to represent 40% of total HSCs.

Adapted from Wilson et al., 2008

3.3 Heterogeneity in the quiescence of HSCs

Due to the very nature of stem cells, the acquisition of mutation by such cells can have dramatic and deleterious consequences on the whole organism, especially in a tissue such as the hematopoietic system that undergoes massive amplification from stem cells to differentiated cells. DNA replication itself is inherently prone to error and is the main underlying cause for spontaneous mutagenesis. Quiescence thus appears as a strategy to prevent DNA replication-induced mutations and stresses. The hematopoietic system has adopted this strategy, most of HSCs being in a quiescent state: ~70% of HSCs are found in the G_0 phase (Figure 11) (Cheshier et al., 1999; Passegue et al., 2005; Wilson et al., 2008).

As I mentioned earlier, one of the best ways to identify HSCs phenotypically is using their LRC property. Initially, such experiments following the long-term incorporation of BrdU *in vivo* in HSCs considered them as a homogeneous pool of rarely dividing cells that regularly enter the cell cycle, thus refuting the existence of a dormant population of HSCs that would not divide for a few months (Cheshier et al., 1999; Kiel et al., 2007). In this model, 6-8% of HSCs would asynchronously enter the cell cycle every day, with a complete turnover of the entire HSC pool within 57 days (Figure 12). Later, the teams of A.Trumpp and H.Hock used fine mathematical modelization to understand the long-term label retention of BrdU or H2B-GFP within HSCs (LSK $CD34^-$ $CD150^+$ $CD48^-$), and showed that a two-population model for HSCs fitted better the observed data (Foudi et al., 2008; van der Wath et al., 2009; Wilson et al., 2008). In this model, a large proportion of HSCs (55-85%) is found in a primed, or activated state (a-HSCs) while the remaining 15-45% of HSCs are in a dormant state (d-HSCs). d-HSCs are slower cycling cells with a more important proportion of G_0 cells, and divide about once every 149-193 days, that is 4-5 times in a mouse's lifetime; on the other hand, a-HSCs are more rapidly cycling cells dividing once every 28-36 days (Foudi et al., 2008; van der Wath et al., 2009; Wilson et al., 2008).Through serial transplant experiments, both teams further showed that d-HSCs display better repopulation potential than a-HSCs, indicating that d-HSCs are more *bona fide* HSCs. Furthermore, Wilson *et al.* observed cell cycle entry of LRCs 2 days after treatment with 5-fluorouracile (5-FU), an injury-inducing chemotherapeutic agent, and loss of BrdU and H2B-GFP labeling 70 days after treatment with 5-FU or G-CSF (induces mobilization of HSCs), indicative of the recruitment of d-HSCs to restore homeostasis (Wilson et al., 2008). After homeostasis restoration, they observed the reemergence of LRCs, indicative of the return of HSCs to a dormant status.

Altogether, this indicates that HSCs can reversibly switch from dormancy to an activated state to meet the demands of the hematopoietic system: in homeostatic conditions, a-HSCs are sufficient to ensure renewal of the tissue; in case of injury, d-HSCs are recruited to restore homeostasis and return to a dormant state once it has been restored. Interestingly, although both subpopulations are negative for the membrane marker CD34, a-HSCs exhibit a 100-fold increase of CD34 transcript levels compared to d-HSCs. This can be interpreted as a transcriptional preparation of activated HSCs for differentiation, and further supports the idea that differentiation of HSCs is a continuum of states rather than a sequential situation.

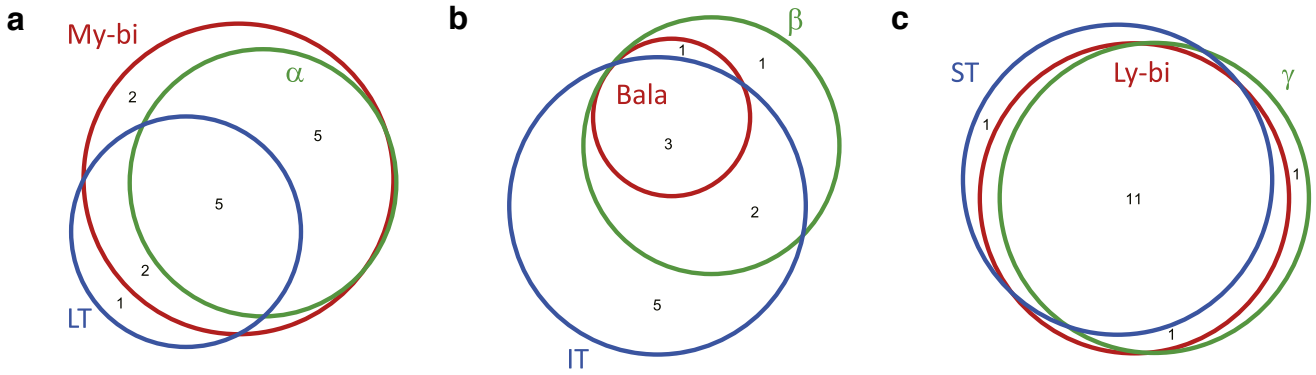

Figure 13. Comparison of α/β/γ/δ HSC, LT/IT/ST HSC and My-bi/Ly-bi/Bala HSC classifications

Ema et al. transplanted 30 single HSC into irradiated hosts, and resultant reconstitution data were classified based on three classifications: α/β/γ/δ *(Dykstra et al.)*, LT/IT/ST *(Benveniste et al.)* and My-bi/Ly-bi/Bala *(Müller-Sieburg et al.)*. Venn diagrams indicate the relationships among (**a**) My-bi, α and LT-HSCs; (**b**) Bala, β and IT-HSCs; and (**c**) Ly-bi, γ and ST-HSCs.

Adapted from Ema et al., 2014

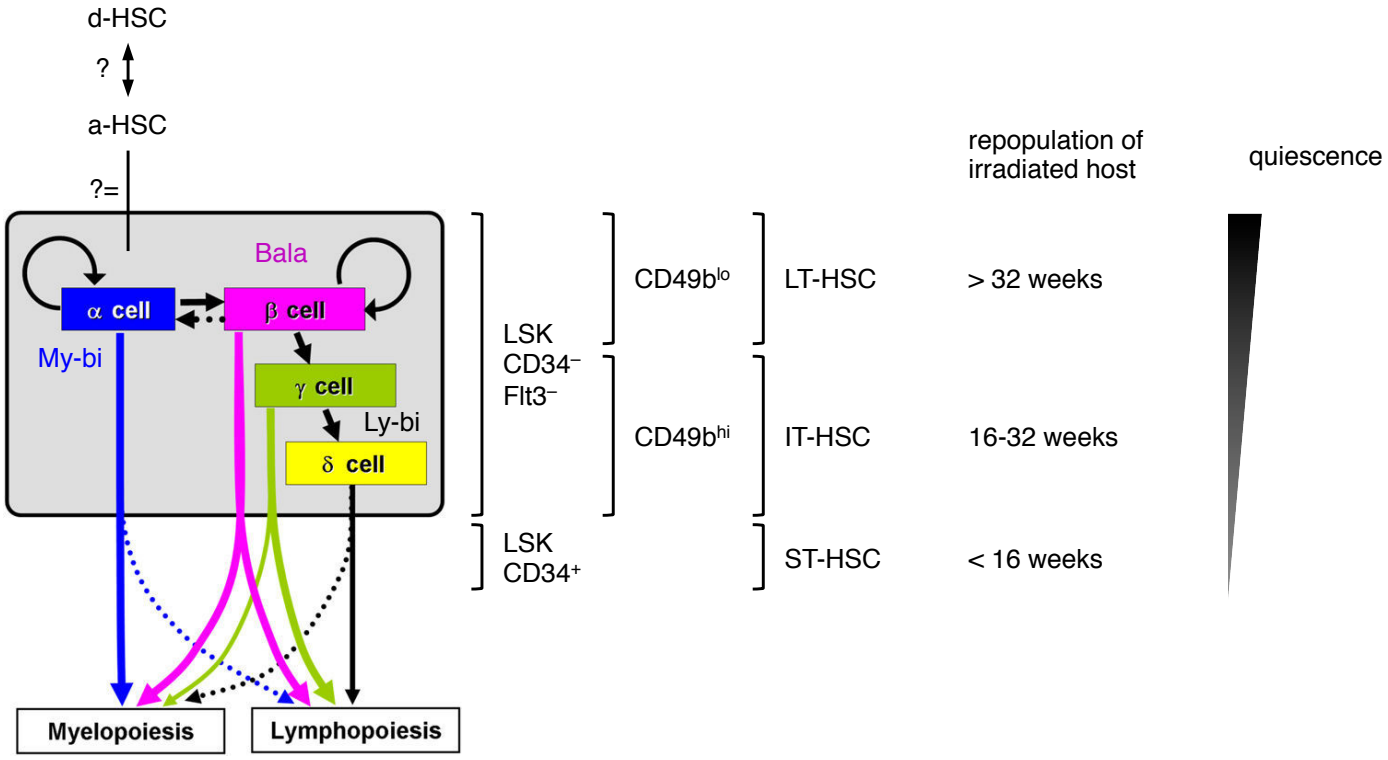

Figure 14. Summary of the heterogeneities observed within HSCs

A hierarchized model composed of a continuum of states can be proposed in light of the different studies. α, β, γ and δ HSCs have been described by *Dykstra et al.* based on their self-renewal and differentiation potential. Within the grey box, cells display repopulation potential for at least 16 weeks after transplant into irradiated hosts. γ and δ HSCs would correspond to IT-HSCs described by *Benveniste et al.* and Ly-bi HSCs described by *Sieburg-Müller et al.*: they can reconstitute an irradiated host for 16 weeks, after what their lineage contribution gradually decreases. Only α and β HSCs are able to repopulate irradiated hosts beyond 32 weeks, and could be compared to My-bi and Bala HSCs described by *Sieburg-Müller et al.* ST-HSCs are not included in the grey box, and should actually not be considered HSCs but rather MPPs. Finally, HSCs at the top of the hierarchy are mostly quiescent as shown by *Wilson et al.*, and the proportion of quiescent HSCs decreases together with their loss of long-term repopulating potential.

3.4 Conclusion: multiple heterogeneities within HSCs, leading to a new model of hematopoietic differentiation

The studies I have presented above highlight several types of heterogeneity within the HSC compartment. Interestingly, other stem cell populations can present heterogeneity in other tissues. In the skeletal muscle, satellite cells (the stem cells of this tissue) display variable self-renewal potential, can undergo different types of divisions –symmetrical or asymmetrical– and have heterogeneous molecular regulations (see (Brack and Rando, 2012) for review). In intestinal crypts, two populations coexist: $Lgr5^+$ stem cells at the bottom the crypt and "+4" stem cells, which are respectively more rapidly cycling and more quiescent (see (Carlone and Breault, 2012) for review). Such studies on the heterogeneity of stem cell populations in various systems contribute to a better knowledge of the biology of stem cells in general.

To reconcile the different types of heterogeneity observed in the hematopoietic system, Ema *et al.* compared the different classifications using data of transplantation with 30 single HSCs (Ema et al., 2014). Their analysis puts My-bi, α and LT-HSCs in one group, Ly-bi, γ and ST-HSCs in another; Bala, β and IT-HSCs were also regrouped but showed more differences (Figure 13). They also raise the question of whether all these different classes of HSCs can be detected using criteria commonly used in transplantation assays. The gold standard for HSC detection is long-term multi-lineage reconstitution, meaning >1% of total chimerism in peripheral leukocytes 16 weeks post-transplant with detectable reconstitution of myeloid, B lymphoid and T lymphoid lineages. However, this criterion does not allow detection of Ly-bi HSCs or the distinction between IT- and LT-HSCs, for instance, due to the different repopulation dynamics. Ideally, the peripheral blood (PB) of recipient individuals should be analyze for as long as they survive, although obvious practical reasons could not allow it. Thus, Ema *et al.* suggest that multi-lineage reconstitution in the PB of recipient animals should be analyzed at least 3 times at 1-2, 4-6 and 8-12 months after transplant, or in the case of serial transplants 1-2 and 4-6 months after primary transplant and 4-6 months after secondary transplant.

Altogether, these different studies and others have challenged the initial "bifurcation" model of HSC differentiation proposed by I.Weissman's group, proposing alternative models such as the "myeloid-based" and the "LMPP" (lymphoid-primed MPP) models (for review see (Ema et al., 2014)). Finally, in light of these studies I propose the model presented in Figure 14, where the HSC population would be composed of a continuum states with different self-renewal and differentiation potentials.

4. Post-transplant *vs* native hematopoiesis: different behavior of HSCs?

Although transplantation experiments are the best way of testing the functionality of HSCs, it is important to keep in mind that transplanted HSCs are not in homeostatic nor physiological environment. In such experiments, only cells that are able to circulate, colonize the niche and proliferate rapidly will be able to give rise to detectable progeny. Furthermore, engraftment procedures inflict a great amount of stress to the transplanted cells, together with dramatic changes

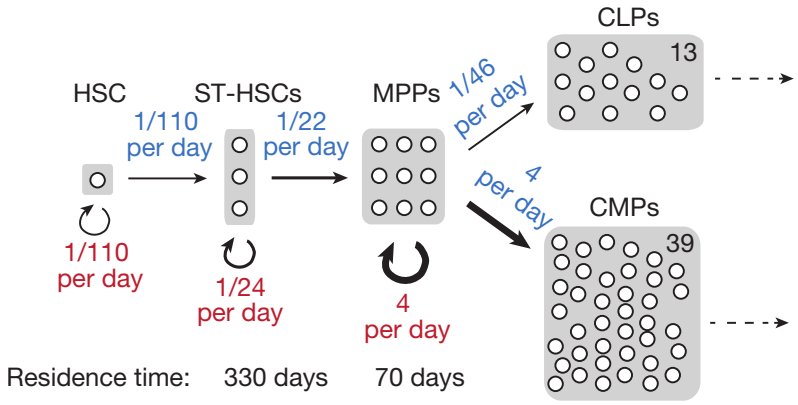

Figure 15. Dynamics of hematopoietic stem and progenitor cells in unperturbed conditions

Busch et al. used a mouse model allowing inducible genetic labeling of the most primitive Tie21 HSCs in the bone marrow, and quantified label progression along hematopoietic development by limiting dilution analysis and data-driven modeling. From their data, they estimated the indicated proliferation rates and residence times for HSCs (LSK CD150^{+} CD48^{-}), ST-HSCs (LSK CD150^{-} CD48^{-}) and MPPs (LSK CD150^{-} CD48^{+}).

Adapted from Busch et al., 2015

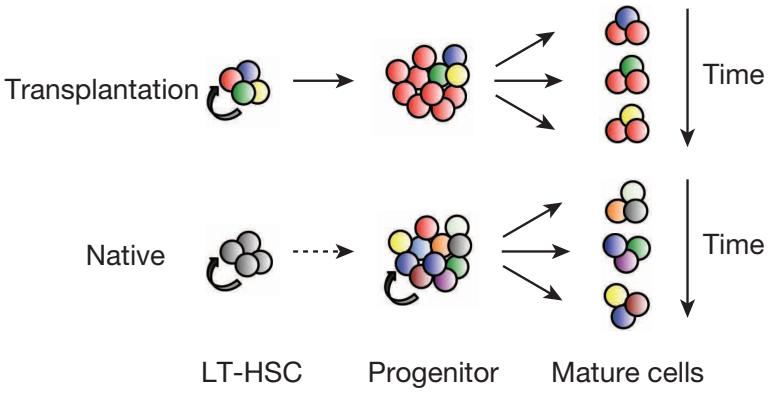

Figure 16. Clonal dynamics of native and post-transplant hematopoiesis

Sun et al. used transposon-mediated genetic barcoding of hematopoietic cells and followed the clonal dynamics of hematopoiesis in unperturbed conditions (native hematopoiesis) or after transplantation. Thus, they show that in native hematopoiesis, HSCs have minor lineage contribution, and that downstream progenitors are the main driver of hematopoiesis. In contrast, in irradiated hosts, transplanted HSCs have major contribution to lineage production, as observed in other studies.

Adapted from Sun et al., 2014

of their environment (cytokines, O_2 levels…): transplanted HSCs may thus display a different behavior compared to unperturbed hematopoiesis, a concern that can be extended to all HSPC populations. Thanks to different method of *in vivo* labeling of HSCs *in situ*, two recent studies have uncovered fundamental differences in the dynamics of hematopoiesis in normal maintenance of the system compared to re-establishment of homeostasis following chemically-induced leukopenia or transplantation after irradiation (Busch et al., 2015; Sun et al., 2014).

The team of H.-R.Rodewald used genetic fluorescent labeling of LT-HSCs and followed the progression of the label along hematopoietic differentiation to measure the output kinetics of *in situ* labeled HSCs by limiting-dilution analysis and data-driven modelization (Busch et al., 2015). They observed that label progression from the LT-HSC compartment to all differentiated lineages was relatively slow: labeled cells appeared in the ST-HSC and MPP compartment only after 4 weeks, and labeled LT-HSCs had contributed to all progenitor and mature lineages only after 16 weeks. They show that a LT-HSC undergoes a division leading to differentiation only once per 110 days, that ST-HSCs are capable of near-complete self-renewal and can reside for up to 330 days before exhaustion (~47 weeks), and that MPPs are key amplifiers: 1 MPP can give rise to up to 280 committed progenitors (Figure 15). In another study, the team of F.Camargo used transposon-mediated barcoding of all hematopoietic cells to investigate the cellular origins of differentiated cells and the dynamics of steady-state hematopoiesis (Sun et al., 2014). Following the overlap of tags present in hematopoietic cells at different levels of differentiation and at different time-points after initiation of the barcoding, they were able to reverse-track the origins of mature cells. Thus, they showed that LT-HSCs have limited lineage output under unperturbed conditions for at least 40 weeks (over a third of the mouse lifespan!) and that most of mature lineage production is sustained by polyclonal bulks of more or less committed progenitors. Using barcoded hematopoietic cells in transplant experiments, they showed that although many clones contribute to early BM and PB repopulation, an oligoclonal pattern arises with time, in accordance with data from other transplant studies.

Together, these two studies show fundamental differences in the clonal dynamics of post-transplant and steady-state hematopoiesis (Figure 16). They point towards a new model where unperturbed hematopoiesis is mainly driven by a large number of long-lived, lineage-restricted progenitors and multi-potent clones (including MPPS and so-called short-term HSCs) that have been specified in early post-natal life, and where the lineage output from the LT-HSC compartment is very limited. Finally, LT-HSCs would act as founding stem cells during development and as replenishing cells in the adult mouse to ensure maintenance of homeostasis in the long run (>1 year); ST-HSCs would act as long-term amplifying cells and primary source of maintenance in mice, and MPPs as intermediate-term amplifying cells. Upon injury such as 5-FU-induced leukopenia, ST-HSCs or LT-HSCs alone would not be sufficient and would act together to maintain homeostasis.

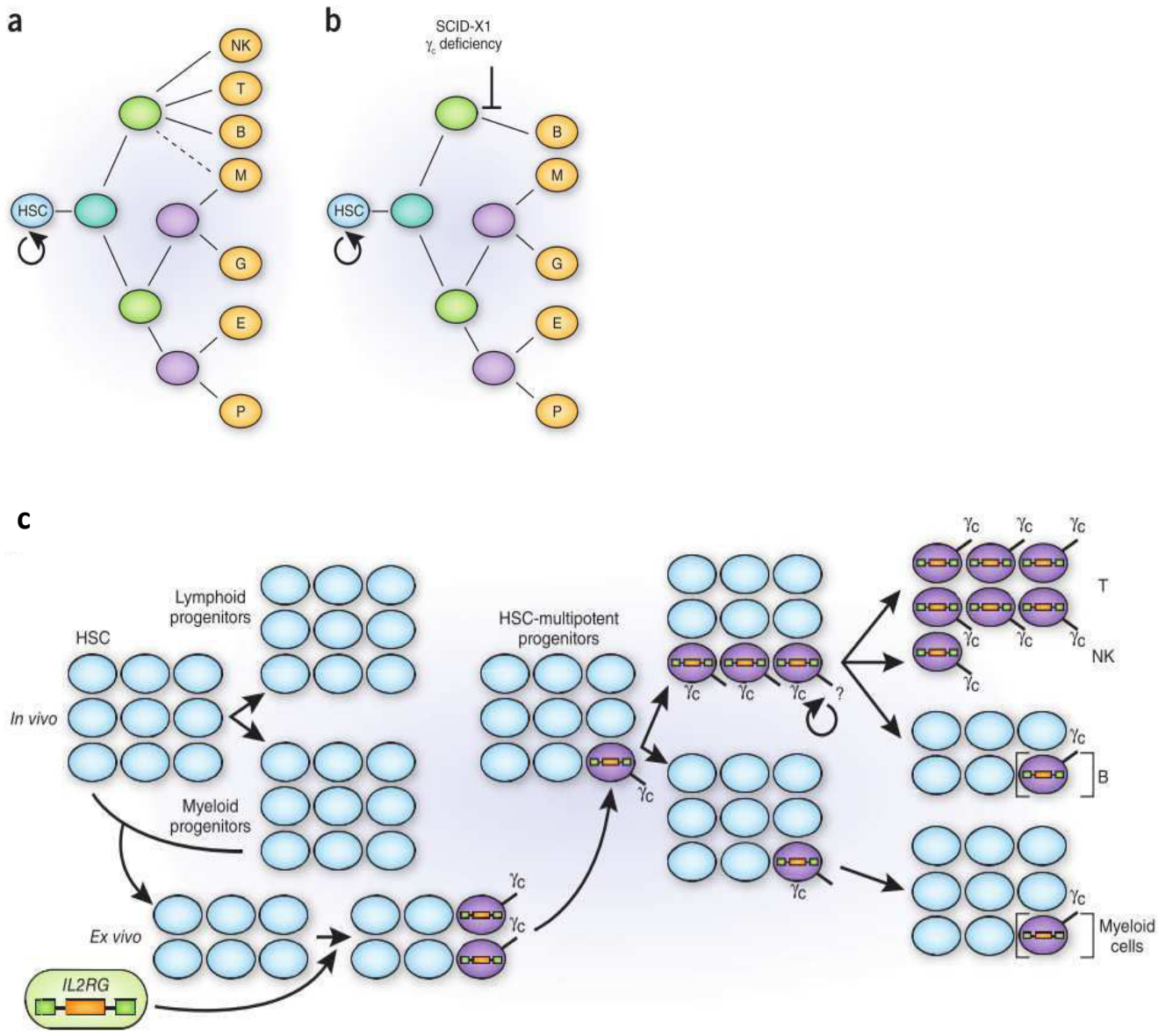

Figure 17. Principle of gene therapy in the treatment of X-linked severe combined immunodeficiency

X-linked SCID is characterized by the absence of T and NK cells due to mutations in the gene encoding the interleukin-2 γ-receptor *(IL2RG)*, which causes defective expression or function of the γ_c subunit of the receptor. **a.** Simplified view of normal hematopoiesis. **b.** Defective expression of the γ_c subunit results in defects in the production of T and NK cells. **c.** Schematic view of the strategy adopted for gene therapy: immature cells are transfected with a retroviral vector containing the *IL2RG* gene. One re-introduced, transfected cells contribute to part of the hematopoiesis (purple cells) and generate lymphoid progenitor capable of producing T cells, and NK cells to a lesser extent. Retroviral insertion is not detected in B and myeloid cells long-term, but is maintained in T cells, suggesting that T progenitors may have acquired self-renewal properties that allow their long-term maintenance.

Adapted from Fischer et al., 2010

5. Conclusion: HSCs, a privileged model for stem cell biology studies

The discovery of HSCs in 1960s has marked the beginning of stem cell research, and the immense advances made since have elevated them to the rank of model of study for stem cell biology in the mouse. The development of tools such as multi-parameter flow cytometry, gene inactivation approaches and mass transcriptomic analyses at the single cell level, has largely contributed to increasing progress in the field of HSCs.

Most advances on HSCs have been motivated by their use for clinical applications. Indeed, not only were HSCs the first adult stem cells to be isolated, but they were also the first to be used for therapeutic purposes. Initially, bone marrow transplant was mainly used to restore hematopoietic function in cancer patients treated with chemotherapy. Today, transplantation of HSC-enriched bone marrow cells is a therapy of choice for the treatment of a variety of malignant and non-malignant diseases such as autoimmune diseases or leukemia, in children and adults. HSCs have also been used in the first attempts of gene therapy, notably illustrated in the early 2000s by the work of A.Fischer at the Necker hospital in Paris in treating children with severe combined immunodeficiency (SCID). Although sever secondary effects were observed, his work demonstrated the benefits of gene therapy. Today, the treatment of X-linked SCID presents promising results (Figure 17 (Fischer et al., 2010)).

The comparison of healthy conditions with pathological situations such as cancer has uncovered similarities in the regulation and behavior of stem and cancer cells. Indeed, in many aspects a leukemic cell resembles a hematopoietic stem cell, notably in their ability to self-renew. Several key pathways required for the maintenance of HSC function involve proto-oncogenes and tumor-suppressor genes such as *PTEN* or *Bmi1*, suggesting that similar mechanisms can be used by HSCs and cancerous cells (Park et al., 2003; Yilmaz et al., 2006; Zhang et al., 2006). In the early 1970s, the notion of tumorigenic leukemia stem cells emerged based on studies showing that only a few leukemic cells were capable of extensive proliferation *ex vivo* and *in vivo* (Park et al., 1971). However, it is only in 1997 that it was clearly demonstrated that most leukemic cells are unable to proliferate extensively and that only a small, defined population of cells displayed consistent clonogenic potential (Bonnet and Dick, 1997). Today, the hematopoietic system is a model of choice to tackle questions regarding cancer such as the nature and origin of tumor initiating cells, the molecular mechanisms of tumorigenesis or the hierarchical organization of cancer cells, and develop therapeutic approaches.

Finally, the integration of knowledge from studies conducted in the hematopoietic tissue and in other systems has lead to better understanding of the biology of stem cells. Several studies have highlighted particularities in the use of some cellular processes by stem cell populations compared to differentiated cells, such as the DNA repair machinery and mechanisms of cell cycle regulation or cell division. Although this has not allowed the identification of molecular markers common to stem cells from different tissues, these processes all seem to be important for the maintenance of their stem cell properties. As a foretaste of things I will discuss later in this manuscript, I will point out now that recent data in the laboratory and other recent studies in the literature suggest a role for ribosome biogenesis in the regulation of stem cells.

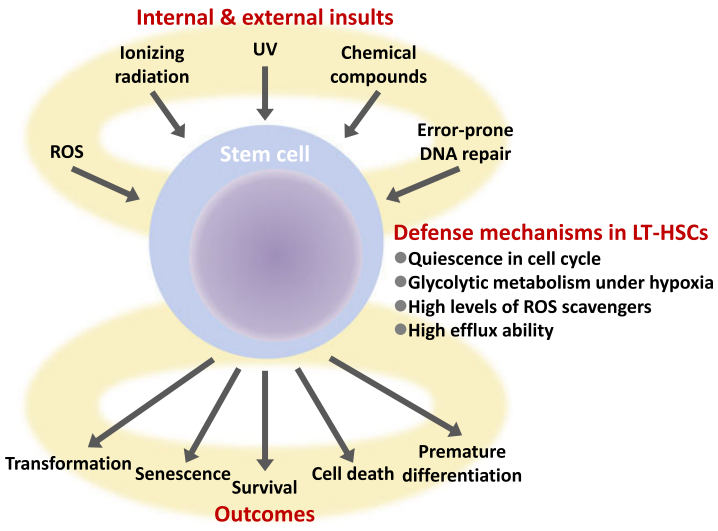

Figure 18. Potential defense mechanisms of HSCs in response to stresses

HSCs are constantly exposed to various stresses. Defense mechanisms have been identified specifically in these cells: quiescence, preferred glycolysis, expression of anti-oxidative defenses and ability to exclude some drugs. Exposure to stress can lead to various outcomes presented below.

Adapted from Suda et al., 2011

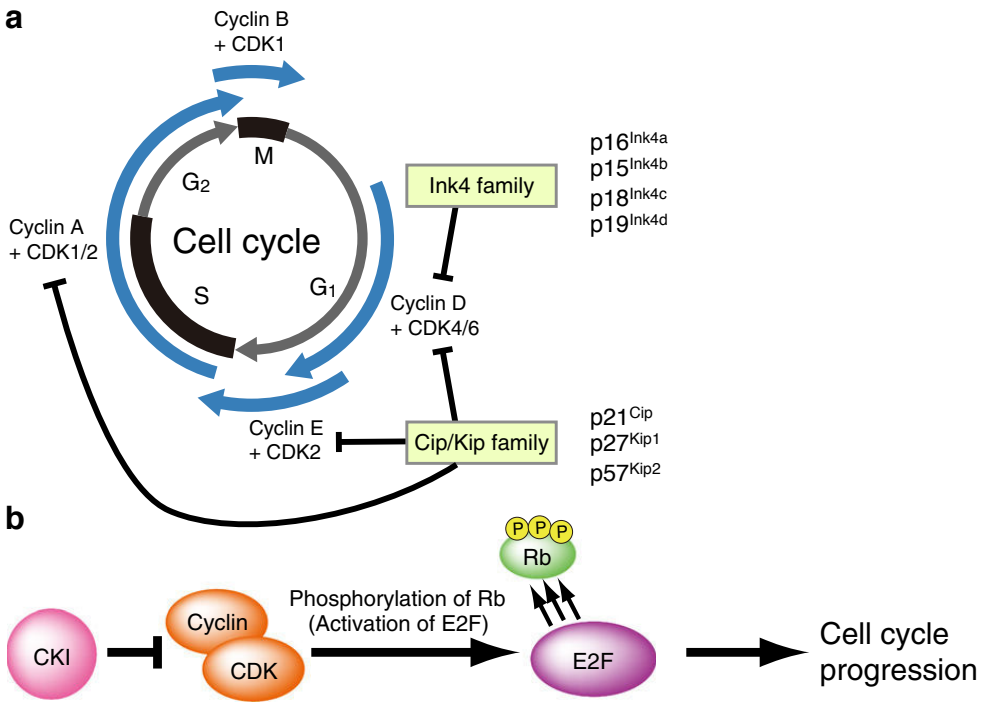

Figure 19. Molecular mechanisms of cell cycle regulation: function of CDK inhibitors

During the G_1 phase, activation of the cyclin D-CDK4/6 complex induces phosphorylation of Rb. This step is negatively regulated by members of CDK inhibitors (CKIs) for the Ink4 and Cip/Kip families. In late G_1, hyper-phosphorylation of Rb by the cyclin E-CDK2 complex promotes transition to the S phas. CKIs of the Cip/Kip family inhibit both the cyclin E-CDK2 complex in late G_1 and the cyclin A-CDK2 complex in the early S phase.

Adapted from Matsumoto et al., 2013

II. Regulation of HSCs

Stem cells are constantly exposed to various kinds of stress: intrinsic stresses due to the normal function of the tissue, such as DNA replication, oxygen metabolism, and extrinsic stresses, such as infections, tissue lesions, and exposure to toxic compounds or ionizing and UV radiations. Furthermore, their constant self-renewal throughout the individual's lifespan makes stem cells likely to accumulate of damages through time. All these stress signals must be sensed by stem cells, which in response can either maintain their stem cell potential, go into premature differentiation or enter senescence or apoptosis (Figure 18).

In this part, we will see how HSCs protect themselves from stress thanks to quiescence, hypoxia, telomere protection or the exclusion of toxic compounds. We will also see how HSCs exposed to stress integrate and respond to stress signals, and use properties of the cellular machinery as defense mechanisms.

1. Balancing quiescence and proliferation: plasticity of HSCs in stress situation

In the hematopoietic system, quiescence is considered as an intrinsic property of stem cells. Balance between HSCs in dormant and activated states provides the hematopoietic system with certain plasticity and adaptability when subjected to various stresses.

1.1 Is quiescence required for self-renewal?

1.1.1 Loss of quiescence induces self-renewal defects and HSC exhaustion

First evidence of a direct link between self-renewal was brought by the study of mice deficient for the cell cycle regulator *$p21^{CIP1/Waf1}$ (p21)*: loss of *p21* induced increased cycling of HSCs and their exhaustion upon transplantation ((Cheng et al., 2000) ; see Figure 19 for an overview of cell cycle regulators). Since, studies of mice deficient for cell cycle regulators such as *p27*, *p57* and members of the *Retinoblastoma (Rb)* family, members of the *FoxO* family of transcription factors, the tumor suppressor *Pten* or several other genes, have shown that loss of quiescence is followed by self-renewal defects in HSCs ((Tothova et al., 2007; Viatour et al., 2008; Yilmaz et al., 2006; Zou et al., 2011) ; see Table 1 for more examples of genes with similar phenotypes). Notably, such deficiencies can result in impaired repopulation capacity of HSCs and exhaustion of the HSC compartment within weeks. Thus, maintenance of a balanced quiescence and self-renewal appear to be crucial for the maintenance of HSCs.

To compare the repopulation capacity of quiescent *vs* cycling HSCs, the team of I.Weissman sorted HSCs in the G_0, G_1 or $S/G_2/M$ phase of the cell cycle. Thus, they showed that the ability of HSCs to engraft and reconstitute the hematopoietic tissue of irradiated hosts was dramatically impaired as soon as they exit quiescence and enter the cell cycle (Passegue et al., 2005). However, *ex vivo* culture of the different HSC subpopulations showed that this engraftment defect of cycling HSCs was not caused by impaired proliferation or differentiation capacity, or by increased susceptibility to apoptosis. Hence, intrinsic molecular mechanisms of cell cycle regulation could

Gene	Type of Mouse	FL	Engraftment Ability in Transplantation Assays						Cell Extr	Canc	Comments	PMID
			Sev	Mod	Mild	After Serial	Norm	Incr				
Gfi1	KO		+								KO HSCs cannot compete with WT HSCs in 2-month-old chimeric mice	15457180
Sox17	KO	+	+				+				decreased fetal HSCs; no impact in adults	17655922
Lkb1	cKO (Mx1-Cre)		+								HSCs profoundly depleted 18 days after deletion; pancytopenia	21124450; 21124456; 21124451
Irgm	KO		+								hyper interferon signaling; increased HSC proliferation	18371424
CD48	KO			+					+	+	increased HSC quiescence; dysregulated cytokine signaling; lymphomas	21576698
Hoxa9	KO	+		+							FL: defective engraftment of *Hoxa9*$^{-/-}$ FL HSCs	17761289; 16091451
PU.1	cKO (Mx1-Cre)	+		+							decrease in FL HSC; block in myelomonocytic differentiation	15914556
IL10	KO			+					+		IL10 expressed in endosteal osteoblasts; hypocellular Pre-TP	17464085
Smad4	cKO (Mx1-Cre)				+						decreased repopulation; Pre-TP: reduction in RBC	17353364
Hif1alpha	cKO (Mx1-Cre)					+		+			increased engraftment after 1°TP, and almost total loss after 2°TP; increased cycling	20804974
CD81	KO					+					severe defect only after 2°TP; CD81 promotes quiescence after TP	21931533
Opn (Spp1)	KO					+		+	+		increased engraftment after KO BM TP, lost by 2°TP; host effect	15928197
Egr1	KO					+		+			increased engraftment and circulating HSCs; defect after 3°TP	18397757
Necdin	KO						+				slightly reduced stress recovery	19770359
Dicer	cKO (Osx-Cre)						+		+	+	increased HSC proliferation and apoptosis; MDS and leukemia; host effect	20305640
Gfi1b	cKO (Mx1-Cre)							+	+		increased engraftment; increased ROS in HSCs	20826720
Cebpa	cKO (Mx1-Cre)	+						+		+	increased engraftment in 1°TP and 2°TP; myeloid diff. block in BM	15589173
Cbl	KO							+		+	increased HSC number and repopulating ability; myeloproliferative disease	18413713
Tet2	KO, cKO (Mx1- and Vav-Cre)							+		+	increased progenitors; development of CMML-like disease; het. phenotype	21723200; 21873190; 21723201
Trp53	KO							+			20%–50% incr after competitive TP; increased HSC number	12829028

Table 1. Examples of genes where KO leads to altered proliferation and self-renewal potential upon transplantation

KO, knockout; cKO, conditional KO; TP, transplant; 1°TP, primary TP; 2°TP, secondary TP; 3°TP, tertiary TP; FL, hematopoietic defect seen at the fetal liver development stage; Sev, Severe defect; Mod, moderate defect; Mild, mild defect. After Serial: defect observed only after serial transplantation (normal hematopoiesis in 1°TP). Incr, Increased function: KO mice that showed enhanced PB production after HSC or BM transplantation. Cell Extr, cell extrinsic effect generally is shown by demonstrating an impact on PB production from WT HSCs after transplantation into KO recipients. Canc, cancer development in KO or transplanted mice. PMID, PubMed ID number.

Adapted from Rossi et al., 2012

impinge on the self-renewal of HSCs. In mice with quiescence defects, cycling HCSs could be more prone to differentiate, which would explain the exhaustion of the HSC pool in some mutant strains.

1.1.2 Increased HSC proliferation does not necessarily cause self-renewal defects

The requirement of quiescence for maintenance of HSC self-renewal potential is well established and even appears to be a dogma in the field. However, surprisingly some studies suggest that increased proliferation of HSCs is not necessarily associated with the loss of their stem cell potential, or stemness.

The study of *Ink4* family member *p18*, a cell cycle inhibitor that specifically blocks the activity of cyclin D-CDK4/6 complexes, lead to surprising results (see Figure 19 for an overview of cell cycle regulators and (Matsumoto and Nakayama, 2013) for review of their role in HSC maintenance). $p18^{-/-}$ HSCs exhibit increased proliferation compared to wild-type (WT) HSCs, but also display increased self-renewal capacity in competitive or serial transplantation experiments and *ex vivo* functional tests, in contrast with $p21^{-/-}$ HSCs (Song et al., 2006; Yu et al., 2006; Yuan et al., 2004). Similar phenotypes have been observed in mice mutated for the ubiquitin ligases *Cbl* or *Itch* and the transcription factor *Egr1* ((Min et al., 2008; Rathinam et al., 2008) ; see Table 1 for more examples of genes with similar phenotypes). Indeed, these mutations induce the exit of HSCs from quiescence, but $Cbl^{-/-}$, $Itch^{-/-}$ and $Egr1^{-/-}$ HSCs still have self-renewing potential and can repopulate the BM of irradiated hosts, even in serial transplant experiments. Such findings can have implications in clinical research, where being able to stimulate the expansion of HSCs without altering their stem cell properties is a real challenge.

1.1.3 Conclusions:

Overall, these contradictory phenotypes associated with increased proliferation –severe HSC defects in some cases *vs* enhanced HSC function in others– illustrate our poor understanding of how the links between HSC proliferation and self-renewal. While quiescence is an intrinsic property of HSCs, cell division is necessary for their self-renewal and provides an opportunity for differentiation. Genes involved in the entry of HSCs into the cell cycle may also play a role in determining the susceptibility of HSCs to the effects of other genes or environmental cues, and could thus promote either HSC self-renewal or their differentiation. In the end, the outcome of HSC division would result of the balance between forces driving self-renewal or differentiation.

Finally, it is worth mentioning that the different studies aforementioned have analyzed the properties of populations enriched in HSCs but have not discriminated activated *vs* dormant HSCs. Revisiting the studies of the different mutants with emphasis on the characterization of the properties of quiescent HSCs could give interesting insight.

1.2 A few insights into the regulation of quiescence

1.2.1 Complex regulation of quiescence by extrinsic and intrinsic factors

As I mentioned above, the maintenance of HSCs relies upon a controlled balance between quiescence and proliferation. This balance is finely regulated, both by intrinsic signaling pathways and by interactions with the niche, through cellular interactions and interactions with the extra-

Category	Effect	Name of quiescent regulators
Extrinsic regulators	Positive regulators	Bone-lining osteoblastic cells and stem cell factor/C-Kit signaling, Tie2/Ang-1 signaling as well as TPO/MPL signaling
		Hypoxic environment
		Other matrix components: N-cadherins, integrins, osteopontin
		Ca^{2+} ions
		Transforming growth factor–β
		Wnt signaling pathway
	Negative regulators	Hedgehog (Hh) signaling pathway
Intrinsic regulators	Positive regulators	Transcription factors: Gfi-1, Pbx1, p53, Scl, Irf2, TXNIP, Nurr1, GATA-2
		Cyclin-dependent kinase inhibitors: p21, p57
		Others: Cdc42, Fbw7, pTEN, PML, TSC1, ATM, FoxOs, STAT5, Rb, Lkb1, Mi-2b, and Wnt5
	Negative regulators	MEF/EFL4
		Lnk
		c-Myc

Table 2. Regulators of quiescence in HSCs

Adapted from Li et al., 2013

cellular matrix. Studies of numerous mouse mutants have identified regulators of the cell cycle in HSCs (for review, see (Matsumoto and Nakayama, 2013)), a number of which are involved in the regulation of quiescence (*p21*, *p57*…). Other regulators of quiescence have been identified among transcription factors (*p53*, *FoxO* family…), molecular signaling pathways (*Pi3K/Akt* pathway…), developmental pathways (*Hedgehog*, *Wnt*), molecules of the extra-cellular matrix (*N-cadherin*, *integrins*…) and environmental conditions (calcium concentration, hypoxia: see *II.3.2*) (Table 2). All these intrinsic and extrinsic signals form a complex network to regulate the quiescence of HSCs (Figure 20). Since this network has been reviewed in several publications (Li, 2011; Matsumoto and Nakayama, 2013; Nakamura-Ishizu et al., 2014; Pietras et al., 2011; Rossi et al., 2012) and I will discuss some of its components later *II.3.3.2*, I will not go into the details here and just give the example of *p57*.

p57 is a member of the Cip/Kip family of cyclin-dependent kinase (CDK) inhibitors (CKIs), along with *p21* and *p27* (Cip/Kip = CDK interacting protein / Kinase inhibitory protein ; Figure 19). *p57* knockout (KO) mice die immediately after birth and show severe developmental defects (Takahashi and Nakayama, 2000; Yan et al., 1997; Zhang et al., 1997). Studies have shown high expression of *p57* in quiescent HSCs, and lower in downstream progenitor populations (Matsumoto et al., 2011; Passegue et al., 2005; Yoshihara et al., 2007). Using *p57* conditional knockout (cKO) mice, Matsumoto *et al.* showed that *p57* inactivation in adult mice leads to a reduction in size of the HSC population resulting from impaired self-renewal capacity of HSCs (Matsumoto et al., 2011). The authors further show that loss of *p57* causes upregulation of CDK activity and entry of HSCs into the cell cycle, making *p57* a key regulator of HSC quiescence. When investigating the potential redundancy of the different Cip/Kip family members, the authors observed that the additional KO of *p27* in *p57*-deficient mice leads to aggravated defects in the maintenance of HSC quiescence. Interestingly, replacement of *p57* by knockin (KI) of *p27* rescued most of developmental defects as well as the abnormalities of HSCs observed in *p57* KO mice suggesting that the total amount of CKIs of the Cip/Kip family is important to determine HSC stemness. However, HSCs lacking both *p21* and *p57* do not exhibit significant differences from those lacking *p57* alone but did show reduced CFU activity, indicating reduced proliferative capacity of progenitor cells and suggesting that the combined deletion of both CKIs may not only affect HSCs but also downstream progenitors. HSC function in mice deficient for both *p21* and *p27* does not differ markedly from that in WT animals, suggesting that *p57* alone is sufficient for maintenance of HSCs in non-stress situation (Figure 21). Interestingly, cell cycle arrest induced by the transforming growth factor β (TGF-β) in human hematopoietic progenitors and mouse HSCs was found to be associated with increased *p57* expression (Scandura et al., 2004; Yamazaki et al., 2009). Altogether, these studies illustrate the key role of CKIs of the Cip/Kip family in the regulation and maintenance of quiescence and self-renewal potential of HSCs.

1.2.2 Quiescence is actively regulated

Interestingly, most molecules and signaling pathways regulating HSC quiescence that have been identified so far are positive regulators of quiescence (Li, 2011; Yamada et al., 2013). The team of I.Weissman has performed transcriptomic analyses to examine how the expression profile

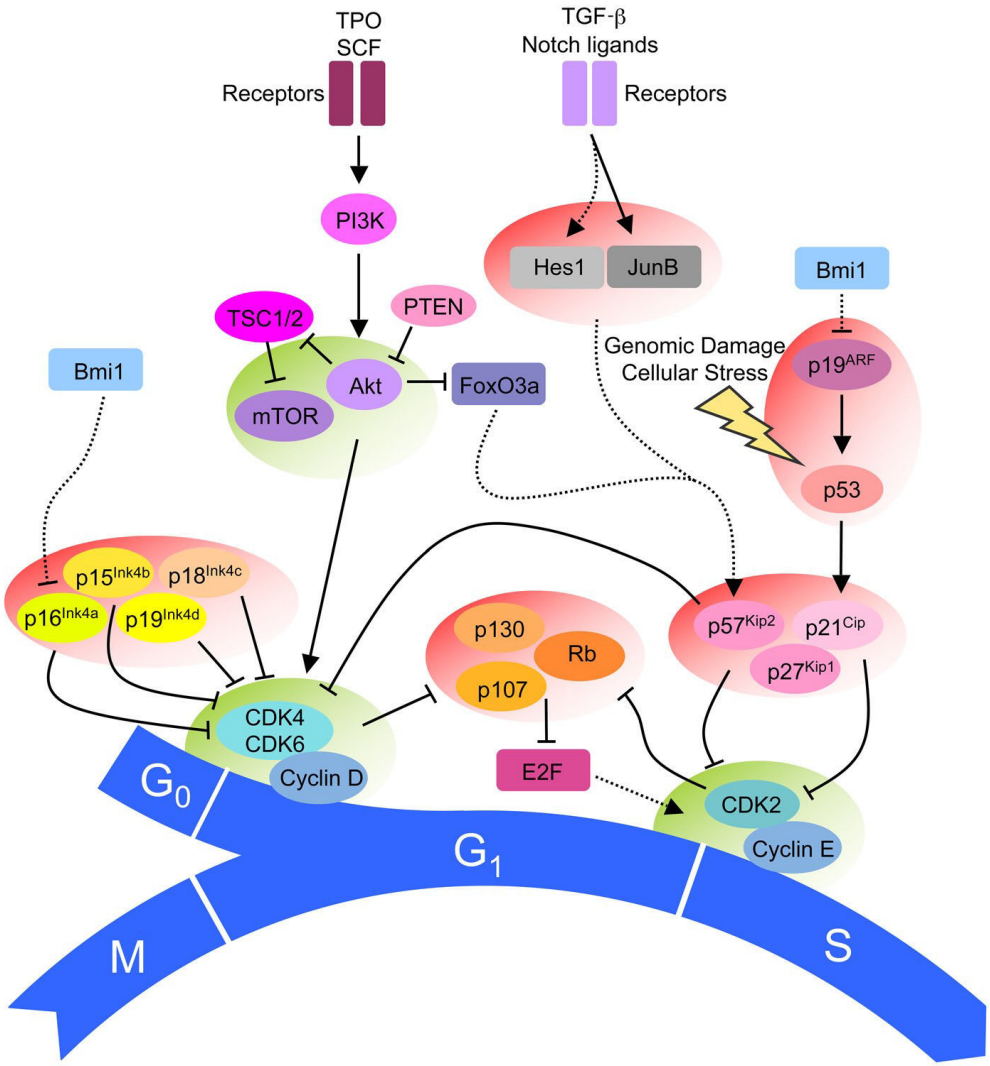

Figure 20. Regulation of cell cycle entry in HSCs

The entry of quiescent HSCs from G_0 into the G_1 phase of the cell cycle is governed primarily via competing activating and inhibitory mechanisms that regulate the activity of cyclin–CDK complexes. The PI3K/Akt/mTOR pathway, which is activated in response to numerous extrinsic signals, is considered a central activator of HSC cell cycle activity, primarily via activation of the cyclin D–CDK4/6 complex. This pathway is heavily regulated, primarily by PTEN and TSC1/2. Moreover, the Ink4 CKI family inhibits cyclin D–CDK4/6 activity, and Cip/Kip family CKIs are also capable of inhibiting CDK4 activity. Progression from the G_1 to the S phase of the cell cycle is regulated by Cyclin E–CDK2. This complex is regulated via the Cip/Kip family of CKIs, as well as by the Rb family. Expression of Cip/Kip family members is in turn regulated by transcription factors such as Hes1, JunB, and FoxO3a, which are activated by extrinsic growth-repressive signals. Furthermore, HSC cell cycle activity is subject to regulation via p53, either in response to cellular damage or $p19^{ARF}$ activity. Solid arrows indicate direct activation/inhibition events, dashed arrows indicate transcriptional regulation events. Functionally related groups of cell cycle activators are shaded in green; function- ally related groups of cell cycle inhibitors are shaded in red.

Adapted from Pietras et al., 2011

of normal, quiescent HSCs changes under three different conditions: normal differentiation into MPPs, cytokine-induced expansion and mobilization, and leukemic transformation (Forsberg et al., 2010). Thus, they identified a network of genes and signaling pathways that are specifically activated in quiescent HSCs and repressed in non-quiescent HSCs and MPPs. Their data highlight the existence of an important and active signaling that regulates positively the quiescence of HSCs and inhibits their proliferation, suggesting that differentiation would be the default fate of HSCs.

This hypothesis is supported by studies of Polycomb group (PcG) proteins. Indeed, the inactivation of PcG genes *Bmi1*, *Mel18*, *Ring1B*, *Rae28*, *Cbx7* or *Suz12* is associated with HSC self-renewal defects, suggesting that PcG proteins participate in the maintenance of self-renewal through the regulation of genes or proteins involved in cell proliferation, lineage specification or cell death (Calés et al., 2008; Kajiume et al., 2004; Kim et al., 2004; Klauke et al., 2013; Lee et al., 2015; Park et al., 2003). Indeed, a very recent publication reports that the PcG repressive complex 1 (PRC1, composed notably of Bmi1, Ring1B, Rae28), together with Hoxb4/Hoxa9, directly regulates the function of Geminin –a regulator of DNA replication and chromatin remodeling– to determine the fate of HSCs, promoting quiescence and preventing proliferation/differentiation (Yasunaga et al., 2016). Altogether, these studies further argue that the default fate of HSCs would be differentiation, and that maintenance of their stem cell properties requires an active regulation.

1.2.3 Specific regulation of quiescence

Strikingly, several regulators of the cell cycle in HSCs do not regulate or have an opposite effect on the cell cycle of other hematopoietic populations. A first example is the transcriptional repressor *Gfi1*, which is a known oncogene in lymphoid cells. Indeed, the *Gfi1* locus is a frequent site of retroviral integrations participating in the development of lymphoid tumors in mice. Under normal conditions, *Gfi1* promotes the proliferation of T cells: *Gfi1*$^{-/-}$ mice display diminished proliferation of thymic cells (Hock et al., 2004). In contrast, *Gfi1* represses HSC proliferation and is required for the maintenance of HSCs. The study of a conditional knockout of *Mll*, a transcriptional coactivator involved in epigenetic regulation, leads to similar results: *Mll* deletion in myelo-erythroid progenitors results in reduced proliferation and response to cytokine-induced cell cycle entry, whereas *Mll*$^{-/-}$ HSCs enter the cell cycle. Finally, the triple KO of *FoxO1, FoxO3, FoxO4* or the single KO of *FoxO3a* lead to defective cell cycle regulation in HSCs but does not affect the proliferation of downstream hematopoietic progenitors (Miyamoto et al., 2007; Tothova et al., 2007).

These examples, among others, illustrate the fact that cell cycle regulation differs depending on the differentiation state and lineage commitment of hematopoietic cells. Quiescence being an important property for HSCs but not for progenitors, this may not be so surprising, nevertheless these studies highlight specific regulations of the cell cycle in HSCs.

1.2.4 Potential applications of our knowledge on HSC quiescence

Understanding how quiescence is regulated in HSCs is very important for the study of physiopathology in numerous diseases. Not surprisingly, several factors involved in the regulation of quiescence and of the cell cycle are found associated with leukemias. For example, chromosomal

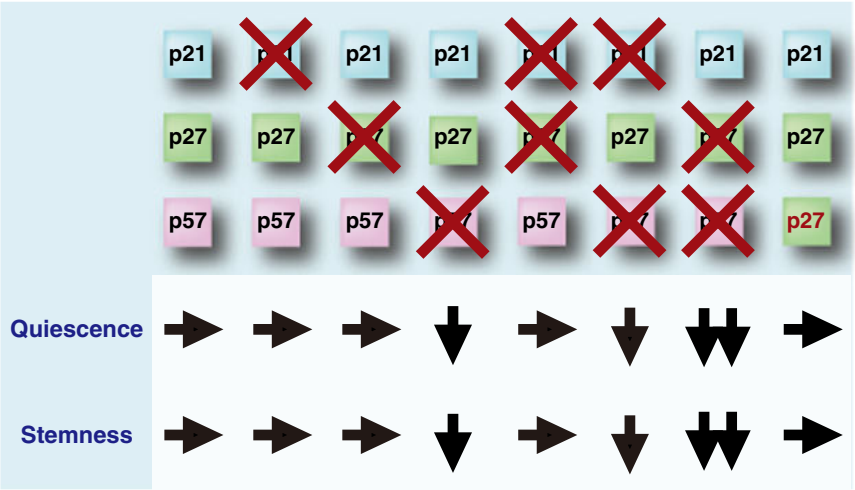

Figure 21. Functional relations among Cip/Kip CKIs in HSCs

Deficiency of p57 in HSCs promotes cell cycle entry and loss of stemness, whereas deficiency of p21 or p27 (or both) does not affect the cell cycle or stemness. Although further ablation of p21 in p57-null HSCs results in defects in colony-forming ability, double-mutant cells do not differ substantially in terms of quiescence and stemness from those lacking p57 alone. In contrast, additional deficiency of p27 in p57-deficient HSCs leads to further defects in stem cell function, and knockin of the p27 gene at the p57 locus corrects the abnormalities of p57-deficient HSCs.

Adapted from Matsumoto et al., 2013

translocations resulting in the fusion of members of the *FoxO* family have been reported in acute myeloid leukemias (Tothova et al., 2007). Furthermore, the maintenance of HSC quiescence involves multiple tumor suppressor genes such as *Pten*, *Fbxw7*, or members of the *Rb* family. Understanding the mechanisms underlying the regulation of HSC quiescence would also be useful for the HSCs *in vitro* for therapeutic purposes. However, to date, our knowledge from these mechanisms mostly comes from studies performed in the mouse and has not yet been validated in human. Finally, while the relationships between cell cycle regulation and HSC quiescence and self-renewal has been elucidated in part, a lot of work still remains to be done to fully understand the regulatory networks involved and how multiple signaling pathways cooperate to regulate precisely the functions of HSCs.

1.3 Quiescence, a safeguard against various stresses?

Why are hematopoietic stem cells quiescent? It has long been proposed that quiescence could be a protective property of HSCs against various stresses, protecting them throughout the lifespan of the organism. Indeed, quiescence prevents the exposition to DNA replication-induced stress. However, we will see that this property is controversial since it does not allow a proper, accurate response to DNA damages in HSCs (see *II.2*). In the case of HSCs, quiescence is also associated with reduced oxidative stress, which is important for the maintenance of HSC properties (see *II.3.3.2*). Finally, quiescent cells are more resistant to cytotoxic factors such as UV or ionizing radiations or chemical compounds, the consequences of which affect more particularly cells in the S or M phases of the cell cycle (Suda et al., 2011). Thus, quiescence appears as a safeguard of HSC maintenance and genetic integrity.

2. DNA damage management in HSCs

By definition, stem cells must be able to persist throughout the life of the organism in order to ensure the long-term maintenance of the tissue. This makes them particularly susceptible to the accumulation of DNA damages through time, which can result from intrinsic, physiological alterations due to spontaneous reactions in the nucleus, oxidative damage by metabolic byproducts or replication-associated defects, or from extrinsic factors such as UV and ionizing radiations or chemical agents. Because they can be transmitted and propagated in daughter cells, DNA damages have more severe consequences than damages to replaceable cellular macromolecules. The accumulation of DNA damage plays an important role in the development of malignancies, especially when it occurs in stem cells. Hence, stem cells are thought to be responsible for the maintenance of genomic integrity of tissues. Because the hematopoietic system undergoes tremendous amplification from HSCs to differentiated progeny, unrepaired genetic lesions in HSCs can have dramatic consequences and lead to hematological defects and malignancies.

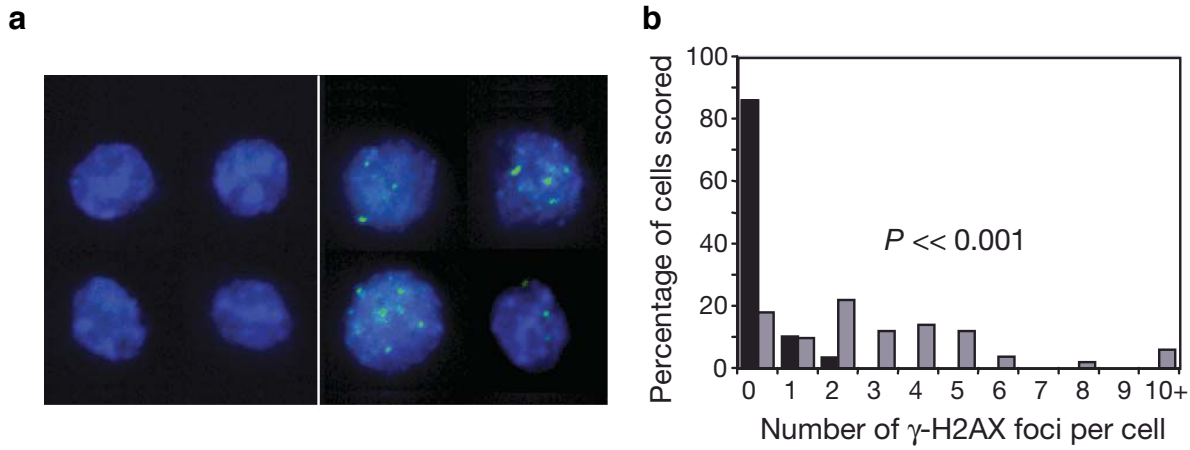

Figure 22. Accumulation of DNA damage in aging HSCs

a. HSCs of 10 weeks old mice (left) or 122 weeks old mice (right) were stained for γ-H2AX (green). **b.** Distribution of the number of γ-H2AX foci per HSC, in 10 weeks old mice (black) and 122 weeks old mice (grey).

Adapted from Rossi et al., 2007

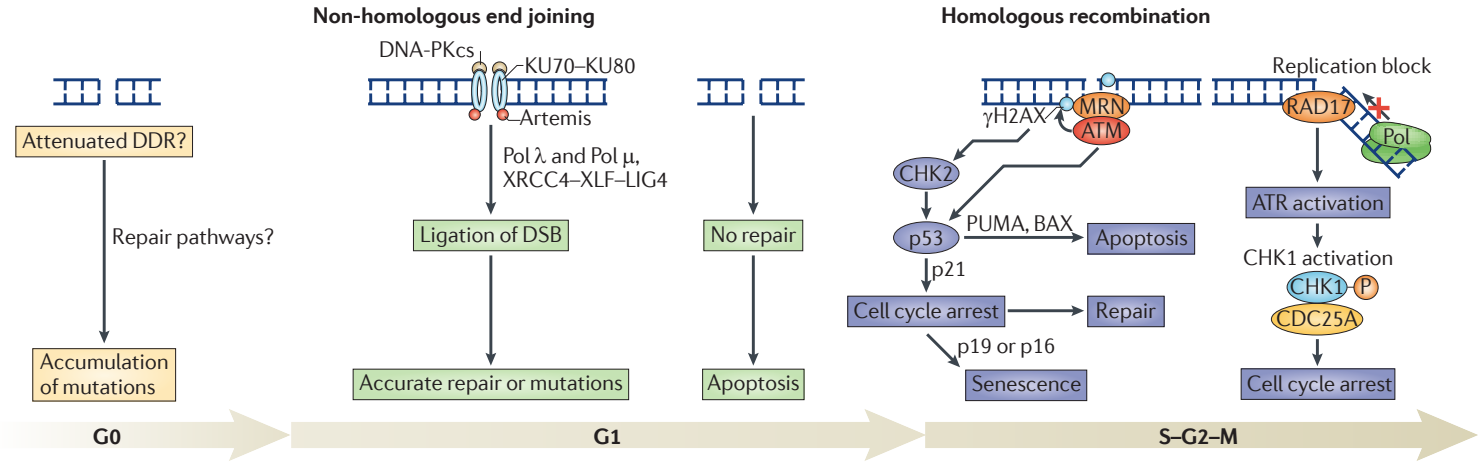

Figure 23. DNA damage repair pathways during the cell cycle

DNA double-strand breaks (DSBs) can be repaired by two main pathways. During the G_1, the non-homologous end joining (NHEJ) pathway is the predominant DSB repair pathway, because it does not use homologous DNA matrix. Briefly, the Ku70/Ku80 heterodimer binds the DSB site and forms a complex with protein kinases DNA-PKcs. This complex interacts with several enzymes, including DNA Ligase IV which performs DNA ligation. However, NHEJ is prone to the generation of new mutations (deletions, insertions, mismatches and translocations). During $S/G_2/M$, cells preferentially use homologous recombination for DSB repair. DSBs are recognized by the MRE11-RAD50-NBS1 complex, which recruits ATM. ATM then phosphorylates histone variant H2AX (which thus becomes γ-H2AX) to mark the break site. ATM also induces activation of CH2K and p53, leading to cell cycle arrest. Block during DNA replication because activate the ATR kinase, resulting in activation of CHK1 and consecutive cell cycle arrest. Many adult stem cells reside in G_0 phase of the cell cycle, and details regarding DNA repair during this phase are poorly understood.

Adapted from Mandal et al., 2011

2.1 Natural accumulation of DNA damage HSCs with aging

2.1.1 DNA repair mechanisms are essential for long-term maintenance of HSCs

2.1.1.1 Accumulation of DNA double-strand breaks with aging

Double-strand breaks (DSB) accumulate with age in mouse and human, in all tissues. In mouse, this can be visualized by the accumulation in multiple tissues of the phosphorylated form of histone H2AX (γ-H2AX) in foci that colocalize with DNA repair proteins such as RAD50 (Sedelnikova et al., 2004). Similarly, γ-H2AX foci accumulation occurs in HSCs of aging mice (Figure 22)(Rossi et al., 2007). Interestingly, γ-H2AX foci observed in HSCs are not detected in downstream progenitors, suggesting that these cells were able to repair DSBs or that severely damaged cells have been eliminated. In human, accumulation of γ-H2AX foci and DSBs has also been observed in HSPCs of old *vs* young donors (Rübe et al., 2011). Altogether, this indicates that the accumulation of DNA damage could play a major role in aging.

2.1.1.2 Mouse models with deficient DNA repair mechanisms

Cells use two major mechanisms for DSB repair: homologous recombination (HR, also called homology-directed repair) and non-homologous end-joining (NHEJ) (Figure 23, for review see (Sancar et al., 2004)). To test the requirement of these mechanisms in stem cells and investigate the effects of accumulated DNA damage on the long-term maintenance of HSCs, several teams have analyzed the phenotypes of mouse deficient for some DNA repair mechanisms.

HR, as suggests its name, relies on sequence homology, using an undamaged DNA template to repair the breaks and thus restoring the original DNA sequence. Hence, HR occurs only during the S/G_2/M phases of the cell cycle. Breaks are recognized by the MRE11-RAD50-NBS1 complex, which then recruits the ATM (Ataxia-Telangiectasia Mutated) and/or ATR (Ataxia-Telangiectasia and Rad3-related) kinases, leading to the phosphorylation and activation of a cascade of repair enzymes. Activation of ATM also leads to the stabilization of p53 and cell cycle arrest. Deletion of *Atm* in mouse leads to severe functional defects in HSCs (Ito et al., 2004; 2007), and functional RAD50 is required in an ATM-dependent manner for the maintenance of HSCs (Bender et al., 2002; Morales et al., 2005). Interestingly, the role of ATM in the regulation of oxidative stress is essential for proper repair of DSBs (see *II.2.2.1*).

NHEJ, in contrast to HR, does not use a homolog DNA template to repair DSBs, and can thus be used during the G_1 phase of the cell cycle or in quiescent cells. This pathway involves the recognition of DSBs by the Ku70/Ku80 heterodimer, which bind to DSB sites and form a complex together with the DNA-dependent protein kinase DNA-PK_{cs}. This complex interacts with DNA ligase IV, which ensures the ligation of the loose ends of DNA. NHEJ thus enable rapid repair of DSBs. Mouse models with NHEJ defects have been studied, such as *Ku80*-deficient mice and mice with the hypomorphic allele of DNA ligase IV, $Lig4^{Y288C}$(Nijnik et al., 2007; Rossi et al., 2007). While in both cases this only lead to partial depletion of HSCs with age, HSC functional capacities were severely affected under stress situations such as competitive transplantation.

Since most HSCs –and adult stem cells– are in a quiescent state, the only available DNA repair mechanism is NHEJ, which more prone to erroneous repair such as translocations and may

participate to the accumulation of DNA damage in these cells. However, the team of D.Rossi recently showed that accumulated DNA damages in quiescent HSCs can be repaired upon reentry into the cell cycle, thus allowing at least partial recovery of genome integrity although it may not be sufficient (Beerman et al., 2014). Finally, Flach *et al.* investigated whether a decline in the ability to repair DNA could explain the accumulation of DNA damage in aging HSCs (Flach et al., 2014). They compared the DNA repair ability of cultured HSCs from old (22-30 months old) *vs* young (6-12 weeks old) mice HSCs: although old HSCs did exhibit a ~8 h delay compared to young HSCs, both populations showed similarly capable of clearing γ-H2AX foci upon irradiation and expressed similar levels of HR and NHEJ genes. If old HSCs have the same ability to deal with DNA damage as young HSCs, this raises the question of what is responsible for the accumulation of γ-H2AX foci observed in aging HSCs?

2.1.1.3 Fanconi anemia

Fanconi anemia is the most frequent cause of inherited BM failure syndromes in human, with a variety of symptoms such as severe medullar aplasia and developmental or cutaneous abnormalities and a predisposition to leukemia (for review, see (Soulier, 2011)). To date, at least 15 *FANC* genes have been identified, involved in a signaling pathway termed "FA" in reference to the disease. This pathway is involved in the management of lesions preventing DNA replication, and thus plays an essential role in the maintenance of genome integrity.

To study the FA pathway, mouse models of Fanconi anemia have been generated such as the *Fancd2*$^{-/-}$ and *Fancg*$^{-/-}$ mouse strains. These mice exhibit progressive depletion of the HSC compartment, possibly resulting from quiescence defects. *Fancd2*$^{-/-}$ HSCs display reduced self-renewal *in vitro* and *in vivo*, and *Fancg*$^{-/-}$ HSCs display impaired functionality and homing defects upon transplantation (Barroca et al., 2012; Parmar et al., 2010; Zhang et al., 2010). Furthermore, the Usp1 enzyme, which plays an important role in the regulation of the FA pathway through de-ubiquitination of Fancd2, is also required for HSC maintenance (Parmar et al., 2010). These studies show how deregulation of the FA pathway could be the underlying cause of the hematopoietic defects observed in patients with Fanconi anemia.

2.1.2 Maintenance of telomeres in stem cells: the telomerase complex

2.1.2.1 Maintaining telomeres to preserve genome integrity

Chromosomes are linear DNA molecules and, therefore, have extremities that are particularly vulnerable to deterioration. During DNA replication in the S phase, these extremities cannot be fully replicated due to intrinsic properties of the DNA replication process that I will not discuss here. To preserve the integrity of genes located near chromosome ends, these extremities are protected by repeated sequences called telomeres that form loop structures protecting them from degradation. Nevertheless, these telomeres are still improperly replicated and, therefore, are shortened with every cell division until they eventually cannot preserve genome integrity anymore, at which point the cell undergoes cells death by apoptosis or senescence. It is widely accepted that stem cells actively protect their telomeres and thus their genome integrity thanks to the ribonucleoproteinic telomerase complex. Telomerase, a reverse transcriptase encoded by the *Tert*

gene, ensures the reverse-transcription of the repeated telomeric sequences form an RNA template encoded by *Terc*. Indeed, telomerase is specifically active in stem cell populations of different organs and tissues, including HSCs, resulting in longer telomeres in these cells than in differentiated cells (Flores et al., 2008; Morrison et al., 1996; Shay and Wright, 2010).

Telomere shortening is often viewed as an intrinsic biological clock, limiting the number of divisions of a cell. Although quiescent HSCs divide rarely, telomere shortening is still observed in HSCs in human with age, or in mouse through serial transplant (Allsopp et al., 2003; Vaziri et al., 1994). On another note, it is interesting to see that mouse telomeres are eight times longer than human telomeres, suggesting that telomerase activity could affect the two species differently and raising questions about the role and efficiency of telomerase in HSCs in human and mouse.

2.1.2.2 Mouse models to study the role of telomerase in HSCs

In mouse, telomere shortening is not associated with a reduction of telomerase activity, the latter being maintained serially transplanted HSCs (Allsopp et al., 2003). Thus, telomere shortening despite telomerase activity could result from the important solicitation of HSCs, or from other cellular mechanisms that impede telomere maintenance.

To understand the role of telomerase activity in the mouse, *Tert*$^{-/-}$ and *Terc*$^{-/-}$ models have been generated. Surprisingly, such mice do not exhibit visible defects, suggesting that telomere shortening is not essential for the survival of mice in homeostatic conditions (Allsopp et al., 2003; Rudolph et al., 1999). However, inbreeding of either strain for over several generations results in pleiotropic defects in homeostasis and impaired responses to various stresses (Rudolph et al., 1999). In the hematopoietic system, this translates into self-renewal defects of HSCs in the third generation of *Terc*$^{-/-}$ mice, which is recapitulated in serial transplants of *Terc*$^{-/-}$ and *Tert*$^{-/-}$ HSCs (Allsopp et al., 2003; Rossi et al., 2007). Thus, the importance of telomerase activity for mouse HSCs seems to be visible only when they are highly solicited. Similarly, mice homozygous for a hypomorphic allele of the *Acd* gene –which is involved in the protection of telomeres and recruitment of telomerase– display pleiotropic abnormalities with no apparent hematopoietic defects, but their HSCs exhibit profound functional defects upon transplantation (Jones et al., 2013). Moreover, complete conditional inactivation of *Acd* induces acute depletion of both fetal and adult HSPC compartments, leading to rapid hematopoietic failure before telomere shortening can be detected.

Finally, the team of M.Blasco has generated mice with three-fold increased telomerase activity by treating adult (one year of age) and old (two years of age) mice with adenovirus vectors expressing *Tert*. The “super-mice” thus obtained exhibited increased longevity and better health and fitness (Bernardes de Jesus et al., 2012). Interestingly, the same team showed that embryonic stem (ES) cells in culture have abnormally longer telomeres than those in embryonic tissues (Varela et al., 2011). They used such ES cells with “hyper-long” telomeres to generate chimeric mice containing cells with both normal and hyper-long telomeres (Varela et al., 2016). Thus, they showed that, with age, highly renewing compartments such as blood were enriched in cells with hyper-long telomeres, and that chimeric mice exhibited increased rates of wound healing in the skin. Altogether, their work suggests that increased telomerase activity has beneficial effects on aging in mouse.

2.1.2.3 Human diseases due to defective telomerase activity

Several human pathologies are associated with defects in the telomere maintenance machinery, further stressing the important role of telomerase activity. A well-known example of such pathologies is *dyskeratosis congenita* (DC), an inherited disease characterized by skin defects, abnormal development and hematopoietic defects that can lead to fatal hematopoietic failure (for review, see (Paiva and Calado, 2013)). Different inheritance patterns have been described in DC (X-linked, autosomal dominant and autosomal recessive), and mutations in several genes involved in the telomerase complex or the shelterin complex (responsible for the protection of telomeres) have been identified, such as *hTERT*, *hTERC*, *DKC1* (aka *Dyskerin*) or *NOP10* (Paiva and Calado, 2013). The NOP10 protein could be involved in the assembly and/or stabilization of the telomerase complex, and Dyskerin is part of this complex. Deficient telomerase activity seems to be responsible for the phenotypes observed in DC, and indeed a correlation between the length of telomeres and the severity of the clinical phenotype has been observed (Alter et al., 2007). Interestingly, Dyskerin also participates to post-transcriptional modifications of ribosomal RNA, and DC associated to mutations in *DKC1* is also classified among ribosomopathies, which I will discuss in the second part of this introduction (see *Part 2*).

Finally, the telomerase complex also plays a key role in tumorigenesis. Indeed, defects in the maintenance of telomeres are a cause of genomic instability, which could contribute to the initiation of malignancies. Conversely, reacquisition of telomerase activity in cancerous cells is required for their maintenance. Altogether, this indicates that the telomerase complex can act as both tumor suppressor and oncogene.

2.1.3 Conclusions

Altogether, these studies underline how the roles of DNA repair mechanisms and the telomerase complex in maintaining genome integrity are essential for the maintenance of stem cells. Strikingly, genetic defects causing dysfunction of either of these mechanisms lead to severe hematopoietic defects, and are associated with increased risks of cancer. Interestingly, even in non-pathological situations these mechanisms do not seem to suffice to fully ensure maintenance of stem cells' genome integrity, leading to the accumulation of DNA damage and thus to increased risks of cancer with age.

2.2 Specific DNA damage responses of HSCs under situations of acute stress

We have just seen how HSCs are particularly susceptible to accumulate DNA damage with age or in case of dysfunctional DNA repair mechanisms or telomerase activity. Recently, studies lead in different tissues have investigated the capacity of adult stem cells to respond to genotoxic stresses. Following irradiation, DNA lesions are observed in both stem and differentiated cells, indicating that stem cells are not protected against such damages, neither by intrinsic properties nor by their environment (Inomata et al., 2009; Mohrin et al., 2010; Sotiropoulou et al., 2010). Nonetheless, we will see here that stem cells use specific defense mechanisms in responses to genotoxic stresses.

2.2.1 To be or not to be? Regulation of stem cell survival upon genotoxic stress

The team of E.Passegué has investigated how HSCs and downstream progenitors respond to low doses of ionizing radiation (2 Gy, IR)(Mohrin et al., 2010). Surprisingly, they showed that HSCs are more resistant to apoptosis than myeloid progenitors. However, in the absence of ATM, both populations are equally sensitive to apoptosis, suggesting that ATM is involved in this differential response. Indeed, they showed that when exposed to ionizing radiation, HSCs elicit a DNA damage response dependent of ATM leading to p53 activation, which induces cell cycle arrest, robust expression of the anti-apoptotic gene *Bcl-2*, and DNA repair by the NHEJ pathway. Interestingly, they also showed even upon *in vivo* or *in vitro* activation, HSCs were still more resistant to apoptosis than progenitors, suggesting that intrinsic mechanisms other than quiescence may participate to this radio-protective property of HSCs.

To investigate the response to genotoxic stress in human hematopoietic cells, Milyavsky *et al.* exposed HSPCs from human cord blood to IR (Milyavsky et al., 2010). In this case, HSCs displayed more apoptosis than progenitors, and less efficient DNA repair. This increased sensitivity was due to robust activation of the *p53* pathway in HSCs and strong expression of *ASPP1*, a pro-apoptotic gene (ASPP: apoptosis-stimulating protein of p53). Thus, in contrast to the observations made in mouse, human HSCs are more susceptible to apoptosis and DNA damage repair is delayed. This discrepancy could be explained by differences in the radiation doses to which cells were exposed in both studies, or by the fact that while mouse HSCs were collected from adult BM, human HSCs were obtained from cord blood, so HSCs of different ages and from distinct environments. Interestingly, another recent study in mice exposed to low doses or IR showed that *Aspp1* plays an important role for the induction of apoptosis in most severely damaged HSCs, *Aspp1*$^{-/-}$ HSCs being even more resistant to IR-induced apoptosis (Yamashita et al., 2015).

It is interesting to see that adult stem cells in other tissues also display increased resistance to apoptosis upon by ionizing radiation. Notably, Sotiropoulou *et al.* showed that hair follicle stem cells are resistant to ionizing radiation-induced apoptosis thanks to robust expression of *Bcl-2* and only transient activation of p53, whereas other cells of this tissue exhibit more sustained p53 activation and cell death (Sotiropoulou et al., 2010). Of note, hair follicle stem cells are mostly quiescent and thus preferably use NHEJ for DNA repair, similarly to HSCs.

2.2.2 To be, but different: differentiation in response to severe DNA damage

Upon DNA damages, another response elicited by stem cells is differentiation. This was first evidenced in melanocyte stem cells (MSCs): exposure to 5 Gy IR induced premature differentiation of MSCs in the niche, resulting in decolorization of the hair (Inomata et al., 2009). In the hematopoietic system, first evidence of premature HSC differentiation following DNA damage was brought by the team of K.L.Rudolph (Wang et al., 2012). In their study, the authors showed that exposition to IR or shortening of the telomeres lead to the activation of an HSC-specific differentiation checkpoint mediated by the transcription factor Batf. This resulted in lymphoid-biased differentiation of HSCs and loss of their long-term repopulating potential. Another, more recent study by Wingert *et al.* showed that upregulation of Gadd45a (growth arrest and DNA

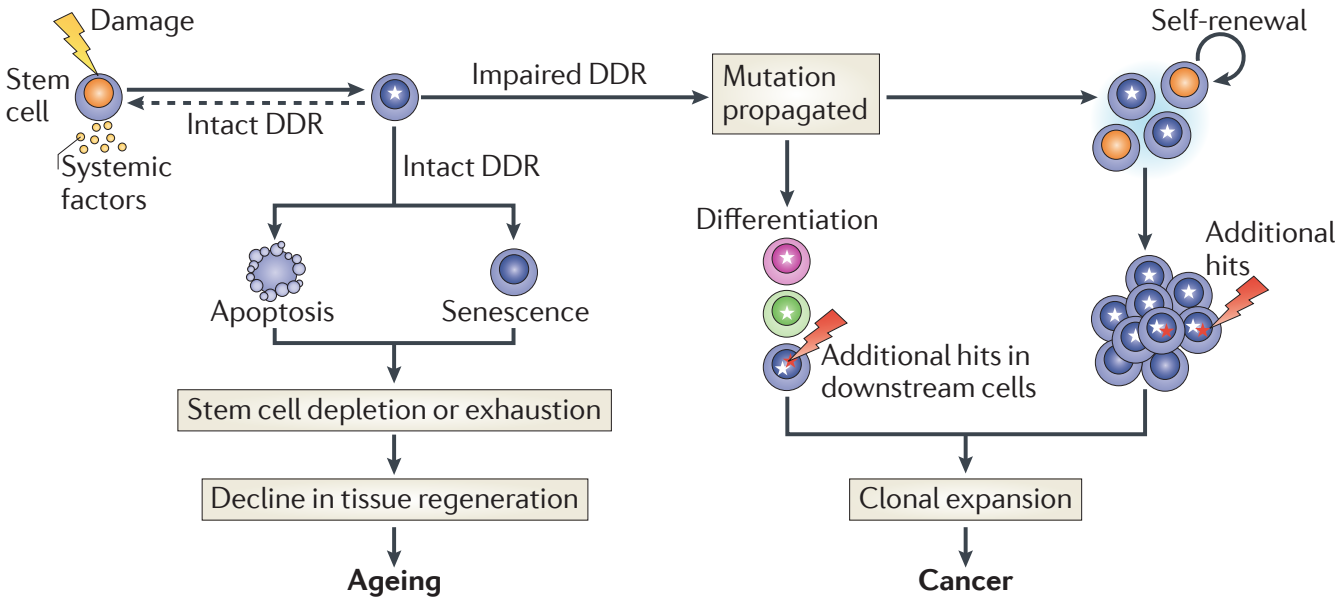

Figure 24. Impact of DNA damage on stem cells

DNA damage in stem cell compartments is followed by the induction of a robust DNA damage response (DDR), which when properly executed leads to DNA repair or elimination of damaged stem cells by apoptosis or senescence. If elimination and senescence prevail over a lifetime, this can lead to stem cell exhaustion and aging. If DNA damage escapes the DDR or is not repaired properly, the stem cell pool may accumulate mutations, which can be propagated and amplified horizontally within the stem cell compartment by self-renewal, and vertically to downstream progeny by differentiation. Mutations conferring selective advantages in stem or progenitor cells can be further amplified through clonal expansion, increasing the pool of cells through which additional mutagenic events can arise, eventually leading to tumorigenesis. (Damaged DNA is represented by a star in the nucleus).

Adapted from O'Sullivan et al., 2010

damage-inducible 45 α) protein in response to DNA damage also leads to terminal, unbiased differentiation of HSCs, without inhibiting cell cycle or survival (Wingert et al., 2016).

2.3 DNA damage responses and tissue physiology

Quiescent stem cells deal with DSBs by using the NHEJ DNA repair pathway, which can be viewed as a double-sided strategy: although it allows a rapid response and survival of HSCs, NHEJ is error-prone and can contribute to genomic instability. Hence, it seems that survival of HSCs could be at the expense of genome integrity.

The different studies I have presented above have contributed to considerable advances in the understanding of the responses elicited by stem cells upon exposure to IR or other genotoxic stresses. Finally, it seems that stem cells can elicit different responses –survival, apoptosis, senescence or differentiation– depending on their tissue of origin, the severity of the damages they endure or the dose of genotoxic stress they are exposed to (Figure 24). These responses to DNA damage, and notably the threshold of stem cells' susceptibility to apoptosis, participate to the physiology of their tissue. Thus, high susceptibility to apoptosis can prevent the accumulation of mutations but strongly impedes tissue regeneration. Conversely, high resistance to apoptosis allows maintenance of the tissue but increases the risk of mutagenesis and can thus lead to malignancies. Finally, the induction of differentiation or senescence allows the short-term maintenance of the architecture and functions of the tissue, while preventing self-renewal of the damaged cells. In the end, the choice of either one of these responses must guarantee an appropriate balance between aging and cancer, and between maintenance of genome integrity at all costs and maintenance of stem cells.

3. HSCs and oxygen: metabolic adaptation to the hypoxic environment and oxidative stress management

As we will see in this part, HSCs are particularly sensitive to oxidative stress. To shield them from oxidative stress, the hematopoietic system has put into place two strategies. First, HSCs are located in a hypoxic environment that favors a low metabolic activity in order to limit the generation of ROS. Then, HSCs are equipped with specific antioxidant responses that protect them efficiently from ROS-induced toxicity.

3.1 ROS and oxidative stress

Oxygen has granted eukaryotic cells with an efficient metabolism thanks to mitochondrial respiration. However, in the presence of radiation, metal ions or some enzymes, oxygen can undergo chains reactions that participate in the production of reactive oxygen species (ROS). The mitochondrial respiratory chain is particularly inclined to the generation of ROS.

The effects of these ROS are somehow double-sided. On one hand, ROS have physiological roles for growth, development and inflammation (such roles in HSCs will be addressed in *II-3.4*). On the other hand, due to their reactivity ROS can be toxic for the cell and generate oxidative lesions at the level of membranes, proteins or DNA (Figure 25).

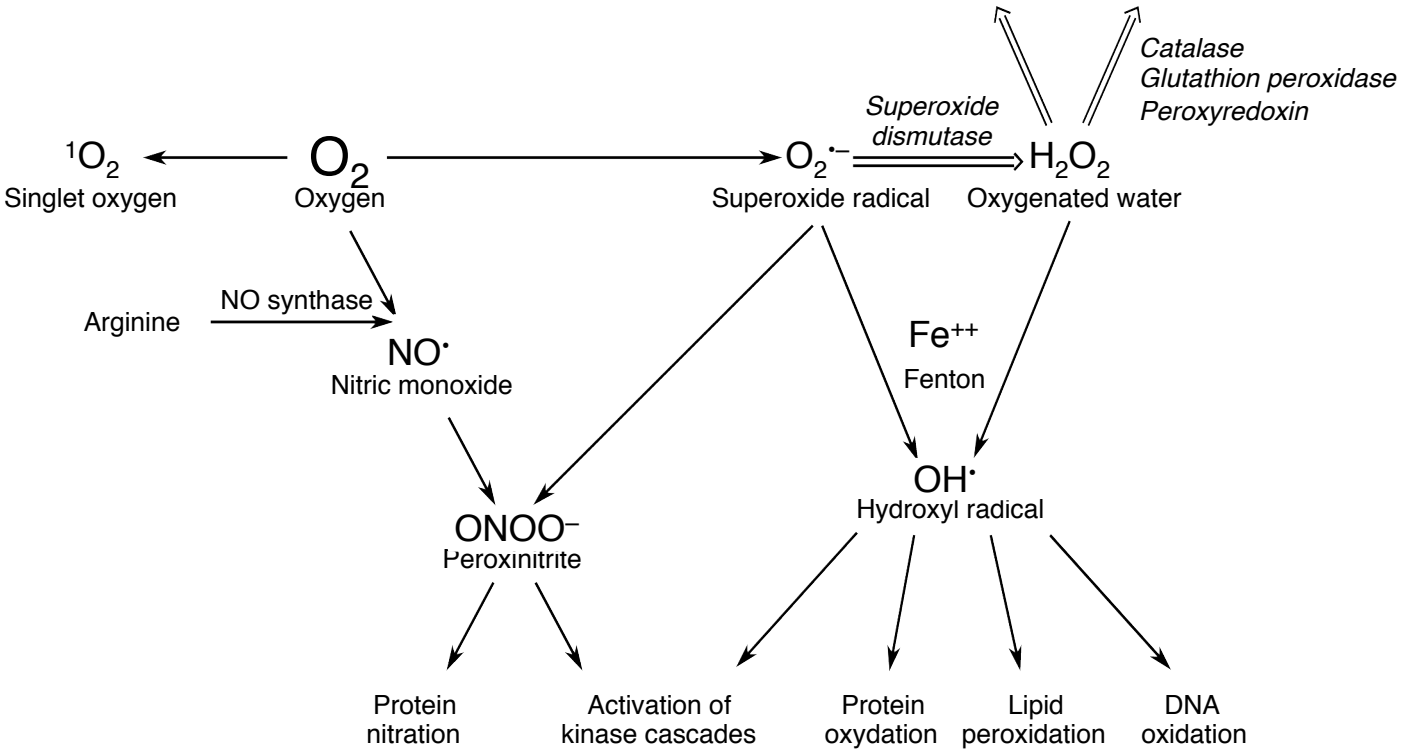

Figure 25. Reactive oxygen species

Oxygen is able to capture a electron to give superoxide $O_2^{\bullet-}$. This radical is the substrate of superoxide dismutase enzymes, which can transform it into oxygenated water H_2O_2. In the presence of metal ions, H_2O_2 can undergo a Fenton reaction and form the hydroxyl radical $OH^{\bullet}$, which is highly reactive. H_2O_2 can also be detoxified by anti-oxidant enzymes (catalase, glutathion peroxidase, peroxidoxin). Under the influence of UV radiation, oxygen can be transformed into singlet oxygen $^1O_2$. Oxygen and nitrogen metabolisms are intercrossed: the superoxide radical can interact with nitric monoxide to form peroxinitrie $ONOO^-$, a toxic compound. $ONOO^-$ and hydroxyl radical can induce direct damages on cellular components (bottom). Double arrows represent detoxifying steps involving the indicated enzymes.

Adapted from Barouki et al., 2006; Naka et al., 2008

Cells have natural antioxidant defense mechanisms to deal with ROS. Detoxifying enzymes such as superoxide dismutases, catalase or gluthation peroxidase catalyze the degradation of some ROS (Figure 25, double arrows). Some proteins, such as ferritin, can also participate in the sequestration or transport of metal ions. Finally, small exogenous molecules have antioxidant properties, such as vitamins E and C or carotenoids supplied by nutrition.

Oxidizing stress occurs when the balance between ROS generation and antioxidant defenses is disrupted in the cell or in intracellular compartment. In case of an accumulation of ROS, the cell will first use these antioxidant defense mechanisms for detoxification. However, accumulation of too much ROS will eventually induce damages, thus triggering specific cellular responses that can lead to cell death by apoptosis or senescence, and participating to aging or pathological situations.

3.2 A hypoxic environment for HSCs

Keeping HSCs in an environment with low oxygen levels is considered as a way of protecting HSCs from ROS. As we will see here, in addition to protecting HSCs, this hypoxic environment is also essential for the regulation and maintenance of HSCs.

3.2.1 HSCs in the hypoxic niche

Oxygen represents 21% of the air we breathe. These levels of oxygen progressively decrease as it enters the lungs, travels through circulating blood throughout the body, and finally reaches organs and tissues. Thus, although the physiological concentration of oxygen –or normoxia– is often described as 21% O_2, it is estimated to a range of 2-9% O_2 for most adult cells *in vivo* (Simon and Keith, 2008). However, mathematical models have estimated that oxygen levels in the endosteal niche of the BM are below 1% O_2, with a gradient from the endosteum to more vascularized regions of the BM (Chow et al., 2001). Since they are located in the endosteal niche, HSCs are hypoxic and can be stained using hypoxia markers such as pimonidazole (Kubota et al., 2008). Similarly, other stem cell populations such as neural and mesenchymal stem cells have been located in hypoxic niches –the subventricular zone and adipose tissues, respectively– suggesting that hypoxia could be a common property to several stem cell populations (Mohyeldin et al., 2010).

3.2.2 Adapting HSC metabolism to the hypoxic environment: the central role of Hif-1α

In response to hypoxia, HSCs activate similar signaling pathways as many other cell types. Notably, a key regulator of this response is the transcription factor Hif-1 (hypoxia-inducible factor 1). Hif-1 is a heterodimer made of a constitutively expressed Hif-1β subunit and a Hif-1α subunit that is highly regulated, mainly by oxygen levels (for review, see (Greer et al., 2012)). Under normoxia, the oxygen-dependent degradation domain of Hif-1α is hydroxylated by prolyl-hydroxylase domain containing proteins (PHDs); hydroxylated Hif-1α is then recognized by the E3-ubiquitin ligase VHL, leading to degradation of Hif-1α by the proteasome. PHDs require oxygen for their catalytic activity: under hypoxia, PHDs are inactive and the Hif-1 heterodimer is stabilized. Stabilized Hif-1 binds to "hypoxia-response elements" sequences in the promoter of its target genes and thus regulates the expression of a large subset of genes involved in various cellular processes such as cell cycle, survival, differentiation, autophagy, proteolysis and metabolism (Figure 26).

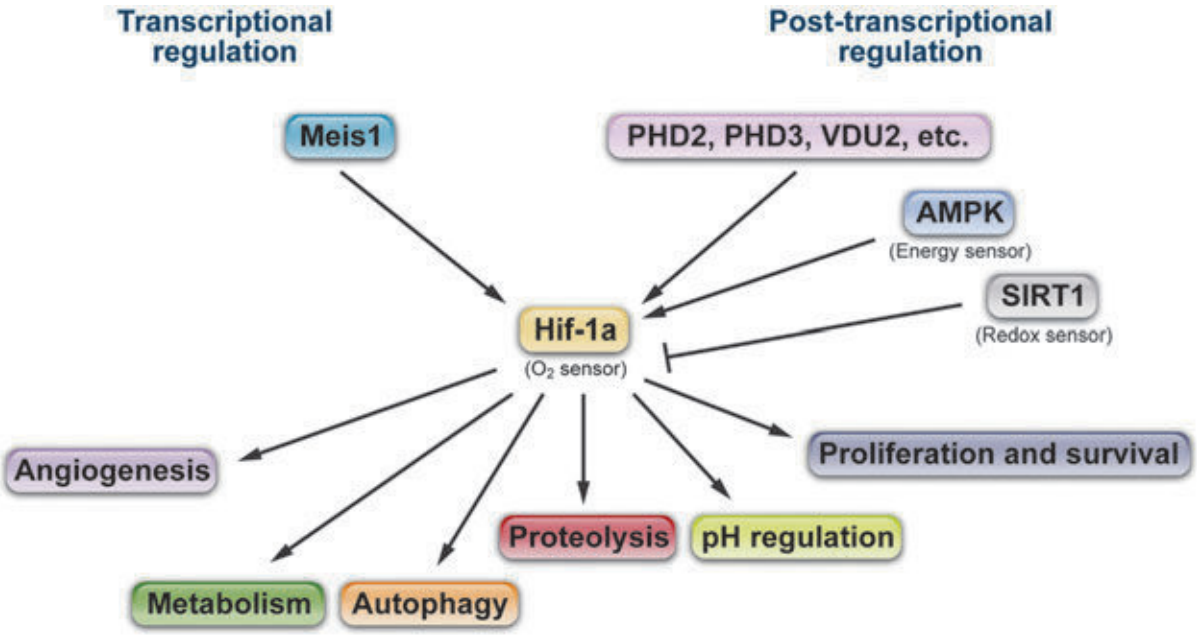

Figure 26. Upstream regulation and down-stream targets of Hif-1α

Regulation of Hif-1α through protein stabilization (by PHD2, PHD3, VDU2, AMPK…) or transcriptional activation (by Meis1) enables cells to survive under hypoxia and to minimize oxidative damage resulting from oxidative phosphorylation. Hif-1α regulates the expression of hundreds of genes with roles in angiogenesis, metabolism, proliferation and survival, autophagy, proteolysis and pH regulation.

Adapted from Zhang and Sadek, 2014

As a consequence of their hypoxic environment, HSCs have adapted their metabolism. Indeed, the team of H.Sadek has shown that HSCs have strongly reduced mitochondrial activity, using preferably anaerobic glycolysis rather than oxidative phosphorylation for the production of ATP (Simsek et al., 2010). This change in metabolism is highly regulated, and Hif-1α plays a central role (for review, see(Zhang and Sadek, 2014)). Of note, the team of H.Sadek also showed that the transcription factor *Meis1* is required for optimal activation of *Hif-1α* and regulates the metabolic phenotype and antioxidant defenses of HSCs (Kocabas et al., 2012; Simsek et al., 2010). Stabilized Hif-1, among its numerous target genes, notably promotes the transcription of glucose transporters, glycolytic enzymes and glycolysis inducing factors such as Cripto. Cripto is secreted by HSCs –and the endosteal niche– and binds the GRP78 receptor, thus promoting glycolysis and reducing mitochondrial activity (Miharada et al., 2011). Strikingly, although glycolysis is anaerobic and generates fewer ROS, it highly inefficient: for 1 mol of glucose, it produces 2 mol of ATP, where oxidative phosphorylation would produce 36 mol (Semenza, 2007). This may participate to the maintenance of a low metabolic activity in HSCs and their quiescence. Interestingly, a recent study showed that in the fetal liver, highly proliferative HSCs are using oxidizing phosphorylation, suggesting that HSCs switch from mitochondrial respiration to anaerobic glycolysis as they colonize the bone marrow, and further supporting that the choice of the metabolic pathway used by HSCs is linked to their cell cycle activity (Manesia et al., 2015).

3.2.3 Regulation of HSCs by hypoxia

Analyses of HSCs in cultures have shown that hypoxia contributes importantly to the maintenance of their functions: self-renewal and quiescence of human HSCs, as well as the SP property of murine HSCs, can be maintained in culture under hypoxic conditions, and HSCs cultured in hypoxic conditions have better repopulating potential (Hammoud et al., 2012; Hermitte et al., 2006; Krishnamurthy et al., 2004; Roy et al., 2012; Wang et al., 2016). *In vivo*, cells located in the most hypoxic regions of the BM display better self-renewal, confirming the observations made in *in vitro* analyses (Parmar et al., 2007).

The importance of *Hif*-1α in the maintenance of HSCs in hypoxic conditions is supported by several studies. *Ex vivo* cultures of human cord blood-derived HSCs under hypoxic conditions leads to the upregulation of *HIF-1α* (Roy et al., 2012). *In vivo*, mouse HSCs express high levels of *Hif-1α*, and its conditional deletion leads to severe functional defects in HSCs: *Hif-1α*$^{-/-}$ HSCs exit quiescence, lose their repopulation capacity and are more susceptible to myelotoxic stress or aging (Simsek et al., 2010; Takubo et al., 2010). Conversely, overstabilization of Hif-1α by biallelic loss of VHL induces cell cycle quiescence in HSCs and their progenitors but results in impairmed transplantation capacity, suggesting that fine regulation of Hif-1α activation is required (Takubo et al., 2010). Finally, a recent comparative cDNA microarray analysis between human ES cells, HSCs, and MSCs found that Hif-1a was the only transcription factor that these cells have in common; this further highlights that hypoxia may be a common property to different stem cell populations (Kim et al., 2006).

The regulation of *Hif-1α* and its role in response to hypoxia is now well documented, yet only little is known about the details of the signaling downstream of *Hif-1α*, especially in specific cell

types. Hopefully, future studies will shed light on this, providing more insight on the intricate regulation of HSC functions.

3.3 Regulation of ROS (1): toxicity of ROS for HSC functions

3.3.1 Maintenance of low levels of ROS by efficient protection mechanisms in HSCs

HSCs are particularly susceptible to increases in the levels of ROS. Treatment with pro-oxidant agents such as BSO (L-Butathionine-sulfoximine) induces a strong increase of ROS levels in all hematopoietic cells, and particularly affects the functions of HSCs, stressing the importance of the regulation of ROS levels in HSCs (Ito et al., 2006).

ROS levels in HSCs in unperturbed conditions are very low: they are estimated to be 100 times lower than in myeloid progenitors (Tothova et al., 2007). This could be explained by the important metabolic activity of proliferating progenitors and their localization in more vascularized regions of the BM. Furthermore, since some differentiated cells can use ROS for various immune strategies, an increase in ROS levels as differentiation progresses would be understandable. To gain insight on the regulation of ROS in the hematopoietic system, Tothova *et al.* performed comparative transcriptomic analyses of HSCs and myeloid progenitors (Tothova et al., 2007). Thus, they highlighted the existence of specific transcriptional programs in these populations: HSCs activate antioxidant responses dependent on *FoxO* transcription factors, whereas progenitors exhibit *FoxO* independent processes. These *FoxO* transcription factors localize to the nucleus, where they are involved in the regulation of cell cycle, apoptosis, differentiation, metabolism, DNA repair and oxidative stress (see (Charitou and Burgering, 2013; Tothova and Gilliland, 2007) for reviews); upon phosphorylation by AKT, FoxOs are excluded from the nucleus and degraded. Indeed, accumulation of FoxO3a is observed in the nucleus of LSK $CD34^-$ cells, whereas it is found in the cytoplasm of LSK $CD34^+$ cells, supporting the differential regulation of *FoxO* transcription factors between HSCs and downstream progenitors. Furthermore, inactivation of *FoxO* genes leads to the downregulation of antioxidant enzymes in HSCs and elevation of ROS levels; conversely, overexpression of *FoxO3a* by retroviral transduction in immature hematopoietic cells upregulates such enzymes (Miyamoto et al., 2007; Paik et al., 2007; Tothova et al., 2007; Yalcin et al., 2008). Altogether, this suggests an important role for *FoxO* transcription factors in the antioxidant defenses of HSCs.

Finally, additional transcriptomic analyses have shown the upregulation of genes involved in antioxidant responses, in HSCs compared to downstream progenitors (Cabezas-Wallscheid et al., 2014). Such observations further suggest that HSCs have efficient antioxidant defense mechanisms to keep low ROS levels.

3.3.2 ROS and regulation of quiescence

As I discussed earlier, the quiescence state of HSCs is strongly associated to hypoxia. Indeed, we will see here that the maintenance of quiescence is tightly linked to the maintenance of low levels of ROS in HSCs, as illustrated by two major signaling pathways: ATM/BID and PI3K/AKT.

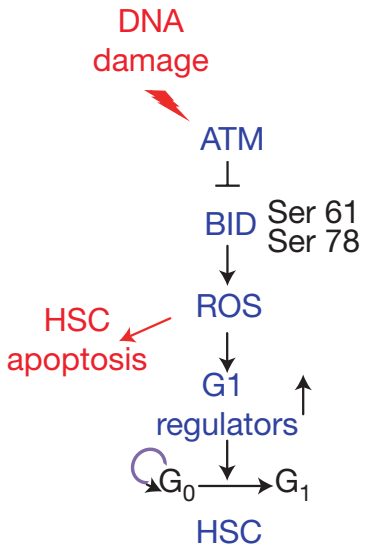

Figure 27. Role of the ATM-BID pathway in the maintenance of quiescence and survival in HSCs

In the bone marrow, the ATM–BID pathway plays a pivotal role in preserving the self-renewal and quiescence of HSCs by regulating oxidative stress, leading to downregulation of G1 cell-cycle regulators (blue pathway). In response to external DNA damage, the ATM–BID pathway has a role in regulating HSC apoptosis also by regulating oxidative stress (red pathway).

Adapted from Maryanovich et al., 2012

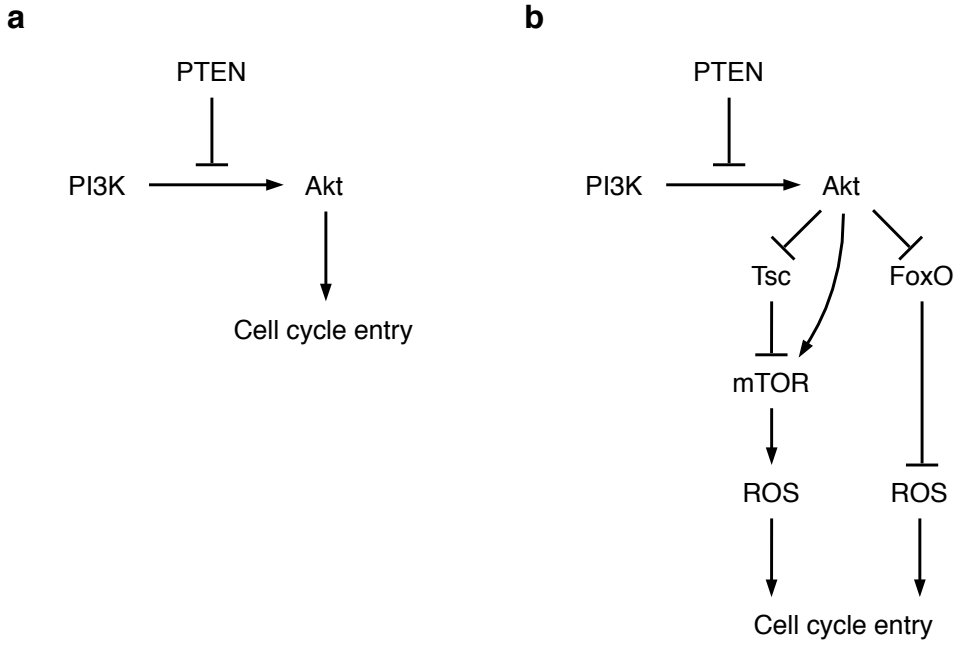

Figure 28. Role of the *PI3K/Akt* pathway in the regulation of HSC quiescence

a. PTEN represses cell cycle entry in HSCs by inhibiting the PI3K/Akt pathway. **b.** Effectors of the PI3K/Akt, FoxO and mTOR, can play a role in the maintenance of quiescence of HSCs. Akt can activate mTOR either by direct phosphorylation of mTORC1, or indirectly through inhibition of Tsc1, member of the mTOR inhibitory complex.

3.3.2.1 ATM and the ATM/BID pathway regulate HSC quiescence through the control of ROS

Atm plays a key role in the maintenance of genome integrity in response to DNA damage, telomeric instability or oxidative stress. In HSCs, ATM is essential for the activation of antioxidant defenses in response to oxidative stress, and loss of *Atm* leads to a decrease in the numbers of quiescent cells in the LSK compartment (Ito et al., 2004; 2006). These defects are restored by the treatment of $Atm^{-/-}$ mice with the antioxidant molecule NAC (N-acetyl-L-cysteine), indicating that increased ROS levels in the absence of ATM participate to the loss of HSC quiescence. In parallel, the team of A.Gross has studied the phenotype of BID^{AA} mice expressing a non-phosphorylatable form of BID, a direct target of ATM activated in response to DNA damage (Kamer et al., 2005). In these mice, they further showed an increase in the proliferation of HSCs, resulting in their depletion, due to exceedingly high levels of ROS (Figure 27) (Maryanovich et al., 2012). Interestingly, BID^{AA} mice also exhibit increased sensitivity to DNA damage, which is rescued by a treatment with NAC. Altogether, this suggests that the ATM/BID pathway is a critical sensor of oxidative stress and DNA damage, and serves as an essential checkpoint for the maintenance of HSC quiescence and genome integrity.

3.3.2.2 Role of the PI3K/Akt pathway in the maintenance of HSC quiescence through the regulation of ROS

The *PI3K/Akt* pathway is an essential signaling pathway for several processes such as insulin metabolism, protein synthesis, proliferation or apoptosis. In response to growth factors, PI3K (phosphatidylinositol 3-kinase) is activated and recruits the serine/threonine protein kinase AKT to the plasma membrane. Activated AKT can then inactivate *FoxO* transcription factors, leading to their degradation, and activate *mTOR*, which results in the exit of quiescence by HSCs (Kharas et al., 2010; Naka and Hirao, 2011; Urao and Ushio-Fukai, 2013). Inhibition or activation of the *PI3K/Akt* pathway has unraveled the key role of this pathway in the regulation of quiescence and the maintenance of low levels of ROS in mouse HSCs.

The tumor suppressor *Pten* acts as a negative regulator of the *PI3K/Akt* pathway. Inactivation of *Pten* leads to cell cycle entry of HSCs accompanied by self-renewal defects (Yilmaz et al., 2006; Zhang et al., 2006). Similar phenotypes are observed in mice with constitutively active AKT (Kharas et al., 2010). Conversely, fetal liver HSCs with reduced PI3K activity or deficient for both *Akt* isoforms *Akt1* and *Akt2* exhibit increased quiescence and thus impaired repopulation potential upon transplantation (Haneline et al., 2006; Juntilla et al., 2010). Altogether, this indicates that inhibition of the *PI3K/Akt* pathway by *Pten* is required to maintain low cycling activity in HSCs (Figure 28.a). As we will see hereafter, several studies suggest that *FoxO* and *mTOR* are involved in this regulation of HSCs' cell cycle by the *PI3K/Akt* pathway (Figure 28.b).

mTOR (mammalian target of rapamycin) is a direct target of AKT. The *mTOR* pathway is a major regulation pathway for cell growth, metabolism and survival. The role of this pathway in the regulation of HSC quiescence is notably illustrated by two observations. The inactivation of *Tsc1* – member of an mTOR inhibitory complex– leads to a similar phenotype as in $Pten^{-/-}$ mice, that is, cell cycle entry of HSCs and reduced self-renewal potential (Chen et al., 2008a; Gan et al., 2008). The consequent activation of mTOR leads to increased ROS levels; NAC treatment of $Tsc1^{-/-}$ mice restores HSC functions, suggesting that *Tsc1* participate to the maintenance of HSCs through the

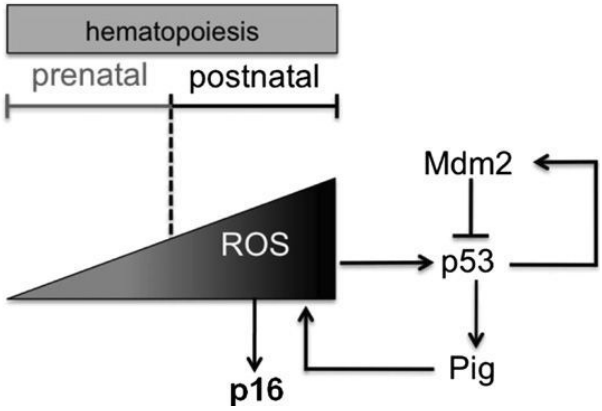

Figure 29. MDM2 is required for maintenance of low ROS levels in HSCs

Basal ROS levels accumulate in hematopoietic tissues during development. Normally, the balance between MDM2 and p53 is highly regulated. In the absence of MDM2 and in the presence of basal oxidative stress, p53 activity is increased. p53 induces increased ROS production via transactivation of Pig genes (p53-induced genes), creating a positive feedback loop. This leads to upregulation of p16 and susequent induction of cell cycle arrest, senescence and ultimately cell death.

Adapted from Abbas et al., 2010

regulation of ROS. Moreover, treatment of *Pten*$^{-/-}$ mice with rapamycin also restores quiescence in HSCs (Yilmaz et al., 2006). Interestingly, rapamycin treatment can, through the inhibition of mTOR complex 2 (mTORC2), induce the inactivation of AKT in HSCs, resulting in increased activity of *FoxO* transcription factors (Sarbassov et al., 2006; Zeng et al., 2007). Thus, *FoxO* factors could also participate to the restoration of quiescence in rapamycin-treated *Pten*$^{-/-}$ mice.

Finally, constitutive deletion of *Foxo3a* or triple cKO of *FoxO1/3/4* in the hematopoietic system both induce cell cycle entry of HSCs, changes in the expression of cell cycle regulators such as the CKI *p27* and cyclins (Miyamoto et al., 2007; Tothova and Gilliland, 2007; Yalcin et al., 2008). These defects are associated to elevated ROS levels and, once again, NAC treatment of *FoxO1/3/4*$^{-/-}$ mice restores HSC quiescence. Thus, the antioxidant program controlled by *FoxO* factors is essential for the maintenance of HSC quiescence.

3.3.3 HSC self-renewal requires the maintenance of low ROS levels

Without surprise, the maintenance of low ROS levels in HSCs is also essential for their self-renewal potential. Indeed, Chow *et al.* tested the properties of ROS^{low} HSCs *vs* ROS^{high} HSCs and showed that only the former exhibit characteristics of *bona fide* HSCs, with better self-renewal potential than ROS^{high} HSCs, both *in vitro* and *in vivo* (Ito et al., 2006; Jang and Sharkis, 2007). Since then, several other studies have shown that increased ROS levels lead to the loss of HSC self-renewal potential. Notably, the loss of HSC quiescence due to increased ROS observed in the studies presented above is also associated to impaired self-renewal potential (Chen et al., 2008a; Ito et al., 2004; 2006; Miyamoto et al., 2007; Tothova et al., 2007).

Interestingly, serial transplants of human HSCs in immunodeficient mice induces the accumulation of ROS in HSCs (Yahata et al., 2011). Such accumulation of ROS is also observed in HSC in transplanted and elderly patients, indicating that transplantation- and aging-induced stress causes an increase in ROS levels, which can lead to the accumulation of DNA damages and self-renewal defects. This can be partially relieved by antioxidant treatments.

3.3.4 ROS-induced senescence

Etymologically, senescence derives from the latin *senex*, meaning old age. In cell biology, it is usually applied to describe cells that have irreversibly lost their ability to divide and have entered a state of permanent growth arrest without really undergoing cell death. Senescence is viewed as a defective state of the cell, usually associated to the accumulation of DNA damage and telomere shortening, but can also be induced in response to stresses such as oxidative stress. In HSCs, it may be more pertinent to consider a continuum between the functional state of HSCs and senescence, with gradual loss of HSC functions, as is observed with aging. Although some markers are associated with senescence, such as upregulation of the CKI *p16*^{Ink4a} or detection of β-galactosidase activity, there is still no good molecular definition of senescence. Whether senescence eventually leads to the death or the disappearance of HSCs, or whether senescent HSCs may remain in the tissue is still not well understood today.

In the hematopoietic system, several studies have proposed that the accumulation of ROS can be associated to the induction of a senescent state in HSCs. Indeed, in *Atm*$^{-/-}$ mice, upregulation of

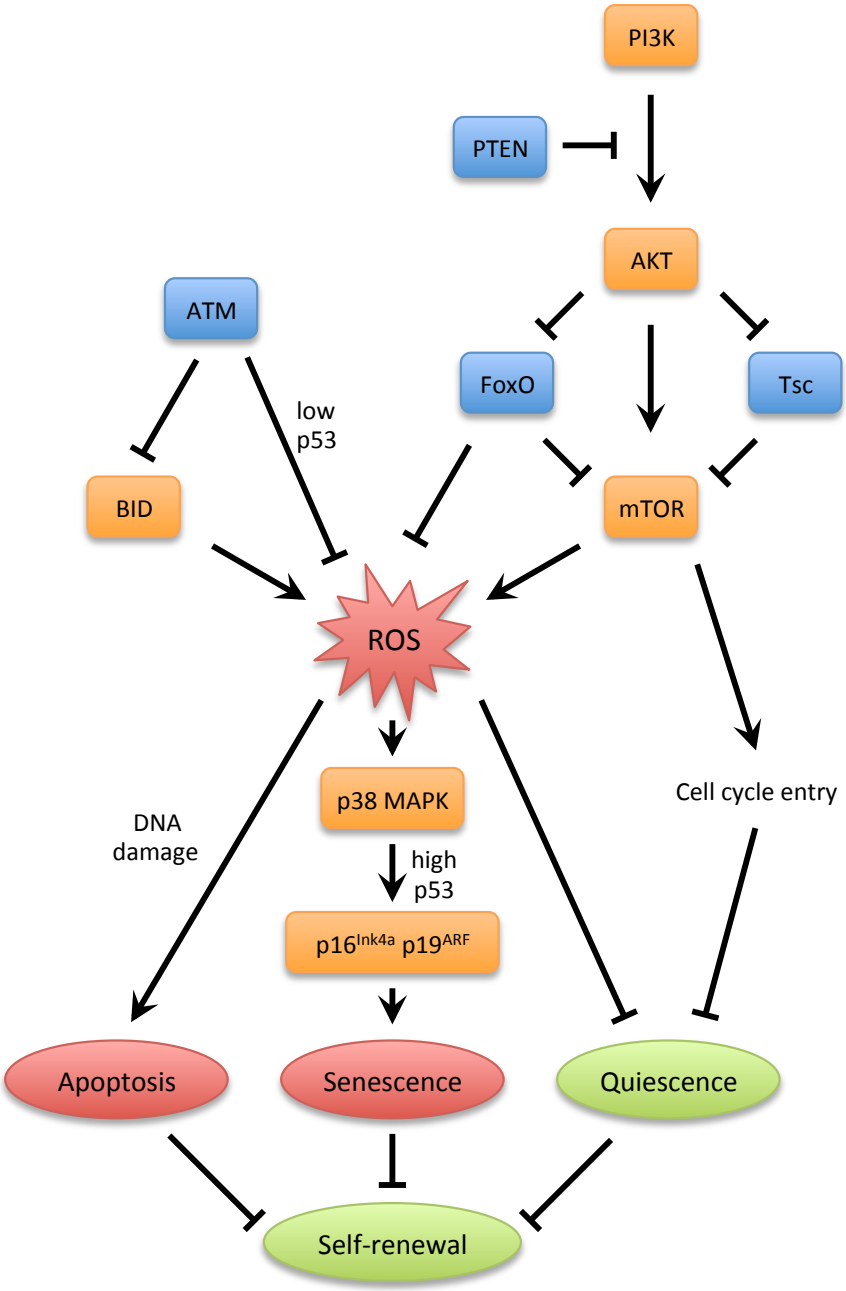

Figure 30. Summary of the pathways regulating ROS levels in HSCs in response to oxidative stress

p16^{Ink4a} in HSCs results in a consecutive block of cell-cycle-induced senescence (Ito et al., 2006). Besides, *p53* has been shown to have a pro-oxidant and senescence-inducing role in the hematopoietic system. Indeed, some *p53* targets can have both anti- and pro-oxidant effects, and *p53* could serve as a sensor of the intensity of oxidizing stress (Sablina et al., 2005). Thus, under normal conditions, low levels of *p53* would promote anti-oxidant, protective responses; conversely, strong *p53* activation would induce pro-oxidant mechanisms and apoptosis. The role of *p53* in the regulation of ROS has been further illustrated by the study of mice deficient for *Mdm2* –a major negative regulator of *p53*– and carrying hypomorphic alleles of *p53* (Abbas et al., 2010). *Mdm2*$^{-/-}$ *p53*$^{515C/515C}$ mice die shortly after birth from hematopoietic failure. Constitutive expression of hypomorphic p53 in hematopoietic cells leads to increased ROS levels through the activation of *Pig* genes (for "*p53*-induced genes"; Figure 29). The consequent accumulation of ROS leads to cell cycle arrest, senescence and apoptosis-independent cell death. Interestingly, in normal conditions, while ROS^{low} HSCs display low p53 levels, p53 is undetectable in ROS^{high} HSCs, further supporting the role of p53 in the downregulation of ROS levels (Jang and Sharkis, 2007). It would be interesting to investigate the role of *p53* in ROS regulation in adult BM at homeostasis and under stress conditions, comparing the responses triggered by p53 in HSCs *versus* downstream progenitors.

3.3.5 Origins and effects of ROS: molecular aspects of models with increased ROS levels

3.3.5.1 The mitochondrial machinery, major producer of ROS

The *Tsc/mTOR* pathway participates to the control of mitochondrial metabolism. *Tsc*-deficient HSCs exhibit increased mitochondrial DNA content and upregulation of genes involved in oxidative phosphorylation; this results in a 7-fold increase of ROS levels in HSCs (Chen et al., 2008a). The BID protein is also involved in the regulation of mitochondrial metabolism: in *BID*$^{A/A}$ or *Atm*$^{-/-}$ HSCs, BID localizes to the mitochondria and is responsible for the aberrant production of ROS (Maryanovich et al., 2012). This suggests that ATM-dependent phosphorylation of BID is required to prevent BID from migrating to the mitochondria and produce ROS.

In these models, ROS production would result from excessive mitochondrial activity in HSCs. Interestingly, the same pathways that are deregulated in these cases are also involved in the physiological generation of ROS required for the physiological activation of HSCs (see part *3.4*).

3.3.5.2 ROS-induced mechanisms participating in HSC defects

In the *Atm*$^{-/-}$ and *FoxO3a*$^{-/-}$ models, increased ROS levels lead to the phosphorylation and subsequent activation of the p38MAPK, which participates to the loss of self-renewal and exhaustion of HSCs, and inhibition of p38MAPK phosphorylation allows better self-renewal of HSCs both *in vitro* and *in vivo* (Ito et al., 2006; Miyamoto et al., 2007). Interestingly, p38MAPK is found to be preferably activated in ROS^{high} HSCs, which could participate to their lower stemness compared to ROS^{low} HSCs (Jang and Sharkis, 2007). In HSCs, ATM and the *Polycomb* repressor BMI-1 promote the maintenance of HSCs by inhibiting the CKIs *p16*^{Ink4a} and *p19*^{ARF}, and increased ROS levels in *Atm*$^{-/-}$ and *Bmi-1*$^{-/-}$ HSCs leads to upregulation of these CKIs due to activation of p38MAPK (Ito et al., 2004; 2006; Liu et al., 2009a; Maryanovich et al., 2012; Park et al., 2003).

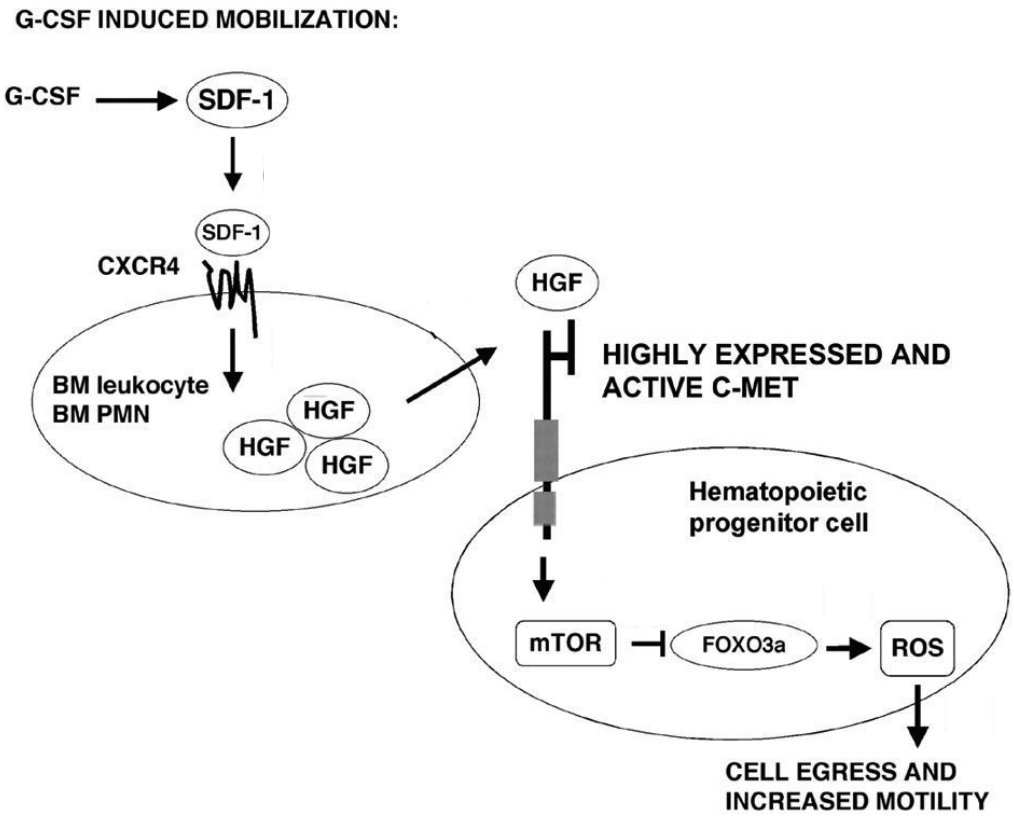

Figure 31. Activation of c-Met allows the mobilization of HSCs through the induction of ROS

G-CSF induces transitory activation of SDF-1, which binds the CXCR4 receptor, inducing the production of HGF in leukocytes and granulocytes of the bone marrow. HGF is secreted and binds to the c-Met receptor on HSCs. Activation of c-Met activates the mTOR pathway, which represses the transcription factor FoxO3, allowing the increase of ROS levels. This signaling cascade results in the mobilization of HSCs and their egress from the niche.

Adapted from Tesio et al., 2011

Thus, ROS levels could control the *Ink4a/Arf* locus, suggesting molecular mechanisms regulating HSC maintenance.

Altogether, these observations make p38MAPK and the *Ink4a/Arf* locus interesting candidates for the understanding of regulation by ROS (Figure 30). However, it is not clear yet how exactly ROS regulate these pathways. One possibility is that the damages induced by ROS accumulation could activate these responses, yet how a response specifically to ROS could be triggered is still unknown. Furthermore, the question remains open whether oxidative stress responses in HSCs necessarily go through p38MAPK and/or *Ink4a/Arf* or if other mediators can regulate the fate of HSCs.

3.4 Regulation of ROS (2): the physiological ROS for HSCs

Besides the deleterious effects of ROS accumulation in case of oxidative stress, ROS also have important physiological roles for HSCs.

As I discussed earlier, constitutive inactivation of *Akt1/2* leads to proliferation and differentiation defects in fetal liver HSCs (Juntilla et al., 2010). This is accompanied by self-renewal defects in competitive or serial transplantation experiments, which could be due to a reduced level of ROS in HSCs. Indeed, induction of ROS by treatment with low doses of BOS restored proliferation and differentiation *ex vivo*. Thus, *Akt* would be required to maintain basal levels of ROS required for cell cycle entry and differentiation of HSCs.

HSCs can be mobilized to the blood in response to stress signals, growth factors… Notably, G-CSF leads to the activation of c-Met by HGF, which is required for the mobilization of HSCs (Figure 31). Tesio *et al.* showed that activation of c-Met induces the activation of the *mTOR* pathway, which leads to downregulation of *FoxO3a* and subsequently to the production of ROS (Tesio et al., 2011). This production of ROS induced by c-Met activation in HSCs is essential for their efficient mobilization in response to G-CSF.

3.5 Conclusions: fine regulation of ROS levels is critical for HSC functions

Several models, such as the ones I presented in this part, have highlighted how hypoxia and the regulation of ROS are important for the function of HSCs. Excessive production of ROS can lead to the exit of HSCs from quiescence, associated with the loss of self-renewal potential and exhaustion of the HSC compartment, and can induce a senescent state of even death of HSCs.

If the origin of ROS production is well known –mostly mitochondrial activity–, the pathways through which ROS impede self-renewal are not clear. Activation of p38MAPK and induction of $p16^{Ink4a}$ are associated with high ROS levels in several studies, yet no molecular link has been made between ROS and self-renewal so far.

Finally, if high ROS levels have deleterious effects on HSCs, null ROS levels do too: low levels of ROS are necessary to maintain HSCs' proliferation and differentiation potential or their mobilization. Thus, while self-renewal requires low levels of ROS, a slight increase of ROS seems to serve as an activation signal for HSCs. In the end, the fine regulation of ROS levels in HSCs appears important to allow maintenance of steady-state hematopoiesis, whilst preserving quiescent HSCs for long-term hematopoiesis and stress-response.

Cellular effect	Target genes	Refs.
Cell-cycle arrest	p21	el-Deiry et al. (1993)
	14-3-3sigma	Chan et al. (1999), Weber et al. (2002)
	Cdc25	Resnick-Silverman et al. (1998)
DNA repair	DDIT4	Ellisen et al. (2002)
	Gadd45	Canman et al. (1995)
Apoptosis	Puma	Han et al. (2001), Nakano and Vousden (2001), Yu et al. (2001)
	Noxa	Oda et al. (2000)
	Slug	Inoue et al. (2002)
	Bid	Mandal et al. (2008)
	Bax	Miyashita and Reed (1995)
Stem cell quiescence	Gfi1	Liu et al. (2009)
	Necdin	Liu et al. (2009)

Table 3. List of p53 target genes involved in the p53-induced response

In response to stresses, several p53 target genes participate to the cellular response and can induce cell cycle arrest, activate the DNA repair machinery or lead to apoptosis. In HSCs, p53 participates in the maintenance of quiescence through the activation of *Gfi1* and *Necdin*.

Adapted from Asai et al., 2011

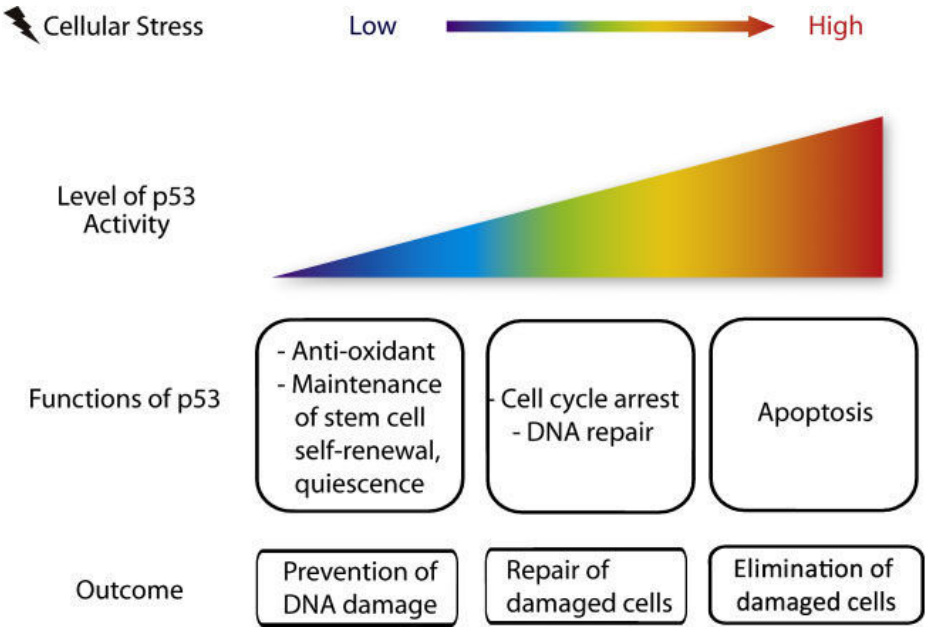

Figure 32. p53 has multiple functions in HSCs, at homeostasis and in stress situations

p53 can induce a variety of cellular responses depending on the nature, intensity and duration of the stress. When p53 is expressed at physiological levels, in homeostatic conditions, it participates to the maintenance of HSC self-renewal and quiescence, regulates the anti-oxidant response and creates cellular competition based on relative p53 expression levels. More severe stresses induce the upregulation of p53, which will then induce cell cycle arrest and activation of the DNA repair machinery. Finally, if p53 levels are excessive, p53 can induce apoptosis or senescence to eliminate damaged cells.

Adapted from Asai et al., 2011

4. The *p53* pathway: at the crossroad between homeostasis and stress management

Stem cells can be defined by their ability to integrate stress signals and trigger specific responses in order to restore/maintain homeostasis, and the *p53* pathway appears as a good example of how HSCs are able to coordinate stress signals and homeostasis.

p53 is a major actor of stress responses. It is activated by a large number of stresses to which cells can be exposed: DNA damage, oxidative stress, cell division defects, metabolic perturbations, ribosomal stress… Upon activation of the *p53* pathway, the p53 protein is stabilized by post-translational modifications and act as a transcription factor to regulate a vast network of target genes. These target genes contribute to the response elicited by the cell, and can induce cell cycle arrest, DNA damage repair, apoptosis or senescence (Table 3). Depending on the severity of the stress HSCs are exposed to, such responses are triggered by *p53* (Figure 32). As we have seen in *II.3.3.4*, *p53* is also capable of triggering pro-oxidant genes. Today, *p53* is known to participate in the regulation of HSCs in steady-state conditions, notably in the maintenance of their quiescence and self-renewal. Finally, following low levels of stress *p53* induces competition within the HSPC populations.

Thus, *p53* coordinates a great number of various signals that report the state of the cell, and triggers specific responses accordingly: maintenance of cellular properties at homeostasis, or stress responses in case of stress.

4.1 Role of *p53* in HSC self-renewal

Several independent studies have investigated the role of *p53* in the self-renewal of HSCs over the past fifteen years. A first observation was that loss of *p53* (also called *Trp53* for transformation-related protein 53) leads to an increase (~2-fold) in the numbers of HSCs defined by the LSK or SLAM markers (Chen et al., 2008b; Liu et al., 2009c; TeKippe et al., 2003). Upon transplantation into irradiated hosts, *p53* KO HSCs exhibit increased (~2-fold) repopulation capacity compared to WT HSCs (Akala et al., 2008; Chen et al., 2008b; TeKippe et al., 2003). Interestingly, chimeric reconstitution by the co-transplantation of $p53^{-/-}$ and WT HSCs resulted in a gradual decrease of *p53* KO cells with time (Chen et al., 2008b; Marusyk et al., 2010). In contrast to *p53* inactivation, constitutively active p53 in $Trp53^{7KR}$ or $Trp53^{T21DS23D}$ mice leads to reduced numbers of HSCs (Liu et al., 2010; Wang et al., 2011). Hence, the impact of the state of *p53* on the number of HSCs is largely accepted. However, the exact role of *p53* in the self-renewal is not clear.

Finally, Akala *et al.* have shown that in the absence of $p16^{Ink4a}/p19^{Arf}$, *p53* activity is required to limit the self-renewal of progenitors (Akala et al., 2008). Indeed, in $p16^{-/-}$ $p19^{-/-}$ $p53^{-/-}$ mice, immature $Lin^- Sca^+ Kit^+ CD150^- CD48^-$ progenitors but not committed progenitors (CMP/GMP/MEP) acquire long-term self-renewal potential, a property normally restricted to HSCs. Thus, their study shows that in multi-potent progenitors *p53* interacts with the *Ink4a/Arf* pathways to downregulate self-renewal, and suggests that other mechanisms inhibit self-renewal of more committed progenitors.

4.2 Role of *p53* in the quiescence of HSCs

The increase of HSC numbers in the absence of *p53* could also be explained by a role of this tumor suppressor in the regulation of HSC quiescence. Indeed, Liu *et al.* observed that the proportion of G_0 HSCs was reduced by ~2-fold in *p53* KO mice (Liu et al., 2009c; 2009b). To dissect the molecular mechanisms involved in HSC quiescence, they studied the impact of *p53* inactivation in mice deficient for the transcription factor *MEF (ELF4)*. $MEF^{-/-}$ mice exhibit increased HSC numbers associated with stronger self-renewal and quiescence (Lacorazza et al., 2005). Crossing these mice with $p53^{-/-}$ mice, they showed that this increased self-renewal potential was *p53*-independent (Liu et al., 2009b; 2009c). However, *p53* was required for the increased quiescence and for protection of $MEF^{-/-}$ HSCs from myelotoxic stresses. Surprisingly, they showed that *p21* was not involved in the control of quiescence in these cells, and identified two new target of *p53* involved in the maintenance of HSC quiescence: *Necdin* and *Gfi1* (you may remember the latter from earlier in *II.1.2.3*). This study highlights the role of *p53* in the quiescence of HSCs, at least in $MEF^{-/-}$ mice. Interestingly, this study also further supports the idea that quiescence and self-renewal are not necessarily coupled, as I discussed in *II.1.1*.

4.3 *p53* in other stem cells

p53 also plays a role in the self-renewal and quiescence of other stem cell populations. Indeed, *p53* is required for the maintenance of both self-renewal and quiescence in adult neural stem cells (NSCs) and mammary stem cells (MaSCs): deletion of *p53* leads to increased proliferation of both NSCs and MaSCs *in vivo* and *ex vivo* (Cicalese et al., 2009; Meletis et al., 2006). *p53* KO NSCs formed more neurospheres when cultured *ex vivo*, and displayed increased self-renewal after several passage compared to WT controls. In MaSCs, loss of *p53* also leads to a change in the polarity of divisions *ex vivo* with an increase in the frequency of symmetric, self-renewing divisions. Through regulation of the polarity of MaSC divisions, *p53* could have a tumor suppressor role by limiting self-renewing symmetric divisions that could lead to tumorigenesis. Finally, increasing evidence indicate that *p53* negatively regulates the self-renewal of ES cells by promoting their differentiation through the activation of differentiation genes and the inhibition of genes involved in pluripotency and self-renewal (Li et al., 2012).

Altogether, these data suggest that the suppression of self-renewal by *p53* could be a conserved mechanism in several systems, which could be activated at homeostasis or in stress situations.

4.4 Competition within HSPCs mediated by *p53*

Using original approaches, two studies have unraveled the existence of cellular competition within the HSC and progenitor compartments that selects for the least damaged cells, based on the relative rather than absolute levels of *p53* in competing cells (Bondar and Medzhitov, 2010; Marusyk et al., 2010).

This competition occurred following exposure to sublethal ionizing radiation (2.5 to 5 Gy), but not at homeostasis, suggesting the involvement of mechanisms distinct from those involved in self-renewal. Furthermore, the enrichment of selected cells compared to outcompeted cells was

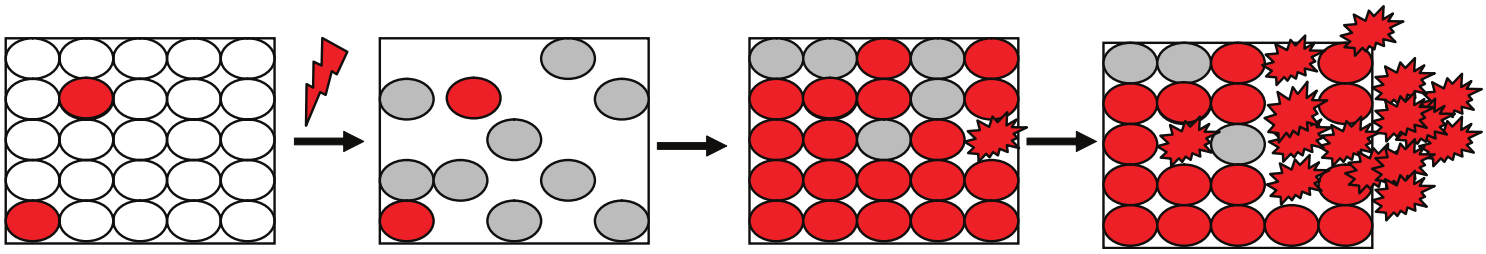

Figure 33. Irradiation promotes p53$^{-/-}$ lymphomagenesis

p53 mutation confers partial resistance to the acute effects of ionizing radiation, and partial protection from the loss of long-term clonogenic potential, leading to selection for hematopoietic cell clones with disrupted p53 (red). Irradiation-induced selection of cells with inactivated p53 leads to an increased pool of target cells for secondary mutations (spiky cell shape), which together with the loss of critical guardian functions of p53 can drive tumorigenic transformation. The resulting malignant cells may then no longer be confined to the niche of normal stem and progenitor cells.

Adapted from Asai et al., 2011

much stronger (10 to 20-fold) than in the models mentioned in *II.4.1*. Here, after exposure to sublethal IR, competition selects for the cells with the lowest levels of *p53* expression. Using dominant-alleles of *p53* (a modified *R172H* allele or the *DDp53* allele encoding the multimerized domain of *p53*) and the $p53^{-/-}$ allele, these two studies show that competition is based on the relative levels of *p53* expression within HSCs and progenitors. This competition settles in a few weeks after IR exposure and is maintained long-term: the loss of *p53* thus appears to protect the functional properties of HSCs. Bondar *et al.* further show how the "winner" cells induce senescence in outcompeted cells, through a non-cell autonomous mechanism (Bondar and Medzhitov, 2010). Such competition could have a major impact on tumorigenesis, and Marusyk *et al.* stress the importance of taking into account the selection of cells that already present oncogenic lesions –here *p53* mutations– and not just the appearance such lesions induced by carcinogenic stress (Figure 33) (Marusyk et al., 2010).

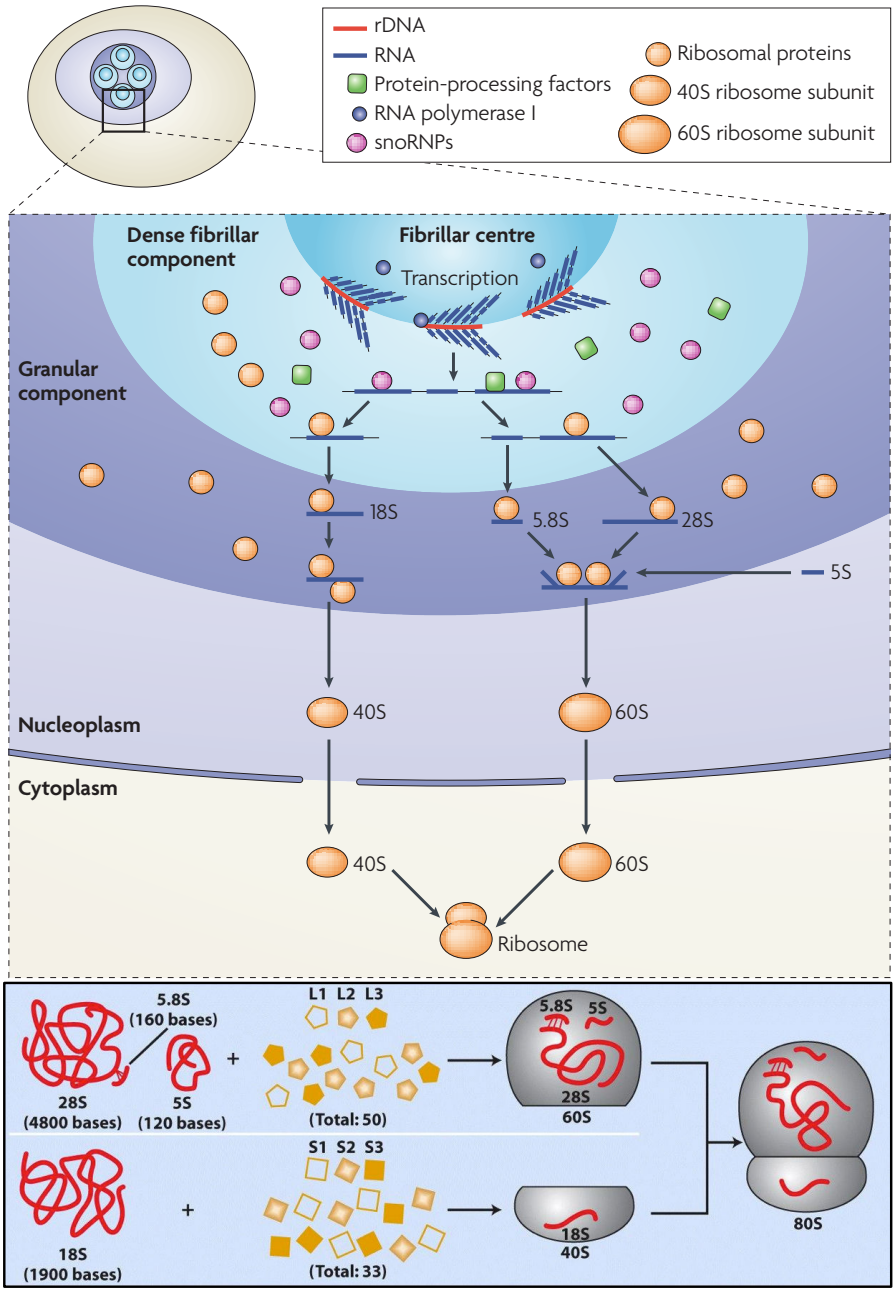

Figure 34. Model for the assembly of ribosomes

RNA Pol I dependent transcription of the rDNA occurs in the fibrillar center of the nucleolus, at the boundary with the dense fibrillar component region. Pre-rRNA transcripts are then cleaved and modified by small nucleolar ribonucleoproteins (snoRNPs) in the dense fibrillar component region. Incorporation of the pre-rRNAs into pre-ribosomal particles with ribosomal proteins occurs mostly in the granular component region: the 5.8S and 28S rRNAs assemble with the 5S rRNA transcript and RPL proteins to form the 60S subunit, whereas the 18S rRNA assembles with RPS proteins to form the 40S subunit. Both 40S and 60S subunits are exported to the cytoplasm, where they bind to mRNA to form functional ribosomes and initiate translation.

Adapted from Boisvert et al., 2007

Part 2 A regulatory role for ribosome biogenesis

Ribosome biogenesis (RiBi) is a complex cellular process crucial for the survival of all living organisms, and involves a large number of factors (Figure 34; see (Kressler et al., 2010) and (Nerurkar et al., 2015) for review). In eukaryotes, RiBi is initiated in the nucleolus –a subcompartment of the nucleus– with the transcription of ribosomal RNAs (rRNAs) from ribosomal genes (or ribosomal DNA; rDNA). Mammalian cells contain several hundreds of copies of rDNA genes organized in tandem-repeat clusters on several chromosomal regions that, when transcribed, are regrouped in the nucleolus. RiBi requires the action of all three RNA polymerases (RNA Pol I, II and III). There are 4 mature rRNAs: the 18S rRNA, which is incorporated into the small subunit of the ribosome, and the 28S, 5.8S & 5S rRNAs that will be incorporated into the large subunit. All rRNAs –with the exception of the 5S rRNA– originate from a 47S precursor (pre-) rRNA, which is transcribed by RNA Pol I in the nucleolus, and undergoes several cleavage and maturation steps to generate the 5.8S, 18S and 28S mature rRNAs. One the other hand, the 5S rRNA is transcribed by RNA Pol III in the nucleoplasm and is then imported into the nucleolus. During their maturation, rRNAs are assembled with ~80 ribosomal proteins (RPs; RPS for the small subunit and RPL for the large) –transcribed by RNA Pol II– to finally form the mature small (40S) and large (60S) subunits of ribosomes in the cytoplasm, which can then assemble into 80S ribosomes on messenger RNAs (mRNAs) to initiate translation. All along this maturation process, hundreds of accessory, non-ribosomal factors are associated to and dissociated from the maturating pre-ribosomal particles (90S, then pre-40S and pre-60S, also called pre-ribosomes), such as endo- and exo-nucleases, helicases, chaperone proteins and small non-coding RNAs, all of which participate to the cleavages, post-transcriptional modifications, conformational changes and other maturation processes of rRNAs (for concise review, see (Thomson et al., 2013)). Finally, the proper execution of RiBi requires fine spatial and temporal coordination by the cell.

Quantifying the net production of ribosomes by a cell is complicated, but it was estimated to ~7500 ribosomes per minute in HeLa cells (Mayer and Grummt, 2006). In yeast, the transcription of rRNAs represents over 60% of the global transcription, more than 60% of total RNA Pol II-dependent transcription is devoted to the production of RPs, and in total RiBi is estimated to represent >80% of the global transcriptional activity (Laferté et al., 2006; Warner, 1999). In addition, many of the proteins involved in the maturation of pre-ribosomal particles are energy-consuming enzymes (AAA-ATPases, GTPases…). Thus, cells have to tightly control their RiBi activity and adapt their growth and proliferation rates depending on the available resources in order to ensure their survival.

It is important to note that RiBi has been mostly studied in yeast (for review, see (Woolford and Baserga, 2013)). Although many of the mechanisms described in yeast seem to be conserved in higher eukaryotes, evolution has brought changes and the regulation of RiBi appears to be even more complex in multi-cellular organisms, with notably the emergence of RiBi surveillance mechanisms.

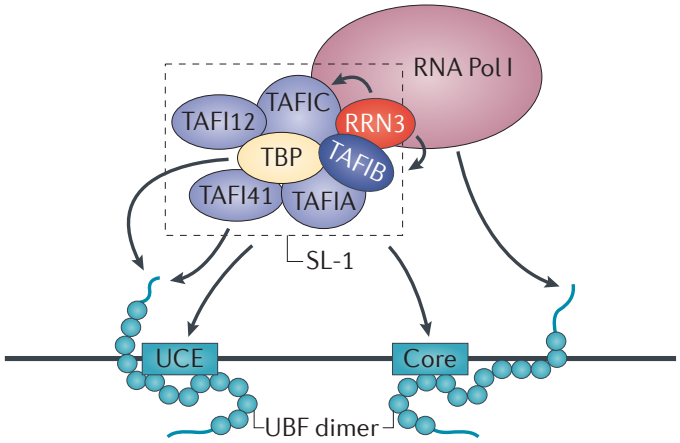

Figure 35. Assembly of the RNA Pol I pre-initiation complex at rDNA promoters

Assembly of the RNA Pol I pre-initiation complex on rDNA promoters starts with the binding of a upstream binding factor (UBF) dimer to the upstream control elements (UCE) and core element (Core) of the rDNA promoter, leading to recruitment of the SL1 initiation complex composed of TATA-box binding protein (TBP) and at least five TATA-box associated factors (TAFs) to the key rDNA promoter sequences. The resultant stable UBF-SL1 complex recruits an initiation competent RNA Pol I associated to RRN3, through interaction between RRN3 and SL1.

Adapted from Bywater et al., 2013

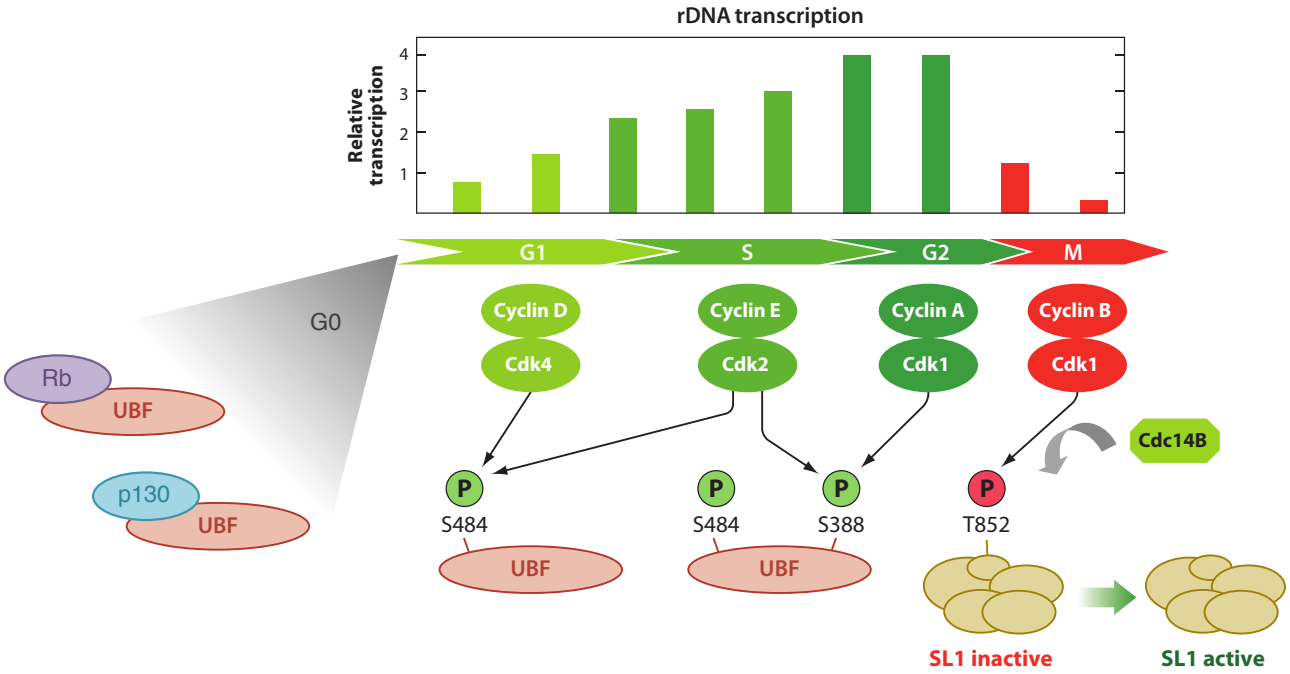

Figure 36. Regulation of the transcriptional activity of RNA Pol I during the cell cycle

UBF is activated during interphase through phosphorylation on Serine 484 and Serine 388 by the cyclin D/CDK4, cyclin E/CDK2 and cyclin A/CDK1 complexes. At the entry into mitosis, the cyclin B/CDK1 complex inactivated the SL1 complex through phosphorylation of TAFI-110 on Threonine 852, impeding its interaction with UBF and thus RNA Pol I dependent transcription. At the end of mitosis, the CDC14B phosphatase is activated an dephosphorylates TAF1-110, thereby reactivating the SL1 complex. In quiescent G0 cells, UBF is inactivated by association with Rb and p130, and reentry into G1 requires CDK4/6-dependent dissociation of p130/Rb. Activating and inactivating phosphorylations are depicted in green and red, respectively.

Adapted from Drygin et al., 2010; Voit and Grummt 2011

In this part, we will see how the regulation of RiBi is inextricably linked to the regulation of cell cycle, growth and metabolism in the cell, focusing mainly on mammalian cells. Then, we will see that studies suggest the existence of heterogeneity in the composition of ribosomes within a same organism, at different levels, which could allow the modulation and specialization of ribosome functions and impinge on gene expression and thus on the regulation of the cell. In the last part, we will see how RiBi participates to the regulation of major events during development and to the regulation of stem cell properties. Finally, I will discuss how dysfunctions of the ribosome biogenesis pathway are associated with severe physiological defects observed in a specific type of pathologies in human known as ribosomopathies.

1. Coordinated regulation of RiBi, cell cycle and cell growth

The regulation of RiBi is intricately coupled with the regulation of fundamental cellular processes such as replication, transcription, translation and energetic metabolism, thus intimately linking RiBi and cell proliferation. However, and probably due to this intricate coupling, understanding and showing the direct links between RiBi and proliferation is quite tortuous and challenging. Notably, one can wonder if it is cell proliferation that leads to the activation of RiBi, or if, conversely, increased production of ribosomes drives proliferation.

1.1 Coupled regulations of RiBi and the cell cycle

1.1.1.1 Oscillation of RNA Pol I activity during the cell cycle

As I mentioned earlier, 3 of the 4 mature rRNAs (5.8S, 18S and 28S) originate from a single precursor 47S pre-rRNA synthesized by a dedicated RNA polymerase: RNA Pol I. Transcription by RNA Pol I requires the formation of a pre-initiation complex (PIC) involving three essential basal transcription factors: UBF (Upstream Binding Factor), TIF-IA (or RRN3, homolog of yeast Rrn3p) and the TIF-IB (aka SL1) complex (composed of TBP –TATA binding protein– and 5 associated TAF factors). As illustrated in Figure 35, a UBF dimer binds to the upstream and core control elements of the rDNA promoter, leading to the formation of a nucleosome-like structure called enhancesome. This allows the SL1 complex to recognize and bind to the key promoter sequences, and the consecutive UBF/SL1 interaction finally recruits the TIF-IA/RNA Pol I complex, thus completing the formation of a functional PIC and allowing the initiation of rDNA transcription.

The cell regulates RNA Pol I-dependent transcription during the cell cycle. This is mainly achieved by the modulation of UBF and SL1 activities by CDK/cyclin complexes, through regulation of their phosphorylation status as illustrated in Figure 36. Thus, rDNA transcription by RNA Pol I reaches its peak during the S and G_2 phases, is silenced during mitosis and gradually increases during the G_1 phase.

1.1.1.2 Role of Arf in the regulations of the cell cycle and ribosome biogenesis

ARF ($p14^{Arf}$ in human and $p19^{Arf}$ in mouse) is one of the proteins encoded by the *Ink4a/Arf* locus, and is involved in both the regulation of RiBi and regulation of the cell cycle. Mice deficient for *Arf* display increased susceptibility to the development of some tumors; the role of *Arf* as a

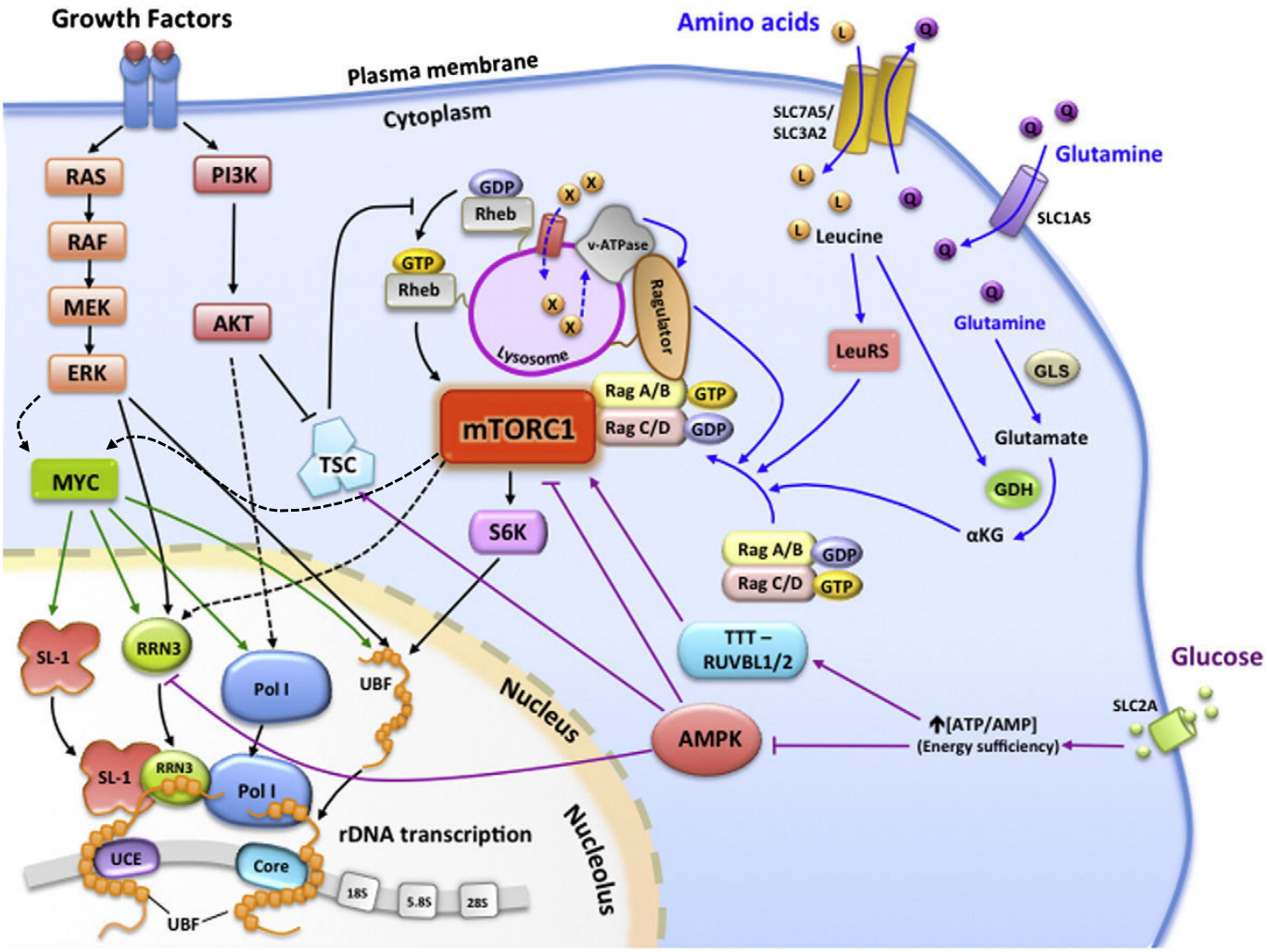

Figure 37. Regulation of rDNA transcription by growth factors, and nutrient and energy availability: the central role of mTORC1

Adapted from Kusnadi et al., 2015

tumor suppressor has been described in details in two recent reviews (Maggi et al., 2014; Ozenne et al., 2010).

ARF is implicated in the *Arf/Mdm2/p53* oncogenic stress pathway. The E3 ubiquitin ligase MDM2 is a main negative regulator of p53, and achieves this role by sequestration and ubiquitination of the p53 protein, which respectively impedes its function as a transcription factor and leads to its degradation by the proteasome. Of note, activation of p53 promotes *Mdm2* expression, revealing an autoregulatory loop. Oncogenic stimuli such as the overexpression of *c-Myc* or a mutated form of *Ras* induce the transcription of *Arf*. The ARF protein then binds and inhibits MDM2, thus stabilizing p53 (Sherr, 2006). Subsequent upregulation of p53 then induces cell cycle arrest. Interestingly, *Arf* can also control cell cycle progression in the absence of *Mdm2* and *p53*, suggesting *p53*-independent mechanisms (Weber et al., 2000). Although these *p53*-independent mechanisms are not clear, several studies have shown a direct role for *Arf* in the regulation of ribosome biogenesis.

First, ARF can impede 47S pre-rRNA transcription by RNA Pol I through the inhibition of UBF (thus preventing transcription initiation) and TTF-1 (transcription termination factors-1)(thus inhibiting transcription termination) (Ayrault et al., 2006; Lessard et al., 2010). Besides, ARF also interacts with Nucleophosmin (NPM or B23), leading to its destabilization (Bertwistle et al., 2004; Itahana et al., 2003). NPM is an endonuclease required for the cleavage of maturating pre-rRNAs at the level of the internal transcribed spacer 2 (ITS2) and the subsequent conversion of the 32S pre-rRNA into the 28S and 5.8S mature rRNAs. Finally, it was recently shown that ARF prevents the localization of RNA helicase DDX5 to the nucleolus, which is also involved in the processing of pre-rRNAs (Saporita et al., 2011).

The tumor suppressor *Arf* thus participates to the regulation of the cell cycle directly through induction of the *p53* pathway, and independently of p53 to the regulation of RiBi at the level of rRNA transcription and maturation. It is still unclear how the different functions of *Arf* are regulated: do they cooperate to better suppress tumorigenesis? Is the control or RiBi by ARF only enforced if the *Arf/Mdm2/p53* pathway is no functioning (for instance in the absence of p53)? To what extent are these mechanisms induced in homeostatic conditions *vs* in response to oncogenic stress? It has been suggested that basal, low levels of ARF may be involved in the regulation of nucleolar structure and function (Maggi et al., 2014).

1.2 Regulation of RiBi by growth factors: the central role of mTORC1

1.2.1 Regulation of rDNA transcription by the PI3K/Ras/Myc control network

It has been well established in several systems that rDNA transcription is regulated by growth factor signaling pathways. Two main pathways are involved in this regulation: the PI3K/AKT/mTORC1 (mTOR complex 1) and the Ras/Raf/ERK pathways, which together form an intricate control network with the transcription factor Myc (Figure 37; for reviews, see (Hannan et al., 2011; Iadevaia et al., 2014; Kusnadi et al., 2015)).

1.2.1.1 Regulation of rDNA transcription by the PI3K/AKT/mTORC1 pathway

Activation of the PI3K/AKT/mTORC1 pathway by growth factors regulates RNA Pol I activity *via* regulation of UBF and TIF-IA activities. Briefly, PI3K activates AKT, which in turn inactivates TSC2, thus relieving repression of the Rheb GTPase, activator of mTORC1 (Inoki et al., 2003a). Activated mTORC1 then phosphorylates and activates S6K1/2 (RPS6 kinases 1 & 2), and S6K1 then activates UBF *via* phosphorylation of its C-terminal activation domain (Hannan et al., 2003). Furthermore, activated mTORC1 is also able to activate TIF-IA, putatively by promoting its activating phosphorylation (on Ser44) and repressing its inactivating phosphorylation (on Ser199) (Mayer et al., 2004). In addition to activating mTORC1, AKT is also able to promote RNA Pol I activation at different levels, although the underlying mechanisms are unclear (Chan et al., 2011).

Moreover, activated mTORC1 can also promote RNA Pol III-dependent transcription or the 5S rRNA. RNA Pol III is repressed by the evolutionary conserved transcriptional repressor Maf1, which is inactivated by the recruitment of mTORC1 to the rDNA promoter. mTORC1 is thought to be recruited by TFIIIC, one of the basal transcription factors required for the formation of the RNA Pol III PIC, and could then phosphorylate and inactivate Maf1 either directly or through activation of S6K1 (Kantidakis et al., 2010; Shor et al., 2010).

1.2.1.2 Regulation of rRNA synthesis by the Ras/Raf/ERK pathway

Growth factors can also regulate rDNA expression through activation the Ras/Raf/ERK pathway. Upon activation of Ras, successive phosphorylation of Raf, MEK and ERK lead to the transport of ERK to the nucleus. ERK then phosphorylates and activates UBF and TIF-IA, thus promoting RNA Pol I transcription (Stefanovsky et al., 2001; Zhao et al., 2003).

In addition, ERK also phosphorylates the TFIIIB complex, another basal transcription factor required for the formation the of RNA Pol III pre-initiation complex, thus leading to activation of RNA Pol III transcription (Felton-Edkins et al., 2003).

1.2.1.3 Activation of Myc promotes rRNA synthesis

The PI3K/AKT/mTORC1 and Ras/Raf/ERK pathways both lead to the upregulation of the transcription factor Myc by promoting translation of *c-Myc* mRNAs and stabilizing the Myc protein, respectively (Csibi et al., 2014; Sears et al., 2000; Tsai et al., 2012). Increased Myc levels can promote RNA Pol I transcription through different mechanisms. First, Myc promotes the RNA Pol II-dependent transcription of a number of target genes, including UBF, TIF-IA and RNA Pol I subunits (Poortinga et al., 2014). Furthermore, Myc binds to the rDNA promoter region and promotes rDNA transcription through remodeling of the rDNA chromatin structure and direct interaction with SL1, thus stabilizing the RNA Pol I PIC (Shiue et al., 2009). Finally, Myc also promotes RNA Pol III-dependent transcription through activation of TFIIIB (Gomez-Roman et al., 2006).

1.2.2 mTORC1 controls the translation of ribosomal proteins

mTORC1 also participates to the control of RP translation. In mammals, all RP mRNAs contain a feature known as a 5'-terminal oligopyrimidine tract (5'-TOP, TOP mRNAs) immediately after the 5'-cap. Of note, TOP mRNAs also include several translation factors and factors involved

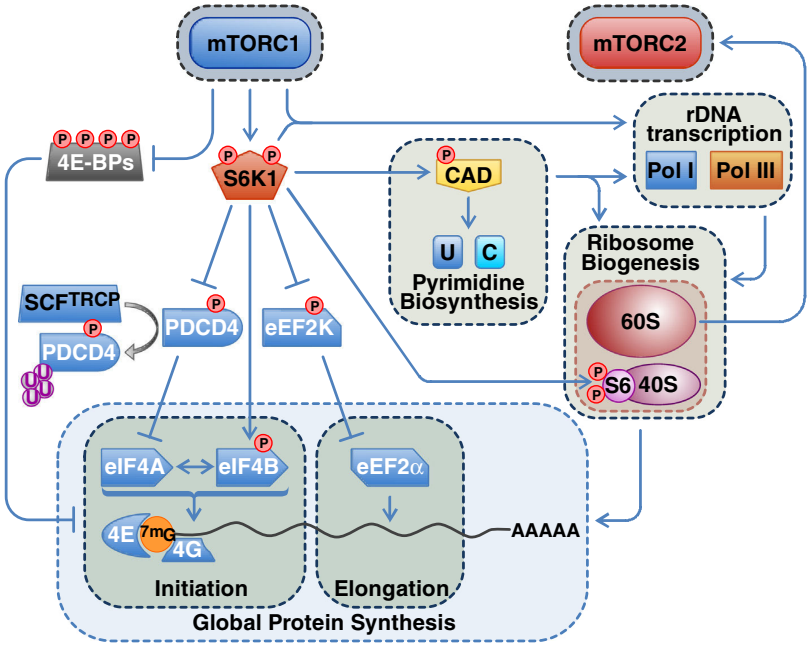

Figure 38. mTORC1 controls general protein synthesis through direct and indirect functional interactions

mTORC1 phosphorylates and activates S6K1, which in turn positively regulates mRNA translation initiation and elongation, and ribosome biogenesis through regulation of pyrimidine biosynthesis and rDNA transcription. mTORC1 phosphorylates 4E-BPs, thus relieving their inhibitory effect on translation initiation.

Adapted from Gentilella et al., 2015

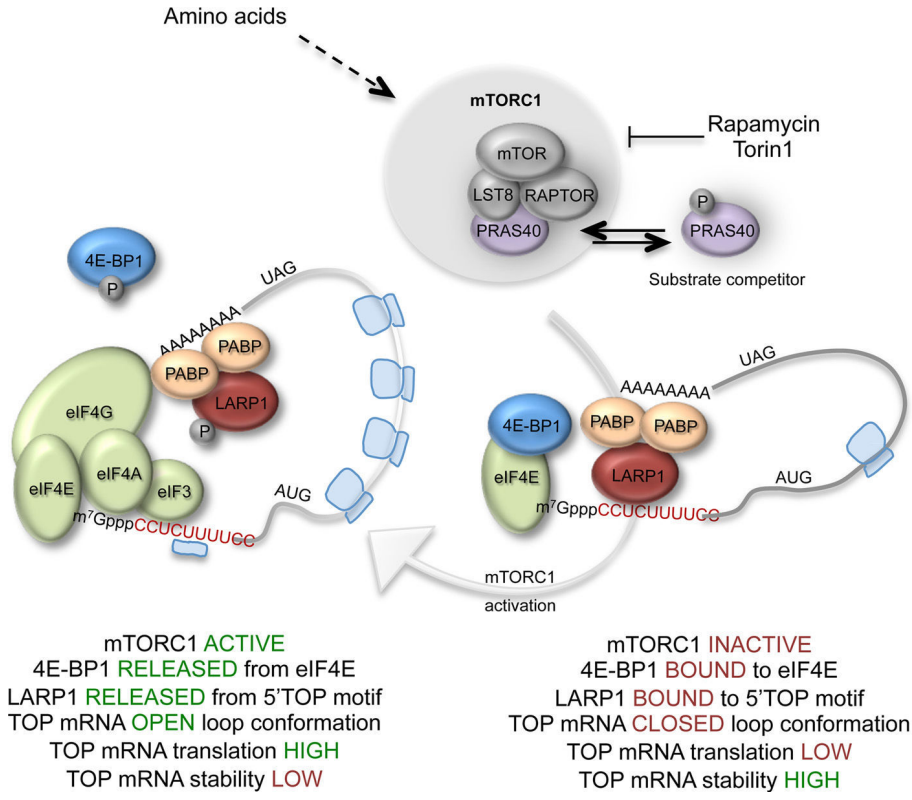

Figure 39. Model for regulation of TOP mRNAs by LARP1 downstream of mTORC1

mTORC1 phosphorylates LARP1 at multiple residues, effectively releasing LARP1 from the TOP motif. mTORC1 also controls the phosphorylation of 4E-BP1, releasing it from eIF4E. eIF4G can thus bind eIF4E, allowing recruitment of the pre-initiation complex to the mRNA and its subsequent translation.

Adapted from Fonseca et al., 2015

in ribosome assembly. Initial work in the 1980's by the team of L. Johnson showed that the rate of RP synthesis is not so much dependent on the levels of RP mRNAs in the cell, but is rather controlled by changes in the efficiency of their translation associated to cellular growth (Geyer et al., 1982). Translation of these mRNAs is inhibited in basal conditions, and is activated upon stimulation with growth factors or serum. Since then, several studies have been aimed at understanding how TOP mRNA translation is regulated and have shown that it is highly sensitive to mTORC1 inhibition, suggesting that mTORC1 plays a central role in this regulation (Hsieh et al., 2012; Jefferies et al., 1997; 1994; Tang et al., 2001; Thoreen et al., 2012).

mTORC1 is known to regulate the translation of mRNAs by two main mechanisms (for review, see(Iadevaia et al., 2014)). First, mTORC1 can inactivate eukaryote initiation factor 4E (eIF4E) binding proteins (4E-BPs), which prevent the formation of the eIF4F complex required for translation initiation; relieved eIF4E can then interact with eIF4G and other partners to promote the initiation of translation (Schalm et al., 2003). Second, mTORC1 can also activate S6K1, which in turn phosphorylates and inactivates EF2K –an inhibitory kinase of elongation factor 2 (EF2)–, thus promoting translation elongation of mRNAs (Wang et al., 2001). These two mechanisms have essential roles in the regulation of global translation (Figure 38) and have been proposed in the past to play a particular role in the control of TOP mRNAs translation by mTORC1. However, several studies suggest that they might not be so essential for this control, indicating that yet another mechanism may be involved (Huo et al., 2012; Jefferies et al., 1997; Miloslavski et al., 2014; Pende et al., 2004; Tang et al., 2001; Thoreen et al., 2012).

A recent study has identified LARP1 (La-related protein 1) as a key negative regulator of TOP mRNA translation (Figure 39) (Fonseca et al., 2015). The authors propose a model where in normal conditions or upon nutrient insufficiency where mTORC1 is inactive, LARP1 binds to the 5'-TOP element of TOP mRNAs in close proximity to the eIF4F complex, disrupting the association of eIF4G with TOP mRNAs and thus impeding translation of TOP mRNAs; in parallel, active 4E-BPs sequester eIF4E, also inhibiting translation initiation. Upon growth factor stimulation, mTORC1 is activated and phosphorylates 4E-BPs and LARP1, releasing them from the 5'-UTR (5' untranslated region) of TOP mRNAs and thereby allowing their translation. Interestingly, the authors also show that binding of LARP1 to TOP mRNAs increases their stability, suggesting that it acts as a bimodal regulator: while it represses translation of TOP mRNAs, it simultaneously ensures their preservation until they are ready to be translated again. Finally, such a mode of action could be a mean for the cell to ensure optimal energy conservation and rapidly respond to nutrient starvation or growth factor stimulation by either repressing or promoting the translation of ribosomal proteins and translation factors encoded by TOP mRNAs.

1.2.3 Regulation of mTORC1 and RiBi by nutrient and energy availability

In addition to responding to growth factors, cells also monitor and respond to nutrient and energy availability, *i.e.* the amount of amino acids and ATP, respectively. We will see here that mTORC1 plays a central role in the response to nutrient and energy availability/deficiency.

1.2.3.1 mTORC1 activity is regulated by nutrient sensing mechanisms

The mechanisms involved in sensing and reacting to changes in amino acid availability are different from those involved in the response to growth factors (Figure 37; for review, see (Bar-Peled and Sabatini, 2014)). Notably, mTORC1 is activated by amino acids independently from the PI3K/AKT/TSC pathway. Briefly, amino acids are transported to the lysosome upon intake, where the v-ATPase (which seems to act as an amino acid sensor) engages in extensive amino acid-dependent interactions with the Ragulator complex. Ragulator is tethered to the lysosome membrane and acts as a guanine exchange factor to activate Rag GTPase heterodimer, which in turn recruit mTORC1 through specific interactions with Raptor (member of the mTORC1 complex required for its substrate specificity). The subsequent recruitment of mTORC1 to the lysosome membrane then allows its activation by the Rheb GTPase. Thus, it appears that amino acid-dependent shuttling of mTORC1 from the cytoplasm to the lysosome membrane is essential for activation of mTORC1 by growth factors, and growth factors cannot efficiently activate mTORC1 in conditions of amino acid deficiency. Altogether, this places mTORC1 as a hub that coordinates the sensing of nutrient availability with growth stimuli, and makes nutrient sensing a major regulator of RiBi activity.

1.2.3.2 Coordination of RiBi activity with the energetic state of the cell

Besides, energy sensing by the cell also plays a critical role in the regulation of mTORC1 (Figure 37; for review, see (Kusnadi et al., 2015)). Energy levels can be defined as the ratio between monophosphate and triphosphate forms of the adenosine nucleotide (respectively AMP and ATP) in the cell: a high AMP/ATP ratio is indicative of deficient energy production and triggers energetic stress responses. The AMP-dependent protein kinase (AMPK) is a crucial sensor of this ratio, and is activated by the binding of AMP. Once activated, AMPK transmits energetic stress signals to mTORC1 through activation of the TSC1/2 complex and inactivation of Raptor, leading respectively to inactivation of the Rheb GTPase and dissociation of Raptor from the mTORC1 complex, which result in mTORC1 inactivation (Gwinn et al., 2008; Inoki et al., 2003b). Furthermore, AMPK has also been reported to directly inactivate TIF-IA by phosphorylation on Ser635, a unique phosphorylation site that is not affected by mTORC1 signaling. TIF-IA phosphorylation at this site disrupts the interaction of the RNA Pol I/TIF-IA complex with SL1, thereby preventing the assembly of the RNA Pol I PIC (Hoppe et al., 2009). Thus, AMPK ensures that cells embark on energy-consuming processes such as RiBi only in sustainable energetic conditions.

1.3 Feedback from ribosome biogenesis regulates cell proliferation

1.3.1 Ribosomes and the mTORC2 complex cooperate to promote cell growth

Besides its role in the mTORC1 complex in the regulation of cell growth and RiBi, mTOR also participates to signaling pathways involved in cell survival and organization of the actin cytoskeleton, through its incorporation into the mTOR complex 2 (mTORC2). Much less is known about the regulation of the mTORC2 pathway compared to mTORC1, but recent studies have highlighted the existence of links between mTORC2 and ribosomes. Notably, two teams have

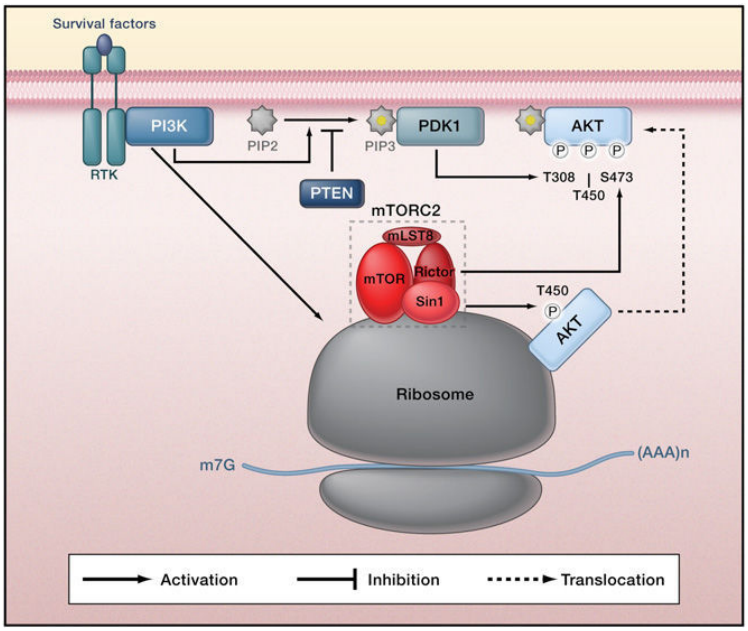

Figure 40. Regulation of mTORC2 by association to ribosomes

In response to upstream stimulation, increased PI3K signaling activates mTORC2 (composed of mTOR, Rictor, Sin1 and mLST8) by promoting its association with ribosomes. mTORC2 can then phosphorylate AKT on Threonine 450 during its translation, and on Serine 473 in a post-translational manner and independently of PI3K signaling.

Adapted from Xie and Guan., 2011

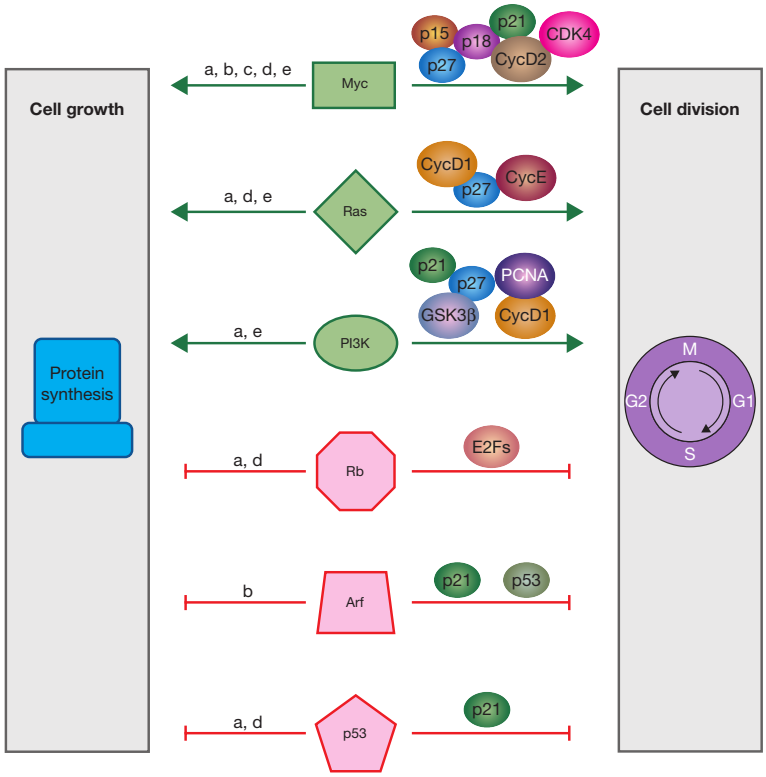

Figure 41. Coordinated control of cell growth and proliferation

Several signaling pathways regulate both cell growth (left) and proliferation (right), with either activating (oncogenic, green) or repressive (tumor suppressor, red) effects. The processes participating to cell growth regulation are: RNA Pol I dependent transcription (a), pre-rRNA processing (b), RNA Pol II dependent transcription (c), RNA Pol III dependent transcription (d) and mRNA translation (e).

Adapted from Oskarsson and Trumpp., 2005

shown that mTORC2 associates to mature ribosomes (Oh et al., 2010; Zinzalla et al., 2011). Zinzalla *et al.* have demonstrated that PI3K activation in mammalian cells leads to the association of mTORC2 with the ribosome, independently of their translation activity. Their findings show that this association is essential for the activation of mTORC2 signaling and suggest that it could have physiological roles in both normal and cancer cells (Zinzalla et al., 2011). In parallel, Oh *et al.* have investigated the downstream effects of the association of mTORC2 with the ribosome, and showed notably that ribosome-bound mTORC2 phosphorylates AKT on Ser450 during its translation, promoting its stability (Figure 40)(Oh et al., 2011).

Why this regulation of mTORC2 by ribosomes? The cellular content in ribosomes is determinant for its growth capacity, and mTORC2 regulates growth-related processes. Thus, regulation of mTORC2 by ribosomes could be a way to ensure that it is not activated unless the cell is able to grow. This also implies that through its regulatory role in RiBi, mTORC1 indirectly regulates mTORC2. Interestingly, mTORC2 regulates the AKT kinase, which regulates mTORC1 and other survival pathways. Thus, ribosomes appear to be involved in a feedback loop with mTOR to promote cell growth.

1.3.2 Ribosomes, at the crossroad between growth and proliferation

An inextricable link exists between the regulations of protein synthesis, RiBi, cell growth and cell division. Indeed, cell division demands an increase of growth, and thus more important protein synthesis. Moreover, cell division also requires the presence of specific proteins involved in the regulation of cell cycle checkpoints. Thus, one cannot reasonably dissociate the regulations of cell growth and cell proliferation. Indeed, several cross- and co-regulations exist, and ribosomes are notably involved in the coupling of cell growth with the cell cycle.

In yeast, cells must reach a certain critical size before they can divide. To understand the underlying mechanisms allowing the coordination of cell cycle regulation with cellular growth and cell size, systematic screening approaches have been used. Such studies have shown that several genes involved in ribosome biogenesis are essential for the coupling between cell size and division (Jorgensen et al., 2002).

In mammals, many signaling pathways regulate both proliferation and growth (Figure 41). Interestingly, these pathways regulate cell growth through the regulation of RiBi at different levels. A striking example of the co-regulation of growth and proliferation is the transcription factor *c-Myc*, which I mentioned earlier. In response to mitogenic signals, Myc induces the expression of genes involved in cell cycle control and promotes RiBi, thus coordinating cell proliferation and growth (for reviews, see (Dang, 2013; Oskarsson and Trumpp, 2005; Poortinga et al., 2014)). Myc promotes ribosome biogenesis at different levels: (1) Myc increases RNA Pol I transcription (see *1.2.1.3*); (2) Myc induces the expression by RNA Pol II of RPs and other genes involved in RiBi such as *nucleolin* and *nucleophosmin*; (3) Myc promotes RNA Pol III-dependent transcription by activating TFIIIB. Besides ribosome biogenesis, Myc also stimulates cell cycle progression: several of Myc target genes are involved in the different phases of the cell cycle (notably Cdks and Cyclins), as illustrated in Figure 42 (for review, see(Bretones et al., 2015)). Finally, these roles in

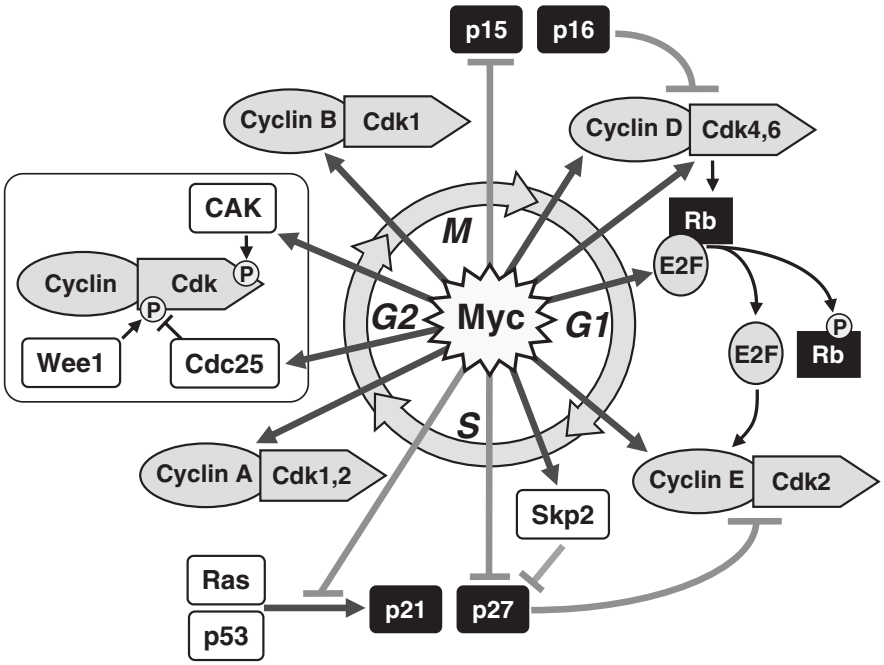

Figure 42. Myc stimulates cell cycle progression

Myc promotes cell cycle progression and thus cellular proliferation, through the induction of several positive regulators of the cell cycle and repression of cell cycle inhibitors.

Adapted from Bretones et al., 2015

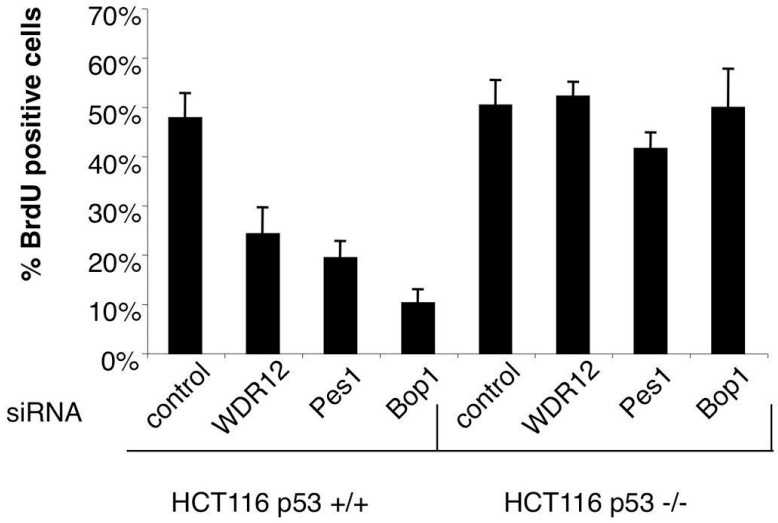

Figure 43. Inactivation of members of the PeBoW complex leads to p53-dependent cell cycle arrest

Inactivation of members of the PeBoW complex (Pes1, Bop1, WDR12) by RNA intereference in $p53^{+/+}$ HCT116 cells leads to cell cycle arrest as illustrated by a net decrease in DNA replication assessed by BrdU staining. In contrast, inactivation in $p53^{-/-}$ HCT116 cells does not affect proliferation, as illustrated by unchanged DNA replication activity.

Adapted from Holzel et al., 2010

the regulation of the cell cycle and cell growth make Myc a major actor in the maintenance of homeostasis, but also a potent driver of tumorigenesis.

1.3.3 Dysfunction of RiBi trigger ribosomal stress responses

Given the fundamental importance of ribosome biogenesis for their functions, cells must monitor the proper progress of this process to sense any perturbation. Here, I will describe the responses that can be induced in response to ribosomal stress triggered by dysfunctional RiBi.

1.3.3.1 Defective RiBi leads to p53-dependent cell cycle arrest and apoptosis

Perturbations of rRNA transcription induced by treatment with different drugs (Actinomycin D, CX-5461…), deletion of transcription factors or disruption of the RNA Pol I complex, lead to the activation of the *p53* pathway, cell cycle arrest and increased apoptosis (for example in response to TIF-IA inactivation in (Yuan et al., 2005)). Defects in the maturation of pre-rRNAs also lead to p53 stabilization. For instance, expression of dominant-negative mutated forms of BOP1, PES1 or WDR12, members of the PeBoW complex, leads to defective maturation of the pre-60S particle associated with increased p53 levels and cell cycle arrest (Ahn et al., 2016; Hölzel et al., 2005; Pestov et al., 2001; Strezoska et al., 2002). Interestingly, p53 inactivation restores the cell cycle defects of these mutations (Figure 43, (Hölzel et al., 2010)). Finally, insufficient expression of some RPs can also activate a p53 response. Several mouse models with invalidated or haploinsufficient expression of some RPs have been developed. Notably, haploinsufficiency of *Rps6* causes defective entry in mitosis and massive apoptosis in gastrulating embryos around the time of implantation; inactivation of p53 in this background mitigates this lethality and extends embryonic development until E12.5 (Panic et al., 2006). In adult mice, conditional homozygous deletion of *Rps6* abrogates T cell development and conditional hemizygous deletion impedes the survival of mature T cells to due impaired cell cycle progression; inactivation of p53 rescued the phenotype in both cases (Sulic et al., 2005). Finally p53 knockdown by RNA interference restore proliferation defects observed in *Rps6*-deficient human cells (Fumagalli et al., 2009). Several other studies in mouse and other models, have similarly shown the role of p53 in the phenotype of other RP mutants, making activation of the p53 pathway a general response to RP deficiency and –as we will see in the next part– to ribosomal stress in general (Danilova et al., 2008; Dutt et al., 2011; Taylor et al., 2012). Whether activation of this pathway can play a role during normal development is still to be determined.

1.3.3.2 Sensing ribosomal stress: the RP-MDM2-p53 pathway

Over the past decades, it has been demonstrated in several studies that alterations in the RiBi pathway can induce specific pathways in response to ribosomal stress (for reviews, see (Deisenroth and Zhang, 2010; Golomb et al., 2014; Zhang and Lu, 2009)). Because RiBi dysfunction can lead to the disruption of nucleolar organization (and vice-versa), ribosomal stress is often associated to nucleolar stress. However, disruption of the nucleolar compartment is not necessary for the induction of ribosomal stress, and perturbations of the RiBi pathway can be detected by the cell before the emergence of morphological changes of the nucleolus (Donati et al., 2011a; Fumagalli et al., 2009). More specifically, ribosomal stress is induced by disequilibrium between the syntheses

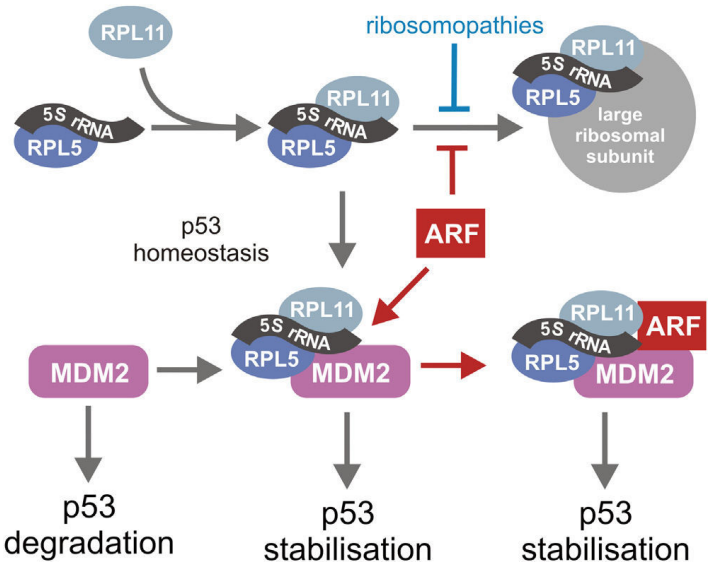

Figure 44. MDM2 inhibition by the 5S RNP is induced by ribosomal stress and ARF activation

In normal conditions, the 5S RNP (composed of 5S rRNA, RPL5 and RPL11) is incorporated into the large ribosomal subunit. Upon ribosomal stress or activation of ARF, this incorporation is impeded and free 5S RNP binds and inhibits MDM2, thus resulting in p53 stabilization. ARF-induced MDM2 inhibition requires interaction of MDM2 with the 5S RNP.

Adapted from Zhang and Lu, 2009

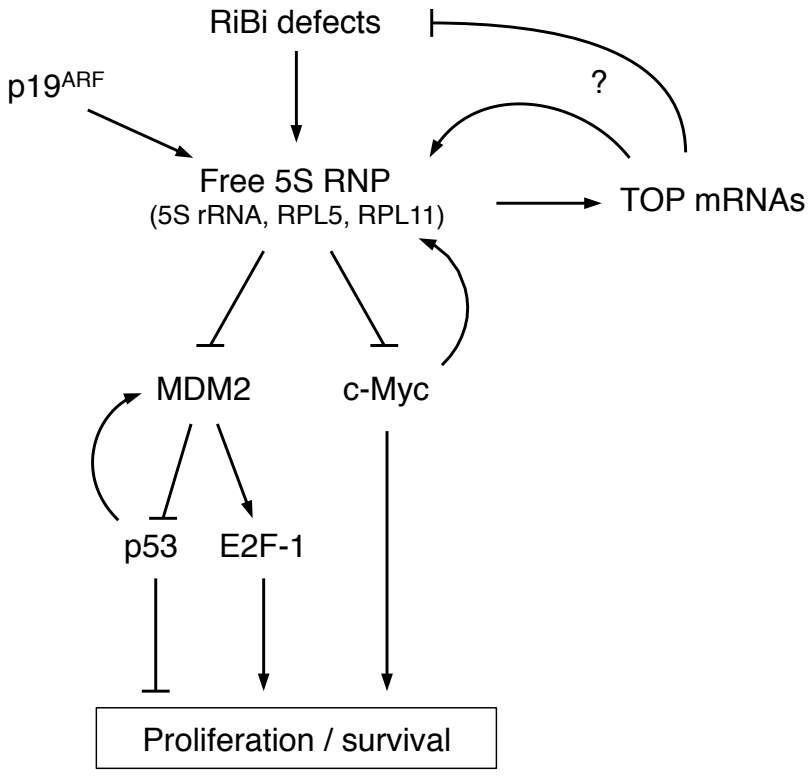

Figure 45. The 5S RNP plays a central role in the response to ribosomal stress

of rRNAs and RPs. It is generally accepted that dysfunctional RiBi leads to the accumulation of unincorporated, free RPs; interestingly, responses to ribosomal stress involve RPs and the MDM2-p53 pathway. Indeed, several RPs have been reported to bind to and inactivate MDM2, thereby upregulating p53 (Chakraborty et al., 2011). However, recent work has shown that only RPL5 and RPL11 are essential for the activation of p53 in response to impaired RiBi (Bursać et al., 2012; Fumagalli et al., 2012; Sun et al., 2010). Furthermore, two more recent studies have elegantly demonstrated that it is actually the association of RPL5 and RPL11 with the 5S rRNA into the 5S RNP (ribonucleoprotein) that is critically required for this activation (Donati et al., 2013; Sloan et al., 2013). Interestingly, both teams also show that inhibition of MDM2 by the tumor suppressor ARF (see *1.1.1.2*) is dependent on the interaction of the 5S RNP and MDM2. Thus, the authors propose that ARF predominantly functions by impeding ribosome biogenesis, leading to the accumulation of unincorporated 5S RNP; the 5S RNP, together with ARF, would then inhibit MDM2 and thus lead to p53 activation (Figure 44).

1.3.3.3 p53-independent responses to ribosomal stress?

In cells deficient for *p53*, the inhibition of RNA Pol I leads to cell cycle arrest, suggesting that p53-independent mechanisms can also be induced in response to RiBi dysfunction (Donati et al., 2011b). Indeed, Donati *et al.* showed that inhibition of MDM2 by RPL11 impedes its function for the stabilization of the transcription factor E2F-1, leading to its degradation; this resulted in the downregulation of E2F target genes that are required for the entry and progression through the S phase (Donati et al., 2011b). Besides, RPL5 and RPL11 have been shown to down-regulate *c-Myc* in response to RiBi defects in a p53-independent manner, resulting in reduced proliferation. They can achieve this repression by different means: (1) RPL11 binding to the promoter of the *c-Myc* gene, thus inhibiting its transcription; (2) recruitment by RPL5 and RPL11 of miRNAs and the RNA silencing machinery to degrade *c-Myc* mRNAs, thereby preventing its translation; (3) direct binding of RPL11 to the Myc protein on its MB II (Myc Box II) domain, hence impeding its transcription factor activity (Figure 45)(Challagundla et al., 2011; Dai et al., 2007; Li et al., 2015; Liao et al., 2013).

Interestingly, two studies have shown that upon RiBi dysfunction, translation of TOP mRNAs is increased or at least sustained despite a decrease in global translation, both in the presence and in the absence of p53 (Fumagalli et al., 2009; Gismondi et al., 2014). Two hypotheses could explain this preferential of TOP mRNAs in response to defective RiBi. TOP mRNAs encode all of the RPs in mammals, as well as actors of the RiBi pathway and translation factors. Thus, increasing/maintaining the translation of these mRNAs could be a mean for the cell to try to compensate the RiBi defects by producing more ribosome components. Alternatively, increasing the production of RPs that would not be incorporated in ribosomes due to RiBi defects, would lead to the accumulation of these RPs and notably of RPL5 and RPL11, which could then activate ribosomal stress responses such as p53 activation.

1.3.3.4 Activation of ribosomal stress responses can lead to various phenotypes

Upon the activation of ribosomal stress responses, cell cycle arrest in the G_1 phase is often observed. It was recently shown that defects in the biogenesis of both ribosomal subunits, by

concomitant deletion of RPs of both subunits, induce a "supra-induction" of p53 in human cells (Fumagalli et al., 2012). Analysis of the cell cycle profile of these cells suggests a blockage of cell cycle progression in either G_1 or G_2/M. It is highly probable that p53 activation can lead to various outcomes, depending on the severity of the RiBi defects, and on the cell types and their intrinsic properties. For instance, activation of the RP-MDM2-p53 pathway in mouse ES cells upon treatment with Actinomycin D or deletion of *Rpl37* leads to apoptosis (Hayashi et al., 2014; Morgado-Palacin et al., 2012).

1.3.3.5 Conclusion: coordinated surveillance of RiBi and proliferation by RPs

Ribosomal proteins have long been considered as sensors of the efficiency of ribosome biogenesis. RPL11 together with RPL5 and the 5S rRNA, and possibly other RPs, appear to function in an internal quality control mechanism, and can trigger ribosomal stress responses in response to defective RiBi. Interestingly, the most frequent outcome is an arrest of the cell cycle before the emergence of nucleolar disorganization and before the depletion of the stocks of ribosomes. Finally, it is also interesting to see that most of the signaling pathways regulating proliferation and pathways involved in responses to other stresses impinge on ribosome biogenesis activity.

2. Heterogeneity of ribosomes confers functional heterogeneity

2.1 The ribosomal filter hypothesis

The idea that ribosomes might display heterogeneity was first suggested in the 1970s, when McConkey and Hauber identified differences in the protein contents in subsets ribosomal subunits from free ribosomes, polysomes and endoplasmic reticulum-bound ribosomes in HeLa cells (McConkey and Hauber, 1975). However, this heterogeneity was not subject to particular attention at the time, and for long ribosomes were still considered as constitutive, homogeneous entities with a "house-keeping" function.

It is only quite recently that renewed interest was granted to the heterogeneity of ribosomes, when studies highlighted the existence of such heterogeneity notably in yeast, invertebrate and mammalian models. Remarkably, such studies have shown that ribosomes can differ from one another at several levels: the primary sequence of rRNAs, post-transcriptional modifications of rRNAs, the presence/absence of some RPs and/or RP paralogs, post-translational modifications of RPs, and factors associated to ribosomes. This has lead to formulation of the "ribosome filter" hypothesis, which proposes the existence of a "ribosomal code" that, in addition to the genetic code, could contribute to an additional layer of regulation of gene expression (Mauro and Edelman, 2007).

In this part, I will present a few examples of ribosome heterogeneity, focusing primarily on studies led in mammalian models.

2.2 Variations in the rRNA sequence: lessons from protozoa and bacteria

In mammals, rDNA genes are present in hundreds of copies in the genome. Whether the transcription of these different copies is subject to differential regulation is unknown, and very little data is available in higher eukaryotes to address this point. However, examples in protozoa and bacteria models suggest that changes in the sequence or mature rRNAs could provide functional heterogeneity.

First evidence of rRNA heterogeneity was brought by the study of the parasite *Plasmodium berghei* (Gunderson et al., 1987). Surprisingly, the authors identified two forms of rRNA in this parasite depending on the phase of its lifecycle: one is found exclusively in the sporozoite stage – when the parasite is in mosquito cells–, whereas another form becomes predominant when the parasite infects mammalian cells. Thus, this parasite expresses two forms of rRNAs during the infection cycle. However, the functional role of these two forms is not clear.

Another example comes from bacteria *E. coli*. Upon stress, the MazF endonuclease is activated, which induces strong repression of global mRNA translation except for a small subset of mRNAs that are specifically involved in stress response and cell death (Vesper et al., 2011). The translation of these mRNAs is in fact ensured by specialized "stress ribosomes". Briefly, MazF cleaves specific subsets of mRNAs around the AUG start codon, thereby generating "leaderless" mRNAs; in addition, MazF also cleaves the rRNA of the small ribosome subunit at the decoding center, which prevents translation initiation of canonical mRNAs, generating modified ribosomes that are selectively translate the leaderless mRNAs. Thus, ribosome heterogeneity at the levels of the rRNA sequence allows efficient response to stress in *E. coli*.

2.3 Post-transcriptional modifications of rRNAs are important for IRES-dependent translation

During their maturation process, rRNAs undergo many post-transcriptional modifications at various sites, catalyzed by enzymes such as Dyskerin (pseudo-uridylation) and Fibrillarin (methylation). Studies in mice expressing a hypomorph Dyskerin encoded by the *Dkc1*^{m} allele display defective post-transcriptional modifications, and cells carrying this allele or cells from *X-linked dyskeratosis congenita* patients (see *Part1 II.2.1.2.3*) exhibit impaired translation initiation of IRES-(Internal Ribosome Entry Site) containing mRNAs (Ruggero et al., 2003; Yoon et al., 2006). Similarly, studies in human immortalized cell lines have shown that Fibrillarin-dependent methylation of rRNAs regulates the translation of IRES-containing mRNAs (Marcel et al., 2013).

2.4 Post-translational modifications of RPs

Ribosomal proteins can undergo different post-translational modifications: methylation, acetylation, phosphorylation, or ubiquitination (Carroll et al., 2008; Lee et al., 2002; Yu et al., 2005). While it is known that many RPs undergo such modifications, their role is not fully understood and the possibility that they contribute to the heterogeneity of ribosomes remains mostly hypothetical. In mammals, the most documented example of RP post-translational modifications is the case of RPS6 phosphorylation by RPS6 kinases (S6Ks), which can phosphorylate RPS6 on 5 different sites in response to mitogenic signals or growth factors (you may remember S6Ks from

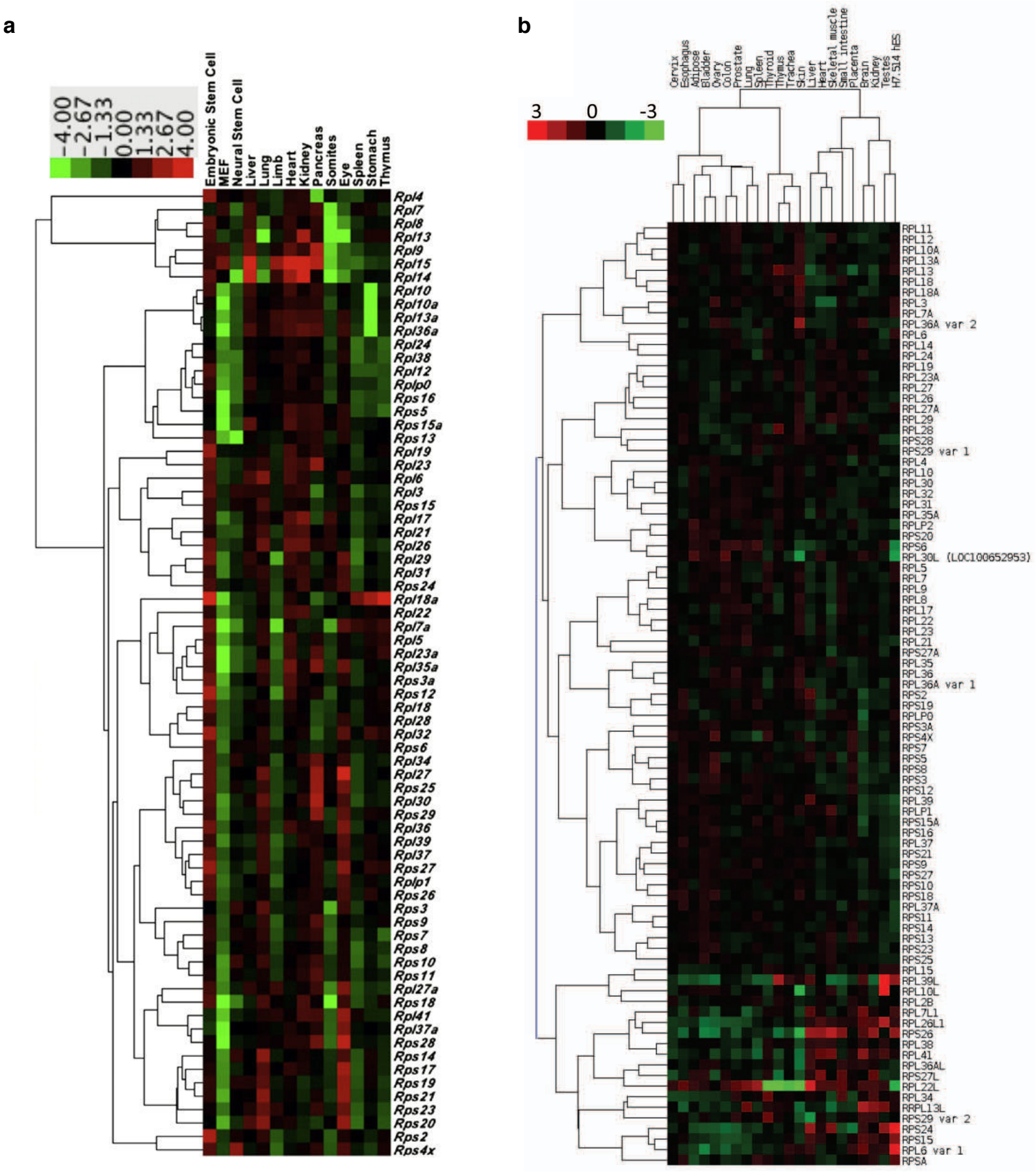

Figure 46. Expression profile of ribosomal proteins in human adult tissues and mouse embryonic tissues

a. Expression profile of RPs in 11 tissues of the developing mouse, mouse embryonic stem cells and fibroblasts or neural stem cells. **b.** Expression profile of RPs in 21 human adult tissues and human embryonic stem cells (H7.514 hES). Color codes indicate the relative gene expression in Log_2 scale.

Adapted from Kondrashov et al., 2011; Wong et al., 2014

part *I.1.2.1.1*). It has been suggested that RPS6 phosphorylation could be required for the translation of TOP mRNAs, although initial studies of *rpS6*$^{P-/-}$ mice homozygous for a non-phosphorylable RPS6 allele indicated that RPS6 was not implicated in this regulation (Ruvinsky et al., 2005). However, *rpS6*$^{P-/-}$ cells are smaller, and a more recent study suggests that RPS6 phosphorylation has a negative regulatory effect on global translation initiation (Chauvin et al., 2014).

2.5 Non-homogeneous expression of RPs within the same organism

2.5.1 Tissue-specific expression of RP paralogs

Numerous RP paralogs have been identified in yeast, plant and drosophila. Resulting from duplications, the different copies of a given RP are not necessarily redundant, and have sometimes evolved specific functions and/or expression patterns (for review, see (Xue and Barna, 2012)). In mammals, while many RP pseudogenes can be found, only few paralogs have been identified, a few examples of which I will present here.

In mouse, paralogs have been identified for RPL10, RPL22 and RPL39, respectively named RPL10-like, RPL-22-like and RPL39-like. Interestingly, all three "original" RPs are highly expressed in liver, mammary gland and testis, wheras their paralogs display restricted expression to testis, except for RPL22-like which is expressed at low levels in mammary gland and liver (Sugihara et al., 2010). A paralog for RPL39 has also been identified in human, which is also specifically expressed in testis at the mRNA level. Furthermore, paralogs have been identified for human RPS4, encoded by three genes: *RPS4X* on the X chromosome, and *RPS4Y1* and *RPS4Y2* on the Y chromosome. Little is known regarding the regulation of *RPS4X* and *RPS4Y1*, but *RPS4Y2* expression is restricted to testis and prostate (Lopes et al., 2010).

These studies show that RPs can be differentially expressed between tissues, and could therefore have different functions. Interestingly, the paralogs mentioned here exhibit specific expression in male genital organs, suggesting a role in male gametogenesis or gonad development.

2.5.2 RPs in general exhibit different expression profiles

A few studies have brought information on the expression profile of several RPs at the mRNA level, in different tissues in human and during mouse development (Figure 46). Surprisingly, this revealed important heterogeneity in the expression of several RPs in the analyzed tissues, which I will discuss in part *II.3.1.1*.

2.6 Conclusion: ribosome heterogeneity for different translational programs?

The different studies presented above highlight different possible sources of ribosome heterogeneity in mammals. However, the data available to date cannot formally ascertain that heterogeneous ribosomes exist within the same cell, tissue or organism or during development. Some studies suggest that distinct ribosomes could have specific affinity for certain subsets of mRNAs, and thus promote specific translational programs. One can propose that the use of different types of ribosomes could allow cells to regulate gene expression directly at the level of mRNA translation, and that changing the composition of some ribosomes could allow a rapid response in particular situations, notably in response to stress.

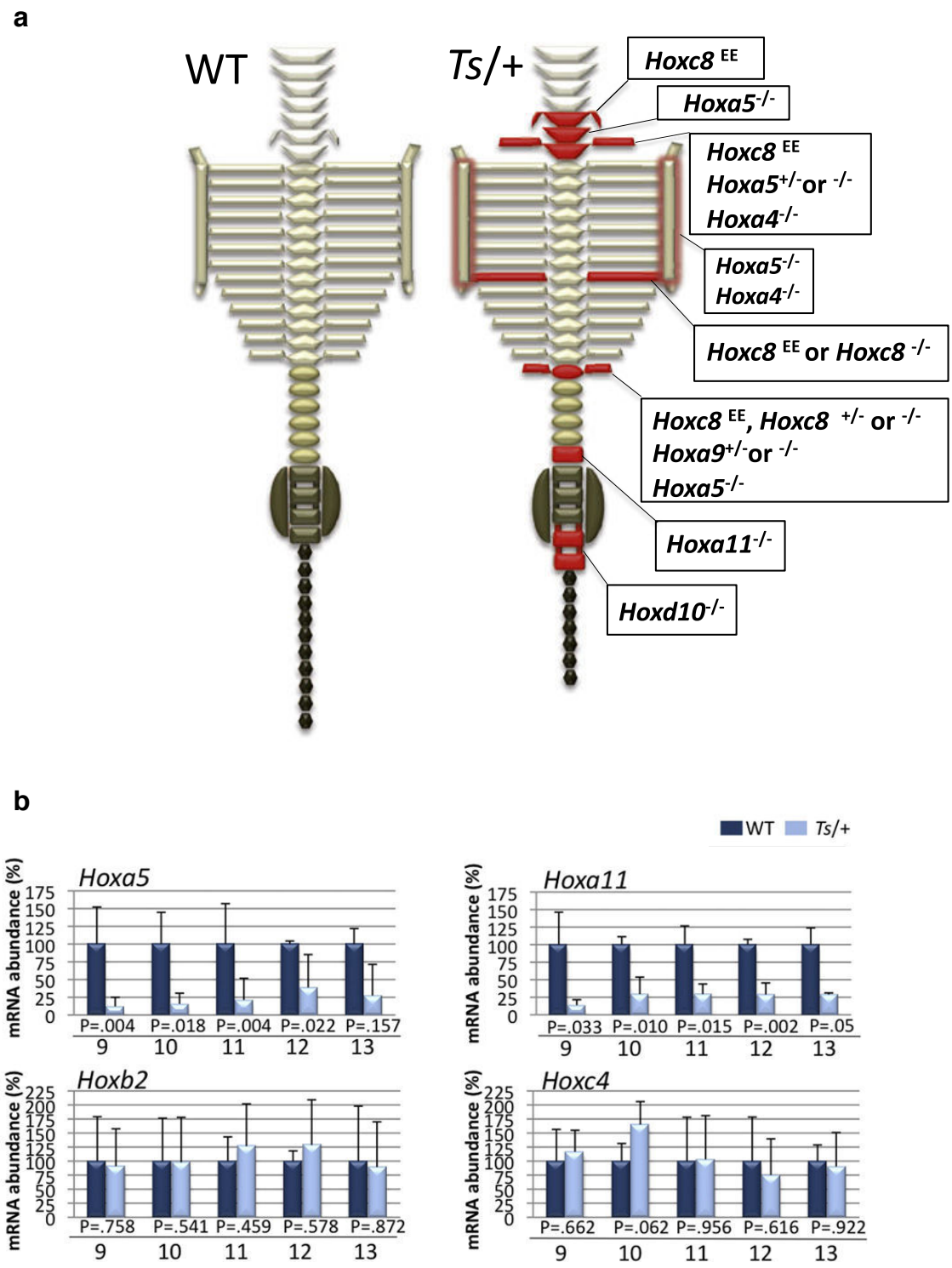

Figure 47. RPL38 regulates the expression of *Hox* gene subsets during mouse development

a. Schematic representation of the skeletal axis in wild-type (WT, left) or *Rpl38* haploinsufficient (*Ts*/+, right) mice. Defects observed in *Ts*/+ mice are indicated in red, and mutations of *Hox* genes leading to similar defects are listed on the right: this shows that defects in *Ts*/+ mice recapitulate those induced by the inactivation of several *Hox* genes. **b.** RT-qPCR analysis of mRNAs being translated in neural tube and somites. Fractions 9 to 13 represent polysome fractions after sucrose gradient separation. The association of mRNA with polysomes in *Ts*/+ vs. WT mice is observed for 8 of the 39 *Hox* genes: representative graphs for *Hoxa5* and *Hoxa11* genes are presented (top row). Graphs for *Hoxb2* and *Hoxc4* genes are representative of *Hox* genes for which mRNA association with polysomes is not affected in *Ts*/+ mice.

Adapted from Kondrashov et al., 2011

Other sources of ribosome heterogeneity have also been proposed, that could also contribute to an additional layer of regulation, such as the subcellular localization of ribosomes. Finally, besides heterogeneity in the composition of ribosomes, the existence of alternative ribosome biogenesis pathways could be proposed, as suggested by the results we have obtained in the laboratory with the study of *Notchless* (see *Results* and *Discussion*). Could such alternative pathways contribute to the production of different ribosomes, with distinct translational programs?

3. Regulatory roles for ribosomes in multicellular organisms in normal or pathological situations

3.1 In normal conditions

3.1.1 Regulatory roles for ribosomes during development

Mutations in genes encoding RPs are associated with developmental defects in several species. In Drosophila the "minute" mutants exhibit various phenotypes including delayed development, shorter and thinner bristles, and infertility (Lambertsson, 1998; Marygold et al., 2007). In plants or zebrafish, mutations in RPs also lead to various developmental defects, and haplo-insufficiency of some RPs is associated to increased tumorigenesis in zebrafish (Byrne, 2009; Horiguchi et al., 2012; Lai et al., 2009). The tissue-specificity of these phenotypes is surprising at first, but can be explained by different rational elements. First, since proliferative cells require important protein synthesis, they could be particularly sensitive to haploinsufficiency of RPs. Furthermore, some RPs can have extra-ribosomal functions particularly required in some tissues and cell types (see (Zhou et al., 2015) for review). Finally, haploinsufficiency in some RPs can lead to qualitative changes of translation, as illustrated by the inhibition of *RPS6* expression in human cells which leads to increased TOP mRNA translation despite decreased global translation (Fumagalli et al., 2009). *In vivo*, such changes could lead to specific defects in some tissues and/or during development.

3.1.2 Role of RPL38 in the regulation of *Hox* genes during development

In a recent study, Kondrashov *et al.* showed that RPL38 is specifically required for the translation of some *Hox* genes and thus for tissue patterning in mouse. Haploinsufficiency of *Rpl38* leads to homeotic transformations that recapitulate the phenotype induced by mutations of several *Hox* genes (Figure 47.a). Global translation was not affected in *Rpl38*-insufficient mice, but RT-qPCR analysis of mRNAs that are being translated in the neural tube and somites showed that RPL38 is required for the translation of some *Hox* genes (8 out of 39) in these tissues (Figure 47.b). Altogether, this indicates that RPL38 exerts specific translational control over these mRNAs, probably by regulating formation of the 80S complex on the mRNAs of the affected *Hox* genes.

Furthermore, the authors analyzed the expression profile of *Rpl38* in mouse embryos: strikingly, *Rpl38* mRNAs are expressed at higher levels in the tissues affected in haploinsufficient mice, notably in developing somites and precursors of the vertebras.

This study showed for the first time in mammals the participation of an RP in regulating developmental processes, through the specific translation of mRNA subsets. Based on the

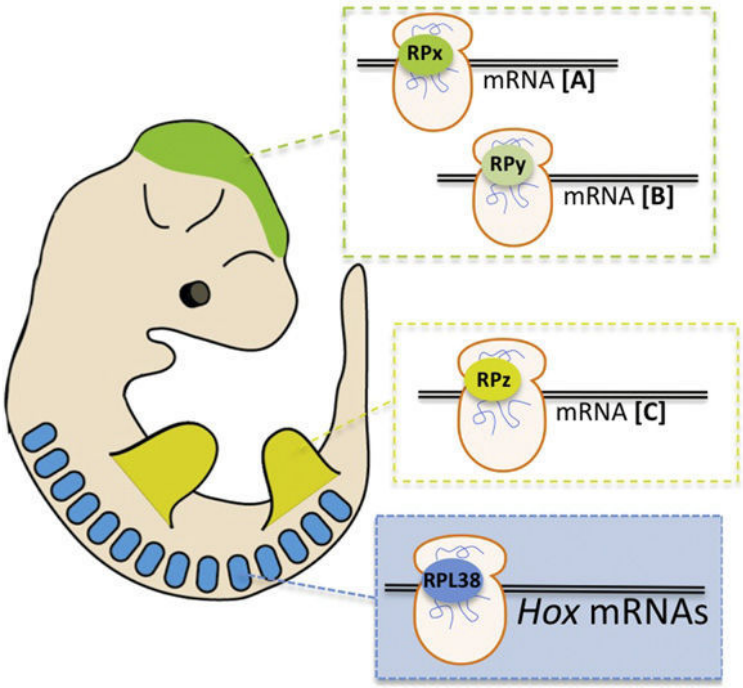

Figure 48. Proposed model for the control of gene expression by RPs during embryogenesis

The expression of some RPs is enriched in some tissues, which could participate in the regulation of developmental processes by specifically regulating the translation of some mRNAs. Notably, RPL38 exerts translational regulation of some *Hox* mRNAs. Blue: somites; yellow: limbs; green: brain.

Adapted from Kondrashov et al., 2011

heterogeneous expression profile of several RPs in the mouse embryo (Figure 46.a), the authors further suggest that other RPs could play a similar regulatory role by controlling the expression of other genes important for development (Figure 48).

3.1.3 A regulatory role for ribosomes in stem cells?

Several independent studies suggest that ribosome biogenesis factors are particularly important for the maintenance of stem cells, in different systems.

Several nucleolar factors have been identified as important regulators of embryonic stem cells. Notably, a gain-of-function screen in mouse ES cells identified Mki67ip as a regulator of pluripotency (Abujarour et al., 2010). Mki67ip and Nucleophosmin are highly expressed in ES cells and during development; in ES cells, they interact to maintain their proliferation and pluripotency. Among its multiple functions, Nucleophosmin regulates RiBi at several levels (for review, see (Lindström, 2011)). Another screen in mouse ES cells has identified that several factors involved in biogenesis of the small subunit or required for their maintenance (You et al., 2015). Nucleolin, another multifunctional nucleolar protein, was also identified as a regulator of ES cell self-renewal, and is an important regulator of rDNA transcription (Durut and Sáez-Vásquez, 2015; Yang et al., 2011). In addition, Nucleostemin was also shown to be highly expressed in ES cells, and is involved in biogenesis of the large ribosomal subunit (Romanova et al., 2009; Tsai and McKay, 2002). Finally, a recent study showed that Fibrillarin, a critical methyltransferase for rRNA processing, is very highly expressed in ES cells (Watanabe-Susaki et al., 2014). Strikingly, maintaining Fibrillarin expression in ES cells prolonged their pluripotency state in the absence of LIF (a factor used in the culture medium of ES cells to promote pluripotency).

In zebrafish, several genes encoding RiBi factors are highly expressed in neuroepithelial progenitors, including *Notchless* which we have shown is involved in biogenesis of the large ribosome subunit in mouse (see *Results* and *Discussion*) (Recher et al., 2013). Similarly, a recent transcriptomics analysis has identified an enrichment of RiBi factors in human naïve pluripotent stem cells (Huang et al., 2014). In Drosophila, several studies have shown that genes involved in ribosome biogenesis are enriched and/or essential in female germline stem cells and neuroblasts (Buszczak et al., 2014; Fichelson et al., 2009; Neumüller et al., 2008; 2011). Important rDNA transcription also seems to be a common feature of stem cells in different systems. In Drosophila, increasing RNA Pol I dependent transcription delays differentiation of female germline stem cells, whereas reduced rRNA production induces morphological and transcriptional changes associated with differentiation (Zhang et al., 2014). Similarly, downregulation of rRNA levels in hematopoietic cell lines and HSCs cultured *ex vivo* was recently shown to induce differentiation (Hayashi et al., 2014).

Altogether, these studies support the idea that regulation of ribosome biogenesis is particularly important for the maintenance of stem cell properties.

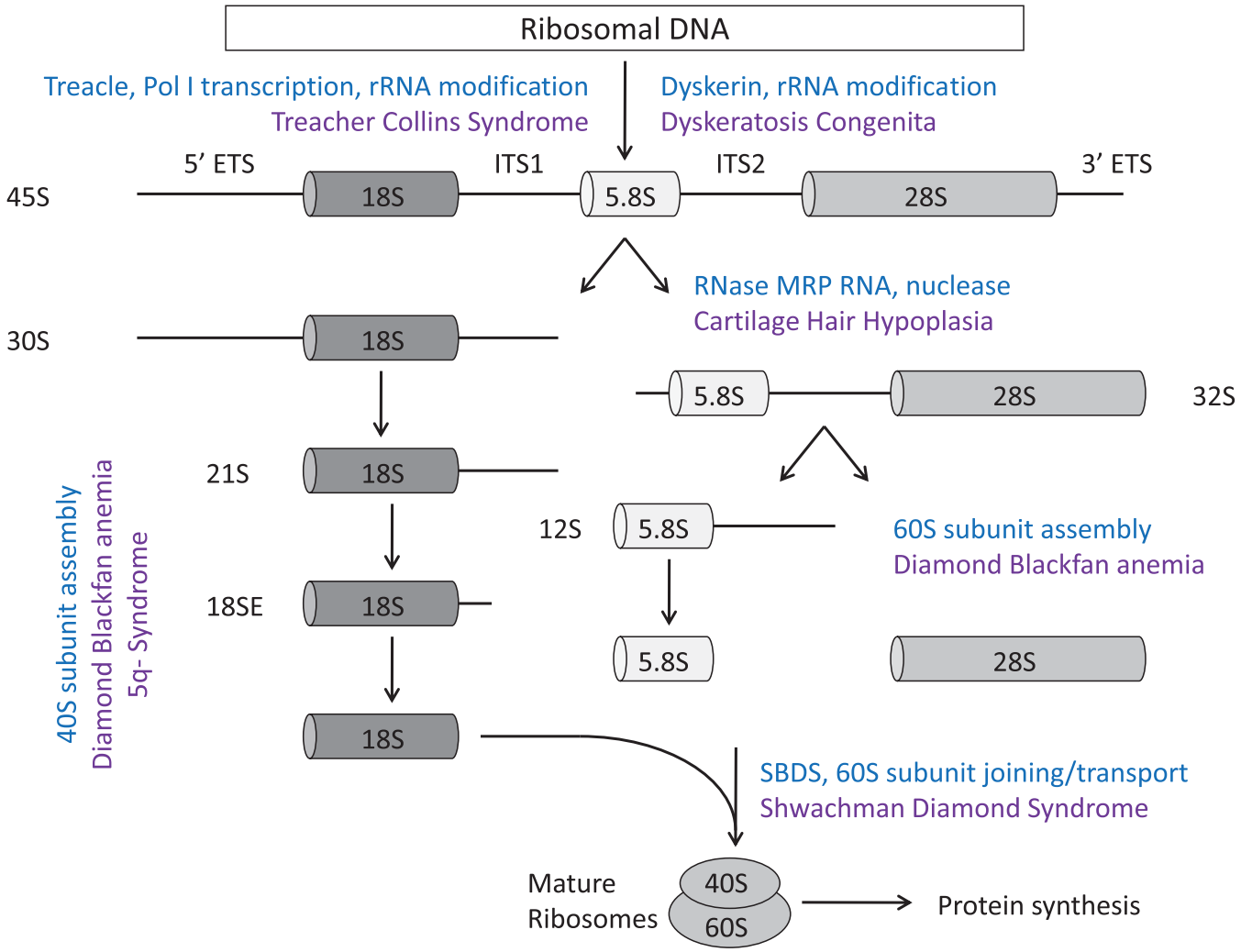

Figure 49. Ribosome biogenesis defects involved in ribosomopathies

Schematic representation of ribosome biogenesis in mammals. Examples of known mutations are noted in blue at the affected steps, and associated ribosomopathies are noted in purple.

Adapted from Narla and Ebert, 2010

3.2 In pathological situations

3.2.1 Ribosomopathies: genetic disorders of ribosome dysfunction

The appellation "ribosomopathy" regroups several syndromes associated to genetic abnormalities affecting genes involved in ribosome function and biogenesis, and that present with specific clinical phenotypes (Figure 49 and Table 4). These rare diseases are the subject of recent studies and reviews (see for instance (Danilova and Gazda, 2015; De Keersmaecker et al., 2015; Narla and Ebert, 2010)). It is in 1999 that mutations in the gene encoding RPS19 were identified for the first time in patients with Diamond-Blackfan Anemia (DBA; (Draptchinskaia et al., 1999)). DBA is a rare congenital disease characterized by severe anemia and other possible hematopoietic defects; malformations and growth retardation are also observed (see (Ball, 2011) for review). Today, heterozygous mutations in several other genes encoding RPs have been associated to DBA. Strikingly, other syndromes linked to defects in RiBi are also associated to abnormal developmental and hematopoietic defects, in particular of the erythroid lineage: (1) the Schwachman-Diamond syndrome, for which 90% of mutations are found in the *SBDS* gene (for Schwachman-Bodian-Diamond Syndrome) encoding a protein implicated in the maturation and transport of the large ribosome subunit; (2) *Dyskeratosis congenital* (DC), for which mutations are found in genes involved in the telomerase complex (see *Part 1 II.2.1.2.3*) and in *Dyskerin* which induces defects in rRNA maturation ; (3) Cartilage hair hypoplasia, for which mutations are found in the *RMRP* gene encoding an RNA that is part of a ribonucleoproteic complex involved in several steps of rRNA synthesis. The 5q- syndrome is an acquired myelodysplastic syndrome (MDS) presenting with macrocytic anemia and similarities with DBA, and is characterized by loss of part of the long arm of chromosome 5 (hence the name 5q-); haploinsufficiency in *RPS14* –which is in the deleted region– has been proposed to cause the erythroid phenotype observed in this syndrome (Pellagatti et al., 2008; Schneider et al., 2016). Finally, the hematopoietic tissue is not always affected in ribosomopathies: for instance, the Treacher-Collins syndrome is characterized by abnormal cranio-facial development associated with mutations in the *TCOF1* gene causing defective rDNA transcription and rRNA methylation.

3.2.2 Why is the hematopoietic system, and especially the erythroid lineage, particularly affected in ribosomopathies?

As we discussed earlier, some RPs are proposed to have extra-ribosomal functions (Warner and McIntosh, 2009). Thus, one can wonder whether the phenotypes observed in ribosomopathies are due to RiBi defects or to these extra-ribosomal functions of RPs. Anemia and some developmental defects are a common trait of several ribosomopathies, associated to mutations in different genes involved in RiBi of ribosome function. Thus, it seems reasonable to think that it is RiBi defects that are responsible for these phenotypes. How can modifications in such a ubiquitous process induce such cell type-specific phenotypes? Why are hematopoietic cells, and particularly cells of the erythroid lineage affected? Here, I discuss some possible explanations.

As I mentioned in *II 3.1.1*, one can reasonable think that highly proliferative cells could be especially sensitive to RP haploinsufficiency and subsequently reduced production of ribosomes. Indeed, hematopoietic progenitors, in particular erythroid-restricted progenitors, exhibit very high

Disease	Genetic defect	Gene function	Congenital or acquired?	Clinical characteristics	Cancer risk
Diamond Blackfan Anemia (DBA)	RPS19, RPS24, RPL35a, RPS17, RPL5, RPL11, RPS7, RPS10, RPS26	Ribosomal proteins required for ribosome biogenesis	Congenital	Macrocytic anemia; growth retardation; craniofacial malformations; thumb, limb and heart defects	Myelodysplastic syndrome (MDS), AML and solid tumors
5q- syndrome	RPS14, one of ~40 genes in CDR	Ribosomal protein required for ribosome biogenesis	Acquired	Macrocytic anemia; micromegakaryocytosis and thrombocytosis	Acute myeloblastic leukemia (AML)
Shwachman–Diamond syndrome (SDS)	SBDS	Maturation of 60S ribosomal subunit and 60S–40S subunit joining	Congenital	Bone marrow dysfunction; pancreatic insufficiency; skeletal abnormalities; short stature	AML and MDS
X-linked dyskeratosis congenital (DKC)	DKC1	Nucleolar protein associated with snoRNPs. Modifies rRNA. Component of telomerase complex	Congenital	Skin and nail abnormalities; bone marrow failure	High risk of cancer
Cartilage hair hypoplasia (CHH)	RMRP	RNA component of RNase MRP complex. Cleaves precursor rRNA. Role in mitochondrial DNA replication	Congenital	Short-limbed dwarfism, hypoplastic hair, defective erythropoiesis and immunity	7-Fold higher incidence of cancer
Treacher Collins syndrome (TCS)	TCOF1 POLR1D POLR1C	Nucleolar protein with role in pre-ribosomal processing and ribosome biogenesis. RNA polymerase I and III components	Congenital	Craniofacial abnormalities	None known

Table 4. Ribosomopathies: characterization and molecular defects

Adapted from Teng et al., 2013

proliferation rates. Therefore, these cells require important protein synthesis and thus important ribosome biogenesis, and so could be particularly affected by RiBi defects. However, other cell types with high proliferative activity in the organism, such as intestinal crypt cells, have not been described affected in patients with ribosomopathies, suggesting that high proliferation alone does not explain the extreme sensitivity of cells of the erythroid lineage.

Some ribosome biogenesis defects or altered composition of ribosomes could also specifically impact on the translation of mRNAs that are particularly important for the erythroid lineage. For instance, RPS19 or RPL11 haploinsufficiencies –which are associated to DBA– affect proliferation and differentiation of p53-deficient murine erythrocytes in culture (Horos and Lindern, 2012). Analysis of mRNAs recruited on polysomes in these cells, it was shown that RPS19 or RPL11 haploinsufficiency affects the translation of IRES-containing mRNAs, including *Bag1* and *Csde1*, which play important for proliferation and differentiation in the erythroid lineage. Interestingly, the protein levels of BAG1 and CSDE1 are decreased in erythroblasts of DBA patients *in vivo*, suggesting that reduced translation of these genes could indeed explain part of the phenotype in DBA, independently of p53. This is supported by the finding that IRES-dependent translation is also affected in mouse cells with hypomorphic Dyskerin and cells from patients with X-linked DC, as we discussed earlier.

Finally, activation of p53 by ribosomal stress in response to perturbed RiBi could also play a role in the physiopathology of ribosomopathies. Indeed, nuclear accumulation of p53 in observed *in vivo* in biopsies from DBA and 5q- syndrome patients (Barlow et al., 2010; Dutt et al., 2011; Pellagatti and Boultwood, 2015; Pellagatti et al., 2010). *Ex vivo*, inactivation of *RPS14* or *RPS19* in human hematopoietic cells in culture leads to accumulation of p53, cell cycle arrest and increased apoptosis, indicative of the activation of a ribosomal stress response. Interestingly, the defects arise specifically in the erythroid lineage and not other lineages, indicating that this lineage is particularly sensitive to reduced expression of RPs (Dutt et al., 2011). Several studies in animal models of ribosomopathies have investigated the role of p53 in these pathologies. In zebrafish, knockdown or *Rps19* or *Rpl11* leads to developmental defects and hematopoietic abnormalities in the erythroid lineage, thus recapitulating phenotypes observed in DBA; in these models, RP deficiency leads to the activation of p53 through induction of ribosomal stress and DNA damage responses (Danilova et al., 2008; 2014; 2011). Inhibition of p53 partially rescues the hematopoietic defects in *Rpl11*-deficien embryos, and treatment with exogenous nucleosides (to inhibit DNA damage response) rescues these defects in both *Rps19*- and *Rpl11*-deficient embryos. In mouse, *Rps19* deficiency also recapitulates the DBA phenotype, and disruption of the 5S RNP-MDM2 interaction in *Rps19*-deficient mice rescues most erythroid defects observed in these mice (Jaako et al., 2015; 2011). Finally, a mouse model of the 5q- syndrome is characterized by macrocytic anemia and decreased number of hematopoietic progenitors, accompanied by p53 activation and important apoptosis of hematopoietic cells (Barlow et al., 2010). Altogether, these studies suggest that activation of the p53 pathway is a common response to RP deficiency that could be implicated in the physiopathology of ribosomopathies. However, it is important to note that these animal models do not recapitulate exactly the pathology in human, and notably erythroid defects do not always reflect those of ribosomopathy patients.

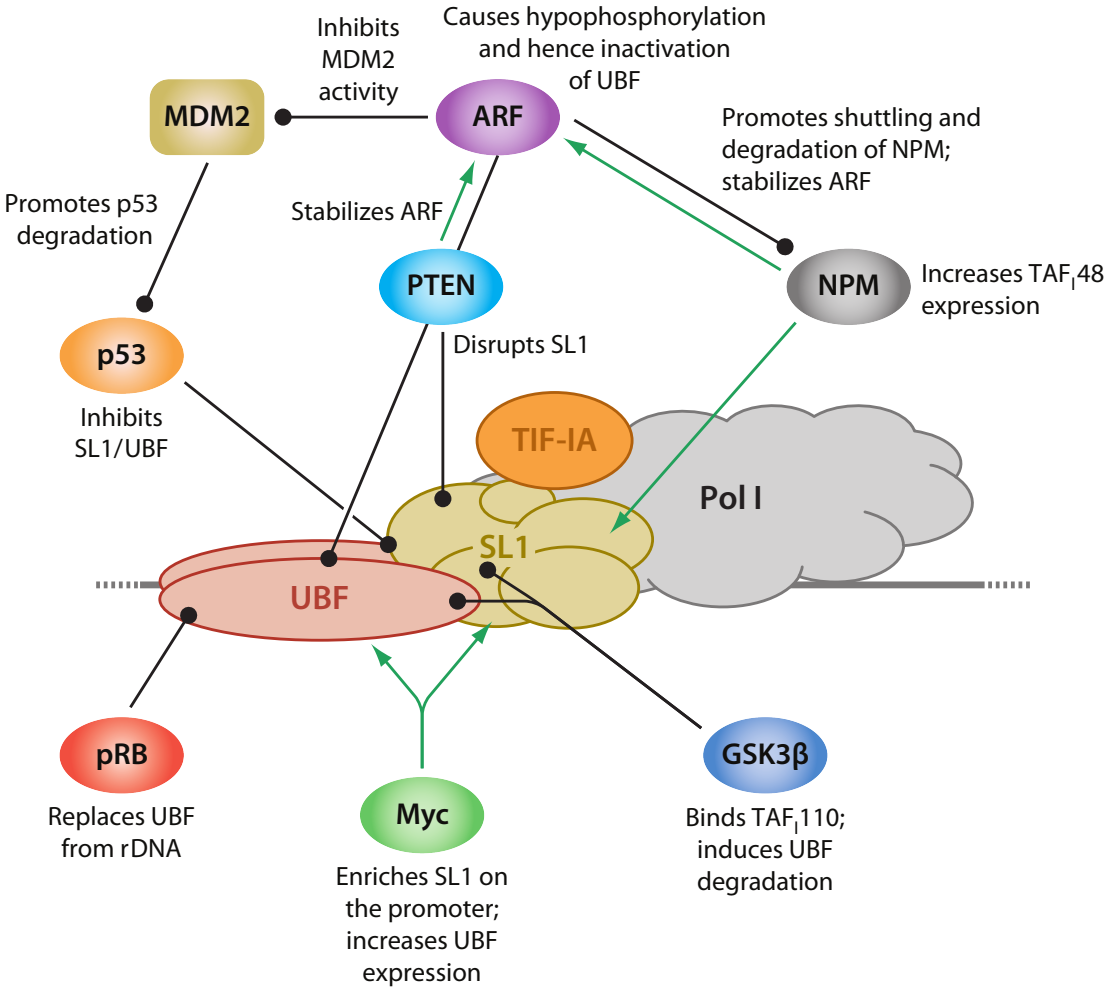

Figure 50. Regulation of RNA Pol I dependent transcription by oncogenes and tumor suppressors

Oncogenes promote rDNA transcription by increasing the expression of factors associated to RNA Pol I, and/or through modifications of the protein-protein or protein-DNA interactions (green arrows). Tumor suppressors inhibit rRNA synthesis through interactions with assembly of the pre-initiation complex (black arrows).

Adapted from Drygin et al., 2010

3.2.3 Complex relationships between ribosomes and cancer

3.2.3.1 Important ribosome biogenesis activity is associated to tumorigenesis

Alterations of RiBi or of the expression of RPs are also often observed in some cancers, suggesting the existence of a link between ribosomes and cancer. Indeed, several oncogenes and tumor suppressors have been identified as regulators of ribosome biogenesis, notably through regulation of rDNA transcription (Figure 50; for reviews, see (Drygin et al., 2013; 2010; Hannan et al., 2013; Stępiński, 2016)). Oncogenes promote RNA Pol I dependent transcription, whereas tumor suppressors impede the assembly of the pre-initiation complex, suggesting a link between high RiBi activity and malignant transformation. Consistently, several inhibitors of rRNA synthesis are used today as anti-cancer therapeutic treatments (Table 5; for review, see (Drygin et al., 2013; Hannan et al., 2013)).

3.2.3.2 Haploinsufficiency of RPs or RiBi factors is also associated to cancer

Surprisingly, haploinsufficiency of RPs or factors involved in RiBi is also associated with increased risk of cancer. In zebrafish, heterozygous loss-of-function mutations of RPs lead to decreased relative expression of the ribosome subunit to which they belong, which could be expected; however, very surprisingly, haploinsufficiency of some of these RPs was associated with the development of tumors of different origins, suggesting a role of tumor suppressor for these RPs (Amsterdam et al., 2004; Lai et al., 2009). This tumor suppressor role could be due to extra-ribosomal functions, although the number of such RPs leads to believe that it is linked to their function in the ribosome. Finally, in human, patients with ribosomopathies also have increased risk of developing cancers, notably of hematopoietic origins (Narla and Ebert, 2010; Xu et al., 2016).

3.2.3.3 Possible explanations: defective p53 activation

Some RPs and RiBi-associated factors are required for the activation of p53. In the context of ribosomal stress, while RiBi defects or haploinsufficiency of some RPs lead to p53 activation, deficiency of *Rpl5* or *Rpl11* fails to activate the tumor suppressor (Teng et al., 2013). Thus, mutations in *RPL5* or *RPL11* observed in some DBA patients could similarly impede activation of p53, which could be in part responsible for their increased risk of cancer. A recent study in mouse has shown that deficiency for *Runx1* –a gene found mutated in myelodysplastic syndromes and leukemia– leads to reduced growth in HSCs due to reduced RiBi activity; strikingly, this was accompanied by a reduction of p53 basal levels and resistance to stress, providing a selective advantage to *Runx1*-deficient HSCs, which eventually outcompete WT HSCs. Furthermore, this suggests that pre-leukemia stem cells that have acquired *Runx1* deficiency could also have a selective advantage, increasing their chances of acquiring additional oncogenic mutations and, in time, leading to the development of leukemia. This could have important implications in the development of myelodysplastic syndromes, as well as in the increased risk of cancer observed in ribosomopathies.

Drug	Mechanism of action	Impact on ribosome biogenesis	Impact on nucleolus	Cancer type(s)
5-Fluorouracil	Thymidylate synthase, incorporates into 47S pre-rRNA	Impairs late rRNA processing	No effect	Colon, esophageal, gastric, rectum, breast, biliary tract, stomach, head and neck, cervical, pancreas, renal cell, and carcinoid cancer
Actinomycin D	Intercalates into GC-rich duplex DNA	Inhibits Pol I transcription at low nano-molar concentrations	Nucleolar disintegration	Wilms tumour and Ewing sarcoma
Camptothecin (Topotecan and Irinotecan)	Inhibits Topoisomerase I	Modulates early rRNA processing	Nucleolar disintegration	Ovarian, lung, colon and cervical cancer
Cisplatin	DNA cross-linking via alkylating DNA bases	Inhibition of Pol I transcription	Nucleolar disintegration	Testicular, bladder, lung, esophagus, stomach, ovarian sarcoma, lymphoma
CX-3543	Disrupts nucleolin/rDNA G-quadruplex complexes	Selective inhibition of Pol I transcription (elongation)	Redistribution of nucleolin, no effect on fibrillarin	Phase I clinical trial Carcinoid and neuroendocrine tumors
CX-5461	Inhibits SL-1 pre-initiation complex formation at the rDNA	Selective inhibition of Pol I transcription (initiation)	Nucleolar disintegration	Phase I clinical trial AML, multiple myeloma, lymphoma
Doxorubicin	Intercalates into DNA and inhibits Topoisomerase II	Inhibition of Pol I transcription	Nucleolar disintegration	Bladder, breast, stomach, lung, ovarian and thyroid cancer, leukemia, Hodgkin's lymphoma, myeloma
Homoharringtonine	Translation inhibitor, prevents elongation	Impairs late rRNA processing	No effect	Chronic myelogenous leukemia (CML)
Mitomycin C	Interstrand DNA cross-linking via alkylating 5-CpG-3 guanosine	Inhibition of Pol I transcription	Nucleolar disintegration	Adenocarcinoma stomach, pancreas, anal, bladder, breast, cervical, colorectal, head, neck, and non-small cell lung cancer
Mitoxantrone	Topoisomerase II inhibitor and intercalates into DNA	Inhibition of Pol I transcription	Nucleolar disintegration	Breast, prostate, liver cancer, myeloid leukemia, non-Hodgkin's lymphoma
Oxaliplatin	DNA cross-linking via alkylating DNA bases	Inhibition of Pol I transcription	Nucleolar disintegration	Esophagus, stomach cancer, colorectal carcinoma
Temsirolimus everolimus	mTOR inhibitors	Inhibition of Pol I transcription	No effect	Renal cell carcinoma, subependymal giant cell astrocytoma (SEGA), progressive neuroendocrine tumors of pancreatic origin (PNET), subependymal giant cell astrocytoma (SEGA) associated with tuberous sclerosis (TS)

Table 5. Clinically approved drugs that have therapeutic effects associated with disruption or RiBi

Adapted from Hannan et al., 2013

4. Conclusion

Although ribosomes have long been considered as homogeneous, constitutive entities with only a house-keeping function, a large number of studies now support the idea that ribosomes could play an important regulatory role, at the level of the cell as well as in multicellular organisms. Several sources of ribosome heterogeneity have been proposed, which could participate in functional heterogeneity; however, clear-cut evidence of the existence of heterogeneous ribosomes are still lacking. The specific recognition of subsets of mRNAs linked to the cap and IRES or TOP sequences seems to participate to the functional specificity of ribosomes. Finally, diseases associated with defective ribosome biogenesis and/or ribosome function, i.e. ribosomopathies and some cancers, strongly support the idea of a regulatory role of ribosomes and also weigh in favor of the existence of ribosome heterogeneity. One of the main challenges today will be to understand whether these dysregulations are due to changes in the translational activity of ribosomes, and/or to the detection of RiBi defects leading to the activation of ribosomal stress responses.

Objectives

The team of Michel Cohen-Tannoudji, in which I did my thesis, is interested in understanding the regulation of fundamental cellular processes in stem cells, and the contribution of such processes in the maintenance of stem cell properties. Indeed, stem cells present particular characteristics in fundamental processes such as cell cycle control, energetic metabolism or DNA damage stress response, which distinguish them from progenitor and differentiated cells. Recently, ribosome biogenesis has been proposed to play an important role in the regulation of stem cells. Thus, during my thesis I have studied the role of ribosome biogenesis regulation in the maintenance of stem cells, and how stem cells respond to defects in this process. To do this, I have used two main approaches.

First, I have participated to the study of the role of *Notchless (Nle)*, coding for a ribosome biogenesis factor, in the regulation of stem cell populations in the mouse. When I joined the team, it had been shown that *Nle* inactivation in the adult mouse leads to the elimination of adult stem cell populations; however the mechanisms underlying stem cells elimination were not fully elucidated. Thus, I investigated the cellular and molecular responses elicited following *Nle* inactivation, using *ex vivo* and *in vivo* models. I asked whether the RiBi defects induced by *Nle* loss-of-function lead to the activation of ribosomal stress responses. In particular, I analyzed whether the RP-MDM2-p53 pathway was activated in *Nle*-deficient cells and I tried to determine how these responses participate to the phenotype observed following *Nle* loss-of-function. To that end, I first turned to an *ex vivo* approach, using embryonic stem cells as a model. In addition, I and colleagues investigated the role of p53 in the response to *Nle* inactivation, using both *in vivo* and *ex vivo* models allowing the deletion of *Nle* in a p53-deficient background. Furthermore, the team has shown that despite the apparently essential role of *Nle* in RiBi in some cells, other cell populations, such as the B lymphoid lineage in the hematopoietic system, do not require *Nle* for the synthesis of ribosomes. This was surprising, and raised the question of whether *Nle* could also dispensable in other populations. To address this point, I investigated the requirement of *Nle* for progenitor and differentiated cells of the T lymphoid lineage, using an *in vivo* model allowing conditional *Nle* inactivation specifically in this lineage. Finally, initial work on *Nle* in our laboratory showed that *Nle* is critically required during early embryonic development at the moment of implantation, but it remained unclear whether *Nle* deficiency affected each of the first embryonic lineages differently. Using new tools available, I participated to the re-visited study of the requirement of *Nle* during the establishment of the first embryonic lineages, *in vivo* in the early embryo and using *ex vivo* models of these lineages.

My second goal was to characterize RiBi activity *in vivo* in the mouse. Indeed, while the regulation of RiBi has been well documented in unicellular organisms and in *ex vivo* models, surprisingly little is known regarding its regulation in multicellular organisms *in vivo*. Motivated by this lack of knowledge, I have developed and used different methods to measure pre-rRNA levels and rRNA neo-synthesis in the mouse hematopoietic system, *in vivo* at homeostasis. My findings have prompted me to also analyze the translational activity of these cells, and to analyze the RiBi activity of stem cells and immature progenitors of the human hematopoietic system. Finally, this work has unraveled previously unsuspected ribosome biogenesis activity in hematopoietic stem cells, suggesting that ribosome biogenesis plays an important role in their regulation.

Results

Results

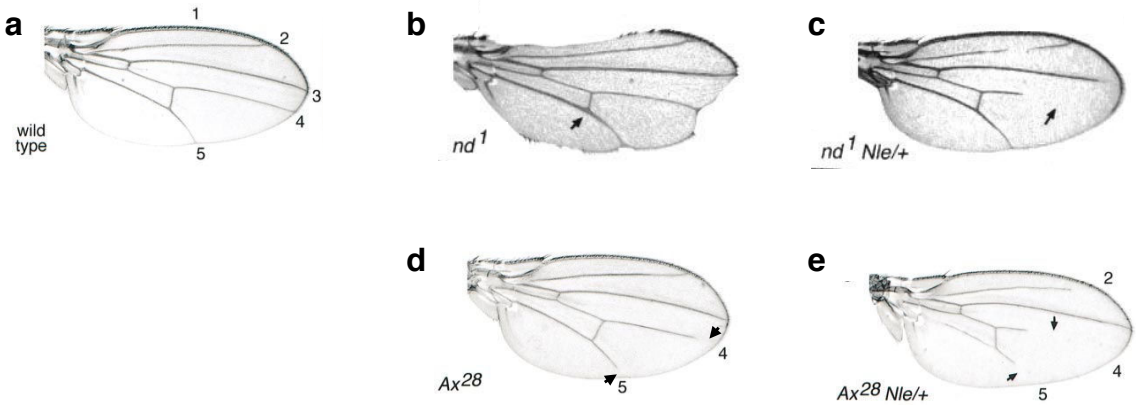

Figure R1. Examples of genetic interactions between *Nle* and *Notch* in Drosophila

a. Wing of a wild-type drosophila; numbers designate wing veins. **b.** Wing in a *Notchoid (nd[1])* background: this phenotype is characterized by notches on the wing, sign of a decreased Notch activity. **c.** Deletion of one *Nle* allele rescues the notches phenotype in the wing. **d.** Wing in an *Abruptex (Ax[28])* background: this phenotype is characterized by shortened veins 4 and 5 in the wing (arrows) due to increased Notch activity. **e.** Deletion of one *Nle* allele enhances this phenotype, leading to even shorter veins in the wing (arrows).

Adapted from Royet et al., 1998

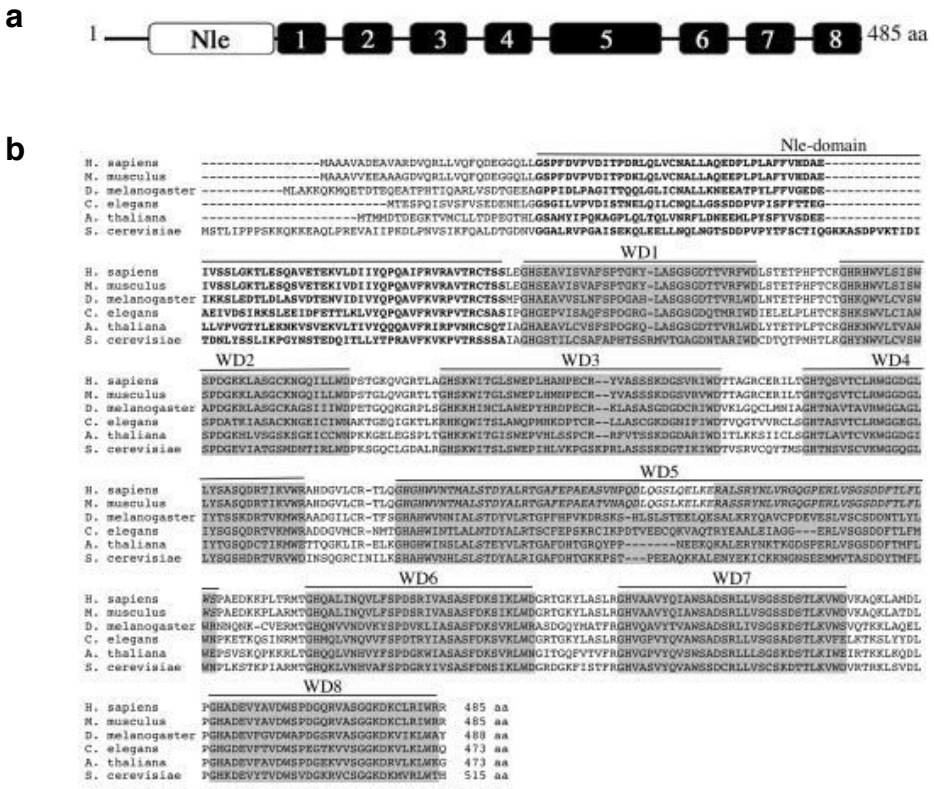

Figure R2. *Nle* is conserved throughout the eukaryote domain

a. Schematic representation of the mNle protein containing a single Nle domain (white box) at its N-terminal region, and 8 WD40 domains (black boxes). **b.** Alignment of amino acid sequences of *Nle* orthologs in the indicated species. Although a search for WD40 domains using bioinformatics tools available at the time of publication of *Cormier et al., 2006* predicted 9 WD40 domains for human and mouse and 8 for other species (highlighted in grey boxes), comparison of amino acid sequences suggest that the fifth and sixth domain found in human and mouse actually correspond to a single domain (in italics). Amino acids corresponding to the Nle domain are in bold characters. The number of amino acids (aa) are indicated at the end of the sequences.

Adapted from Cormier et al., 2006

I. Study of the role of *Notchless (Nle)* in the mouse

1. Introduction: *Nle*, from the Notch pathway to ribosome biogenesis

1.1 *Nle* and the Notch pathway in Drosophila

Notchless was initially identified in Drosophila, in a genetic screen aimed at identifying modifiers of Notch activity (Royet et al., 1998). In their study, Royet *et al.* used strains of *D. melanogaster* carrying mutated alleles of *Notch:* (1) *notchoid*^{1} *(nd*^{1}*),* which leads to notches in the fly's wings due to decreased Notch activity; (2) *Abruptex*^{28} *(Ax*^{28}*)* which causes reduced number of bristles and shorter wing veins due to increased Notch activity. In an *nd*^{1} genetic background, heterozygous deletion of *Nle* suppressed this notched appearance of the wings, suggesting that haploinsufficiency of *Nle* leads to increased Notch activity (Figure R1.a-c). Consistently, deletion of one allele of *Nle* in an *Ax*^{28} genetic background aggravated the *Ax*^{28} phenotype caused by increased Notch activity (Figure R1.a,d-e). Altogether, these observations suggest that *Nle* negatively regulates Notch activity, hence the name *"Notchless"*. The authors further showed the interaction of NLE and NOTCH in *in vitro* fusion-protein experiments, however this was never confirmed *in vivo*. However, as of today no further evidence of the interaction between *Nle* and *Notch* observed by Royet *et al*. has been documented.

1.2 *Nle* ortholog Rsa4 is an essential actor of ribosome biogenesis in yeast

Notchless encodes protein that is evolutionary conserved among eukaryotes, including unicellular organisms and plants where the Notch signaling pathway does not exist (Figure R2). Studies in yeast suggest that the ancestral role of *Nle* is in the export of the maturating large ribosome subunit. Indeed, *Rsa4*, the yeast ortholog of *Nle*, is an essential gene for ribosome biogenesis and cell viability. It encodes a nucleolar, non-ribosomal protein that acts as a ribosome assembly factor associated with the pre-60S subunit of ribosomes. Yeast cells depleted in Rsa4 display defects in biogenesis of the 60S ribosome subunit: the processing of 27S pre-rRNA (equivalent of the 32S of higher eukaryotes) into mature 25S (equivalent of the 28S) and 5.8S rRNAs is disrupted in absence of Rsa4, leading to an accumulation of 27S pre-rRNA(la Cruz et al., 2005). Moreover, lack of Rsa4 impairs the export of pre-60S subunits to the cytoplasm (Baßler et al., 2010). Prior to its nucleo-cytoplasmic export, several trans-acting factors need to be actively removed from the mature 60S subunit. Rea1, an AAA-type ATPase bound to the pre-60S subunit, performs removal of some of these factors by acting like a mechano-chemical spring that will dissociate the factors from the immature ribosomal particle (Baßler et al., 2010; Ulbrich et al., 2009). Interaction between Rsa4 and the MIDAS (metal ion-dependent adhesion site) domain of Rea1 is critical for this removal and is thus critical for export of the pre-60S subunit (Figure R3.a). It was recently shown this Rsa4-Rea1 interaction plays an essential role in the maturation of the peptidyl-transferase center of the ribosome, the catalytic center where peptide bond formation occurs. Indeed, the mechanical force induced by this interaction is required for proper topological conformation of the 25S rRNA and the 5S RNP (composed of the 5S rRNA, Rpl5 and Rpl11), and

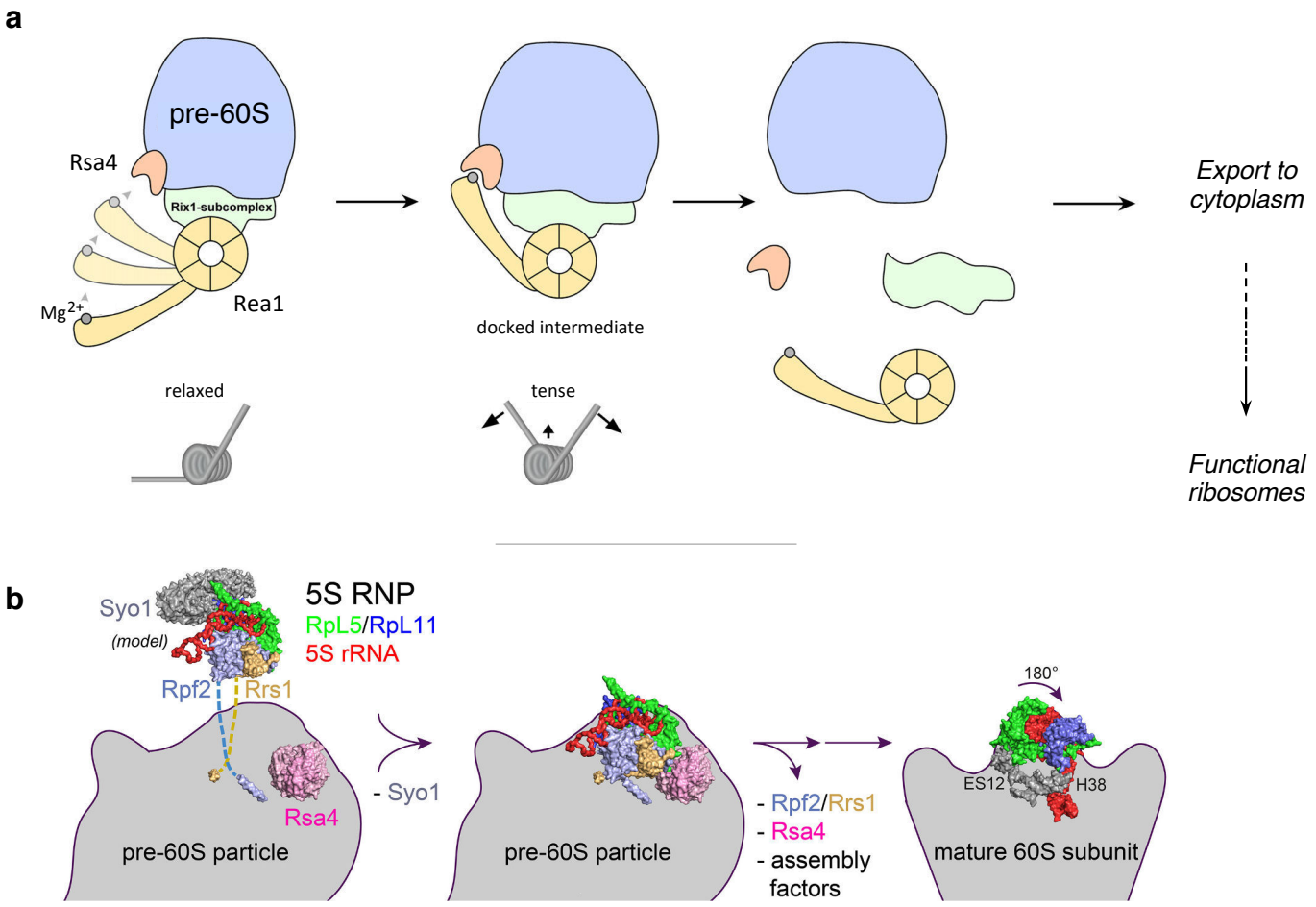

Figure R3. NLE yeast ortholog Rsa4 interacts with AAA ATPase Rea1 in the maturating pre-60S particle to facilitate incorporation of the 5S RNP

a. Schematic representation of the role of Rsa4 in the removal of extra-ribosomal factors from the pre-60S ribosomal particle. Rea1 is composed of a hexameric AAA ATPase ring and a protruding tail, the tip of which harbors a MIDAS domain that coordinates the MIDAS ion (Mg^{2+}). The AAA ring of Rea1 is attached to the pre-60S particle via the Rix1 sub-complex. The MIDAS tail can move up and contact the pre-60S at the site where Rsa4 is located. ATP hydrolysis in the AAA ATPase domain creates a tensile force that pulls off Rsa4, the Rix1 sub-complex and Rea1 from the pre-60S particle. The two different states of Rea1 –tail not bound and bound to Rsa4, respectively– can be compared to a tensile spring in its relaxed or loaded (tense) states. **b.** Schematic representation of incorporation of the 5S RNP (5S rRNA, Rpl5, Rpl11) into the pre-60S particle. In the pre-60S containing Rsa4, the latter interacts with the Rpf2/Rrs1 complex bound to the 5S RNP, allowing its incorporation to the pre-60S. The tensile force created by the Rea1/Rsa4 interaction causes removal of Rsa4 and the Rpf2/Rrs1 complex, and the concurrent topological conformation change of the 5S RNP within the pre-60S, which is required to form the peptidyl-transferase catalytic center of the ribosome.

Adapted from Ulbrich et al., 2009; Kharde et al., 2010

incorporation of the latter into the pre-60S particle (Figure R3.b) (Baßler et al., 2014; Kharde et al., 2015; Leidig et al., 2014).

1.3 *Nle* is required for early embryonic development and maintenance of adult stem cells in the mouse

Initially, work on *Nle* in the laboratory started from its isolation during the clonal positioning of the *Ovum mutant* locus responsible for a conditional pre-implantation lethal syndrome (Le Bras et al., 2002). The mouse *Nle* gene is composed of 13 exons, and is expressed throughout development and in all analyzed tissues and organs (Cormier et al., 2006). It encodes a 485 amino-acid protein composed of a Nle domain followed by 8 WD40 motifs (Figure R2.a).

The laboratory has first shown that *Nle* deficiency is lethal for the blastocyst at the time of implantation, due to the selective apoptosis of inner cell mass (ICM) cells in $Nle^{null/null}$ embryos (Figure R4) (Cormier et al., 2006). Interestingly, their data also suggested that *Nle* was dispensable for the survival of trophectoderm (TE) cells. To analyze the function of *Nle* at later stages, the laboratory has developed conditional *Nle* inactivation approaches *in vivo*, using the Cre/*LoxP* strategy (see part *I-1.5* for *Nle* inactivation models). Using strains where conditional inactivation of *Nle* can be induced, the team investigated the effects of *Nle* loss-of-function later during embryonic development and in adult mice. Thus, they showed that inactivation of *Nle* in the developing embryo leads to multiple developmental defects, in particular during axial skeletal formation (Beck-Cormier et al., 2014). In the adult mouse, they showed that *Nle* is critically required for the maintenance of stem cell populations, notably hematopoietic and intestinal stem cells (Le Bouteiller et al., 2013; Stedman et al., 2015). Briefly, Marie Le Bouteiller (a former PhD student in the laboratory) showed that inactivation of *Nle* led to the exit of quiescence by HSCs and rapid and drastic exhaustion of HSCs and MPPs, resulting in bone marrow failure (Le Bouteiller et al., 2013). In parallel, Aline Stedman (a former post-doctoral fellow in the laboratory) showed that *Nle* was critically required for the maintenance of the intestinal epithelium, and that *Nle* loss-of-function in this tissue led to the rapid elimination of intestinal stem and progenitor cells by apoptosis, cell cycle arrest and differentiation (Stedman et al., 2015). Importantly, mice where *Nle* was ubiquitously inactivated died rapidly after induction of *Nle* loss-of-function. Altogether, these results show that *Nle* is a crucial factor for proper embryonic development and the maintenance of stem cell populations and thus homeostasis in the adult mouse.

1.4 *Nle* function in ribosome biogenesis is conserved in mouse

Interestingly, our team and another one have both shown that the lethality of $Nle^{null/null}$ embryos is independent of Notch signaling (Lossie et al., 2012; Souilhol et al., 2006). Together with the finding that Rsa4 plays a critical role in RiBi in yeast, this raised the question of whether *Nle* function in this process was conserved in mouse and could explain the phenotypes observed following its inactivation.

To test the effects of *Nle* loss-of-function on RiBi, Marie Le Bouteiller first used ES cells where *Nle* inactivation can be induced (see part *I-1.5*). Thus, she showed that *Nle* inactivation led a block of the pre-60S maturation at the levels of the conversion of the 32S pre-rRNA into 5.8S and

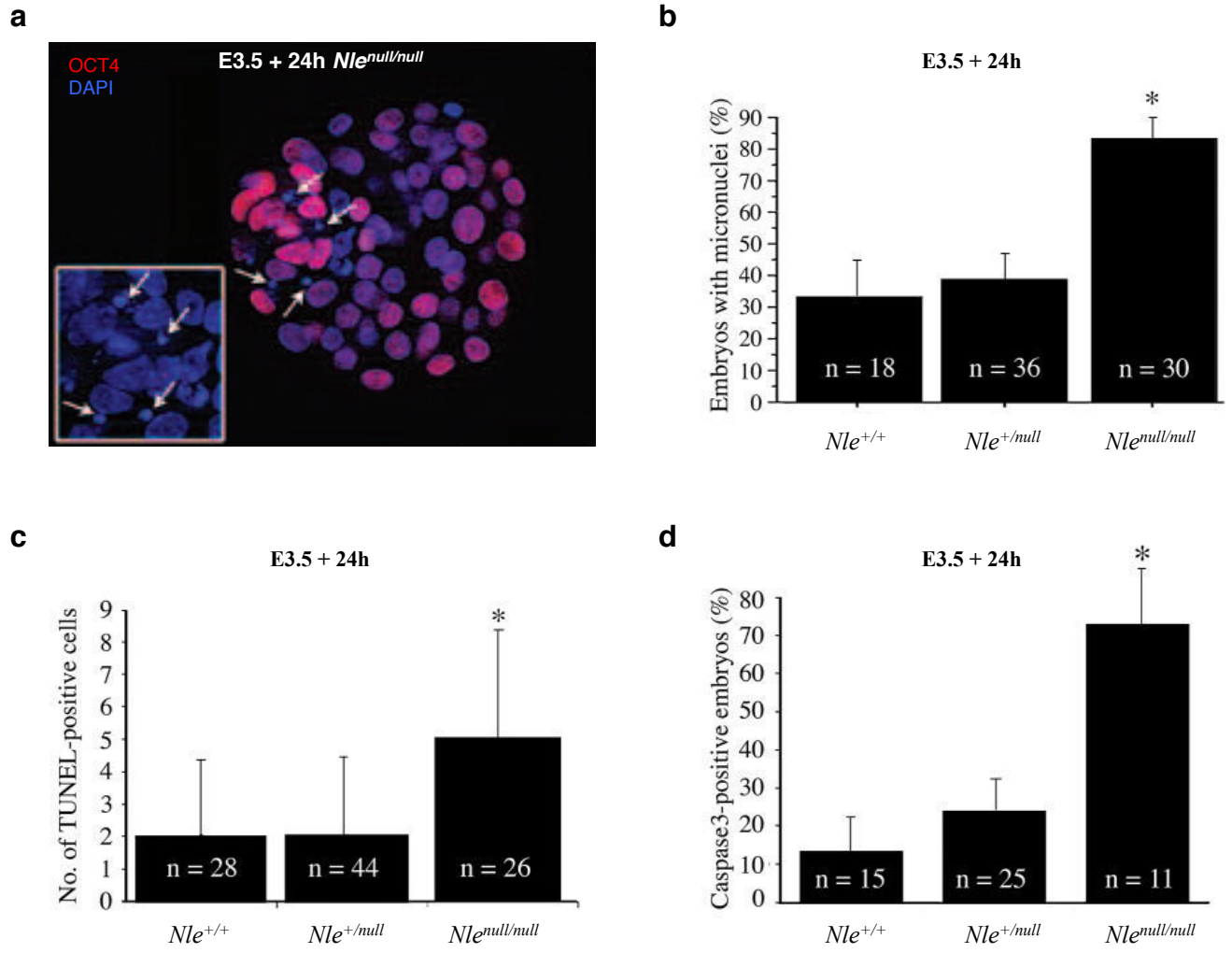

Figure R4. ***Nle*** **is required for the survival of Inner Cell Mass cells during pre-implantatory embryonic development**

Nle$^{+/+}$, *Nle*$^{+/null}$ and *Nle*$^{null/null}$ embryos were collected at E3.5 and cultured *ex vivo* for 24h. **a.** Immunodetection of Oct4, strongly expressed in cells of the Inner Cell Mass (ICM) at this stage. Staining of nuclei using DAPI reveals the presence of pycnotic nuclei (or micro-nuclei), indicative of cell death. **b.** Quantification of the percentage of embryos of each genotype displaying cells with micro-nuclei. **c.** Number of cells positive for TUNEL staining, indicative of apoptosis, in embryos of each genotype. **d.** Quantification of the percentage of embryos of each genotype where the active form of Caspase 3 (marker of apoptosis) is detected. Numbers of embryos for each genotype are indicated in histogram bars. Statistical significance was calculated using χ^2 tests: * $p<0.01$.

Adapted from Cormier et al., 2006

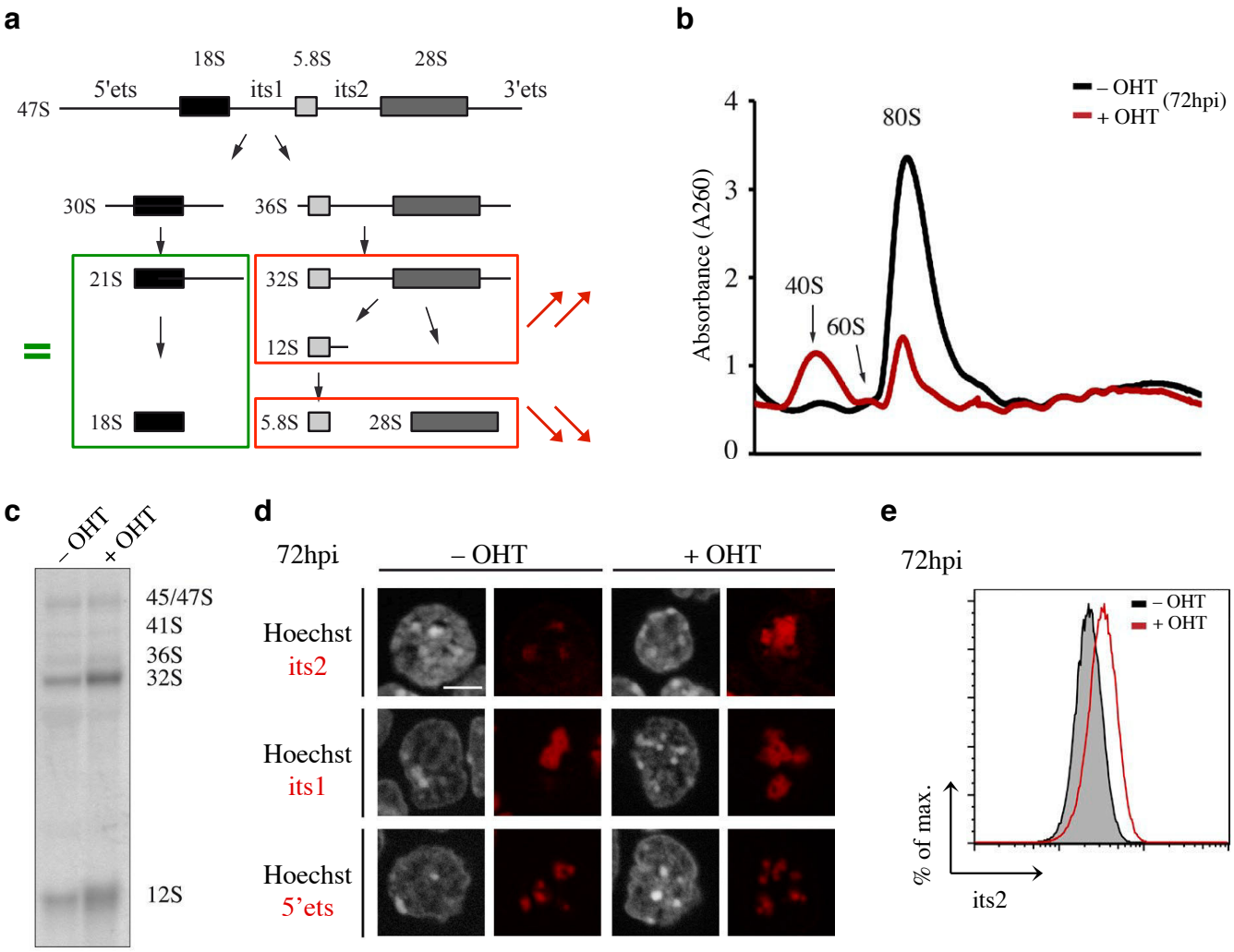

Figure R5. ***Nle* is required for synthesis of the large ribosome subunit in mouse**

Rosa$^{CreERT2/+}$ *Nle*$^{flox/null}$ *(Nle*^{cKO}*)* ES cells were cultured in the presence or absence of hydroxytamoxifen (OHT) for 48h to inactivate *Nle* and were harvested 72h post-induction with OHT (72hpi). **a.** Overview of the pre-rRNA maturation process in mammalian cells, from the 47S primary transcript to the mature 18S (small ribosome subunit), 5.8S and 28S rRNAs (large ribosome subunit; 5S is not presented here). Colored boxes and arrows summarize the effects of *Nle* inactivation. **b.** RNA profiles measured by absorbance at 260nm in a sucrose gradient loaded with extracts from OHT-treated (red line) or untreated cells (black line). This analysis shows that OHT-treated cells have a dramatic decrease in the quantity of 80S assembled ribosomes, leading to an increase of free 40S subunit. **c.** Northern blot analysis of of total RNA from untreated or treated ES cells, using a probe directed against its2, shows the levels of rRNA precursors (pre-rRNAs) of the large ribosomal subunit. This shows that *Nle* inactivation leads to an accumulation of 32S and 12S pre-rRNAs, indicating that NLE is involved in the maturation of the 32S. **d.** Untreated and treated cells were stained using FISH probes directed against its1, its2 or 5'ets, and imaged by microscopy. This shows that the 47S pre-rRNA and the small subunit's pre-rRNAs are not affected by *Nle* inactivation (similar levels of 5'ets and 18S, respectively), but pre-rRNAs of the large subunit are affected (increased its2 levels). **c.** FACS profile of cells stained with the its2 FISH probe, showing the levels of its2. OHT-treated cells do indeed display increased its2 levels, confirming that *Nle* inactivation affects the maturation of pre-60S rRNA precursors.

Adapted from Le Bouteiller et al., 2013

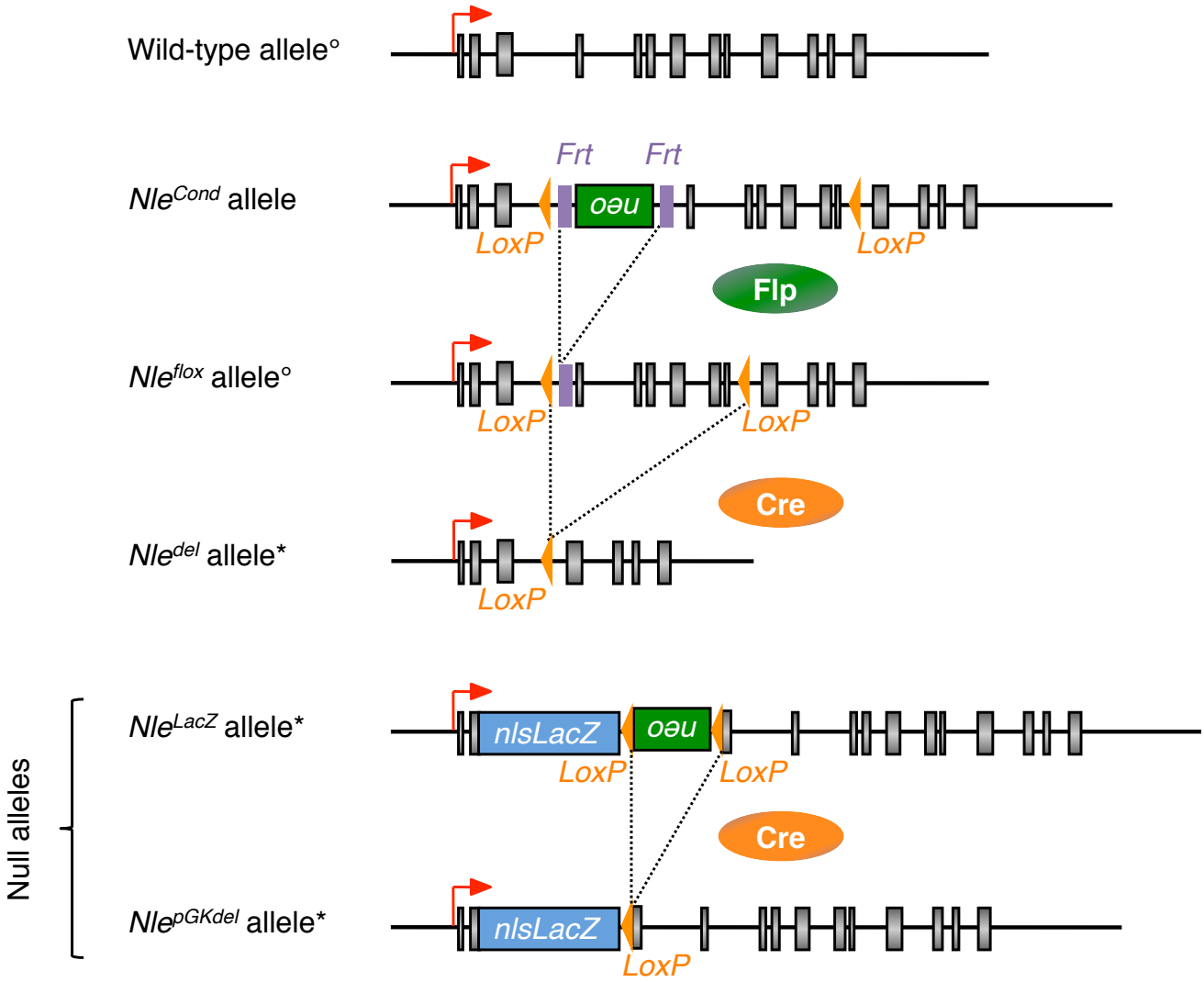

Figure R6. ***Nle*** **alleles generated and available in the laboratory**

The wild-type allele of *Nle* is composed of 13 exons and is under the control of a single promoter. Various functional (°) and non-functional (*) alleles have been generated in the laboratory to study the function of *Nle*. The Nle^{null} appellation I use in my manuscript can refer to either Nle^{LacZ} or Nle^{pGKdel} non-functional alleles, whereas Nle^{+} always refers to the wild-type allele. Conversion of the Nle^{flox} allele into the Nle^{del} allele is induced in cells expressing an active form of the Cre recombinase. A constitutively active Cre will directly induce this conversion, whereas an inducible Cre such as the CreERT2 –fusion protein between Cre and the modified estrogen receptor ERT2– requires the binding of hydroxytamoxifen to be active and induce recombination.

28S, resulting in a dramatic diminution of the quantity of 60S particles, whereas biogenesis of the small subunit remained unaffected (Figure R5, (Le Bouteiller et al., 2013)). To investigate whether similar RiBi defects occurred in the hematopoietic system *in vivo*, Marie developed an approach allowing the quantification of pre-rRNA levels of both ribosome subunits in multiple hematopoietic populations simultaneously, combining fluorescent *in situ* hybridization (FISH) and classical flow cytometry methods (this approach is described in more details in my article, presented in part *II*). Thanks to this approach, she showed that ubiquitous *Nle* inactivation in the adult mouse did indeed induce RiBi defects in hematopoietic stem and progenitor cells (Le Bouteiller et al., 2013). Finally, Aline Stedman showed that *Nle* inactivation in the intestinal epithelium also causes similar RiBi defects (Stedman et al., 2015). Altogether, their work shows that the role of *Nle* in ribosome biogenesis is also conserved in mouse.

1.5 Conditional and inducible inactivation of *Nle* in the mouse

1.5.1.1 Nle alleles available in the laboratory and models I used during my thesis

To study the function of *Nle* in the mouse, different *Nle* alleles have been generated in the laboratory, which are presented in Figure R6. First, constitutively inactive alleles have been generated, which I will refer to as Nle^{null} alleles. However, since *Nle* knockout leads to embryonic lethality, a *Nle* allele that could be inactivated in a conditional and/or inducible manner was necessary to study the role of *Nle* at later stages of development or in the adult mouse. Thus, *LoxP* sites flanking exons 4 to 9 have been inserted in the endogenous *Nle* gene, generating a functional "floxed" Nle^{flox} allele that can be converted into a non-functional Nle^{del} allele in cells expressing an active form of the Cre recombinase (Figure R6).

Different approaches have been developed in the laboratory to induce *Nle* inactivation in a conditional and/or inducible manner *in vivo* and *ex vivo*. Using mice (or cell lines) carrying the Nle^{flox} allele and a Nle^{null} allele, and expressing a Cre recombinase, one can inactivate *Nle* in a conditional and/or inducible manner in several tissues (or cell lines). During my thesis, I have used both *in vivo* and *ex vivo* models. *In vivo*, I have mainly used two Cre strains: the $Rosa26^{CreERT2}$ strain, which allows ubiquitous *Nle* inactivation upon tamoxifen injection, and the *Lck-Cre* strain, which induces constitutive *Nle* inactivation specifically in progenitors of the T cell hematopoietic lineage. In both cases, I compared the phenotypes of $Nle^{flox/null}$ mice to control $Nle^{flox/+}$ mice. In terms of nomenclature, in my thesis I will usually refer to $Rosa26^{CreERT2/+}$, $Nle^{flox/null}$ cells or mice as Nle^{cKO}, and use Nle^{ctrl} for $Rosa26^{CreERT2/+}$, $Nle^{flox/+}$ controls; for the *Lck-Cre* strain, I will use the appellation $Nle^{Lck\text{-}cKO}$ for *Lck-Cre/+*, $Nle^{flox/null}$ mice and $Nle^{Lck\text{-}ctrl}$ for *Lck-Cre/+*, $Nle^{flox/+}$ mice. *Ex vivo*, I have mainly used $Rosa26^{CreERT2/+}$, $Nle^{flox/null}$ (Nle^{cKO}) cell lines where inactivation of *Nle* can be induced by addition of 4-hydroxytamoxifen (OHT) in the culture medium. In the following paragraph, I present the general *modus operandi* I used during my thesis when working with Nle^{cKO} ES cells.

1.5.1.2 Mode of operation I used to inactivate Nle in ES cells during my thesis

To induce *Nle* inactivation in *Nle cKO* ES cells, I cultured them in the presence of 1µM 4-hydroxytamoxifen (OHT) for up to 48h, and used cells cultured in the same conditions but without

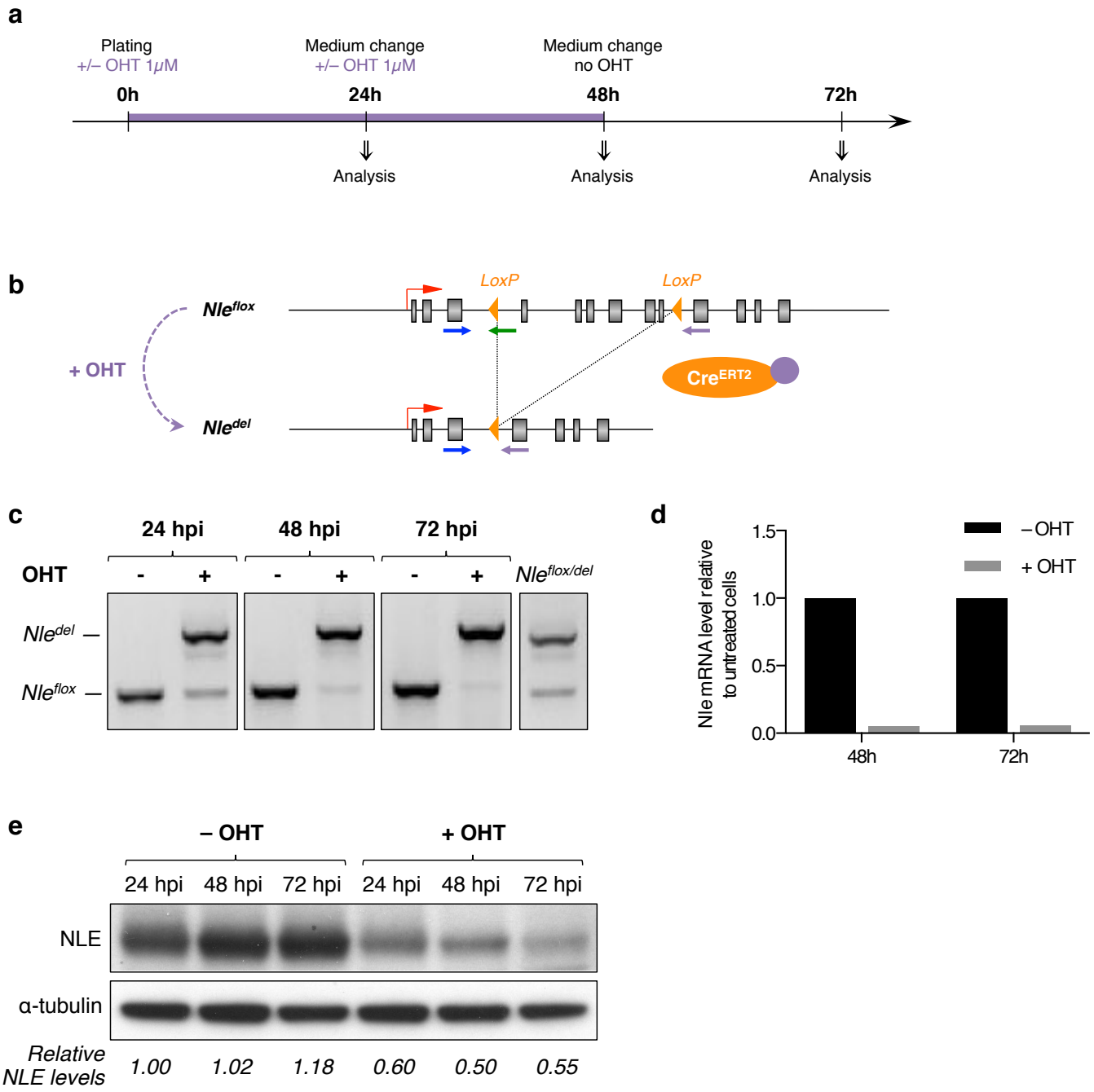

Figure R7. ***Nle* inactivation in *Rosa26*$^{CreERT2/+}$, *Nle*$^{flox/null}$ ES cells**

a. Protocol used to induce *Nle* inactivation in ES cells. **b.** Addition of 4-hydroxytamoxifen (OHT) to the culture medium activates the CreERT2 recombinase, which recognizes the *LoxP* sites flanking exons 4-9 of the *Nle*^{flox} allele, converting it into the non-functional *Nle*^{del} allele. Blue, green and purple arrows represent the position of PCR primers used for the specific detection of both alleles. **c.** Verification of the conversion of the *Nle*^{flox} allele into the *Nle*^{del} allele by PCR on total DNA using primers presented in a. Heterozygous *Nle*$^{flox/del}$ DNA is used as control. **d.** RT-qPCR analysis of relative *Nle* mRNA levels in OHT-treated at 48hpi and 72hpi compared to their respective untreated controls. **e.** Western blot analysis of NLE protein levels in OHT-treated at 24hpi, 48hpi and 72hpi compared to their respective untreated controls. α-tubulin protein levels are used for normalization and quantification of NLE levels. NLE levels indicated are relative to 24hpi untreated cells.

OHT as controls. First, I monitored the efficiency of *Nle* deletion in this model. For this, I harvested cells at 24h, 48h or 72h post-induction (hpi) and extracted their total DNA, mRNA and protein contents (Figure R7.a). First, I analyzed the conversion of the Nle^{flox} allele into the non-functional Nle^{del} (or Nle^{Δ}) by genomic PCR using a combination of 3 primers that allow the detection of both alleles. In the absence of OHT, only the Nle^{flox} allele could be detected, as expected. In contrast, the addition of OHT in the medium allowed the rapid conversion of the Nle^{flox} allele into Nle^{del} (Figure R7.b-c). *Nle* inactivation was already very efficient at 24hpi. However, even at 72hpi the Nle^{flox} allele remained detectable at very low levels, suggesting that a small fraction of cells are resistant to *Nle* inactivation under the conditions used. I then analyzed the levels of *Nle* mRNA by real-time quantitative PCR (RT-qPCR) at 48hpi and 72hpi and observed a strong decrease of *Nle* expression in OHT-treated cells compared to controls (Figure R7.d). Finally, I performed western blot analyses on total protein extracts and also observed a strong reduction of NLE protein levels starting 24h after addition of OHT to the medium (Figure R7.e). Taken together, these results show that *Nle* inactivation is rapid and efficient in *Nle cKO* ES cells.

2. *Nle* loss-of-function induces a ribosomal stress responses in mouse

2.1 ES cells elicit a ribosomal stress response mediated by the RP-MDM2-p53 pathway following *Nle* inactivation

Given the critical role of *Nle* in the biogenesis of the large ribosome subunit, we asked whether the RiBi defects induced by *Nle* loss-of-function could trigger a ribosomal stress response, and notably whether the RP-MDM2-p53 pathway was activated. Since molecular analyzes would require a rather large amount of biological material, I decided to use an *ex vivo* cell culture approach and used $Rosa26^{CreERT2/+}$, $Nle^{flox/null}$ (Nle^{cKO}) ES cells where *Nle* inactivation can be induced by the addition of 4-hydroxytamoxifen (OHT) to the medium (see part *I-1.5.2*).

2.1.1 *Nle* inactivation in ES cells induces impaired proliferation accompanied by alteration of their cell cycle profile

2.1.1.1 Nle-deficient ES cells exhibit impaired proliferation and/or survival

First, I asked whether *Nle* inactivation in ES cells had an effect on their proliferative capacity. To address this, I plated Nle^{cKO} ES cells at the same density, in the presence or absence of OHT (as described in *I-1.5.1.2*), and assessed their proliferation capabilities by counting the number of cells obtained at 24hpi, 48hpi, and 72hpi. During the first 48h after induction, I did not observe any difference in the proliferation or survival of cells between both conditions. However, at 72hpi I observed a strong reduction in the total number of OHT-treated cells compared to untreated controls (Figure R8.a). I wondered if this was accompanied by an increase in cell death, so I assessed cell viability using Trypan blue staining but could not see any significant increase in the proportion of dying cells at this time-point (Figure R8.b). Interestingly, at 72hpi I observed that the medium of OHT-treated cell cultures contained significantly more "floating" cells that in untreated cultures, suggesting that *Nle* loss-of-function in ES cells is associated with reduced viability (Figure R8.c).

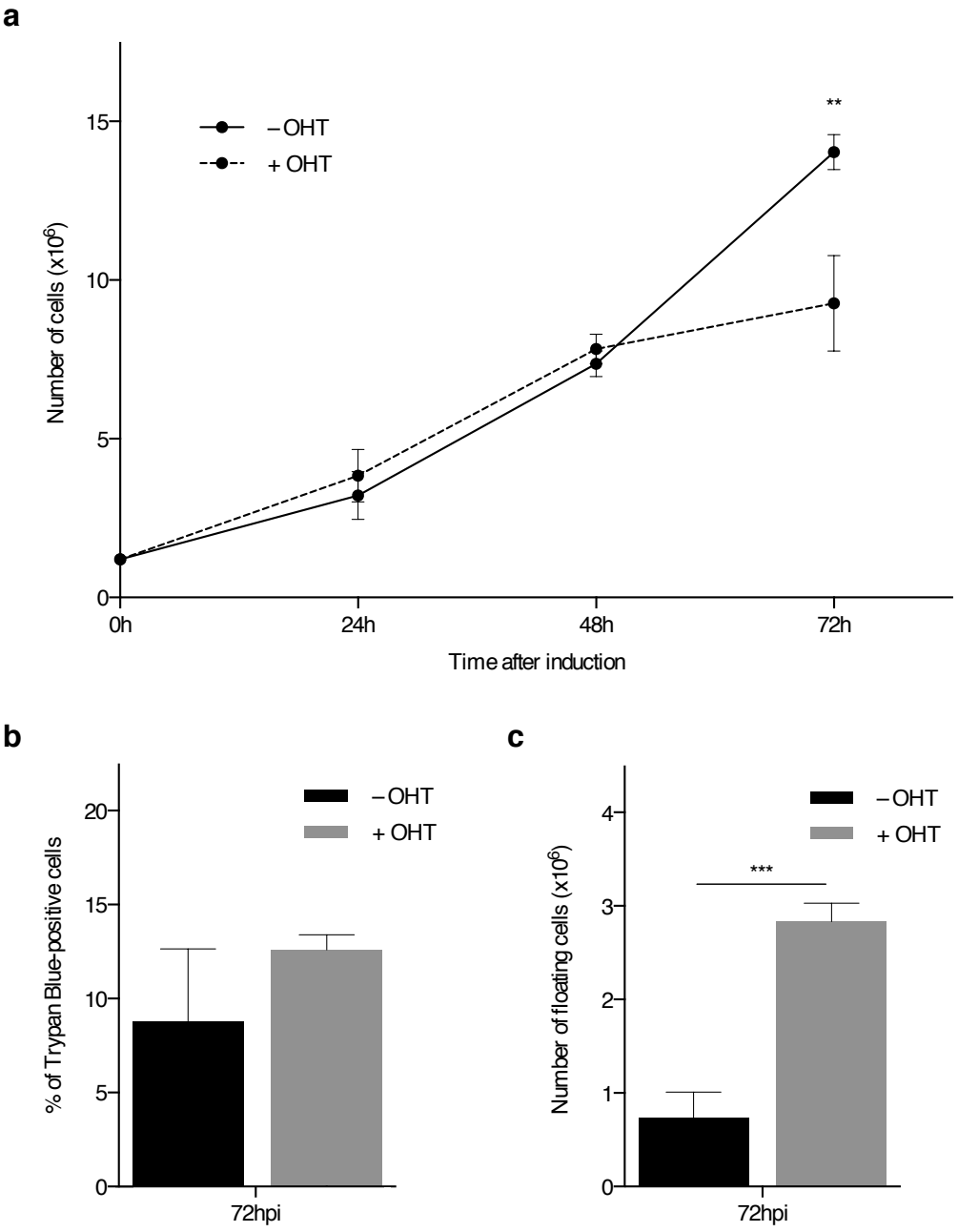

Figure R8. Proliferation and survival analysis of *Nle*-deficient ES cells

Rosa26$^{CreERT2/+}$, *Nle*$^{flox/null}$ ES cells were cultured for up to 72h in the presence or absence of OHT during the first 48h of culture. **a.** Total cell numbers counts after dissociation with Trypsin-EDTA at 24hpi, 48hpi and 72hpi in OHT-treated vs. untreated cultures (n=3 for each condition and time-point). **b.** Percentage of Trypan Blue-positive cells after dissociation with Trypsin-EDTA at 72hpi (n=3 for each condition). **c.** Number of cells present in the culture medium before dissociation with Trypsin-EDTA at 72hpi (n=3 for each condition). **a-c.** Representative results of repeated experiments. Statistical significance was assessed using unpaired two-tailed Student's t tests: ** $p<0.01$; *** $p<0.001$

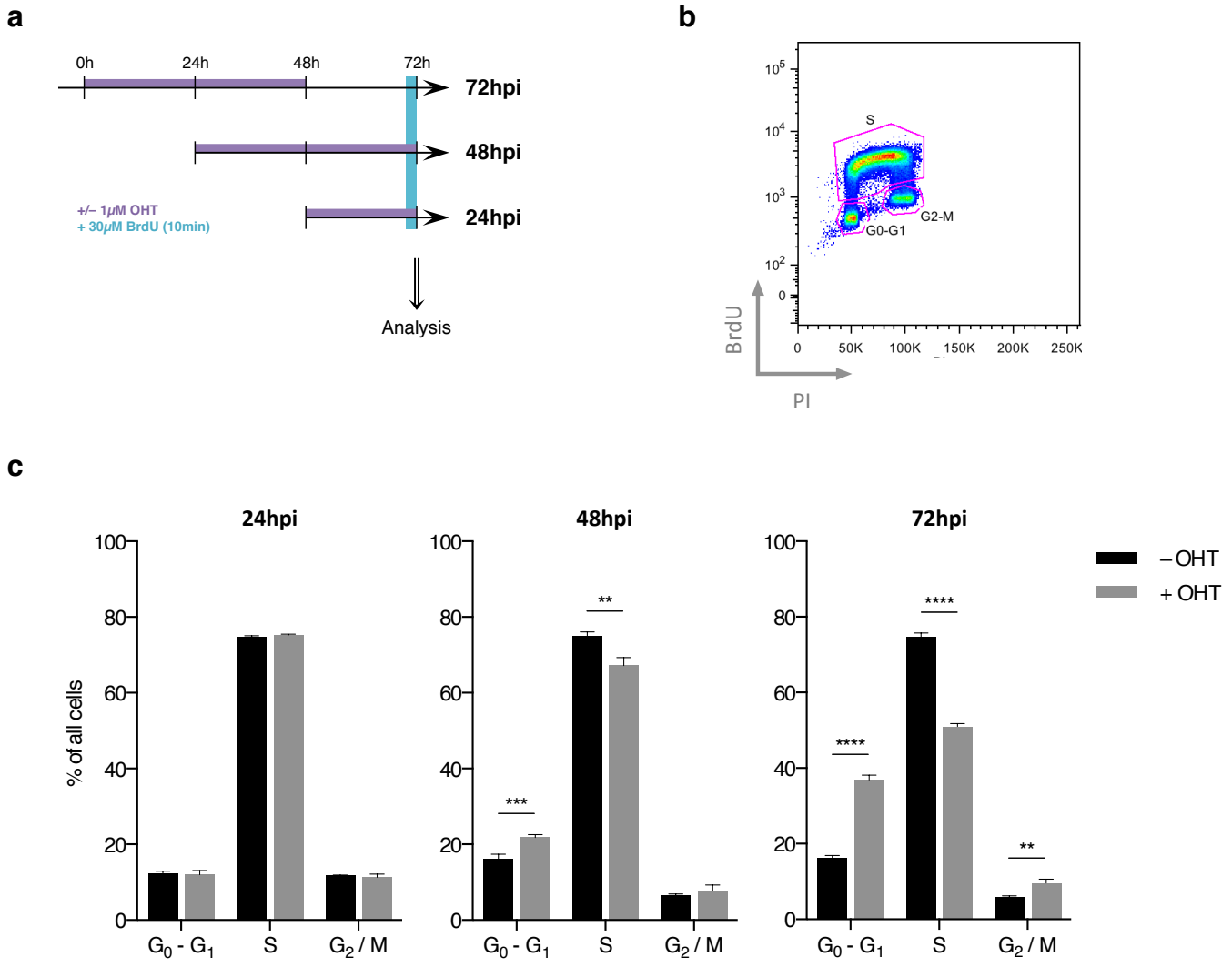

Figure R9. Cell cycle profile analysis of *Nle*-deficient ES cells

a. *Nle*^{cKO} ES cells were cultured for 24h, 48h or 72h in the presence or absence of OHT (purple line), in order to be harvested at the same time. Prior to dissociation with Trypsin+EDTA, cells were incubated 10min in the presence of 30µM BrdU (cyan box). Cells were then harvested and fixed for cell cycle analysis by BrdU/Propidium Iodide (PI) staining and flow cytometry. **b.** Gating strategy for separation of G_0-G_1, S and G_2/M phases on the BrdU/PI profile visualized by flow cytometry. **c.** Quantification of the percentage of cells in each phase of the cell cycle in OHT-treated cells at 24hpi, 48hpi and 72hpi compared to their respective untreated controls (n=4 for each condition; representative results of 3 independent experiments). Statistical significance was assessed using unpaired two-tailed Student's t tests: ** $p<0.01$; *** $p<0.001$; **** $p<0.0001$

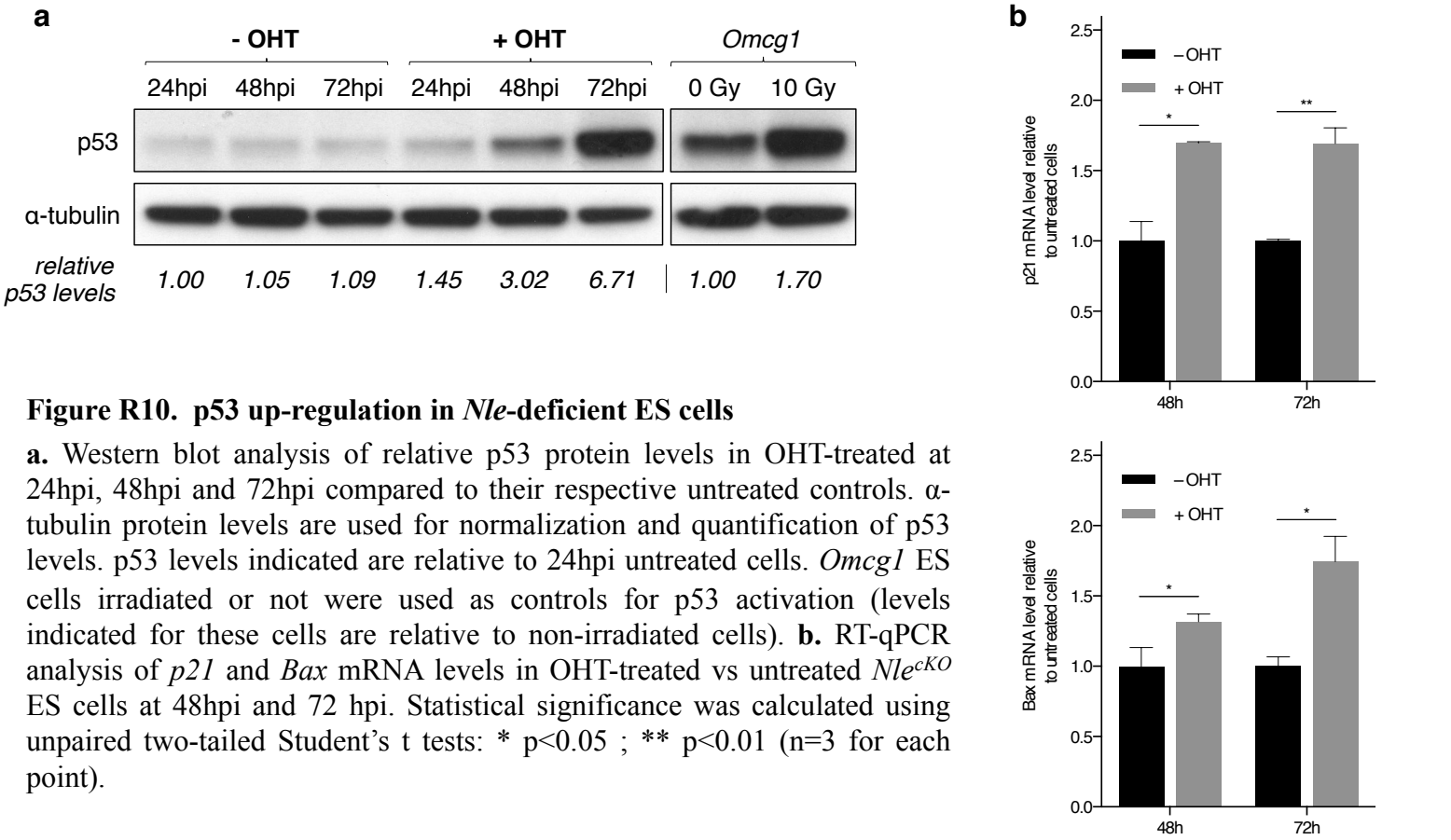

Figure R10. p53 up-regulation in *Nle*-deficient ES cells

a. Western blot analysis of relative p53 protein levels in OHT-treated at 24hpi, 48hpi and 72hpi compared to their respective untreated controls. α-tubulin protein levels are used for normalization and quantification of p53 levels. p53 levels indicated are relative to 24hpi untreated cells. *Omcg1* ES cells irradiated or not were used as controls for p53 activation (levels indicated for these cells are relative to non-irradiated cells). **b.** RT-qPCR analysis of *p21* and *Bax* mRNA levels in OHT-treated vs untreated Nle^{cKO} ES cells at 48hpi and 72 hpi. Statistical significance was calculated using unpaired two-tailed Student's t tests: * $p<0.05$; ** $p<0.01$ (n=3 for each point).

Figure R11. Knockdown of *Rpl11* partially impedes p53 activation in *Nle*-deficient ES cells

a. Nle^{cKO} ES cells were cultured for 24h with or without addition of OHT to their medium. After 24h, media were replaced with media with or without OHT and containing Dharmafect transfection reagent with either no siRNA, a non-targeting siRNA (NT-siRNA) or a siRNA targeting the *Rpl11* mRNA (*Rpl11*-siRNA). Cells were further cultured in these media for 16h (30hpi), at which point media were replaced by media with or without OHT only. Finally, from cells were cultured in medium without OHT from 48hpi and were harvested at 72hpi. **b.** Western blot analysis on protein extracts from cells obtained in a. using antibodies directed against NLE, RPL11, p53 and α-tubulin. Protein levels of NLE, RPL11 and p53 were normalized using α-tubulin levels, and relative levels between samples were calculated in comparison to untreated, non-transfected cells (–OHT no siRNA).

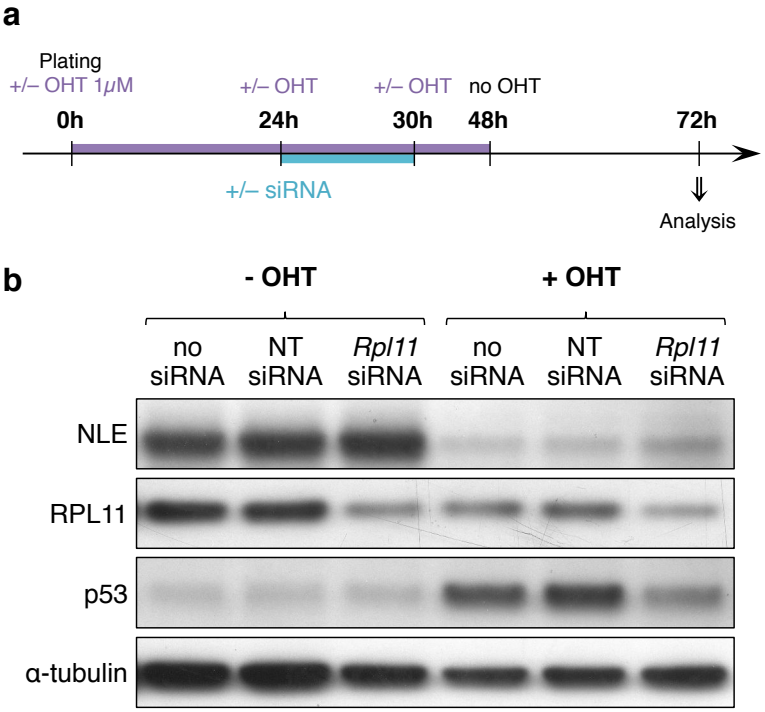

NLE levels	1.00	1.12	1.07	0.30	0.37	0.30
RPL11 levels	1.00	0.94	0.63	0.92	1.00	0.47
p53 levels	1.00	1.11	1.40	5.60	6.10	4.44

2.1.1.2 Alteration of the cell cycle profile in ES cells lacking NLE

In light of these results, I wondered if the impaired proliferation of *Nle*-deficient ES cells was accompanied by an alteration of their progression through the cell cycle. To address this question, I cultured ES cells in similar conditions as above for 24h, 48h or 72h; just before harvesting cells, I incubated them for 10min in the presence of 30µM BrdU (see Figure R9.a for protocol overview). I then fixed the cells and stained them with Propidium Iodide (PI) and an anti-BrdU antibody: these stainings allow the visualization of the cell cycle profile of the cells using flow cytometry as illustrated in Figure R9.b. Thus, I quantified the proportion of cells in the G_0-G_1, S and G_2/M phases of the cell cycle. At 24hpi, I could not see any difference between OHT-treated vs. untreated cells. However, at 48hpi I observed a significant increase in the proportion of cells in the G_0-G_1 phase accompanied by a significant reduction of the proportion of cells in S phase. This was further accentuated at 72hpi, where I also observed a small yet significant increase in the proportion of cells in the G_2/M phase (Figure R9.c).

There are two possible and non-exclusive explanations for this modification of the cell cycle profile: first, *Nle* deficiency could induce cell cycle arrest of ES cells in G_1; second, *Nle*-deficient ES cells could undergo cell death when they are about to enter the S phase. Interestingly, the increase of cells found in the supernatant of OHT-treated cells at 72hpi could almost account for the reduction in total cell numbers compared to untreated cells at this time-point, which weighs in favor of the second possibility. My observations are consistent with two recent studies where RiBi defects in ES cells induced by a treatment with low levels of Actinomycin D or the knockdown of *Rpl37* led to cell cycle arrest and/or apoptosis (Morgado-Palacin et al., 2012; Sasaki et al., 2011). These two studies further showed that this response was induced by RPL11-dependent p53 stabilization, demonstrating that ES cells have a functional ribosomal stress response.

2.1.2 Activation of the RP-MDM2-p53 pathway in response to *Nle* inactivation in ES cells

Given the role of *Nle* in biogenesis of the large ribosomal subunit and the phenotype I observed in *Nle*-deficient ES cells, I wondered if RiBi defects induced by *Nle* inactivation in these cells led to the stabilization of p53 mediated by RPL11.

2.1.2.1 p53 is up-regulated in Nle-deficient ES cells

To investigate the activation of the RP-MDM2-p53 in *Nle*-deficient ES cells, I first wanted to test whether p53 was up-regulated in these cells. To that end, I harvested Nle^{cKO} cells cultured in similar conditions as above, at 24h, 48h and 72h after induction with OHT, and extracted their total protein content. I then performed western blot analyses to compare the levels of p53 protein in OHT-treated vs. untreated cells at the different time-points. As early as 24hpi, I noticed a slight accumulation of p53 in OHT-treated cells, which continued to increase afterwards, reaching 3-fold and 6-fold increases at 48hpi and 72hpi, respectively (Figure R10.a). To further ascertain the up-regulation of p53 in OHT-treated cells, I analyzed the expression levels of two classical p53 target genes: the cell cycle regulator *p21*, and the pro-apoptotic gene *Bax*. I extracted total mRNAs from cells cultured in similar conditions as above for 48 h or 72 h and analyzed the expression levels of *p21* and *Bax* using quantitative real-time PCR. For both genes, I observed a significant increase of

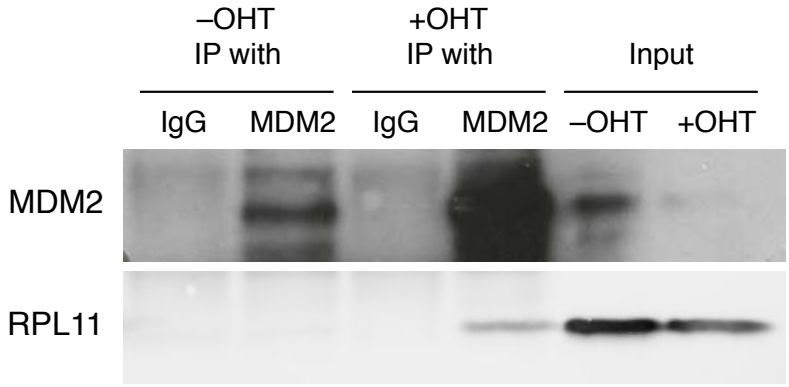

Figure R12. Co-immunoprecipitation of MDM2 and RPL11 in *Nle*^{cKO} ES cells

ES cells were cultured in the presence or absence of OHT for 48h and were harvested at 72h after induction to prepare protein extracts. Immunoprecipitation (IP) was then performed on these extracts using an antibody directed against either MDM2 or non-targeting immunoglobulin (IgG) as control. Equivalent quantities of protein from the obtained immunoprecipitates were then analyzed by western blot using antibodies directed against MDM2 (top lane) and RPL11 (lower lane), and whole protein extracts were used as control (Input).

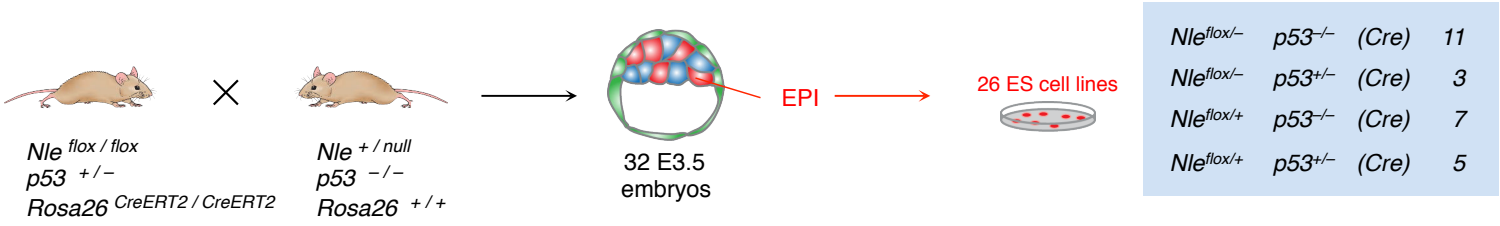

Figure R13. Derivation of *p53* deficient ES cells with inducible *Nle* inactivation

Nle$^{flox/flox}$, *p53*$^{+/–}$, *Rosa26*$^{CreERT2/CreERT2}$ female mice were crossed with *Nle*$^{flox/flox}$, *p53*$^{+/–}$, *Rosa26*$^{CreERT2/CreERT2}$ males. **day 1.** Embryos were collected at the blastocyst stage (E3.5) and incubated 2 days in 4-well plates with KSOM medium complemented with PD0325901 and PD173074. **day 2.** After 2 days, if embryos had not hatched, the *zona pellucida* was removed by treatment with Tyrode's acid. They were then put in culture on gelatin-coated 4-well plates, in N2B27 medium complemented with 2i (PD0325901 + CHIR99021) and LIF (N2B27+2i/LIF) for 3-4 days to allow attachment of embryos to the dishes and proliferation of ICM (inner cell mass) cells. **day 6-8.** Once ICM cells had expanded enough, they were recovered and dissociated using Trypsin+EDTA, and were put back in culture in gelatin-coated 96-well plates with N2B27+2i/LIF. **day 10-12.** Cells were dissociated, a small portion was collected for DNA extraction and the rest re-plated in gelatin-coated 24-well plates. **day 12-14.** Cells were dissociated and re-plated in gelatin-coated 6-well plates. **day 14 onwards.** Once cells had reached confluence in 6-well plates, they were either frozen or further expanded by additional passages.

mRNA levels in treated cells at 48 hpi and 72 hpi (Figure R10.b). While *p21* overexpression was similar at both time-points, *Bax* expression further increased from 48hpi to 72hpi suggesting that cell cycle arrest may be elicited more rapidly than apoptosis in response to *Nle*-deficiency. Additional experiments with more markers and earlier time-points will be required to confirm this hypothesis. Altogether, these data indicated that inactivation of *Nle* in ES cells does indeed induce up-regulation of p53.

2.1.2.2 p53 stabilization in Nle-deficient ES cells is mediated by RPL11

I interpreted the accumulation of p53 I observed in OHT-treated Nle^{cKO} ES cells as the result of the activation of the RP-MDM2-p53 ribosomal stress pathway. However, I could not exclude that p53 up-regulation may be an indirect consequence of RiBi defects in these cells. To address this point, I decided to knock down *Rpl11* and follow the consequences on p53 up-regulation induced by *Nle* deficiency. To do this, I used an RNA silencing approach. I tried different protocols to find conditions allowing simultaneous *Rpl11* knockdown and NLE depletion. I cultured Nle^{cKO} ES cells for 72h as follows: cells were plated and treated or not with OHT; at 24hpi, cells were transfected for 16h with either no siRNA, a siRNA directed against no mouse mRNA (non-targeting siRNA: NT-siRNA), or a siRNA targeting the *Rpl11* mRNA (Rpl11-siRNA) (see Figure R11.a for protocol overview). Cells were harvested at 72hpi (48h after transfection) and I extracted their total protein content. Then, I analyzed by western blot the levels of NLE, RPL11 and p53 proteins. As expected, I observed a strong reduction in the levels of NLE in OHT-treated cells compared to untreated controls (Figure R11.b, top lane). Furthermore, I observed that transfection with the Rpl11-siRNA led to a ~50% decrease in RPL11 levels in both OHT-treated and untreated cells, whereas transfection with no siRNA or the NT-siRNA had no significant effect on the protein levels (Figure R11.b, second lane). The knock-down of any ribosomal gene is expected to interfere with RiBi, thus inducing a ribosomal stress response and leading to up-regulation of p53, with the exception of RPL5 and RPL11 which, as we saw in the introduction (*Introduction Part 2-1.3.3.3*), are both required for the stabilization of p53. Accordingly, the Rpl11-siRNA had no or modest effect on p53 levels in untreated cells (Figure R11.b, third lane). In contrast, while p53 levels were strongly increased in *Nle*-deficient cells transfected with either no siRNA or the NT-siRNA, this increase was reduced upon *Rpl11* knock-down (Figure R11.b, third lane). These data suggest that stabilization of p53 in NLE-depleted cells is indeed at least in part mediated by RPL11.

This prompted us to test whether RPL11 interacted with MDM2 in OHT-treated cells. To that end, with Aline Stedman we immunoprecipitated MDM2 from protein extracts of treated and untreated cells at 72hpi. Preliminary results showed that RPL11 co-immunoprecipitated with MDM2 in OHT-treated cells (Figure R12). However, we could not determine whether this interaction was more pronounced in OHT-treated cells vs. untreated controls due to technical problems, and the experiment will have to be repeated to answer this point.

Altogether, these results indicate that in response to RiBi defects induced by *Nle* loss-of-function, ES cells elicit a ribosomal stress response leading to the up-regulation of p53, mediated at least in part by the interaction between RPL11 and MDM2, suggesting activation of the RP-MDM2-p53 pathway.

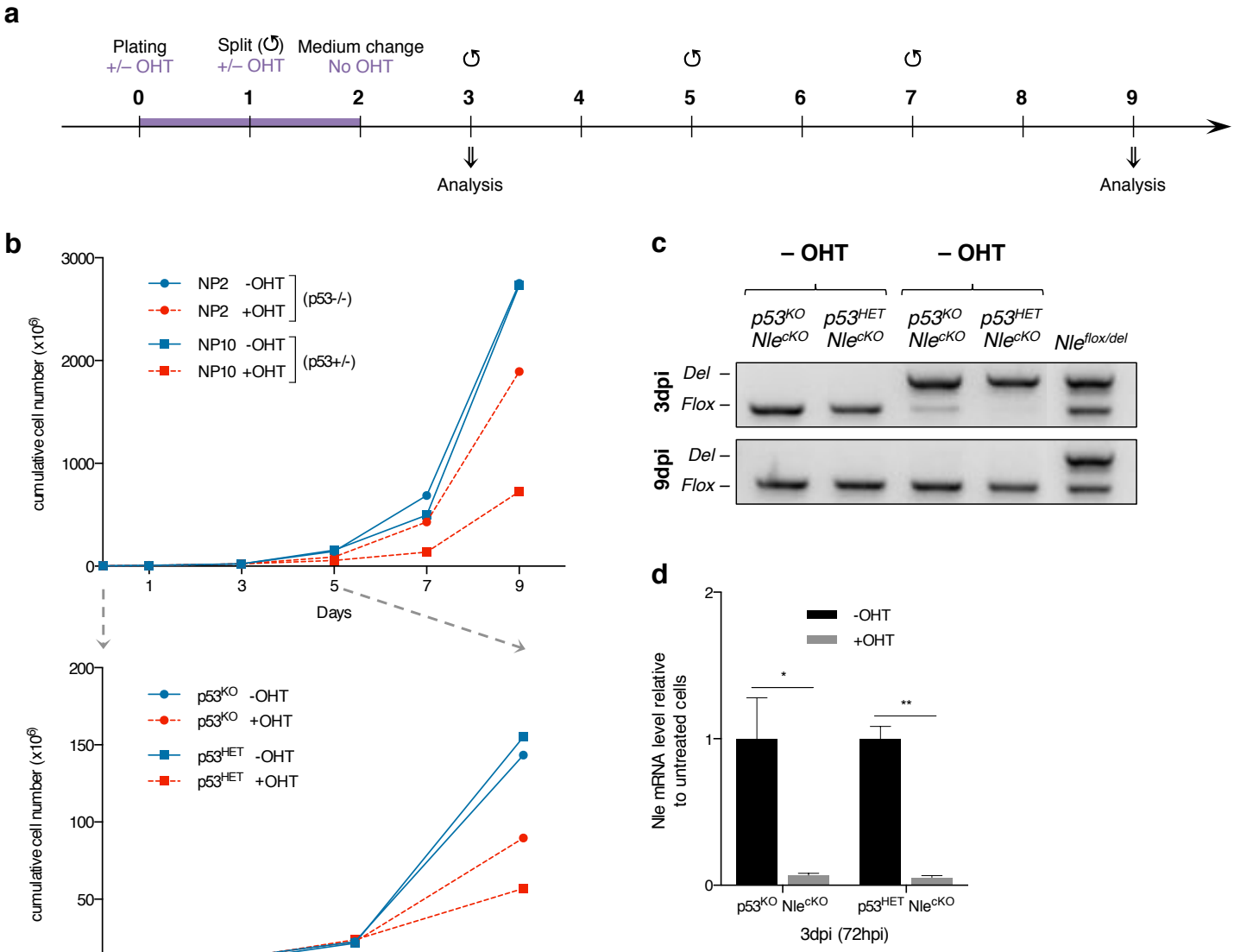

Figure R14. *p53* deficiency partially rescues proliferation defects induced by *Nle* inactivation

a. *p53*$^{-/-}$, *Nle*$^{flox/null}$, *Rosa26*$^{CreERT2/+}$ (*p53*^{KO} *Nle*^{cKO}) and *p53*$^{+/-}$, *Nle*$^{flox/null}$, *Rosa26*$^{CreERT2/+}$ (*p53*^{HET} *Nle*^{cKO}) ES cells were cultured for 24h in the presence or absence of OHT, split (↺) and cultured for another 24h +/– OHT and then cultured in OHT-free medium until 9dpi with passages at 3dpi (72hpi) and 5dpi. **b.** Cumulative cell numbers in OHT-treated vs. untreated cells. Cells were counted after dissociation with Trypsin-EDTA at each split (1, 3, 5, and 7dpi) and at 9dpi; cumulative cell numbers were then calculated based on the proliferation between counts. Counts from 1 to 5dpi are represented again at a smaller scale to highlight differences at 5dpi. (n=1 for each point) **c.** Efficiency of *Nle* deletion was assessed by genomic PCR as in Figure R7, using DNA extracts prepared at 3dpi and 9dpi. *Nle*$^{flox/del}$ DNA was used as control. **d,e.** RT-qPCR analysis of transcripts levels of *Nle* (**d**) and p53 target genes (**e**) *Bax, Noxa, Pidd, Puma* and *p21*, in OHT-treated vs untreated *p53*^{KO} *Nle*^{cKO} and *p53*^{KO} *Nle*^{cKO} cells at 3dpi. Statistical significance was calculated using unpaired two-tailed Student's t tests: * $p<0.05$; ** $p<0.01$ (n=3 for each point).

2.1.3 *Nle* inactivation in *p53*-deficient ES cells

Activation of the RP-MDM2-p53 ribosomal stress response could be responsible for the effects of *Nle* inactivation I observed in these cells regarding their proliferation and their cell cycle profile, however I could not exclude that other cellular responses independent of p53 could be elicited as well.

2.1.3.1 Derivation of p53-deficient ES cells with inducible Nle inactivation

To investigate possible p53-independent responses and understand the role of p53 in the phenotype I observed in Nle^{cKO} ES cells, with the help of Jérôme Artus (a post-doctoral fellow in the laboratory) I derived ES cell lines deficient for *p53* in which *Nle* could be inactivated. To do this, we crossed $Nle^{flox/flox}$, $p53^{+/-}$, $Rosa26^{CreERT2/CreERT2}$ females with $Nle^{flox/null}$, $p53^{-/-}$, $Rosa26^{+/+}$ males and collected embryo at E3.5. Embryos were then cultured in a medium known as "2i medium" containing two inhibitors: PD0325901, which inhibits MEK1/2, thus blocking pro-differentiation FGF signaling and promoting the maintenance of pluripotency; and CHIR99021, which inhibits GSK3β, thus promoting Wnt signaling and pluripotent stem cell survival (Ying et al., 2008). This allowed us to derive 26 ES cell lines from 32 embryos, including 11 $Nle^{flox/null}$, $p53^{-/-}$, $Rosa26^{CreERT2/+}$ ($p53^{KO}$ Nle^{cKO}) lines and 3 $Nle^{flox/null}$, $p53^{-/-}$, $Rosa26^{CreERT2/CreERT2}$ ($p53^{HET}$ Nle^{cKO}) lines (Figure R13).

2.1.3.2 p53 deficiency partially rescues the phenotype of Nle-deficient ES cells but does not prevent their elimination

We then used ES cells from two of the cell lines we derived, one $p53^{KO}$ Nle^{cKO} and one $p53^{HET}$ Nle^{cKO}, to analyze and compare their phenotypes after induction of *Nle* inactivation. For this, cells were plated at the same density and we followed their proliferation activity up to 9 days post-induction (dpi; cells were split in-between to ensure optimal growth conditions: see Figure R14.a). For both cell lines, untreated cells displayed similar proliferation capabilities at all time-points. Up to 72hpi (3dpi), we did not observe any difference in the proliferation of OHT-treated vs. untreated cells in either cell lines (Figure R14.b). However, at 5dpi OHT-treated cells exhibited impaired proliferation compared to their respective untreated controls, which was accentuated at 7dpi and 9dpi (Figure R14.b). Interestingly, OHT-treated $p53^{HET}$ Nle^{cKO} cells displayed a markedly more important decrease in proliferation compared to OHT-treated $p53^{KO}$ Nle^{cKO} cells, suggesting that p53 deficiency suppresses part of the survival and/or proliferation defects of *Nle*-deficient ES cells.

During this analysis, we harvested cells at 72hpi (3dpi) and 9dpi to prepare DNA, RNA and protein extracts. First, I analyzed the efficiency of *Nle* deletion in OHT-treated cells at the genomic level. The conversion of Nle^{flox} into Nle^{del} was efficient in $p53^{HET}$ Nle^{cKO} and $p53^{KO}$ Nle^{cKO} cells, as only little Nle^{flox} was detected in OHT-treated cells at 3dpi (Figure R14.c, top). At the mRNA level, *Nle* transcript levels were very low in OHT-treated cells of either cell lines by RT-qPCR (Figure R14.d), confirming that *Nle* had been indeed correctly inactivated upon OHT addition. Importantly, in cells harvested at 9dpi only the Nle^{flox} allele and no Nle^{del} allele could be detected in OHT-treated cells of either genotype (Figure R14.c, bottom), indicating that the remaining cells at this time-point originated from cells that had escaped *Nle* deletion during OHT treatment. This suggests that even in the absence of p53, *Nle*-deficient ES cells cannot be maintained and are counter-selected.

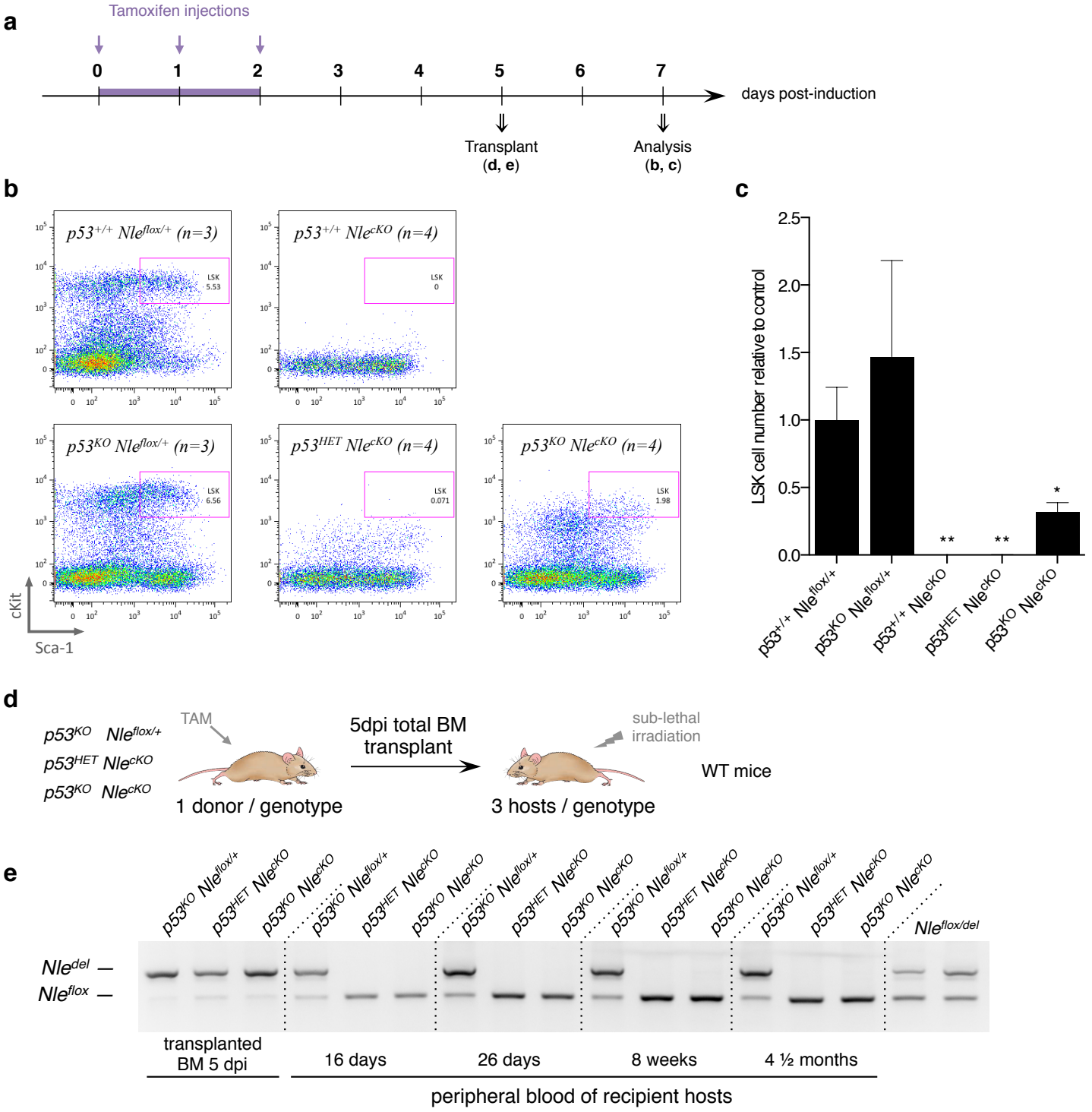

Figure R15. Lack of p53 does not allow maintenance of *Nle*-deficient HSCs and MPPs

a. Mice of the different genotypes were injected with tamoxifen 3 consecutive days to induce *Nle* inactivation. Mice were euthanized at 5dpi for transplantation experiments, and at 7dpi for FACS analysis of LSK cells. **b.** FACS profile of lineage-negative (Lin⁻) cells from the BM of $p53^{+/+}$ $Nle^{flox/+}$, $p53^{KO}$ $Nle^{flox/+}$, $p53^{+/+}$ Nle^{cKO}, $p53^{HET}$ $Nle^{flox/null}$ *and* $p53^{KO}$ $Nle^{flox/null}$ mice, using fluorescent antibodies directed against Lin, cKit and Sca-1 markers. Gates used for the quantification of LSK cell numbers are shown, with frequency of LSK cells relative to Lin⁻ cells. **c.** Number of LSK cells from each genotype, relative to LSK cell numbers from $p53^{+/+}$ $Nle^{flox/+}$ mice (the number of mice for each genotype is indicated in panel b). Statistical significance of the differences with $p53^{+/+}$ $Nle^{flox/+}$ mice was assessed using one-way ANOVA with Dunnett's correction for multiple comparisons: * $p<0.05$; ** $p<0.01$. **d.** For trans-plantation experiments, total bone marrow was collected from $p53^{-/-}$ $Nle^{flox/+}$ ($p53^{KO}$ $Nle^{flox/+}$), $p53^{HET}$ $Nle^{flox/null}$ *and* $p53^{KO}$ $Nle^{flox/null}$ mice at 5dpi (1 mouse per genotype), and each BM was transplanted in the retro-orbital sinus of 3 wild-type, sub-lethally irradiated recipient hosts. **e.** Genomic PCR detecting Nle^{flox} and Nle^{del} alleles was performed on DNA from transplanted BM and DNA from peripheral blood collected from recipient hosts at the indicated times. $Nle^{flox/del}$ DNA samples were used as controls.

In *(p53$^{+/+}$) Nle^{cKO}* cells, *Nle* inactivation induced the up-regulation of p53 target genes *p21* and *Bax* at 48hpi, and proliferation defects appeared at 72hpi. In *p53^{HET} Nle^{cKO}* cells, proliferation defects seem to appear between 72hpi (3dpi) and 5dpi. Thus, I wondered whether OHT-treated *p53^{HET} Nle^{cKO}* cells would also exhibit up-regulation of p53 target genes in response to *Nle* inactivation. For this, I analyzed the expression of *p21* and *Bax*, as well as other p53 pro-apoptotic target genes –*Noxa, Pidd* and *Puma*– in *p53^{HET} Nle^{cKO}* harvested at 72hpi. Interestingly, OHT-treated *p53^{HET} Nle^{cKO}* cells only exhibited significant up-regulation of *Noxa* but not the other target genes (Figure R14.e, bottom panel). I also analyzed this in *p53^{KO} Nle^{cKO}* cells: consistent with their p53 deficiency, none of the p53 targets I analyzed were up-regulated in these cells upon OHT treatment; surprisingly, some of these targets even appeared to be down-regulated (Figure R14.e, top panel).

These are preliminary results, and will need to be confirmed in further studies. Still, they suggest that p53 does indeed play an important role in the proliferation/survival defects of *Nle*-deficient ES cells. However, *p53* deficiency is not sufficient to maintain *Nle*-deficient ES cells, which are eventually counter-selected, suggesting that p53-independent mechanisms lead to the elimination of these cells.

2.2 p53 is up-regulated in other systems in response to *Nle* inactivation

In parallel to my work showing the activation of the RP-MDM2-p53 pathway in ES cells upon *Nle* deletion, our team also showed the up-regulation of p53 in response to *Nle* inactivation in other systems.

2.2.1 Early elimination of *Nle*-deficient HSCs is mediated by p53 activation

In the hematopoietic tissue, Marie Le Bouteiller showed that in *Nle cKO* mice, *Nle* inactivation led to the up-regulation of p53 protein levels in HSCs and MPPs (LSK cells) (Le Bouteiller et al., 2013). This was accompanied by the transcriptional activation of several p53 target genes in these cells, further validating the activation of p53 following *Nle* inactivation. To determine the implication of p53 in the severe hematopoietic phenotype of *Nle^{cKO}* mice, Marie then analyzed the BM of *p53^{KO} Nle^{cKO}* mice. Strikingly, p53 deficiency rescued the elimination of LSK cells she observed in the BM at day 5 after induction of *Nle* inactivation in p53-proficient *Nle^{cKO}* mice (Le Bouteiller et al., 2013).

To further study the hematopoietic phenotype of *Nle*-deficient mice in the absence of p53, I started the analysis of *p53^{KO} Nle^{cKO}*, *p53^{HET} Nle^{cKO}* and *(p53$^{+/+}$) Nle^{cKO}* mice at 7dpi. Preliminary results showed that LSK cells from *p53^{KO} Nle^{cKO}* mice at 7dpi are eliminated at this time-point and exhibit a similar profile as in *(p53$^{+/+}$) Nle^{cKO}* mice at 5dpi (Figure R15.b,c). In addition, Marie and I have performed a transplantation experiment, transplanting BM from *p53^{KO} Nle$^{flox/+}$*, *p53^{HET} Nle^{cKO}* and *p53^{KO} Nle^{cKO}* mice at 5dpi into wild-type, sub-lethally irradiated recipient hosts (R15.d). We then collected peripheral blood from recipient mice at different time-points after transplant, and analyzed the reconstitution of mature lineages by analyzing the presence of *Nle^{flox}* and *Nle^{del}* alleles in these samples (R15.e). In mice that received *p53^{KO} Nle$^{flox/+}$* BM, the *Nle^{del}* allele was retained at all time-points, despite a resurgence of the *Nle^{flox}* allele, indicative that some of the transplanted

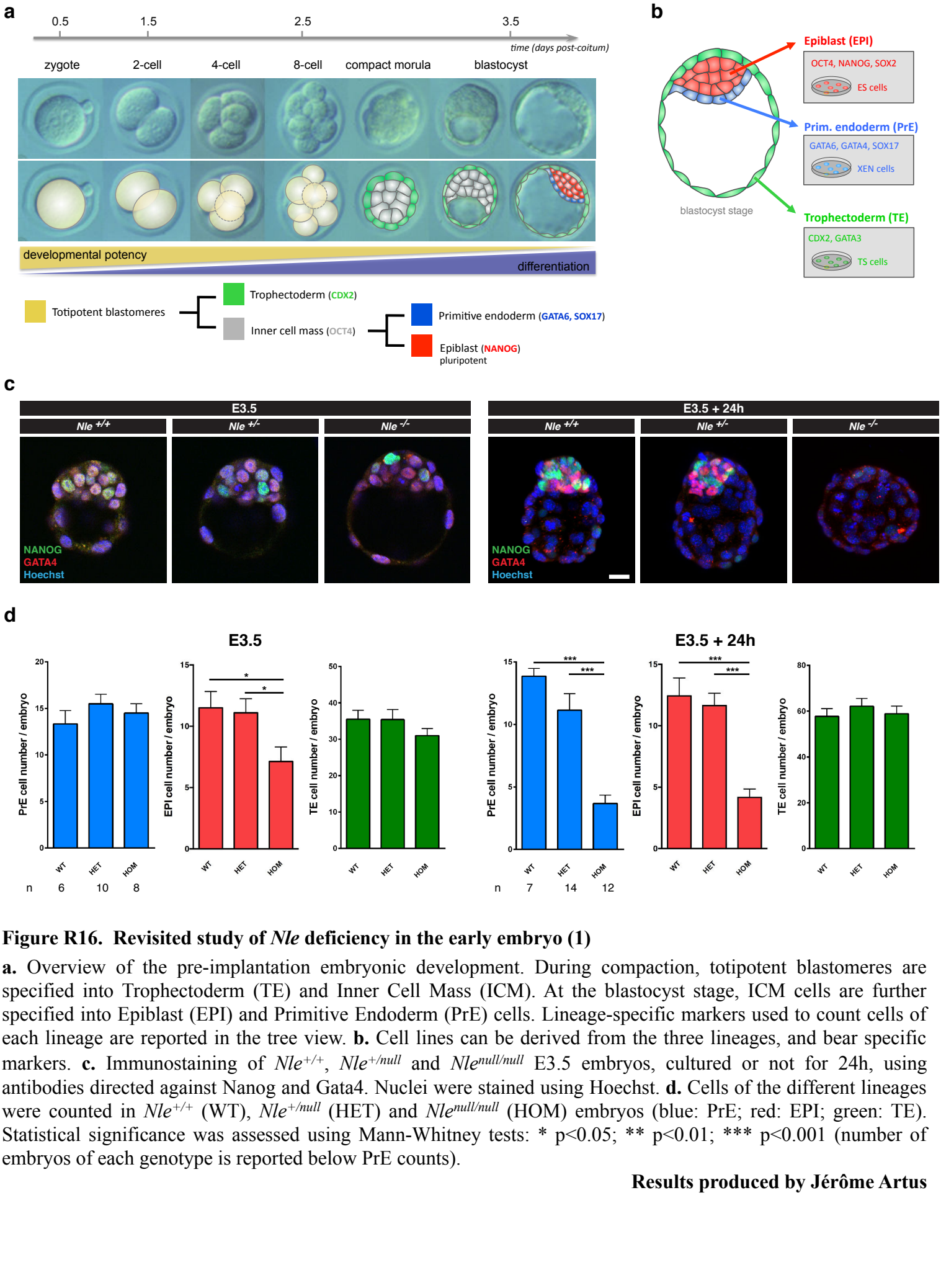

Figure R16. Revisited study of *Nle* deficiency in the early embryo (1)

a. Overview of the pre-implantation embryonic development. During compaction, totipotent blastomeres are specified into Trophectoderm (TE) and Inner Cell Mass (ICM). At the blastocyst stage, ICM cells are further specified into Epiblast (EPI) and Primitive Endoderm (PrE) cells. Lineage-specific markers used to count cells of each lineage are reported in the tree view. **b.** Cell lines can be derived from the three lineages, and bear specific markers. **c.** Immunostaining of $Nle^{+/+}$, $Nle^{+/null}$ and $Nle^{null/null}$ E3.5 embryos, cultured or not for 24h, using antibodies directed against Nanog and Gata4. Nuclei were stained using Hoechst. **d.** Cells of the different lineages were counted in $Nle^{+/+}$ (WT), $Nle^{+/null}$ (HET) and $Nle^{null/null}$ (HOM) embryos (blue: PrE; red: EPI; green: TE). Statistical significance was assessed using Mann-Whitney tests: * $p<0.05$; ** $p<0.01$; *** $p<0.001$ (number of embryos of each genotype is reported below PrE counts).

Results produced by Jérôme Artus

cells had escaped *Nle* inactivation. In contrast, in mice that received either $p53^{HET}$ Nle^{cKO} BM or $p53^{KO}$ Nle^{cKO} BM, only the Nle^{flox} allele could be detected at each time-point, indicating that only cells that had escaped *Nle* inactivation could repopulate the bone marrow, consistent with the loss of LSK cells I observed in $p53^{HET}$ Nle^{cKO} and $p53^{KO}$ Nle^{cKO} mice at 7dpi.

Unfortunately, due to breeding problems at the time, I could not continue the analysis of mice deficient for both *p53* and *Nle*. It will be interesting to investigate what cellular mechanisms lead to the elimination of *p53*-deficient HSCs following *Nle* inactivation.

2.2.2 Inactivation of *Nle* in intestinal stem cells activates the p53 pathway

Another system in which our team has investigated the role of *Nle* is the intestinal epithelium. As I mentioned in part *I-1.3*, Aline Stedman showed that specific inactivation of *Nle* in this tissue (using Nle^{VilcKO} mice) leads to the rapid elimination of intestinal stem and progenitor cells (ISPCs) by cell cycle arrest, apoptosis and biased differentiation (see article in *Annex*). Furthermore, she showed that this was driven by the activation of p53 in *Nle*-deficient ISPCs. However, ISPC elimination persisted in the absence of p53, suggesting the existence of p53-independent responses to defective RiBi in these cells in $p53^{KO}$ Nle^{VilcKO} mice. Interestingly, she observed a diminution, although non-significant, in protein synthesis of *p53*-deficient ISPCs after *Nle* inactivation, suggesting that deregulation of protein synthesis could contribute to the elimination of *Nle*-deficient ISPCs in the absence of p53. In the process of the revision of her publication, I contributed to the analysis of *Nle* deletion in $p53^{KO}$ Nle^{VilcKO} ISPCs (Figure 8.a of the article in *Annex*).

3. Differential requirement of *Nle* for ribosome biogenesis?

3.1 Revisiting the requirement of *Nle* for the establishment of the first embryonic cell lineages

As I mentioned in part *I-1.3*, previous work in the laboratory showed that *Nle* was critically required for the survival of ICM cells, but seemed to be dispensable for cells of the trophectoderm (TE) (Cormier et al., 2006). However, the role of *Nle* in RiBi was unknown at the time, and it remained unclear whether *Nle* is required in both lineages of the ICM –the epiblast (EPI) and the primitive endoderm (PrE)–, and what was the effect of *Nle* deficiency on TE cells. In light of our new knowledge on the role of *Nle* in RiBi, Jérôme Artus and I decided to re-investigate the requirement of *Nle* in these three early embryonic lineages using both *in vivo* and *ex vivo* paradigms (Figure R16.a,b).

3.1.1 *Nle* loss-of-function affects both the epiblast and primitive endoderm, but primarily the epiblast

In vivo, Jérôme used lineage-specific markers to compare lineages formation and maintenance in $Nle^{+/+}$, $Nle^{+/null}$ and $Nle^{null/null}$ embryos. $Nle^{+/-}$ males and females were crossed, and Jérôme collected embryos at E3.5. First, he counted the number of cells of each lineage in these embryos. At E3.5, $Nle^{null/null}$ embryos exhibited significantly reduced numbers of EPI cells compared to controls, but no difference in PrE and TE cells (Figure R16.c,d left panels). After 24h of culture, this reduction was accentuated and accompanied by a significant reduction in the number of PrE

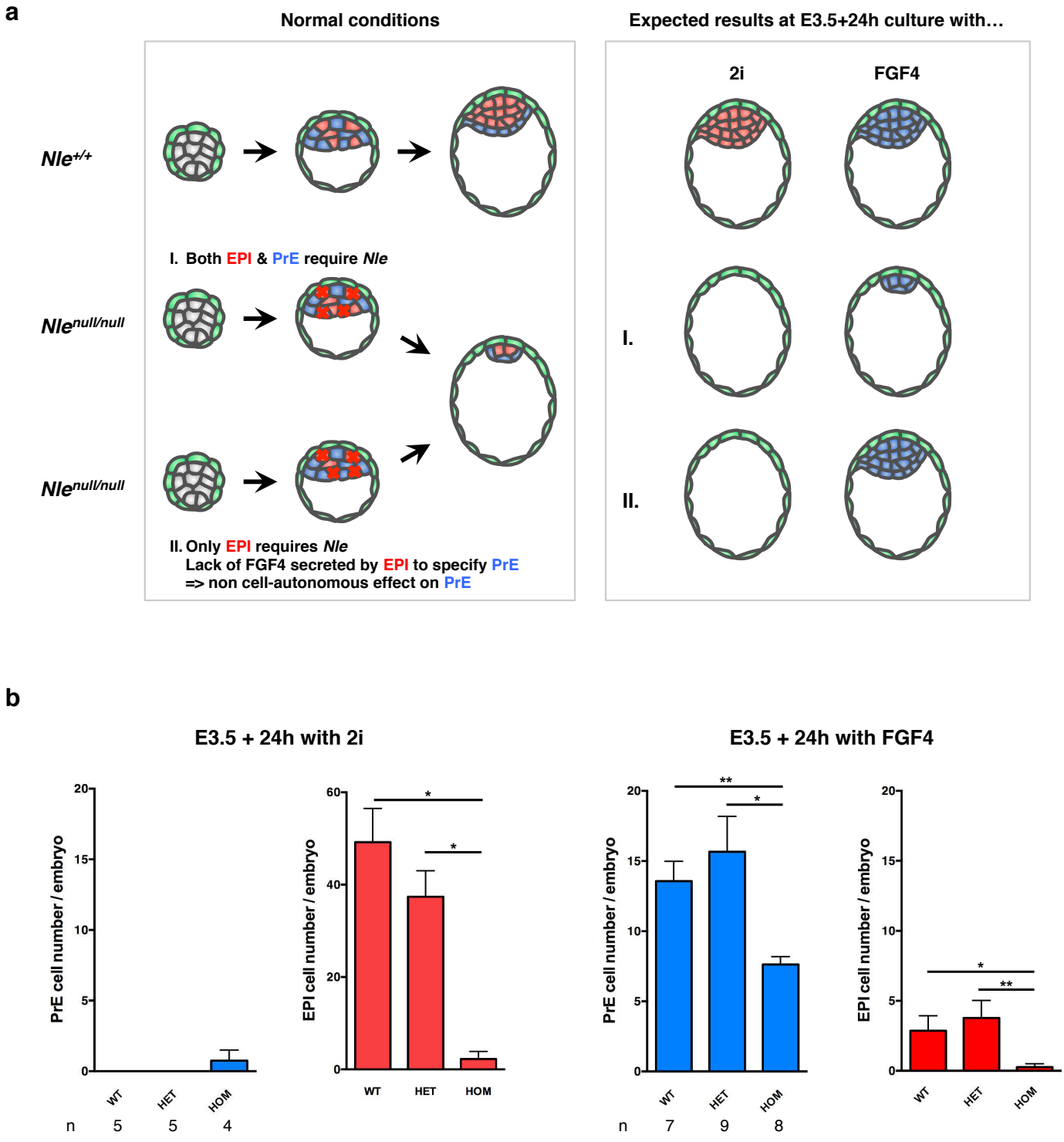

Figure R17. Revisited study of *Nle* deficiency in the early embryo (2)

a. Left panel: hypotheses to explain the loss of PrE cells in *Nle*$^{null/null}$ embryos. Right panel: expected results for both hypotheses in E3.5 embryos cultured 24h in medium complemented with either 2i or FGF4. **b.** EPI (red) and PrE (blue) cells were counted in *Nle*$^{+/+}$ (WT), *Nle*$^{+/null}$ (HET) and *Nle*$^{null/null}$ (HOM) embryos after 24h of culture in the presence of either 2i (left panel) or FGF4 (right panel). Statistical significance was assessed using Mann-Whitney tests: * $p<0.05$; ** $p<0.01$; *** $p<0.001$ (number of embryos of each genotype is reported below PrE counts).

Results produced by Jérôme Artus

cells as well, but TE cells remained unaffected (Figure R16.c,d right panels). These results show that *Nle* is critically required for EPI cells and PrE cells, but apparently not for TE cells. However, since the establishment of PrE cells requires FGF secretion by EPI cells, the loss of PrE cells in *Nle*-deficient embryos could result from the loss of EPI cells (Figure R17.a). To test whether *Nle* was required for PrE in a cell-autonomous manner, Jérôme then cultured E3.5 embryos in medium containing either 2i –forcing ICM cells into EPI cells– or FGF4 –forcing ICM cells into PrE cells– and counted the number of EPI and PrE cells obtained (Figure R17.b). Consistent with the requirement of *Nle* for EPI cells, $Nle^{null/null}$ embryos cultured with 2i displayed dramatic loss of almost all ICM cells (Figure R17.b, left panels). In embryos cultured with FGF4, most ICM cells were converted to PrE cells: a few EPI cells remained in $Nle^{+/+}$ and $Nle^{+/null}$ embryos, but were completely eliminated in $Nle^{null/null}$ embryos; strikingly, these $Nle^{null/null}$ embryos exhibited a significant reduction in the number of PrE cells compared to controls (Figure R17.b, right panels). These data indicate that even in the presence of FGF4 to maintain PrE specification, *Nle* inactivation impedes PrE cell proliferation or survival, meaning that *Nle* is required in a cell-autonomous manner for PrE cells. Altogether, these results show that *Nle* inactivation affects both lineages of the ICM, but primarily the epiblast.

3.1.2 Activation of the p53 pathways in response to *Nle* loss-of-function in cell culture models of early embryonic lineages?

In addition, Jérôme also looked at p53 activation in E3.5 embryos, and saw a notable increase in p53 levels by immunofluorescence in all ICM cells as well as a slight increase in TE cells, suggesting that all three lineages activate the p53 pathway in the absence of *Nle* (data not shown). Since investigating the molecular responses in these lineages is quite arduous, we decided to use *ex vivo* models of each lineage: ES cells as a model for the EPI lineage, XEN (extraembryonic endoderm stem) cells for the PrE lineage and TS (trophectoderm stem) cells for the TE lineage (see Figure R16.b). Nle^{cKO} cell lines where *Nle* inactivation can be induced were used.

In addition to my work on Nle^{cKO} ES cells I presented in part *I-2.1*, I also performed RT-qPCR experiments on mRNA extracts of 48hpi and 72hpi OHT-treated vs. untreated cells, to investigate whether *Nle*-deficient ES cells display transcriptional signatures of differentiation. Although this analysis gave mixed and inconclusive results, I did observe a general deregulation of genes involved in differentiation and the maintenance of pluripotency of ES cells, suggesting that some ES cells may indeed undergo differentiation in response to *Nle* inactivation (data not shown).

In Nle^{cKO} XEN cells, addition of OHT to the medium led to proliferation and/or survival defects 4 days after induction, consistent with the requirement of *Nle* for PrE cells (Figure R18.a). At this time-point, RT-qPCR analysis showed that *Nle* inactivation had been efficient (Figure R18.b). I also observed the up-regulation of p53 target genes *Bax*, *Noxa*, *Pidd*, *Puma* and *p21* in OHT-treated cells, indicating that the p53 pathway is activated in these cells (Figure R18.c). Although these are very preliminary data, they are consistent with the results obtained by Jérôme Artus *in vivo* in the early embryo.

Regarding TS cells, the study of *Nle* in this model proved to be more challenging than expected. Indeed, *Nle* inactivation in Nle^{cKO} TS cells is very inefficient, and these cells proliferate

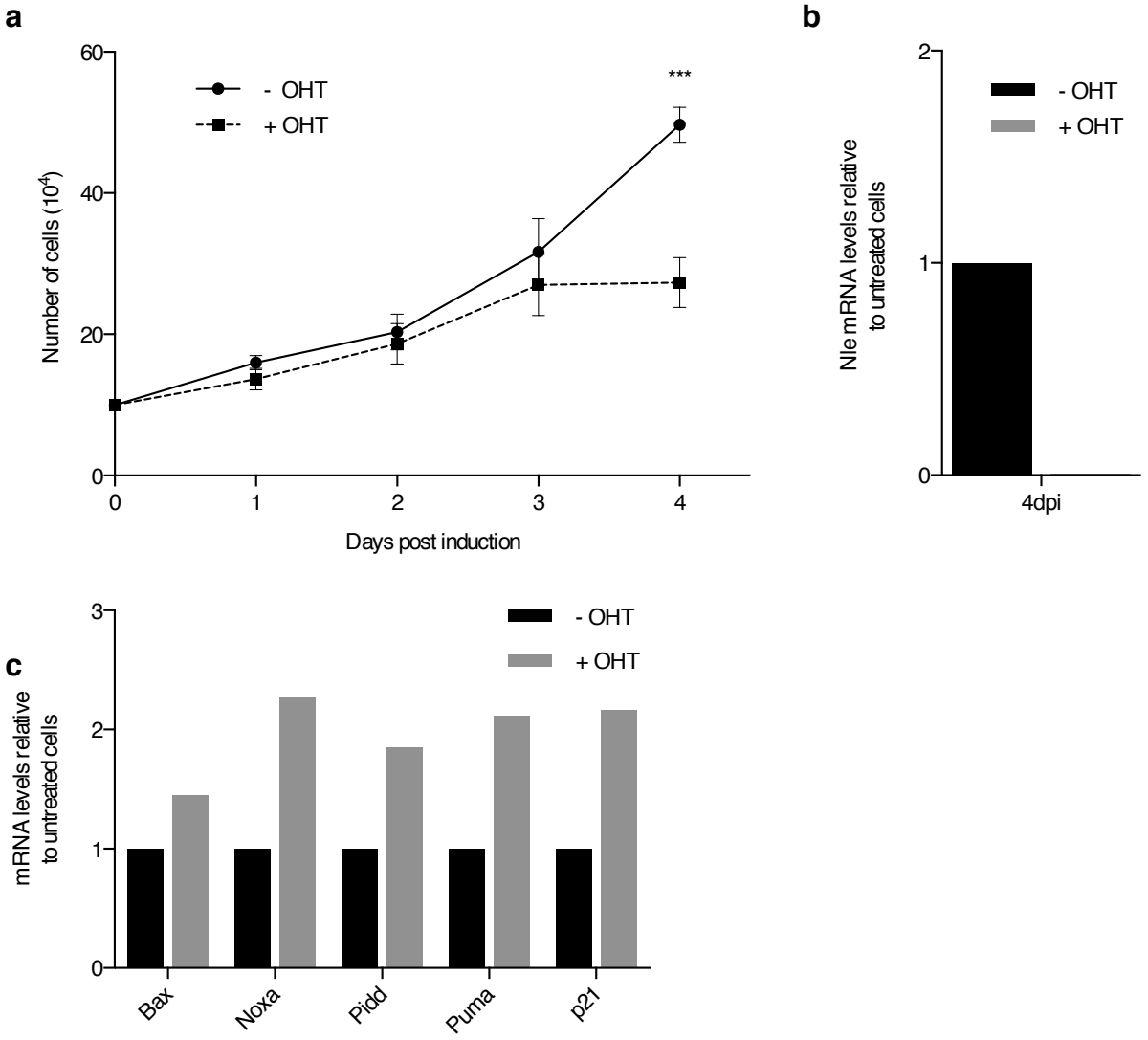

Figure R18. ***Nle*-deficient XEN cells exhibit impaired proliferation and activate p53 target genes**

Nle^{cKO} XEN cells were cultured in the presence or absence of 1µM OHT for 48h and were maintained in culture up to 4 days. **a.** Cell counts of OHT-treated vs. untreated cells, at the indicated time-points (n=3 at each point). Statistical significance was assessed using unpaired two-tailed Student's t tests: *** $p<0.001$. **b,c.** Cells were harvested at 4dpi and total mRNA extracts were prepared. RT-qPCR analysis of the mRNA levels of *Nle* (**b**) and p53 target genes *Bax*, *Noxa*, *Pidd*, *Puma* and *p21* (**c**) in OHT-treated cells relative to untreated cells (n=1).

much more slowly than ES and XEN cells. Thus, I haven't had the opportunity to pursue their study, but first analyses by Sandrine Vandormael-Pournin in the laboratory suggest that *Nle*-deficient TS cells are counter-selected to the benefit of cells that have escaped *Nle* deletion. Future work, maybe using a different Nle^{cKO} cell line, will allow better understanding of the consequence of *Nle* inactivation in this system.

Altogether, these results indicate that *Nle* is required for all three of the first embryonic lineages. Interestingly, although *Nle* deficiency does not affect the TE *in vivo*, it appears to be important for TS cells.

3.2 *Nle* is dispensable in lymphoid lineages?

While studying the role of *Nle* in the mouse hematopoietic system, Marie Le Bouteiller also investigated its requirement in the B lineage using a mouse strain expressing a constitutively active Cre recombinase specifically in progenitors of the B lymphoid lineage. B progenitors are known to proliferate rapidly and mature B cells have an important protein synthesis activity to produce immunoglobulins, thus RiBi defects induced by *Nle* inactivation in this lineage were expected to lead to dramatic defects. However, strikingly Marie showed that in this lineage, *Nle* inactivation did not impede ribosome biogenesis and thus had no effect on cell survival or proliferation, neither in B progenitors nor in mature B-lymphocytes (Le Bouteiller et al., 2013). Furthermore, she showed that the general population of lineage-positive cells in the BM was not affected by *Nle* inactivation, at least regarding RiBi. This was very surprising and questioned the critical role of *Nle* for ribosome biogenesis, and suggested that some cells may use alternative RiBi pathways where *Nle* is not required for maturation of the large ribosome subunit.

This prompted us to ask whether *Nle* could be dispensable in other lineages. Thus, I took advantage of the *Lck-Cre* mouse strain, where a constitutively active Cre recombinase is expressed specifically in progenitors of the T-cell lineage (pro-T cells), to investigate the requirement of *Nle* in this lineage (see Figure R19.a for an overview of the T lineage development). I crossed *Lck-Cre* mice to $Nle^{null/+}$ to obtain a $(Lck\text{-}Cre)^2$, $Nle^{null/+}$ strain (homozygous for the *Lck-Cre* transgene). Crossing such mice to $Nle^{flox/flox}$ mice, I studied the phenotype of *Lck-Cre,* $Nle^{flox/null}$ ($Nle^{Lck\text{-}cKO}$) vs. *Lck-Cre,* $Nle^{flox/+}$ ($Nle^{Lck\text{-}ctrl}$). Importantly, I did not notice any difference in terms of survival between mice of either genotype, indicating that *Nle* inactivation in T cells did not lead to major, pathogenic defects. To analyze the phenotype of T-cells, I collected the thymus of 4 weeks old $Nle^{Lck\text{-}cKO}$ and $Nle^{Lck\text{-}ctrl}$ mice, and analyzed thymocytes using flow cytometry. First, I wanted to check if *Nle* inactivation led to any block in the maturation of T cells, as it has been observed in case of *Rps6* of *Rpl22* inactivation (Anderson et al., 2007; Stadanlick et al., 2011; Sulic et al., 2005). Thus, I used antibodies directed against the CD4 and CD8 markers and looked at the proportion of single-positive ($CD4^+$ $CD8^-$ or $CD4^-$ $CD8^+$) mature T cells, and double-positive ($CD4^+$ $CD8^+$) and double-negative ($CD4^-$ $CD8^-$) pro-T cells. Although there seemed to be some variation in the proportion of each subset between $Nle^{Lck\text{-}cKO}$ and $Nle^{Lck\text{-}ctrl}$ mice, it was not significant (Figure R19.b). Consistently, analysis of the different DN stages (DN1 to DN4, using antibodies directed against the CD44 and CD25 markers) did not show any significant difference

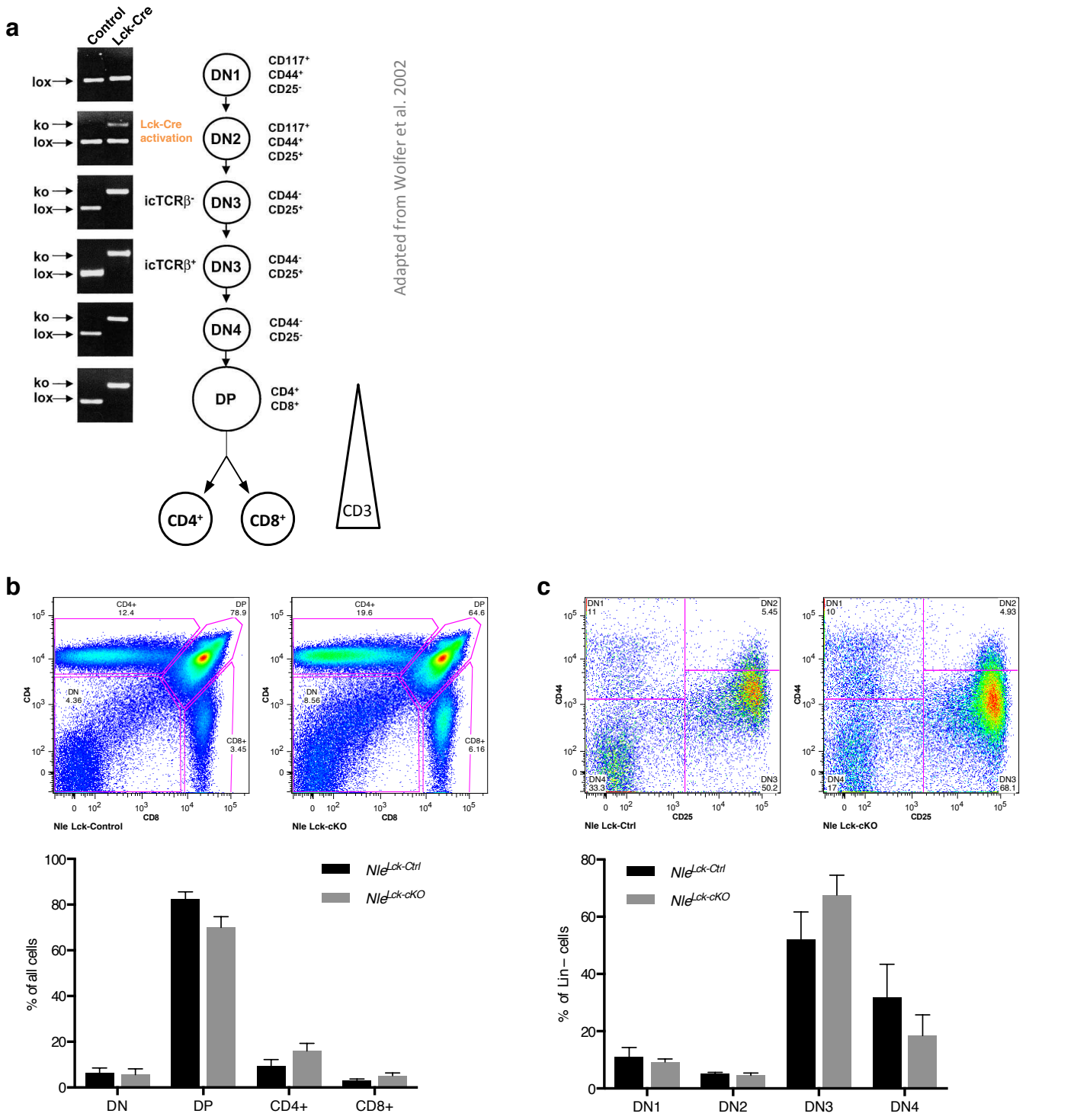

Figure R19. Inactivation of *Nle* in the T lineage using the *Lck-Cre* mouse strain

a. Overview of the T cell development in the thymus: double-negative progenitors (DN1-DN4) give rise to double-positive (DP) T progenitor cells, which in turn become either CD4 or CD8 single-positive mature T cells. The Lck-Cre transgene is expressed from the DN2 stage, allowing recombination of a flox allele into a knock-out (ko) allele (Wolfer et al, 2002). **b,c.** FACS analysis of mature T cells (b) or DN cells at the different stages (c) in thymocytes isolated from the thymus of 4 weeks old $Nle^{Lck\text{-}Ctrk}$ and $Nle^{Lck\text{-}cKO}$ mice. **b.** Upper panel: CD4/CD8 FACS profile on whole thymocytes used to separate DN progenitors from DP and single-positive ($CD4^+$ and $CD8^+$) mature T cells. Lower panel: quantification of the proportion of each subset in the whole thymocyte population. **c.** Upper panel: CD44/CD25 FACS profile of lineage-negative (Lin–) cells ($CD4^-$ $CD8^-$ $CD3^-$) used to separate DN1, DN2, DN3 and DN4 subsets. Lower panel: quantification of the proportion of DN cells at the different stages, in the Lin– population. Statistical analyses using upaired, two-tailed Student's t tests revealed no significant differences between $Nle^{Lck\text{-}Ctrk}$ vs. $Nle^{Lck\text{-}cKO}$ mice (n=3 mice for each genotype).

either, despite a seemingly increased proportion of DN3 cells at the expense of DN4 cells (Figure R19.b).

These are preliminary results, and I did not have time to pursue the analysis of these mice. It will be important to verify the efficiency of *Nle* inactivation in $Nle^{Lck\text{-}cKO}$ and $Nle^{Lck\text{-}ctrl}$ mice, and investigate whether *Nle* loss-of-function in developing T cells impedes their ribosome biogenesis activity. However, the lack of apparent phenotype in $Nle^{Lck\text{-}cKO}$ mice suggests that *Nle* may not be required for RiBi in the T lineage.

II. Article: analysis of the ribosome biogenesis activity of hematopoietic stem cells and immature progenitors

1. Article: synopsis

When I arrived in the laboratory, Marie Le Bouteiller had just set up an approach to analyze RiBi defects in different hematopoietic populations simultaneously, in *Nle*-deficient vs. control mice. This approach combined FISH and flow cytometry, hence we called it "Flow-FISH". Using Flow-FISH, Marie was able to show in HSCs the accumulation of pre-rRNAs of the large ribosome subunit compared to the unaffected small subunit (Le Bouteiller et al., 2013). In addition to allowing analysis of RiBi defects in mutant mice, this method also opened a window of opportunity to document the relative ribosome biogenesis activity of HSCs and other immature hematopoietic populations in unperturbed conditions. This was exciting, especially since studying the regulation and activity of ribosome biogenesis is particularly challenging in rare populations such as HSCs (there are only ~20 000 HSCs per mouse) due to the little amount of biological material available. Thus, I dedicated a major part of my work to the analysis of RiBi activity in immature hematopoietic populations, which led to the writing of the article presented in the following pages. Here, I will briefly present the key results of this article.

Using Flow-FISH, I showed that immature hematopoietic populations display important levels of rRNA precursors (pre-rRNA) of both ribosome subunits, suggesting notably that HSCs actively synthesize ribosomes. This was unexpected, and prompted me to test whether Flow-FISH really reflects the dynamics of ribosome biogenesis. To this end, I used different approaches. First, I used inhibitors of the RNA polymerase I (RNA Pol I) to inhibit neo-synthesis of rRNA; *ex vivo* treatment with these inhibitors prior to Flow-FISH analysis resulted in a significant reduction of the pre-rRNA levels observed in all hematopoietic populations analyzed. In parallel, I used an analog of the uridine nucleotide to label newly synthesized rRNAs in hematopoietic cells *ex vivo* and observed similar results as those obtained with Flow-FISH.

As we saw in the second part of the introduction, ribosome biogenesis and cell growth are tightly linked. Therefore, we also wanted to address whether the RiBi activity I observed in hematopoietic cells was correlated to their protein synthesis activity. To this end, I used the ribopuromycylation method (RPM) developed by Alexandre David to measure the translation rate of immature hematopoietic populations. Thus, I showed that although HSCs and MPPs display similar RiBi activity, HSCs exhibit significantly lower protein synthesis activity than MPPs. The results I obtained using this method are consistent with another study (Signer et al., 2014).

Altogether, the results presented in this article highlight unsuspected ribosome biogenesis activity in HSCs despite their mostly quiescent state, and bring previously unavailable information regarding RiBi activity in the different immature populations of the hematopoietic system. Furthermore, they show that ribosome biogenesis is not coupled to the translational activity or the proliferative index of immature hematopoietic populations. Finally, the observations I made in HSCs support the idea that RiBi may play an important role in the regulation of hematopoietic stem cells independently from the regulation of protein synthesis.

The different approaches I used for this study have required important development and adjustments, some of which are presented in the article as supplementary information. After the article, I will discuss other issues that I have been confronted to, and results that I could not integrate for publication.

Mouse adult hematopoietic stem cells actively synthetize ribosomes

Léonard Jarzebowski[1], Marie Le Bouteiller[1, 2], Sabrina Coqueran[1], Aurélien Raveux[1], Sandrine Vandormael-Pournin[1], Ana Cumano[3] and Michel Cohen-Tannoudji[1,#]

[1] : Institut Pasteur, CNRS, Unité de Génétique Fonctionnelle de la Souris, UMR 3738, Department of Developmental & Stem Cell Biology, 25 rue du docteur Roux, F-75015 Paris Cedex.

[2] : present address, Biotech Research and Innovation Center, University of Copenhagen, DK-2200 Copenhagen N, Denmark

[3] : Lymphocyte Development Unit, Institut Pasteur, Paris, France

[#] Correspondence:

Michel Cohen-Tannoudji : Unité de Génétique Fonctionnelle de la Souris, Department of Developmental & Stem Cell Biology, 25 rue du docteur Roux, F-75015 Paris, France; E-mail: m-cohen@pasteur.fr; Phone: 33 1 45 68 84 86; Fax: 33 1 45 68 86 34; website: https://research.pasteur.fr/en/team/group-michel-cohen-tannoudji/.

Running title: Ribosome biogenesis in HSCs

Keywords : Hematopoietic Stem Cell; Ribosome biogenesis; rRNA maturation;

ABSTRACT

Contribution of basal cellular processes to the regulation of tissue homeostasis has just started to be appreciated. However, our knowledge on the modulation of ribosome biogenesis activity *in situ* within specific lineages remains very limited. This is largely due to the lack of assays that enable quantitation of ribosome biogenesis in small numbers of cells *in vivo*. We developed a technique, named Flow-FISH, combining cell surface antibody staining and flow cytometry with intracellular ribosomal RNA (rRNA) FISH and allowing to measure the levels of pre-rRNAs of hematopoietic cells *in vivo*. Here, we show that Flow-FISH reports and quantifies ribosome biogenesis activity in hematopoietic cell populations, thereby providing original data on this fundamental process notably in rare populations such as hematopoietic stem cells (HSCs). We unravel variations in ribosome biogenesis between different hematopoietic progenitor compartments and during erythroid differentiation. In particular, our data indicate that, contrary to what may be anticipated from their quiescent state, HSCs have significant ribosome biogenesis activity. Moreover, variations in ribosome biogenesis activity do not correlate with proliferation rate suggesting that cell type specific mechanisms might regulate ribosome biogenesis in hematopoietic stem cells and progenitors. Our study contributes to a better understanding of the cellular physiology of the hematopoietic system *in vivo* in unperturbed situation.

INTRODUCTION

Continuous blood cells production over the lifetime of the organism requires the coordinated activity of hematopoietic stem cells (HSCs) and progenitor cells (Orkin and Zon, 2008). Tight regulation of renewal, proliferation and differentiation of the different populations is key during both steady-state and stress hematopoiesis and involves the complex interactions between intrinsic and extrinsic factors. Because of their ubiquitous nature, direct contribution of basal cellular processes to the regulation of tissue homeostasis (Buszczak et al., 2014) has been largely underappreciated for a long time.

Ribosome biogenesis is a fundamental and universal cellular process tightly coupled to cell growth and proliferation (Lempiäinen and Shore, 2009). Ribosome biogenesis occurs in the nucleolus of eukaryotic cells starting with transcription by RNA polymerase I of the 47S pre-rRNA (precursor of the 5.8S, 18S and 28S mature rRNAs), which then undergoes a series of cleavages and modifications while being assembled into ribosomal pre-particles upon hierarchical addition of ribosomal proteins. Large and small ribosomal pre-particles are then exported to the cytoplasm to terminate their maturation and assemble into functional ribosomes.

Ribosome biogenesis is highly connected to diseases. In humans, disorders of ribosome dysfunction are called ribosomopathies and correspond to a collection of inherited or somatically acquired human syndromes associated with haploinsufficiency in genes encoding ribosomal proteins or mutations in ribosome biogenesis factors. They represent a set of clinically distinct diseases presenting with tissue specific developmental defects (bone marrow failure, skeletal abnormalities, asplenia, …) and increased risk of cancer (Narla and Ebert, 2010). The fact that mutations of ribosomal proteins or ribosome biogenesis factors cause tissue-specific diseases in human is puzzling (McCann and Baserga, 2013) and several mechanisms have been put forward to explain the physiopathology of these diseases. Since

the availability of ribosomes is a rate-limiting step in translation initiation (Shah et al., 2013), a shortage in ribosome supply will affect translation efficiency but not equally for all mRNA species.

The existence of differences in ribosome biogenesis between stem cells and their progenies is supported by several studies (Brombin et al., 2015). For example, ribosomal small subunit processing factors are downregulated during mouse embryonic stem (ES) cell differentiation and knockdown of the corresponding genes in undifferentiated ES cells impairs pluripotency maintenance (You et al., 2015). Similarly, genes coding for ribosomal proteins and ribosome biogenesis factors were identified in screens for genes regulating maintenance or differentiation of drosophila germ stem cells (Fichelson et al., 2009; Sanchez et al., 2015; Yu et al., 2016; Zhang et al., 2014), drosophila neuroblasts (Neumüller et al., 2011) and ES cells (Fortier et al., 2015). In the hematopoietic tissue, we recently identified previously unsuspected differences in 60S ribosomal subunit production between stem cells and committed progenitors (Le Bouteiller et al., 2013). Contrasting with these data, our knowledge on the variation of ribosome biogenesis activity *in vivo* within specific lineages remains very poor.

Because extracellular growth and stress signals impinge upon the production of ribosomal components and biogenesis factors, studies on ribosome biogenesis activity in cultured cells cannot be informative on the *in vivo* situation. In addition, the paucity of HSCs has largely impeded direct measurements of ribosome biogenesis activity using traditional methods. Recently, we developed a technique combining rRNA FISH with Flow cytometry to reveal unbalanced 40S and 60S subunit biosynthesis *in situ* in hematopoietic cells following disruption of *Notchless* (Le Bouteiller et al., 2013). Here, we used this approach to quantify ribosome biogenesis activity within the hematopoietic lineage of the adult mouse with special emphasis on the rare populations of HSCs and immature progenitors.

RESULTS

HSCs display low translational activity

We first looked at active ribosomes in the immature cell populations of the bone marrow using the RiboPuromycylation Method (RPM) (David et al., 2012; Seedhom et al., 2016). This method is based on puromycin incorporation into the A site of elongating ribosome and specific and covalent association with nascent peptidic chains. 8-10 weeks old C57Bl/6 mice were injected with a single dose (2 mg) of puromycin and killed 10 min after injection. Immediately after, bone marrow cells were harvested and placed at 4°C in emetine-containing medium in order to freeze ribosome elongation and block the eventual release of puromycylated nascent chains from ribosomes. Bone marrow cells were first stained using cell surface antibodies and then processed for intracellular puromycin immunodetection before flow cytometry analysis. Because labelling is limited to a short period of time (about 15 min), incorporation of puromycin is likely limited to one round of translation and puromycin immunodetection is therefore a good proxy of translation rate.

Total bone marrow cells from injected mice showed a marked increase in puromycin staining compared to untreated mice (**Figure 1A**). When mice were treated with harringtonine, an inhibitor of the initial steps of translation, 15 min prior to puromycin administration, staining was significantly reduced (**Figure 1A-B**) confirming that RPM indeed measured translation activity in bone marrow cells. The wide distribution of fluorescence intensity suggested the existence of differences in translation rate between bone marrow cells. Interestingly, hematopoietic stem cells (Lin^- $Sca1^+$ $cKit^+$ $CD34^+$; "HSC") exhibited lower puromycin incorporation compared to other immature progenitors including multipotent progenitors (Lin^- $Sca1^+$ $cKit^+$ $CD34^-$; "MPP"), common myeloid progenitors (Lin^- $Sca1^-$ $cKit^+$ $CD34^+$ $FC\gamma R\text{-}II/III^{hi}$; "CMP"), granulocyte and macrophage progenitors (Lin^- $Sca1^-$ $cKit^+$ $CD34^{low}$ $FC\gamma R\text{-}II/III^{lo}$; "GMP") and megakaryocyte and erythrocyte

progenitors (Lin^- $Sca1^-$ $cKit^+$ $CD34^-$ FCγR-II/III^{lo} ; MEP) (**Figure 1B**). Consistently with a previous study (Signer et al., 2014), our data suggest that HSCs have a reduced protein synthesis rate compared to committed progenitors.

Flow-FISH allows quantification of pre-rRNA levels in the hematopoietic tissue:

To monitor ribosome biogenesis activity of hematopoietic cells, we combined cell surface antibody staining and flow cytometry with intracellular RNA FISH using rRNA probes. This method, named Flow-FISH, allows quantifying rRNAs levels at the single cell level in the different hematopoietic cell populations. We used its1 and its2 FISH probes hybridizing to nucleolar rRNA precursors but not to the mature rRNA species found in cytoplasmic ribosomes and specific for precursors of the small and the large subunit respectively.

First, we used Flow-FISH to determine ribosome biogenesis activity during erythroid differentiation. Indeed, terminal differentiation of erythroid progenitors is characterized by a gradual decrease of the cell volume and ribosomes content (Dolznig et al., 1995). A decrease in ribosome production is therefore expected during this process although this hasn't been documented *in vivo* so far. Bone marrow cells were collected from femurs and tibias of 6-to-12 week-old, wild type C57Bl/6J mice, and stained using fluorescently-labelled antibodies against CD71 and Ter119 allowing to separate different steps of erythroid maturation: $CD71^+$ $Ter119^{low}$ pro- and early-erythroblasts, $CD71^+$ $Ter119^+$ intermediate erythroblasts, $CD71^{low}$ $Ter119^+$ late erythroblasts and $CD71^-$ $Ter119^+$ early normoblasts (Socolovsky et al., 2001) (for gating strategy, see supplementary figure S1). Cells were then fixed and hybridized with either its1 or its2 fluorescently-labelled probes. We found that $CD71^+$ $Ter119^{low}$ pro- and early-erythroblasts expressed high levels of its1 and its2 (**Figure 2**, 4.3-fold and 4.2-fold increase compared to whole bone marrow cell). Strikingly, pre-rRNA levels dropped

dramatically at the transition from early to intermediate erythrobasts and remained at similar levels in more mature cells (**Figure 2**). We conclude from these experiments that ribosome biogenesis is tightly regulated during bone marrow erythroid maturation.

Immature populations of the hematopoietic tissue display important pre-rRNA levels

We then used Flow-FISH to measure pre-rRNA levels in different populations of immature hematopoietic cells of the bone marrow. Immature Lin– cells, which represent around 10% of whole bone marrow cells, displayed higher levels of its1 and its2 than more mature Lin+ cells (**Figure 3A**). Amongst Lin– cells, megakaryocyte and erythrocyte progenitors (Lin^- $Sca1^-$ $cKit^+$ $CD34^-$; "MEP") showed the highest levels of its1 and its2 and HSCs the lowest (**Figure 3A**). HSCs are in a vast majority quiescent, with very low division rate and low mitochondrial metabolic activity (Chandel et al., 2016; Nakamura-Ishizu et al., 2014) and therefore are expected to require less ribosome production than more active cells. However, we found that pre-rRNA levels in HSCs were similar to that of actively dividing MPPs (1.4-fold and 1.3-fold reduction for its1 and its2 respectively) and higher than Lin+ progenitors and differentiated cells of the bone marrow (3.8-fold and 2.5-fold increase for its1 and its2 respectively).

These relatively high levels of pre-rRNA levels suggest that ribosomes are actively produced in HSCs. However, they could also correspond to a pool of stored pre-ribosomal particles that could be rapidly mobilized to produce new ribosomes upon HSCs activation. To discriminate between these two possibilities, we first looked at the subcellular distribution of pre-rRNAs in HSCs and progenitors. We performed Flow-FISH staining on Lin+-depleted bone marrow cells and then FACS-sorted the different immature bone marrow cell populations before imaging. As shown on **Figure 3C**, its1 staining in HSCs appeared as a few discrete spots located in DNA sparse regions of the nucleus likely corresponding to

nucleoli. Importantly, the subcellular distribution of its1 staining was identical in HSCs (Lin^- $Sca1^+$ $cKit^+$ $CD34^-$), MPPs (Lin^- $Sca1^+$ $cKit^+$ $CD34^+$), CMPs (Lin^- $Sca1^-$ $cKit^+$ $CD34^{hi}$), GMPs (Lin^- $Sca1^-$ $cKit^+$ $CD34^{lo}$) and MEPs (Lin^- $Sca1^-$ $cKit^+$ $CD34^-$) (**Figure 3C**). Identical results were obtained with the its2 probe (not shown). These data argue against the idea that Flow-FISH would measure the levels of different types of pre-rRNAs in HSCs (stored pre-ribosomal particles) versus other cells (pre-ribosomal particles neo synthesis).

We next examined the effects of the inhibition of rRNA transcription on the levels of pre-rRNAs in hematopoietic cells. Bone marrow cells were harvested and cultured for 3 hours in presence of 10µM CX-5461, a selective inhibitor of RNA polymerase I driven rRNA transcription (Bywater et al., 2012; Quin et al., 2014), prior to Flow-FISH staining. CX-5461 treatment resulted in a significant decrease of its1 and its2 levels in HSCs, MPPs, CMPs GMPs and MEPs (**Figure 4**). Because only a modest reduction in its1 and its2 levels was observed, we analyzed in more details the effects of CX-5461 on pre-rRNAs processing using mouse embryonic stem cells. We found that although CX-5461 efficiently inhibited rRNA transcription, as visualized by the drastic reduction in the nucleolar incorporation of the nucleotide analog 5-ethynyl-uridine (EU), it also caused a delay in pre-rRNA processing as suggested by the retention of previously labelled nucleolar RNAs (**Figure S2**). Such inhibitory effects of CX-5461 on pre-rRNAs processing likely explain its limited impact on its1 and its2 levels in hematopoietic cells. Recently, BMH-21 was reported as another selective inhibitor of RNA polymerase I (Peltonen et al., 2014). Importantly, BMH-21 was shown to repress rRNA synthesis without affecting its processing (Peltonen et al., 2014). We thus repeated the experiment using BMH-21 and obtained similar but more pronounced reduction of its1 and its2 levels in HSCs, MPPs, CMPs GMPs and MEPs (**Figure 4**). We conclude from these experiments that *de novo* rDNA transcription largely contributes to pre-rRNAs levels measured by Flow-FISH in HSCs and other bone marrow cell populations.

Finally, we measured transcription in HSCs (Lin^- $Sca1^+$ $cKit^+$ $CD34^-$), MPPs (Lin^- $Sca1^+$ $cKit^+$ $CD34^+$), CMPs (Lin^- $Sca1^-$ $cKit^+$ $CD34^{hi}$ FCγR-II/III^{hi}), GMPs (Lin^- $Sca1^-$ $cKit^+$ $CD34^{lo}$ FCγR-II/III^{lo}) and MEPs (Lin^- $Sca1^-$ $cKit^+$ $CD34^-$ FCγR-II/III^{lo}) by labelling nascent RNAs with a pulse of uridine analog. Because rRNA synthesis represents the majority of transcription, levels of labelled nascent RNAs after a short pulse should reflect the levels of rRNA transcription. We incubated bone marrow cells for 15 min or 1h in presence of 1mM 5-ethynyl-uridine (EU) and measured the levels of incorporated EU in the different hematopoietic subsets using a fluorescently-labelled azide (Jao and Salic, 2008). Bone marrow cells showed a clear EU staining, which increased with the duration of incubation (**Figure 5**). Similarly to pre-rRNA levels, we found that EU incorporation was higher in Lin– cells compared to Lin+ progenitors and differentiated cells and that amongst immature cell populations MEPs showed the highest levels EU staining and HSCs the lowest (**Figure 5B**). However, levels of nascent RNA in HSCs was not massively reduced compared to MPPs (1.1-fold reduction for both 15 min and 60 min incubation) and higher than in Lin+ cells (2.6-fold and 2.8-fold increase for 15 min and 60 min incubation respectively) suggesting that rRNA transcription is effective is HSCs.

Altogether, these experiments demonstrate that ribosome biogenesis is active in HSCs.

DISCUSSION

Here, we describe a new method for measuring the levels of pre-rRNAs in hematopoietic cells *in vivo*, that is, Flow-FISH. We show that Flow-FISH reports and quantifies ribosome biogenesis activity in hematopoietic cell populations, thereby providing original data on this fundamental process notably in rare populations such as HSCs. We unravel variations in ribosome biogenesis between different hematopoietic progenitor compartments and during erythroid differentiation. Thus our study contributes to a better knowledge of the cellular physiology of the hematopoietic system in vivo in unperturbed situation.

An important parameter known to modulate ribosome biogenesis activity is the proliferation rate (Ruggero and Pandolfi, 2003). Using Flow-FISH, we found that oligopotent myeloid progenitors, CMPs, MEPs and GMPs, which are highly proliferative cells, had higher levels of pre-rRNAs compared to HSCs and MPPs, which are non- and slowly-proliferative cell populations, respectively (Busch et al., 2015; Passegué et al., 2005). However, amongst oligopotent myeloid progenitors pre-rRNAs levels do not match with the proliferation index. Indeed, GMPs have the highest proliferation index but the lowest pre-rRNAs levels while MEPs have the lowest proliferation index but the highest pre-rRNAs levels. On the same line, our data show that pre-rRNAs levels are only slightly higher in MPPs compared to HSCs, although their proliferation status is completely different. Therefore, our data demonstrate that ribosome biogenesis activity is not simply a reflection of proliferation and suggest that cell type specific mechanisms might regulate ribosome biogenesis in hematopoietic stem cells and progenitors. Consistent with our conclusion is the recent observation that ANGIOGENIN, a niche-specific factor, stimulates rRNA transcription in MEPs, CMPs and GMPs but not in HSCs and MPPs (Goncalves et al., 2016).

Amongst Lin– undifferentiated cells, MEPs showed the highest activity of ribosome biogenesis. Although classically defined as bipotent progenitors, the Lin^{-} $Sca1^{-}$ $cKit^{+}$ $CD34^{-}$ $FC\gamma R\text{-}II/III^{low}$ population of the bone marrow was recently shown to be composed almost exclusively of cells having erythroid differentiation potency (Paul et al., 2015). We also detected high levels of pre-rRNAs further down along the erythroid differentiation program, in proerythroblasts. Contrary to ribosome biogenesis, global protein translation is not increased in MEPs compared to CMPs and GMPs (this study and (Signer et al., 2014)) indicating that high ribosome biogenesis activity in these progenitors is not driven by a particularly high need in translation. Importantly, a critical role for ribosome in erythroid development was uncovered more than a decade ago by the demonstration that mutations in ribosomal genes causes erythroid defects in patients suffering from Diamond-Blackfan anemia and the 5q syndrome (Narla and Ebert, 2010). Our observation of a particularly high level of ribosome biogenesis activity in erythroid progenitors will eventually help to understand why developing erythrocytes are highly sensitive to suboptimal levels of ribosomal proteins.

We also documented a sharp diminution in pre-rRNAs levels at the transition between pro-erythroblasts and early erythroblasts. This is contrasting with the progressive modulation of other parameters (diminution of cell size, chromatin change or hemoglobin accumulation) observed during erythroid differentiation. Interestingly, the polycomb group protein Bmi1 has been shown to positively regulate ribosome biogenesis in proerythroblasts and therefore is likely involved in the regulation of ribosome biogenesis activity during normal erythroid maturation (Gao et al., 2015). However, *Bmi1* expression is turned off in late erythroblasts (Gao et al., 2015) after the sharp downregulation of ribosome biogenesis, indicating that additional regulators of ribosome biogenesis during erythroid differentiation remain to be discovered. Interestingly, recent studies suggests that down-regulation of rRNA transcription

may actually trigger differentiation (Hayashi et al., 2014; Zhang et al., 2014). In the future, it will be important to address whether the sharp down regulation of pre-rRNAs levels is actually the cause or the consequence of proerythroblast differentiation into early erythroblast.

An unexpected result uncovered by Flow-FISH is the existence of sustained ribosome biogenesis in HSCs. Because a vast majority of HSCs are quiescent and have a low metabolic activity, it was expected to find much lower pre-rRNAs levels in HSCs compared to other hematopoietic cells. This is not the case. The reasons why ribosome activity in HSCs is similar to that of MPPs and higher than that of Lin+ progenitors and differentiated cells is currently unclear. Because of ribosome degradation, a certain level of ribosome biogenesis is required for renewing ribosomes and maintain protein translation above a threshold compatible with HSCs homeostasis. Protein translation is lower in HSCs compared to others hematopoietic cells (this study and (Signer et al., 2014)) and variation in the rate of translation are associated with defects in HSCs function (Signer et al., 2014). Recently, it was shown that reduced translation is not due to a reduction in the number of ribosomes in HSCs but involves 4E-BP-mediated translation inhibition (Signer et al., 2016). Cell-type specific ANGIOGENIN-mediated production of tRNA-derived stress-induced small RNAs was also recently shown to contribute to the reduced levels of global protein synthesis in HSCs and MPPS (Goncalves et al., 2016). Low protein translation rate in HSCs seems therefore to be primarily regulated at the levels of translation inhibition rather than through reduced ribosome supply.

Active ribosome biogenesis in HSCs may also play important roles beyond *de novo* ribosome production. Indeed, while its assembly and structure are dictated by the rate of rRNA transcription and ribosome biogenesis, the nucleolus also regulates other cellular processes (Boulon et al., 2010; Stępiński, 2016). In particular, the activity of several factors

involved in cell cycle regulation, differentiation or stress responses has been shown to be regulated through nucleolar sequestration (Korgaonkar et al., 2005; Kuroda et al., 2011; Sasaki et al., 2011). Interestingly, *Runx1*-deficient phenotypic HSCs have decreased ribosome content and reduced cell size, yet they maintain long term repopulation capacity (Cai et al., 2015) indicating that HSCs self-renewal does not critically rely on a precise level of ribosome biogenesis activity. Importantly, RUNX1 directly regulates the transcription of ribosome component and of ribosome biogenesis factors and in absence of *Runx1*, HSCs show a lower unfold protein response and decreased p53 protein levels conferring them an attenuated apoptotic response following endoplasmic reticulum or genotoxic stresses (Cai et al., 2015). These observations raise the possibility that decreased ribosome biogenesis may participate to the development of multiple hematopoietic malignancies that are associated with *RUNX1* mutations (Mangan and Speck, 2011). They might also explain why ribosome biogenesis is not lower in HSCs since this would attenuate their responses to stress and thus increase the risk of stem cell dysfunction and transformation.

In summary, *in vivo* Flow-FISH allows us to quantify the activity of ribosome biogenesis at the single cell level within a given lineage, the adult hematopoietic system, composed of cells with very different proliferation, growth and metabolic profiles. It has uncovered higher than anticipated ribosome production in adult bone marrow HSCs and sharp downregulation of ribosome biogenesis during erythroid differentiation. Previously, we showed that Flow-FISH could reveal unbalanced ribosomal subunit processing caused by mutation in a factor involved in pre-60s ribosomal particle processing (Le Bouteiller et al., 2013). Adapted to humans, this approach should prove useful to identify dysregulation of ribosome biogenesis in patients suffering from hematologic disorders.

MATERIAL AND METHODS

Mouse Husbandry

All experiments were performed on 8-12 weeks old C57Bl/6J mice of either sex obtained from Charles River and/or bred in our animal facility. For RPM analyses, mice were injected intra-peritoneally with 2mg/100µL puromycin and/or 20µg/100µL harringtonine, 10 and 25min prior to euthanasia, respectively. For bone marrow collection, mice were euthanized and femurs and tibias were collected and kept on ice in medium containing serum; bones were split at one end and spinned shortly in eppendorf tubes at 4°C to recover whole bone marrow. All experiments were conducted according to the French and European regulations on care and protection of laboratory animals (EC Directive 86/609, French Law 2001-486 issued on June 6, 2001) and were approved by the Institut Pasteur ethics committee (n° 2014-0053).

Flow cytometry analysis

Single cell suspensions of bone marrow cells were stained using different combinations of antibodies. All antibody stainings were performed in HBSS medium containing 2% fetal calf serum (FCS). For Flow-FISH analyses on the erythroid lineage, cells were stained using PeCy7-conjugated anti-Ter119 and biotin-conjugated anti-CD71 antibodies. For analyses on immature hematopoietic populations, cells were stained using biotin-conjugated Lineage (B220, Nk1.1, Gr-1, Ter119, CD3, CD11c, Mac-1), PeCy7- or BV510-conjugated anti-Sca1, APC- or PeCy7-conjugated anti-cKit, and FITC- or eFluor660-conjugated anti-CD34 antibodies. For RPM and EU staining analyses, cells were also stained using PE-conjugated anti-FCγRII/III antibody. Biotin-conjugated stainings were revealed using Pacific Blue-conjugated streptavidin. The list of antibody clones is available in **Table S1**. LSR Fortessa (BD) analyzer was used for analysis; AutoMACS Pro (Miltenyi) separator was used for depletion of Lin+ cells; MoFlo Astrios (Beckman Coulter) cell sorter was used for cell

sorting. All cytometry data were analyzed using FlowJo (Treestar) software.

RiboPuromycylation

For the RiboPuromycylation Method, mice were injected with 2mg (in 1X PBS) of puromycin (Sigma P8833) and euthanized 10 min later. For mice treated with harringtonine, 20µg (in 1X PBS) of harringtonine (Santa-Cruz sc-204771) was injected 15min prior to puromycin injection. Importantly, puromycin and harringtonine solutions were warmed at 37°C prior to injections. Bone marrow cells were collected in cold HBSS medium containing 2% fetal calf serum (FCS) and 208µM emetine (Sigma E2375) to block protein elongation, and kept on ice. Cells were then stained using surface marker antibodies as described above. After surface staining, cells were permeabilized and fixed as follows: cells were rinsed in cold PBS, then incubated 2min in permeabilization buffer consisting of "polysome buffer" (50mM Tris-HCl pH 7.5; 5mM $MgCl_2$; 25mM KCl) complemented with EDTA-free protease inhibitors (Roche 11836170001) and 0.015% digitonin (Sigma D141). Cells were then quickly rinsed with polysome buffer complemented with protease inhibitors (added to permeabilization buffer, then rinsed again), and then fixed for 15min at room temperature (RT) in 1X PBS containing 3% PFA. Cells were then rinsed with PBS and incubated in staining buffer (0.05% saponin, 10mM Glycine, 5% FCS, 1X PBS final) for 15min. Puromycin detection was then performed by staining with Alexa647-conjugated anti-puromycin antibody in staining buffer for 1h (see **Table S1** and (Seedhom et al., 2016)). Finally, cells were rinsed in 1X PBS with BSA and kept at 4°C until analysis. For quantification of puromycin levels, mean fluorescence intensity (MFI) was measured for each mouse in each cell population analyzed and was then normalized to the average MFI of the BM population of mice injected with puromycin only.

FISH analysis

For Flow-FISH stainings, BM cells were collected from femurs and tibia and stained with surface marker antibodies as described above. Of note, not all fluorochrome-conjugated antibodies sustain the different protocols, and each antibody should thus be tested. Cells stained with surface marker antibodies were fixed for 30min at RT in 1X PBS containing 4% PFA and rinsed twice in 1X PBS. Cell were then dehydrated as follows: cells were first resuspended in 1 volume of 1X PBS, and 1 volume of 70% ethanol was added drop by drop; cells were then centrifuged, resuspended in 70% ethanol and left at 4°C over-night. The next day, cells were rehydrated for 5min in 2X SSC (saline-sodium citrate) buffer containing 10% formamide and 0.25mg/mL BSA. Cells of each analyzed mouse were then incubated for 3h at 37°C in FISH-staining buffer prepared as indicated in **Table S2** with DNA probes directed against its1 (5'-tagacacggaagagccggacgggaaaga-3') and its2 (5'-ccagcgcaagacccaaacacacacaga-3') or a non-targeting "scramble" probe (scr; 5'-cggaatagtgcgtcacgaactcgctata-3'). After incubation, cells were washed twice in 2X SSC buffer containing 10% formamide and 0.25mg/mL BSA, for 30min at 37°C. Finally, cells were rinsed three times in 1X PBS containing 0.25mg/mL BSA and kept at 4°C until analysis. For quantification of its1 and its2 levels, mean fluorescence intensity (MFI) was measured for each mouse in each cell population of samples stained with its1, its2 or scr probes and MFI of the scr was subtracted from the MFI of its1 and its2. The obtained "corrected" MFI (cMFI) of each cell population was then normalized to the average cMFI of unsorted bone marrow cells. For fluorescent microscopy analyses on sorted cells stained with Flow-FISH, cell nuclei were stained using Hoechst prior to analysis.

EU staining

For EU staining experiments, bone marrow cells were collected from tibias and femurs in OptiMEM medium containing 10% FCS, and were incubated 15min or 1h in the presence of 1mM 5-ethynyl-uridine (EU, Molecular Probes E10345) or without EU, at 37°C and 5%

CO_2. Cells were then rinsed in cold PBS and stained with surface markers antibodies as described above, and fixed and permeabilized 15min using the Foxp3 Staining Buffer set (eBioscience 00-5523-00). Detection of EU was then performed using the Click-iT Plus Alexa Fluor 488 picolyl azide toolkit (Molecular Probes C10641). Cells were then kept in 1X PBS with BSA at 4°C until analysis. For quantification of EU levels, MFI was measured for each mouse in each cell population of samples incubated without EU or in the presence EU for 15min and 60min, and MFI of the cells incubated without EU was subtracted from the MFI of 15min and 60min EU-incubated samples. The obtained "corrected" MFI (cMFI) of each cell population was then normalized to the average cMFI of the unsorted bone marrow cells of samples incubated with EU for 15min.

RNA Pol I inhibition

For treatments with RNA Pol I inhibitors, BM cells were collected from tibias and femurs in OptiMEM medium containing 10% FCS. They were then incubated for 3h in the presence of either 10µM CX-5461 (Axon 2173) or 2.5µM BMH-21 (Sigma SML1183) at 37°C and 5% $C0_2$. Cells were then rinsed in cold HBSS containing 2% FCS and analyzed by Flow-FISH as described above.

Cell culture

Wild-type CK35 embryonic stem cells (Kress et al., 1998) were cultured in DMEM medium complemented with 15% FCS, 100µM β-mercaptoethanol and 10^3units/mL leukemia inhibitory factor. Cells were seeded on Matrigel-coated coverslips, at density allowing near-confluence at the moment of analysis. Cells were then incubated 15min in the presence of 1mM EU, followed by up to 2h incubation in the presence or absence of 10µM CX-5461 for EU pulse-chase analysis. As controls of the efficiency of CX-5461 treatment, cells were incubated 2h in the presence or absence of 10µM CX-5461, followed by 15min with both

1mM EU and 10μM CX-5461. Cells were then fixed in 4% PFA in PBS for 15min at RT and permeabilized 15min in 0.5% Triton in PBS. EU detection was then performed using the Click-iT RNA Alexa Fluor 488 Imaging Kit (Molecular Probes C10329), and nuclei were stained with Hoechst.

Microscopy

All fluorescence microscopy analyses were performed using Apotome.2 (Zeiss) microscope and the Zen blue (Zeiss) software.

Statistical analysis

All bar graphs show mean ± SEM of normalized levels of the indicated variable; results presented are representative of at least 2 independent experiments. Statistical analyses were performed using Prism 6 (GraphPad). For comparisons between different populations within the same sample group, one-way ANOVA with Dunnett's correction for multiple comparisons was used, and significance was indicated as follows. For comparisons to HSC: † $p<0.05$, †† $p<0.01$, ††† $p<0.001$ and †††† $p<0.0001$; for comparisons to BM: ¥ $p<0.05$, ¥¥ $p<0.01$, ¥¥¥ $p<0.001$ and ¥¥¥¥ $p<0.0001$. For comparisons between different sample groups within the same population, unpaired two-tailed Student's t tests were used, and significance was indicated as follows: * $p<0.05$, ** $p<0.01$, *** $p<0.001$ and **** $p<0.0001$.

AKNOWLEDGMENTS

Imaging and cell sorting analyses was performed at the Imagopole of Institut Pasteur. We are grateful to P.-H. Commere for his assistance with FACS analysis and sorting. We thank F. Morlé, L. Da Costa, and all members of the lab for technical advices and helpful discussions. This work was supported by the Institut Pasteur, the Centre National de la Recherche Scientifique and the Agence Nationale de la Recherche (ANR-10-LABX-73-01 REVIVE). L.J. was supported by the DIM biotherapies Ile-de-France, the Société Française d'Hématologie and the REVIVE Labex. M.L.B. was supported by the Ligue Nationale Contre le Cancer.

COMPETING INTERESTS

The authors declare no competing interest.

AUTHORS CONTRIBUTIONS

REFERENCES

Boulon, S., Westman, B. J., Hutten, S., Boisvert, F.-M. and Lamond, A. I. (2010). The nucleolus under stress. *Molecular Cell* **40**, 216–227.

Brombin, A., Joly, J.-S. and Jamen, F. (2015). New tricks for an old dog: ribosome biogenesis contributes to stem cell homeostasis. *Current Opinion in Genetics & Development* **34**, 61–70.

Busch, K., Klapproth, K., Barile, M., Flossdorf, M., Holland-Letz, T., Schlenner, S. M., Reth, M., Höfer, T. and Rodewald, H.-R. (2015). Fundamental properties of unperturbed haematopoiesis from stem cells in vivo. *Nature* **518**, 542–546.

Buszczak, M., Signer, R. A. J. and Morrison, S. J. (2014). Cellular Differences in Protein Synthesis Regulate Tissue Homeostasis. *Cell* **159**, 242–251.

Bywater, M. J., Poortinga, G., Sanij, E., Hein, N., Peck, A., Cullinane, C., Wall, M., Cluse, L., Drygin, D., Anderes, K., et al. (2012). Inhibition of RNA Polymerase I as a Therapeutic Strategy to Promote Cancer-Specific Activation of p53. *Cancer Cell* **22**, 51–65.

Cai, X., Gao, L., Teng, L., Ge, J., Oo, Z. M., Kumar, A. R., Gilliland, D. G., Mason, P. J., Tan, K. and Speck, N. A. (2015). Runx1 Deficiency Decreases Ribosome Biogenesis and Confers Stress Resistance to Hematopoietic Stem and Progenitor Cells. *Cell Stem Cell* **17**, 165–177.

Chandel, N. S., Jasper, H., Ho, T. T. and Passegué, E. (2016). Metabolic regulation of stem cell function in tissue homeostasis and organismal ageing. *Nature Cell Biology* **18**, 823–832.

David, A., Dolan, B. P., Hickman, H. D., Knowlton, J. J., Clavarino, G., Pierre, P., Bennink, J. R. and Yewdell, J. W. (2012). Nuclear translation visualized by ribosome-bound nascent chain puromycylation. *The Journal of Cell Biology* **197**, 45–57.

Dolznig, H., Bartunek, P., Nasmyth, K., Müllner, E. W. and Beug, H. (1995). Terminal differentiation of normal chicken erythroid progenitors: shortening of G1 correlates with loss of D-cyclin/cdk4 expression and altered cell size control. *Cell Growth Differ.* **6**, 1341–1352.

Fichelson, P., Moch, C., Ivanovitch, K., Martin, C., Sidor, C. M., Lepesant, J.-A., Bellaiche, Y. and Huynh, J.-R. (2009). Live-imaging of single stem cells within their niche reveals that a U3snoRNP component segregates asymmetrically and is required for self-renewal in Drosophila. *Nature Cell Biology* **11**, 685–693.

Fortier, S., MacRae, T., Bilodeau, M., Sargeant, T. and Sauvageau, G. (2015). Haploinsufficiency screen highlights two distinct groups of ribosomal protein genes essential for embryonic stem cell fate. *Proceedings of the National Academy of Sciences* **112**, 2127–2132.

Gao, R., Chen, S., Kobayashi, M., Yu, H., Zhang, Y., Wan, Y., Young, S. K., Soltis, A., Yu, M., Vemula, S., et al. (2015). Bmi1 promotes erythroid development through regulating ribosome biogenesis. *STEM CELLS* **33**, 925–938.

Goncalves, K. A., Silberstein, L., Li, S., Severe, N., Hu, M. G., Yang, H., Scadden, D. T. and Hu, G.-F. (2016). Angiogenin Promotes Hematopoietic Regeneration by Dichotomously Regulating Quiescence of Stem and Progenitor Cells. *Cell* **166**, 894–906.

Hayashi, Y., Kuroda, T., Kishimoto, H., Wang, C., Iwama, A. and Kimura, K. (2014). Downregulation of rRNA Transcription Triggers Cell Differentiation. *PLoS ONE* **9**, e98586.

Jao, C. Y. and Salic, A. (2008). Exploring RNA transcription and turnover in vivo by using click chemistry. *Proceedings of the National Academy of Sciences* **105**, 15779–15784.

Korgaonkar, C., Hagen, J., Tompkins, V., Frazier, A. A., Allamargot, C., Quelle, F. W. and Quelle, D. E. (2005). Nucleophosmin (B23) targets ARF to nucleoli and inhibits its function. *Mol. Cell. Biol.* **25**, 1258–1271.

Kress, C., Vandormael-Pournin, S., Baldacci, P. A., Cohen-Tannoudji, M. and Babinet, C. (1998). Nonpermissiveness for mouse embryonic stem (ES) cell derivation circumvented by a single backcross to 129/Sv strain: establishment of ES cell lines bearing the Omd conditional lethal mutation. *Mamm Genome* **9**, 998–1001.

Kuroda, T., Murayama, A., Katagiri, N., Ohta, Y.-M., Fujita, E., Masumoto, H., Ema, M., Takahashi, S., Kimura, K. and Yanagisawa, J. (2011). RNA content in the nucleolus alters p53 acetylation via MYBBP1A. *The EMBO Journal* **30**, 1054–1066.

Le Bouteiller, M., Souilhol, C., Cormier, S., Stedman, A., Burlen-Defranoux, O., Vandormael-Pournin, S., Bernex, F., Cumano, A. and Cohen-Tannoudji, M. (2013). Notchless-dependent ribosome synthesis is required for the maintenance of adult hematopoietic stem cells. *Journal of Experimental Medicine* **210**, 2351–2369.

Lempiäinen, H. and Shore, D. (2009). Growth control and ribosome biogenesis. *Current Opinion in Cell Biology* **21**, 855–863.

Mangan, J. K. and Speck, N. A. (2011). RUNX1 mutations in clonal myeloid disorders: from conventional cytogenetics to next generation sequencing, a story 40 years in the making. *Critical Reviews™ in Oncogenesis*.

McCann, K. L. and Baserga, S. J. (2013). Genetics. Mysterious ribosomopathies. *Science* **341**, 849–850.

Nakamura-Ishizu, A., Takizawa, H. and Suda, T. (2014). The analysis, roles and regulation of quiescence in hematopoietic stem cells. *Development* **141**, 4656–4666.

Narla, A. and Ebert, B. L. (2010). Ribosomopathies: human disorders of ribosome dysfunction. *Blood* **115**, 3196–3205.

Neumüller, R. A., Richter, C., Fischer, A., Novatchkova, M., Neumüller, K. G. and Knoblich, J. A. (2011). Genome-wide analysis of self-renewal in Drosophila neural stem cells by transgenic RNAi. *Cell Stem Cell* **8**, 580–593.

Orkin, S. H. and Zon, L. I. (2008). Hematopoiesis: An Evolving Paradigm for Stem Cell Biology. *Cell* **132**, 631–644.

Passegué, E., Wagers, A. J., Giuriato, S., Anderson, W. C. and Weissman, I. L. (2005). Global analysis of proliferation and cell cycle gene expression in the regulation of hematopoietic stem and progenitor cell fates. *Journal of Experimental Medicine* **202**, 1599–1611.

Paul, F., Arkin, Y., Giladi, A., Jaitin, D. A., Kenigsberg, E., Keren-Shaul, H., Winter, D., Lara-Astiaso, D., Gury, M., Weiner, A., et al. (2015). Transcriptional Heterogeneity and Lineage Commitment in Myeloid Progenitors. *Cell* **163**, 1663–1677.

Peltonen, K., Colis, L., Liu, H., Trivedi, R., Moubarek, M. S., Moore, H. M., Bai, B., Rudek, M. A., Bieberich, C. J. and Laiho, M. (2014). A targeting modality for destruction of RNA polymerase I that possesses anticancer activity. *Cancer Cell* **25**, 77–90.

Quin, J. E., Devlin, J. R., Cameron, D., Hannan, K. M., Pearson, R. B. and Hannan, R. D. (2014). Targeting the nucleolus for cancer intervention. *Biochim. Biophys. Acta* **1842**, 802–816.

Ruggero, D. and Pandolfi, P. P. (2003). Does the ribosome translate cancer? *Nat Rev Cancer* **3**, 179–192.

Sanchez, C. G., Teixeira, F. K., Czech, B., Preall, J. B., Zamparini, A. L., Seifert, J. R. K., Malone, C. D., Hannon, G. J. and Lehmann, R. (2015). Regulation of Ribosome Biogenesis and Protein Synthesis Controls Germline Stem Cell Differentiation. *Cell Stem Cell* **18**, 276–290.

Sasaki, M., Kawahara, K., Nishio, M., Mimori, K., Kogo, R., Hamada, K., Itoh, B., Wang, J., Komatsu, Y., Yang, Y. R., et al. (2011). Regulation of the MDM2-P53 pathway and tumor growth by PICT1 via nucleolar RPL11. *Nature Medicine* **17**, 944–951.

Seedhom, M. O., Hickman, H. D., Wei, J., David, A. and Yewdell, J. W. (2016). Protein Translation Activity: A New Measure of Host Immune Cell Activation. *The Journal of Immunology* **197**, 1498–1506.

Shah, P., Ding, Y., Niemczyk, M., Kudla, G. and Plotkin, J. B. (2013). Rate-limiting steps in yeast protein translation. *Cell* **153**, 1589–1601.

Signer, R. A. J., Magee, J. A., Salic, A. and Morrison, S. J. (2014). Haematopoietic stem cells require a highly regulated protein synthesis rate. *Nature*.

Signer, R. A. J., Qi, L., Zhao, Z., Thompson, D., Sigova, A. A., Fan, Z. P., DeMartino, G. N., Young, R. A., Sonenberg, N. and Morrison, S. J. (2016). The rate of protein synthesis in hematopoietic stem cells is limited partly by 4E-BPs. *Genes & Development* **30**, 1698–1703.

Socolovsky, M., Nam, H., Fleming, M. D., Haase, V. H., Brugnara, C. and Lodish, H. F. (2001). Ineffective erythropoiesis in Stat5a(-/-)5b(-/-) mice due to decreased survival of early erythroblasts. *Blood* **98**, 3261–3273.

Stępiński, D. (2016). Nucleolus-derived mediators in oncogenic stress response and activation of p53-dependent pathways. *Histochem. Cell Biol.*

You, K. T., Park, J. and Kim, V. N. (2015). Role of the small subunit processome in the maintenance of pluripotent stem cells. *Genes & Development* **29**, 2004–2009.

Yu, J., Lan, X., Chen, X., Yu, C., Xu, Y., Liu, Y., Xu, L., Fan, H.-Y. and Tong, C. (2016). Protein synthesis and degradation are essential to regulate germline stem cell homeostasis in Drosophila testes. *Development* **143**, 2930–2945.

Zhang, Q., Shalaby, N. A. and Buszczak, M. (2014). Changes in rRNA transcription influence proliferation and cell fate within a stem cell lineage. *Science* **343**, 298–301.

FIGURES

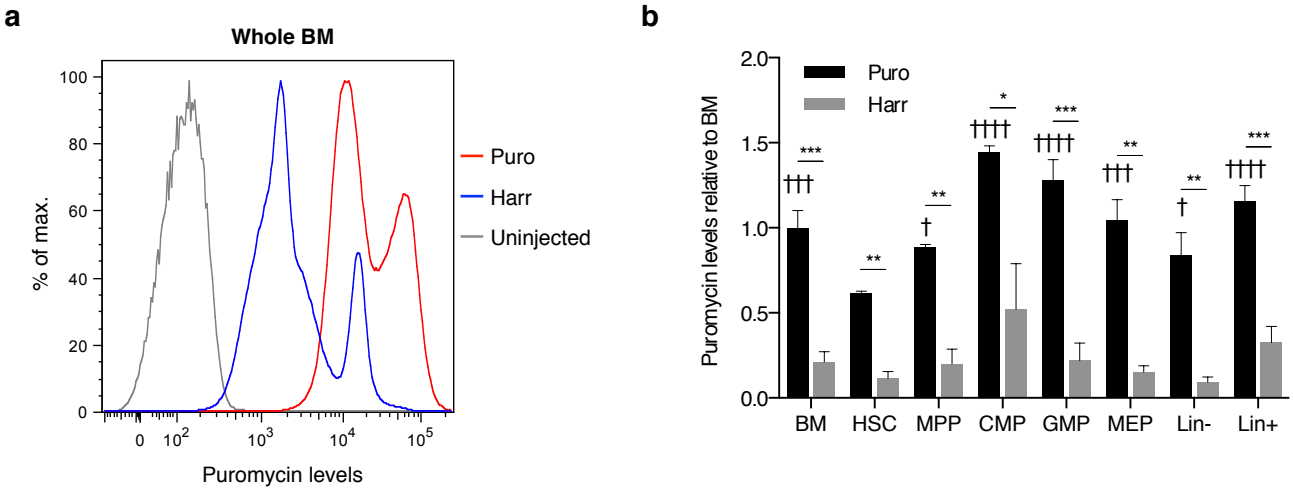

Figure 1: Low translation activity in HSCs

Mice were injected with 2mg puromycin only for 10min (Puro) or with 20µg harringtonine for 15min then 2mg puromycin for 10min (Harr), and non-injected mice were used as controls. **a.** FACS profile of puromycin levels in whole bone marrow cells (BM) of control mice (grey), mice injected with puromycin only (red) or harringtonine and puromycin (blue). **b.** Quantification of puromycin levels in the indicated populations, relative to puromycin levels in the unsorted bone marrow cells of Puro mice (HSC: Lin^- $Sca1^+$ $cKit^+$ $CD34^-$; MPP: Lin^- $Sca1^+$ $cKit^+$ $CD34^+$; CMP: Lin^- $Sca1^+$ $cKit^+$ $CD34^{hi}$ $FC\gamma RII/III^{hi}$; GMP: Lin^- $Sca1^+$ $cKit^+$ $CD34^{lo}$ $FC\gamma RII/III^{lo}$; MEP: Lin^- $Sca1^+$ $cKit^+$ $CD34^{lo}$ $FC\gamma RII/III^{lo}$). For comparisons of puromycin levels between HSCs and other populations in Puro mice, statistical significance was calculated using one-way ANOVA with Dunnett's correction for multiple comparisons: † $p<0.05$, †† $p<0.01$, ††† $p<0.001$, †††† $p<0.0001$. For comparisons between Harr and Puro mice in each population, statistical significance was calculated using unpaired two-tailed Student's t tests: * $p<0.05$, ** $p<0.01$, *** $p<0.001$. n=3 mice for each sample group; results representative of two independent experiments.

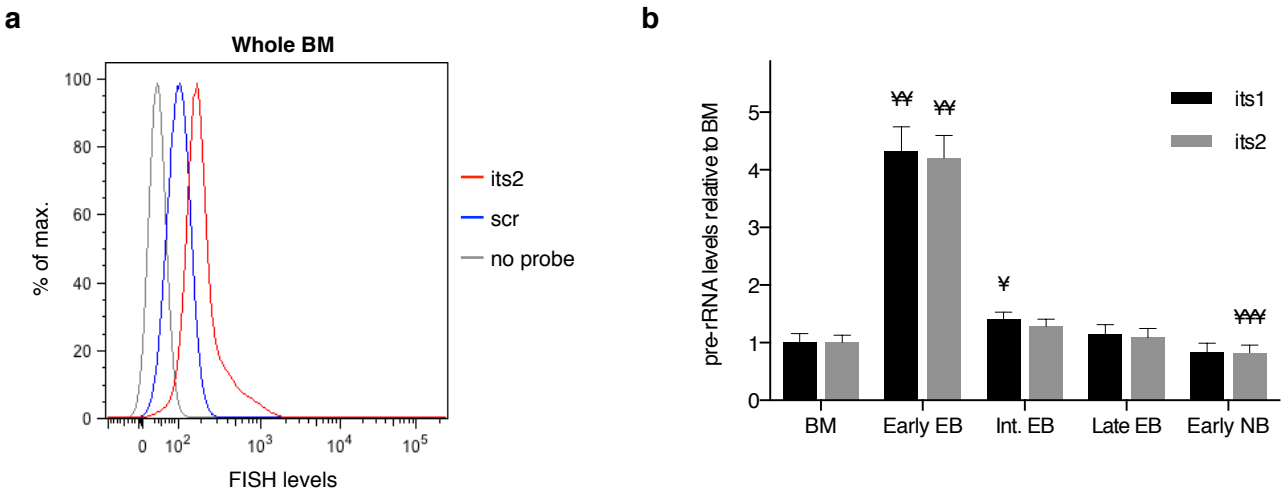

Figure 2: Flow-FISH allows quantification of pre-rRNA levels during erythroid differentiation

Bone marrow (BM) cells were stained using Flow-FISH with probes directed against its1 or its2 or a non-targeting probe (scr). **a.** FACS profile of FISH levels in the whole BM population of samples stained with either no probe (grey) or the scr (blue) and its2 (red) probes. **b.** Quantification of its1 and its2 levels in cells of the erythroid lineage, relative to its1 and its2 levels in the BM population: pro- and early erythroblasts (early EB, $CD71^{+}$ $Ter119^{lo}$), intermediate erythroblasts (int. EB, $CD71^{+}$ $Ter119^{+}$), late erythroblasts (late EB, $CD71^{lo}$ $Ter119^{+}$) and early normoblasts (early NB, $CD71^{-}$ $Ter119^{+}$). For comparisons of pre-rRNA levels between BM and erythroid populations of samples stained with the same probe, statistical significance was calculated using one-way ANOVA with Dunnett's correction for multiple comparisons: ¥ $p<0.05$, ¥¥ $p<0.01$ and ¥¥¥ $p<0.001$. n=3 mice; representative results of 4 independent experiments.

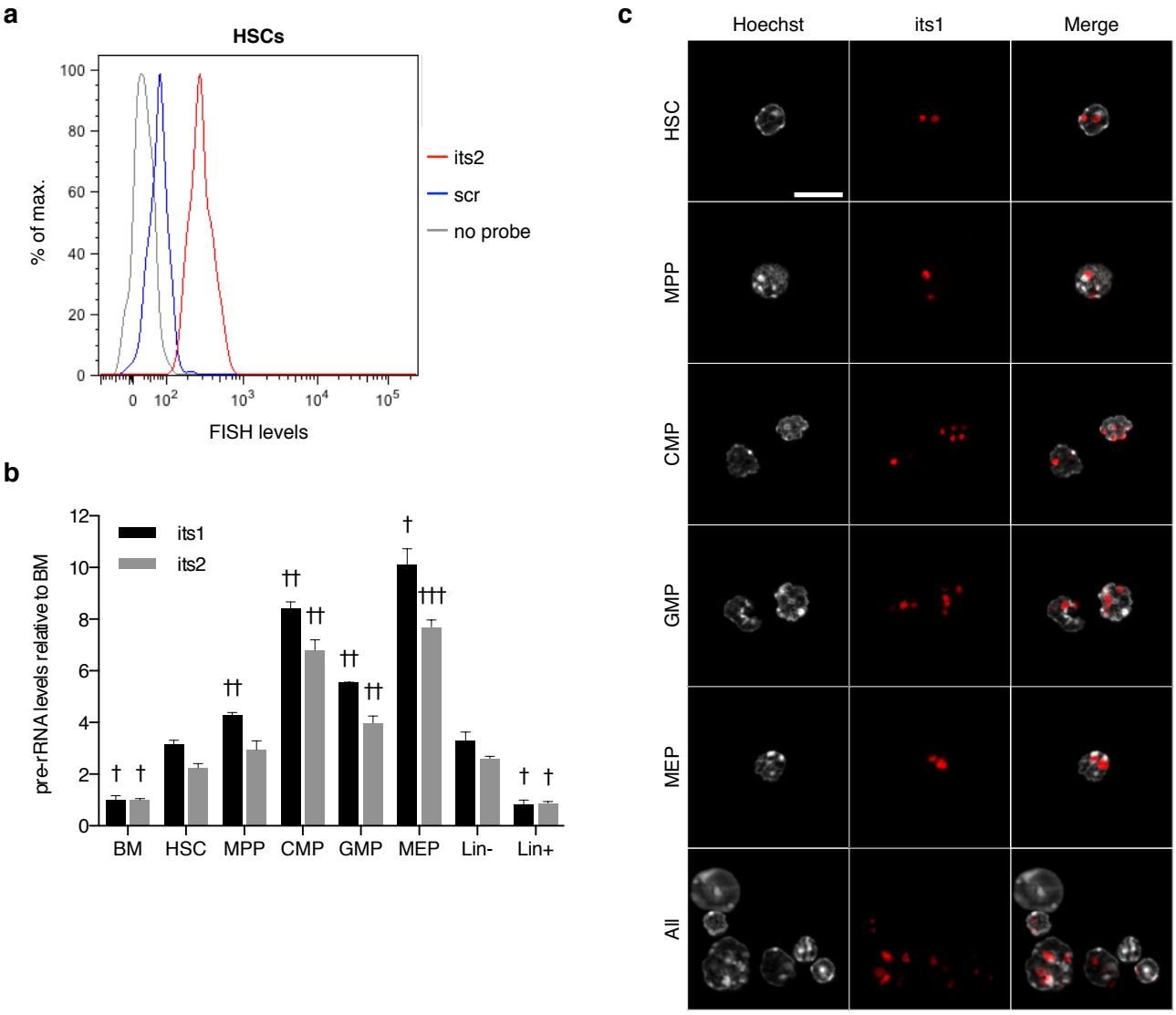

Figure 3: Flow-FISH uncovers variations in pre-rRNA levels of immature hematopoietic populations

Bone marrow (BM) cells were stained using Flow-FISH with probes directed against its1 or its2 or a control probe (scr). **a.** FACS profile of FISH levels in the HSC population of samples stained with either no probe (grey) or the scr (blue) and its2 (red) probes. **b.** Quantification of its1 and its2 levels in the indicated populations, relative to its1 and its2 levels in the BM population (HSC: Lin^- $Sca1^+$ $cKit^+$ $CD34^-$; MPP: Lin^- $Sca1^+$ $cKit^+$ $CD34^+$; CMP: Lin^- $Sca1^+$ $cKit^+$ $CD34^{hi}$; GMP: Lin^- $Sca1^+$ $cKit^+$ $CD34^{lo}$; MEP: Lin^- $Sca1^+$ $cKit^+$ $CD34^{lo}$). Statistical significance of the difference in pre-rRNA levels between HSCs and

other populations of samples stained with the same probe was calculated using one-way ANOVA with Dunnett's correction for multiple comparisons: † $p<0.05$, †† $p<0.01$ and ††† $p<0.001$. n=3 mice; representative results of 4 independent experiments. **c.** Lin-depleted BM cells were stained using Flow-FISH with the its1 probe and sorted to obtain HSC, MPP, CMP, GMP and MEP cells. Nuclei were then stained using Hoechst.

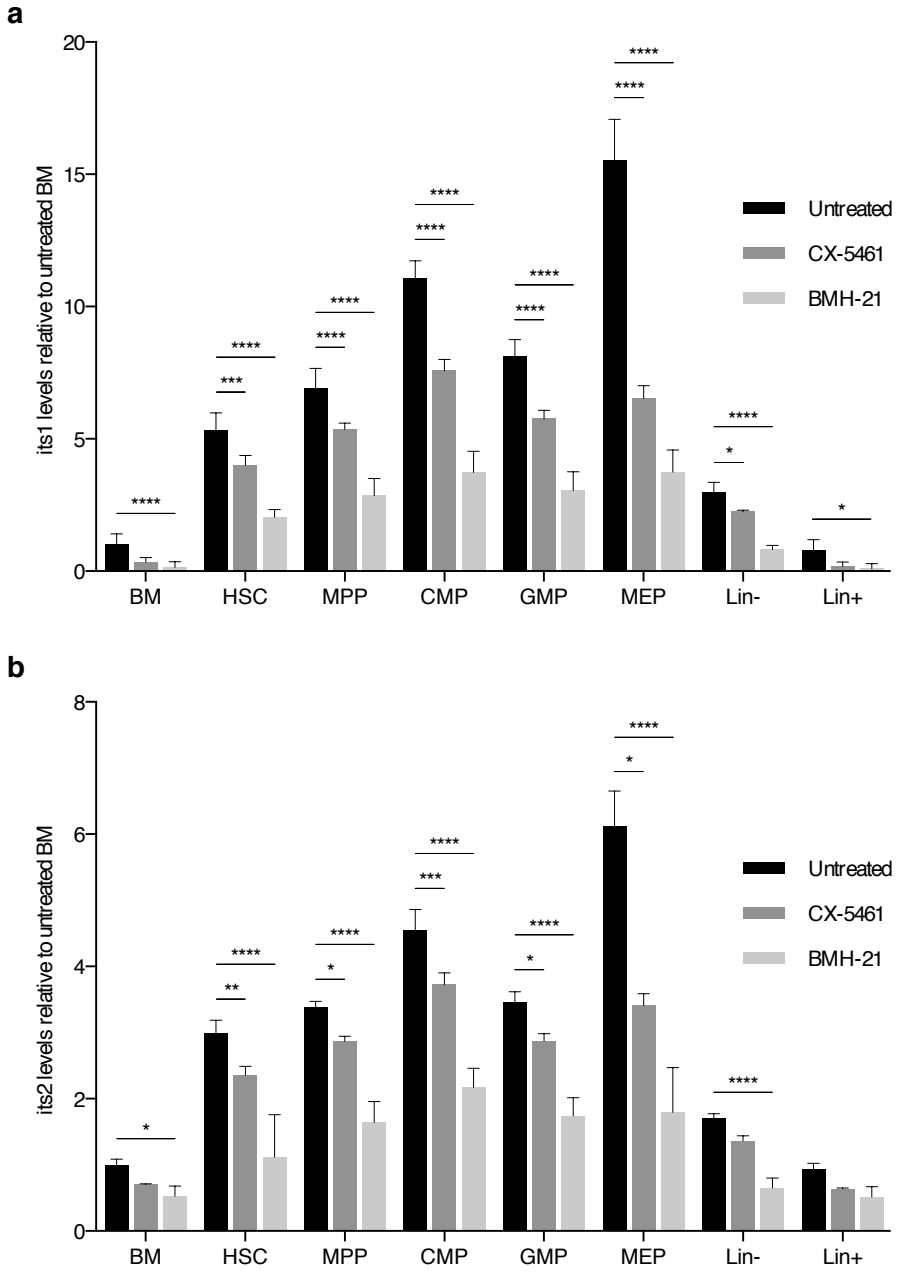

Figure 4: RNA Pol I inhibitors lead to significant decrease of pre-rRNA levels detected by Flow-FISH

Bone marrow (BM) cells were incubated or not in the presence of 10µM CX-5461 or 2.5µM BMH-21 for 3h, and were then stained using Flow-FISH with probes directed against its1 or its2 or a non-targeting probe (scr). **a,b.** Quantification of its1 (a) and its2 (b) levels in the indicated populations, relative to levels in the BM population (HSC: Lin^- $Sca1^+$ $cKit^+$ $CD34^-$; MPP: Lin^- $Sca1^+$ $cKit^+$ $CD34^+$; CMP: Lin^- $Sca1^+$ $cKit^+$ $CD34^{hi}$; GMP: Lin^- $Sca1^+$ $cKit^+$

$CD34^{lo}$; MEP: Lin^{-} $Sca1^{+}$ $cKit^{+}$ $CD34^{lo}$). Statistical significance of the differences between treated and untreated cells was calculated using unpaired two-tailed Student's t tests: * $p<0.05$, ** $p<0.01$, *** $p<0.001$. n=3 mice for each sample group.

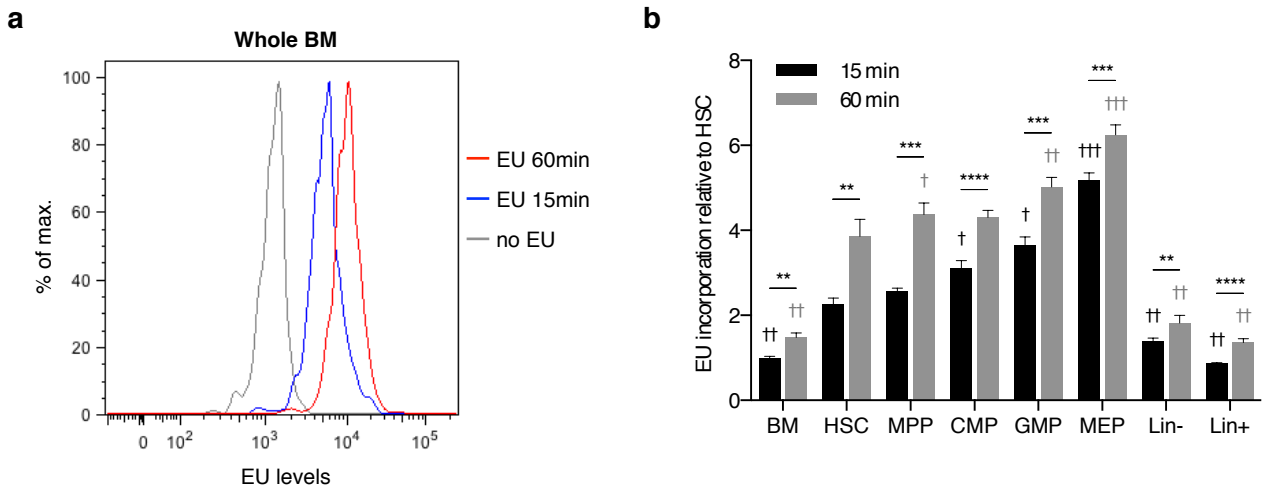

Figure 5: RNA transcription in bone marrow cells

Bone marrow (BM) cells were incubated or not in the presence of 1mM 5-ethynyl-uridine (EU) for 15min or 1h. **a.** FACS profile of EU levels in HSC population of samples incubated without EU (grey) or with EU for 15min (blue) or 60min (red). **b.** Quantification of EU levels in the indicated populations, relative to EU levels in the BM population of cells incubated 15min with EU (HSC: Lin^- $Sca1^+$ $cKit^+$ $CD34^-$; MPP: Lin^- $Sca1^+$ $cKit^+$ $CD34^+$; CMP: Lin^- $Sca1^+$ $cKit^+$ $CD34^{hi}$ $FC\gamma RII/III^{hi}$; GMP: Lin^- $Sca1^+$ $cKit^+$ $CD34^{lo}$ $FC\gamma RII/III^{lo}$; MEP: Lin^- $Sca1^+$ $cKit^+$ $CD34^{lo}$ $FC\gamma RII/III^{lo}$). For comparisons of EU levels between HSCs and other populations in samples incubated 15min or 1h, statistical significance was calculated using one-way ANOVA with Dunnett's correction for multiple comparisons: † $p<0.05$, †† $p<0.01$ and †† $p<0.001$. For comparisons between 15min and 60min incubations in each population, statistical significance was calculated using unpaired two-tailed Student's t tests: * $p<0.05$, ** $p<0.01$, *** $p<0.001$ and *** $p<0.0001$. n=4 mice; results representative of two independent experiments.

SUPPLEMENTARY FIGURES & TABLES

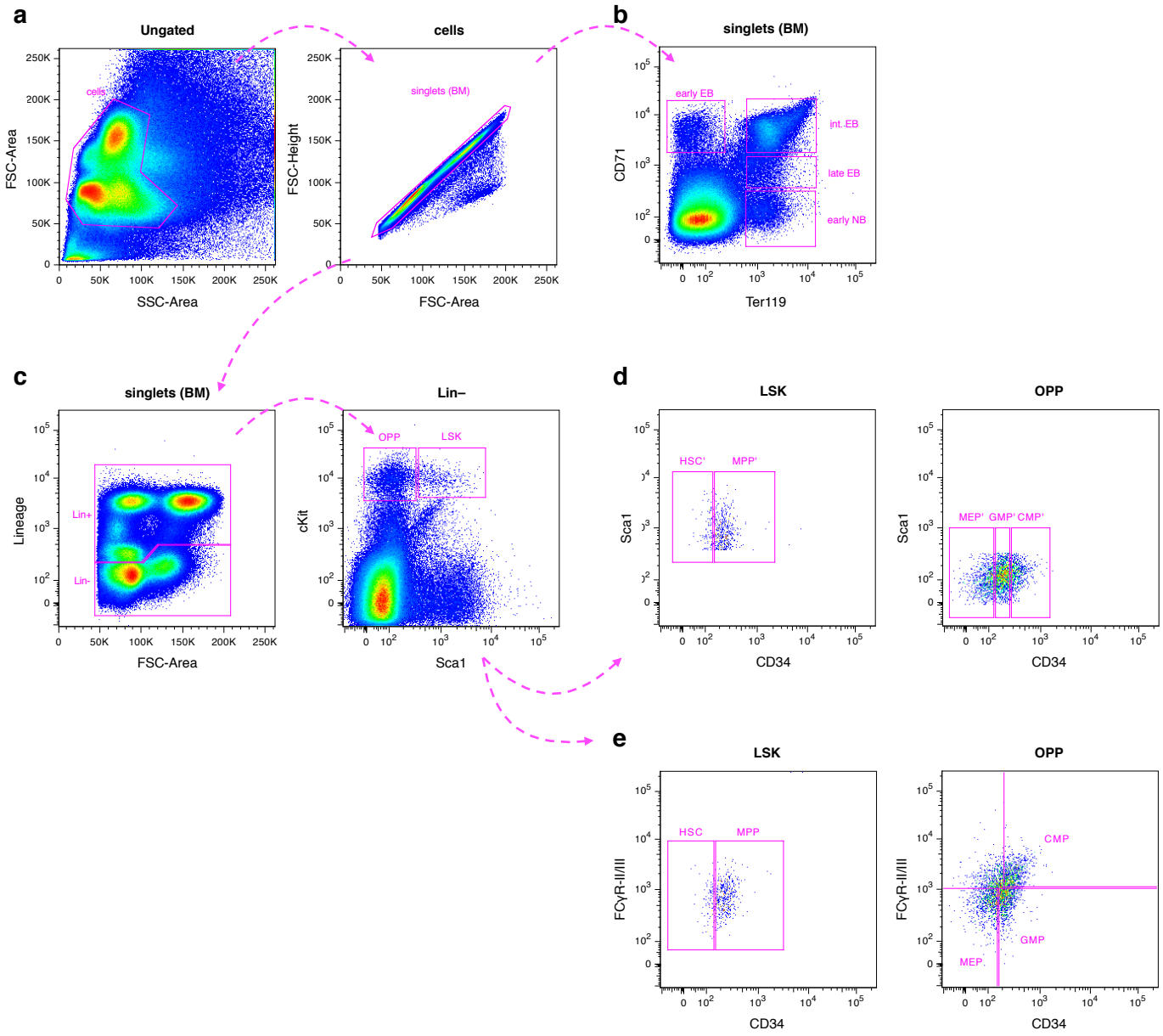

Figure S1: Gating strategies for flow cytometry analyses

a. For all flow cytometry analyses, cell debris and doublets were eliminated using forward and side scatter plots as indicated. **b.** For Flow-FISH analysis of the erythroid lineage, singlets (BM) were plotted using CD71 and Ter119 and the indicated gate were drawn to separate pro- and early erythroblasts (early EB), intermediate erythroblasts (int. EB), late erythroblasts (late EB) and early normoblasts (early NB). **c.** For analyses on the immature

hematopoietic populations, singlets (BM) were plotted using Lineage markers and forward-scatter to separate Lin+ and Lin– cells. Lin– cells were then plotted using Sca1 and cKit to separate oligopotent progenitors (OPP) and HSCs and MPPs (LSK). **d.** For Flow-FISH analyses of immature populations, LSK and OPP were plotted using Sca1 and CD34 to separate HSC and MPP or CMP, GMP and MEP populations as indicated. **e.** For RPM and EU analyses, LSK and OPP were plotted using FCγR-II/III and CD34 to separate HSC and MPP or CMP, GMP and MEP populations as indicated.

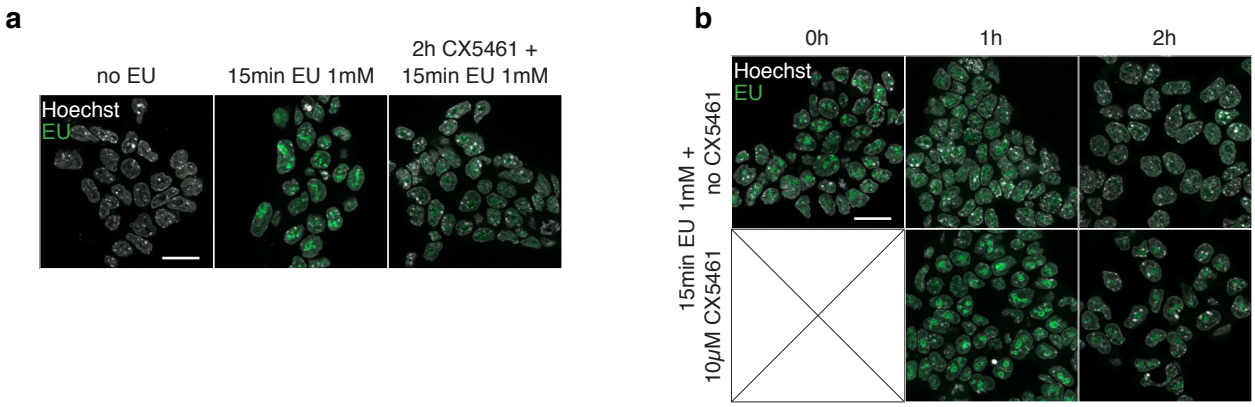

Figure S2: CX-5461 treatment blocks processing of previously synthesized rRNA

a. Embryonic stem cells were incubated in the presence or absence of 10μM CX-5461 for 2h, and then incubated for 15min in the presence or absence of 1mM EU. Cells incubated with neither compound were used as controls. **b.** Embryonic stem cells were incubated in the presence of 1mM EU for 15min, and were then incubated in the presence or absence of 10μM CX-5461 up to 2h. Cells were analyzed at the indicated time-points after EU incubation. **a,b.** EU staining (green) was revealed using Click-iT chemistry, and nuclei were stained with Hoechst (white).

Antibody information			
Antigen	**Fluorochrome**	**Clone**	**Supplier**
CD71	Biotin	C2	BD Biosciences
B220	Biotin	RA3-6B2	BioLegend
Nk1.1	Biotin	PK136	BD Biosciences
Gr-1	Biotin	RB6-8C5	BD Biosciences
Ter119	Biotin	TER-119	BD Biosciences
CD3ε	Biotin	145-2C11	BD Biosciences
CD11c	Biotin	N418	BioLegend
Mac1	Biotin	M1/70	BioLegend
Sca-1	PeCy7	D7	BD Biosciences
Sca-1	BV510	D7	DB
cKit	APC	2B8	BioLegend
cKit	PeCy7	2B8	BioLegend
CD34	FITC	RAM34	eBioscience
CD34	eFluor660	RAM34	eBioscience
FCγR-II/III	PE	2.4G2	BD Biosciences
Streptavidin	Pacific Blue	–	Invitrogen
Puromycin	Alexa647	2A4	Seedhom et al., 2016

Table S1: Antibodies

List of antibodies used for surface marker staining and intra-cellular puromycin staining.

	Volume per well	Comments
Solution A		
Formamide	5µL	
2X SSC	2,5µL	
tRNA (10mg/mL)	2,5µL	SIGMA R1753
H2O (*QS* 21,25µL)	8,75µL	adjust volume
FISH probe (50ng/µL)	2,5µL	
	final vol. 21,25µL	
Solution B		
4X SSC, 20% dextran sulfate	25µL	
BSA 10mg/mL	1,25µL	
VRC 200mM	2,5µL	SIGMA R3380
	final vol. 28,75µL	
Solution (A+B)	**final vol. 50µL**	heat solution A 5min at 95°C before mixing

Table S2: FISH staining buffer preparation

For preparation of FISH staining buffer, solutions A and B were prepared separately as indicated. Solution A was heated for 5min at 95°C, and mixed with solution B for stainings.

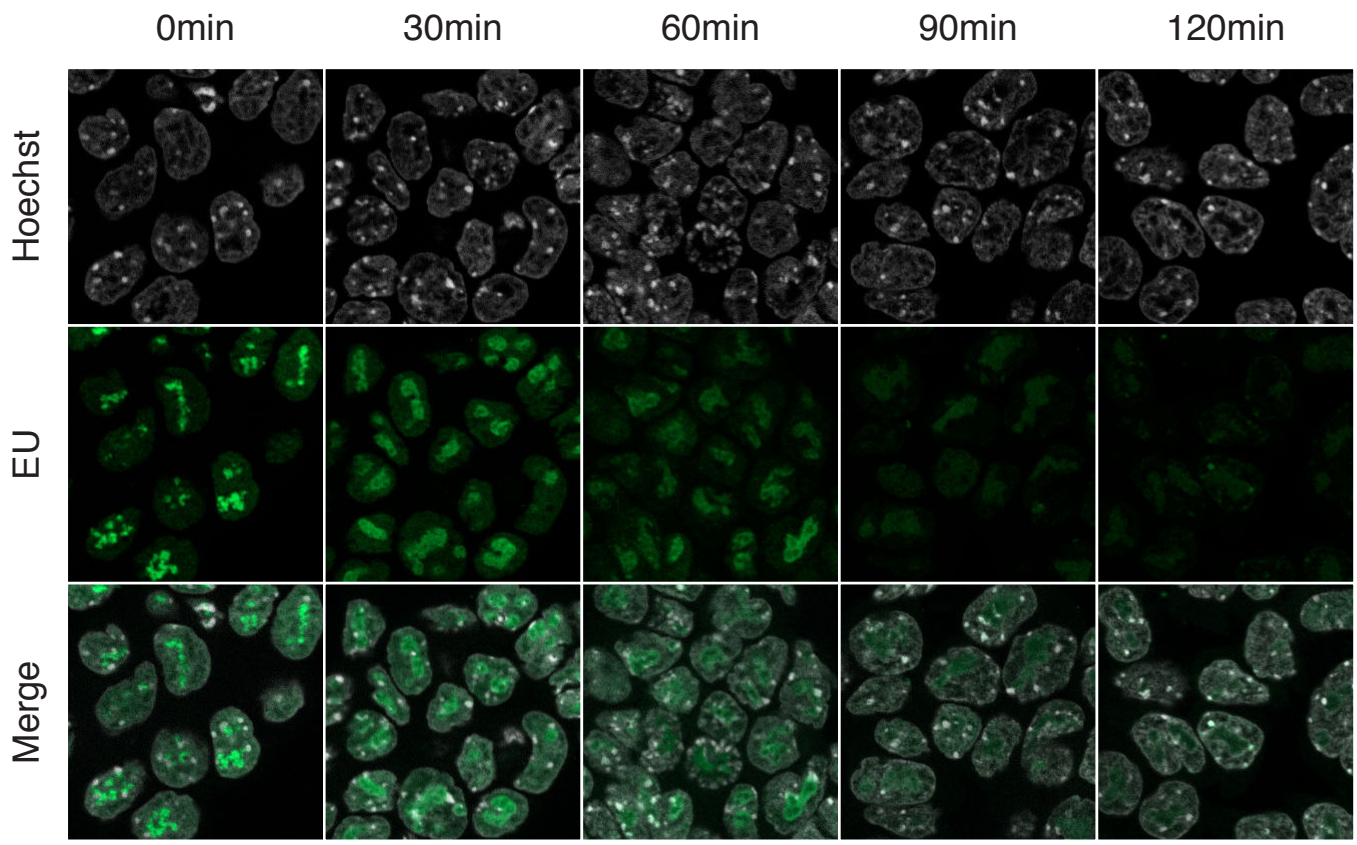

Figure R20. EU incorporation allows following of pre-rRNA processing

cK35 embryonic stem cells were cultured on Matrigel-coated coverslips in order to reach near-confluence. Cells were then incubated 15min in the presence of 1mM 5-ethynyl-uridine (EU), and label progression was analyzed by chase every 30min up to 2h. Cells were then fixed and permeabilized, and EU labeling was revealed by Click-iT chemistry using a fluorochrome-conjugated azide (green). Nuclei were stained using Hoechst (white).

2. Article: making-of and deleted scenes

2.1 Monitoring neo-synthesis of rRNA using EU

In the article, to measure the neo-synthesis of rRNAs I incubated cells in the presence of 1mM 5-ethynyl-uridine (EU), a nucleotide analog that is incorporated in neo-nascent transcripts. Using this method required several adjustments. First, I used wild-type (CK35) ES cells to find optimal conditions: a short pulse of 15min with 1mM EU was sufficient to label newly-synthesized RNAs and gave a mostly nucleolar staining (article Figure S2, extended here in Figure R20.a). Consistent with the processing of pre-rRNAs from the nucleolus to the cytoplasm, pulse-chase experiments showed that the nucleolar staining gradually progressed from the center of nucleoli to the nucleoplasm, and was eventually too faint to be detected (Figure R20.a). This fading could be explained by degradation of the cleaved pre-rRNA specific sequences, and dilution of the signal as ribosome biogenesis progresses.

2.1.1 Adjustment of the EU method to study the hematopoietic system

I wanted to adapt the EU approach to quantify the levels of rRNA neo-synthesis in bone marrow cells. To this end, I stained BM cells with surface marker antibodies, and then used the same EU staining protocol that I used in ES cells, that is, the Click-iT RNA Alexa 488 Imaging Kit (Molecular Probes). There I faced two obstacles. First, the levels of EU detected in BM cells were too weak and too close to control cells that had not been incubated with EU. To circumvent this, I had to incubate cells with EU for 1h instead of the 15min in ES cells. Second, revelation using this kit was very deleterious for many of the fluorochromes of surface marker antibodies I used for identification of BM cells. Therefore, I could not analyze these cells with enough precision (notably, I could not distinguish HSCs from MPPs, or the different oligo-potent progenitor populations). Initially, I thought this was due to the fixation I used: therefore, I tested various fixation/permeabilization methods, but eventually this did not solve the problem. I then tried different combinations of fluorochromes, but was faced with limitations due to the cytometer set-up, and available fluorochromes that resisted the EU revelation. I also tried using a different fluorochrome for the azide used to detect EU (Cyanine 3 instead of Alexa 488), but this still could not solve the issue. Eventually, I realized that the cause of the deterioration of antibody fluorochromes was the free copper present in the copper sulfate solution used for the Click-iT chemistry reaction. Thus, I tested the Click-iT Plus Alexa 488 Picolyl Azide Toolkit (Molecular Probes), where a copper protectant is added and a modified azide is used to reveal ethynyl-conjugated molecules. Using this kit, I was finally able to use all the fluorochrome conjugates that did not sustain the other kit. Interestingly, I realized that EU levels detected with this new kit were much higher than previously. Therefore, I tested whether 15min incubation with EU would be detectable with the new kit. As illustrated on Figure 5 of the article, I was indeed capable of detecting EU in cells incubated only 15min with EU.

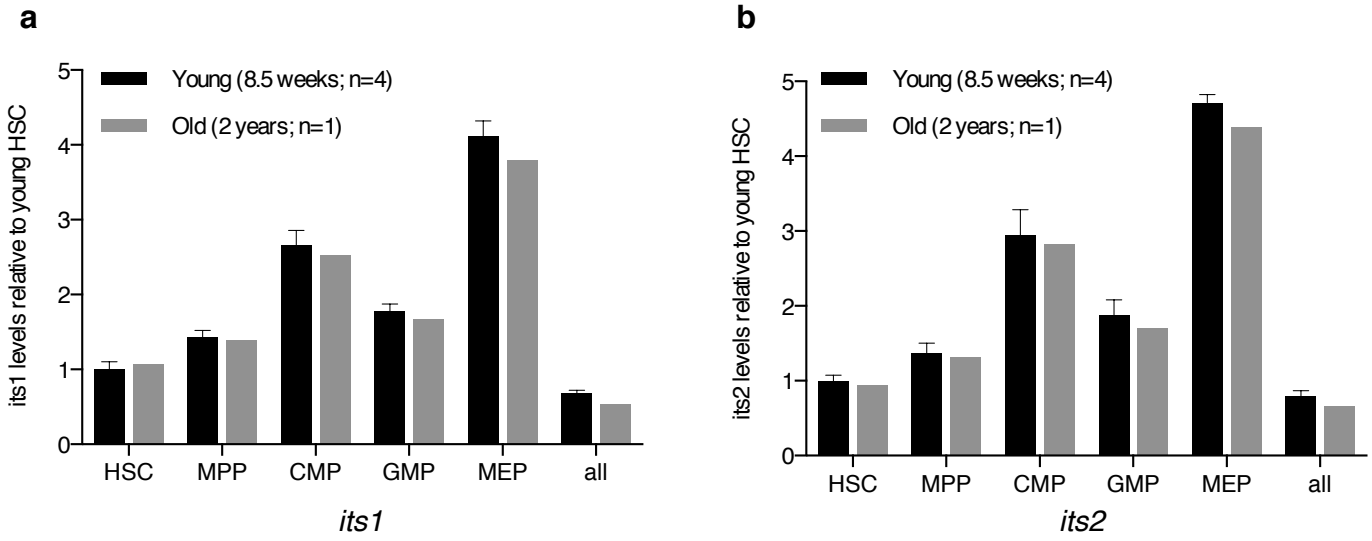

Figure R21. Immature hematopoietic populations from old and young mice display similar pre-rRNA levels

Bone marrow cells were collected from 8.5 weeks old (young, black histogram bars) and 2 years old (old, grey histogram bars) C57Bl/6J mice, and pre-rRNA levels were measure in immature hematopoietic populations using Flow-FISH with its1, its2 or scr probes. Quantification of its1 and its2 levels are presented in **a** and **b**, respectively. In each graph, pre-rRNA levels are normalized against levels measured in HSCs of young mice. n=4 individuals for young mice and n=1 individual for old mice.

2.2 Adjustments of the ribopuromycylation method

Recently, the ribopuromycylation method (RPM) has been developed, which allows measurement of the quantity of ribosomes engaged in protein translation (David et al., 2013; 2012; Seedhom et al., 2016). This is the method I used for the analysis of translational activity of hematopoietic cells presented in the article. Importantly, adapting this method to the hematopoietic system proved to be more complicated than expected. Aurélien Raveux (a fellow PhD candidate in the laboratory) set up the protocols to use RPM *in vivo* in the intestinal epithelium and *ex vivo* in cell culture, based on protocols obtained from the team of A. David. Since these protocols used for fixed solid tissues or cultured cells was suspected to impede the surface marker stainings of hematopoietic populations, we obtained another protocol that was supposed to allow analysis of hematopoietic cells (more precisely lymphocytes).

Thus, I performed first RPM experiments on hematopoietic cells using this adapted protocol. Strikingly, the levels of puromycin I quantified in the different populations analyzed were very low and comparable to background levels observed in mice that had not been injected with puromycin. I first wondered if this could be due to low accessibility of puromycin to bone marrow cells. Indeed, mice were injected intra-peritoneally and euthanized 10min later, which might not have allowed incorporation of enough puromycin in BM cells. Thus, I tested other puromycin administration methods, by injecting intra-venously or incubated BM cells with puromycin *ex vivo*. However, this did not improve detection by FACS of puromycin, as all conditions gave very similar results. Increasing the time of incubation did not help either. Interestingly, western blot analysis of BM cells treated *ex vivo* with puromycin for 10min or 1h showed that puromycin was indeed detectable at the protein level, which increased between 10min and 1h (data not shown), indicating that accessibility of puromycin to BM cells was not the issue. Therefore, I then wondered if the low levels were due to the puromycin detection method I used, and tested different signal amplification methods, without success. I also tested different fixation/permeabilization protocols. Finally, it appeared that the protocol that was supposedly adapted to the analysis of hematopoietic cells was responsible for the low puromycin detection. Indeed, the protocol we used to analyze solid tissues or cultured cells did not seem to impede the surface marker stainings, contrary to what was initially suggested, and allowed efficient detection by FACS of puromycilated peptides in injected mice. This is the protocol I used for the analyses presented in the article (Figure 1 of the article).

2.3 Similar RiBi activity in hematopoietic stem cells of aged and young mice?

Aging is associated with dysfunction of stem cell populations and loss of their intrinsic properties. Therefore, we asked whether RiBi activity could be altered in HSCs of aged mice compared to young adults. Furthermore, a recent publication showed that in aging mice, old HSCs display accumulated DNA damage in rDNA regions, leading to reduced RiBi activity and functional decline in these cells (Flach et al., 2014). Therefore, I decided to compare pre-rRNA levels in young vs. old mice using Flow-FISH. To this end, I measured relative its1 and its2 levels in four 8.5 weeks old mice and one 2 years old mouse, and did not notice any difference in HSCs or any other population analyzed (Figure R21). These preliminary results suggest that age does not affect the RiBi activity of HSCs. I did not have the opportunity to repeat this analysis because

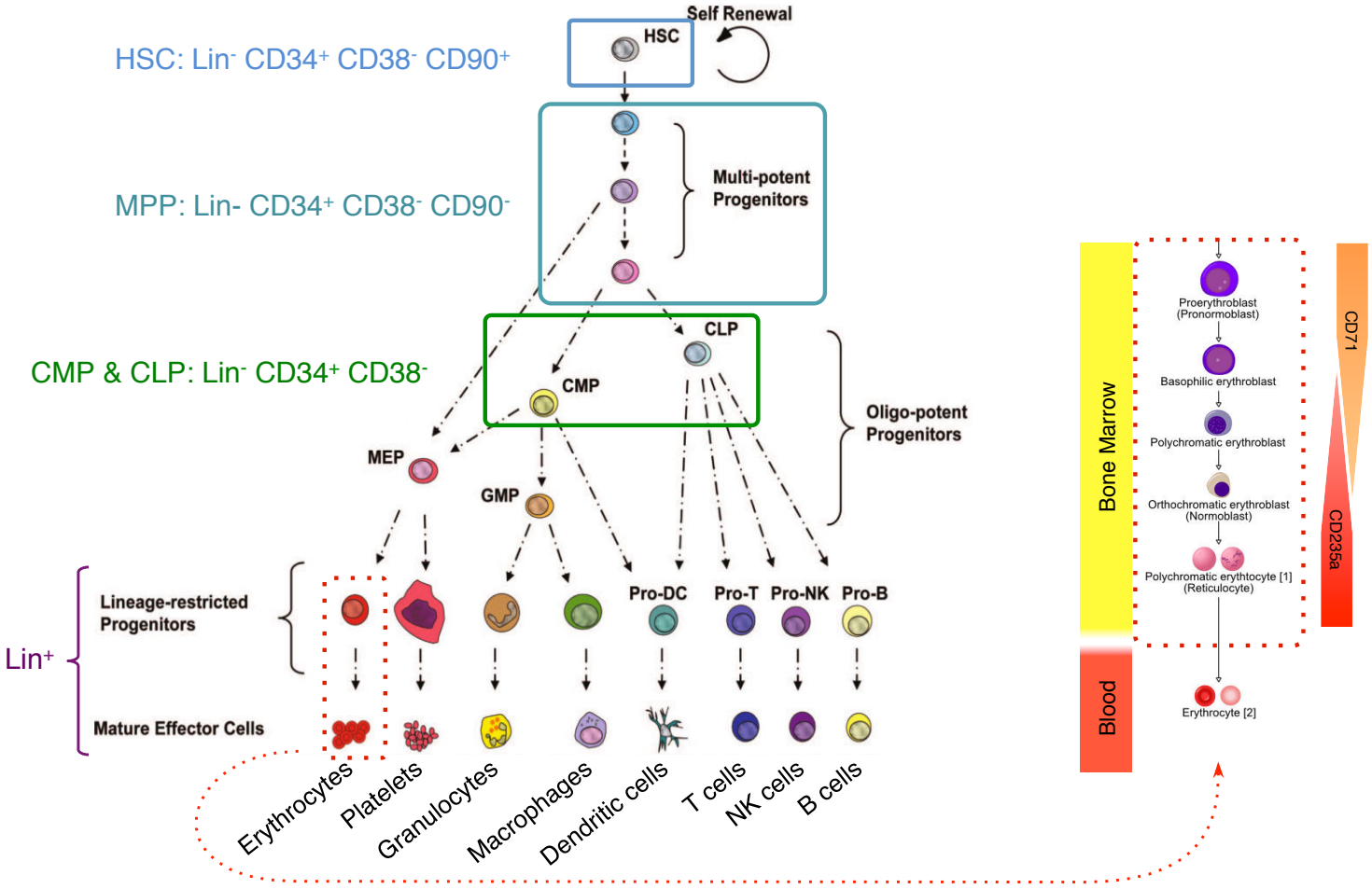

Figure R22. Human markers for the analysis of hematopoietic populations using flow cytometry

For analysis of the human immature hematopoietic populations highlighted in full-line boxes, I used fluorochrome-coupled antibodies directed against human CD34, CD38, CD90 and lineage (Lin: CD3, CD14, CD15, CD19, CD56 and CD235a) markers. For analysis of the erythroid lineage (dotted red line and boxes), I used markers CD71 and CD235a (equivalent of mouse Ter119).

Adapted from Bryder et al., 2006

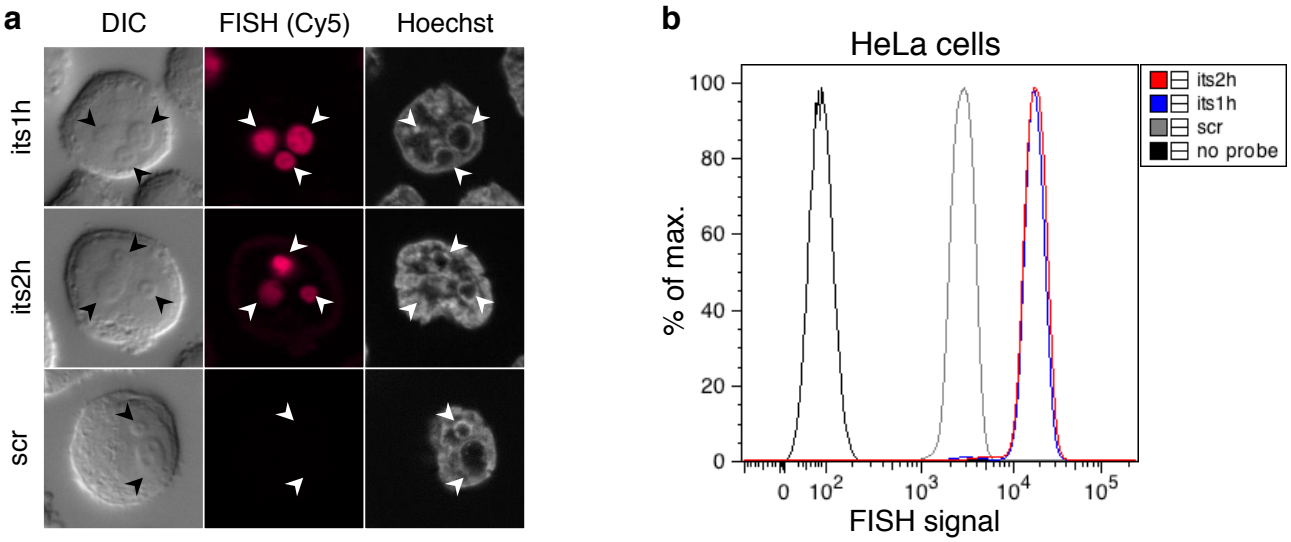

Figure R23. FISH probes specific to human its1 and its2 (1)

HeLa cells were stained using FISH probes specific to the human its1 and its2 sequences (its1h, its2h) or a non-targeting "scramble" probe (scr). **a.** Visualization by fluorescence microscopy of FISH signal. Hoechst was used to label nuclei. Differential interference contrast (DIC) allowed visualization of nucleoli (arrowheads, reported on other channels). **b.** Detection of the FISH signal by FACS analysis in HeLa cells stained with the different probes, compared to non-stained cells.

keeping mice to old age is not easy (out of 4 mice I had kept to age, 3 died before I could analyze them); it will be important to validate these observations using aged mice from mouse facility suppliers.

2.4 Analysis of pre-rRNA levels in human immature hematopoietic populations

The sustained RiBi activity I observed in mouse HSCs was very surprising, and in strong contrast to what could be anticipated from their quiescent state. Therefore, we asked whether the results obtained in mouse were reflective of a general and conserved HSC property. This motivated us to analyze RiBi activity in HSCs of another organism. Because ribosome biogenesis dysfunction is often associated with hematological defects in human, we thought that analyzing human BM cells would be interesting on a fundamental aspect to address the question mentioned above, but also as it may represent an interesting diagnostic tools in order to screen patients with hematologic disorders for RiBi dysfunction. Thus, I had to adapt the Flow-FISH protocol to the analysis of human BM cells. For this, we established a collaboration with Pr. Jérôme Larghero at the Hôpital Saint-Louis and Dr. Lydie da Costa at the Hôpital Robert Debré, to work on human bone marrow and cord blood samples. The use of such samples required the submission of a clinical research project, which was approved by the *Comité de recherche clinique* under the number 2012-46.

2.4.1 Adapting the Flow-FISH method to the human hematopoietic system

To analyze human hematopoietic cells by flow cytometry, I first had to find combinations of fluorescently-labelled antibodies allowing the separation of the different populations I wanted to analyze, which would be compatible with the Flow-FISH protocol. Together with Marie Le Bouteiller, we established the combinations of markers presented in Figure R22, using human bone marrow or cord blood samples provided by the team of Lydie da Costa.

We also had to design FISH probes specific to the human its1 and its2 sequences (respectively its1h and its2h), which I then validated using HeLa cells. Using fluorescence microscopy, I observed that both its1h and its2h stainings localized specifically to the nucleolus of HeLa cells, whereas a non-targeting “scramble” (scr, used as a control for background noise) probe gave no detectable signal (Figure R23.a). The scr probe was detected by FACS analysis, although at lower levels than its1h and its2h probes (Figure R23.b).

Once I had validated the human FISH probes, I could start analyzing human BM samples. To this end, I obtained from Jérôme Larghero leftover samples from human bone marrow used for transplantation. Strikingly, the first experiments I performed showed no or very little difference in the signal intensity of cells stained with its1h or its2h probes compared to those stained with the scr probe (Figure R24.a). This was a big issue, and meant that I could not use the data from this experiment. I wondered whether the final concentration of FISH probes (2.5ng/µL) I used impinged on the discrimination of specific signal over background noise. To test this, I stained HeLa cells with each probe, using final probe concentrations ranging from 0.25ng/µL to 6.25ng/µL (Figure R24.b). Thus, I showed that the higher the concentration is, the more background signal is detected and impedes the detection of specific signals. Therefore, I decided to analyze human BM cells using

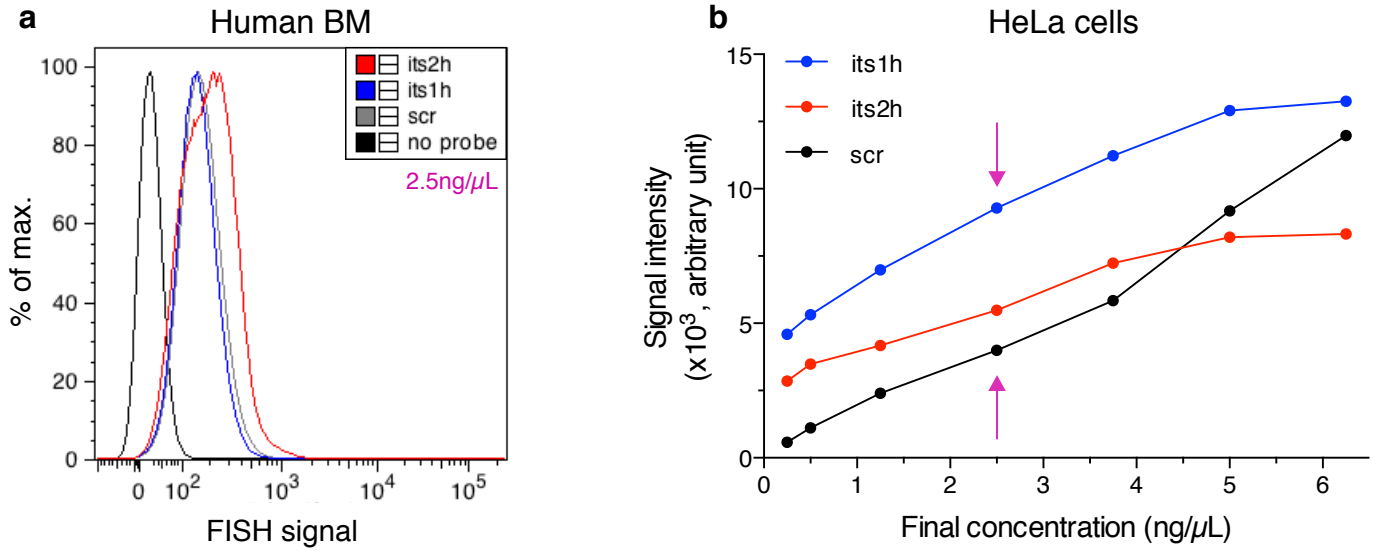

Figure R24. FISH probes specific to human its1 and its2 (2)

a. Human bone marrow (BM) cells were stained using its1h, its2h and scr FISH probes at a final concentration of 2.5ng/µL, and FISH signal was measured by FACS analysis. **b.** HeLa cells were stained using its1h, its2h an scr FISH probes at final concentrations ranging from 0.25ng/µL to 6.25ng/µL, and FISH signal was measured by FACS analysis. Signal intensity for each probe was measured and plotted against the final probe concentration used. Pink arrows show the intensities obtained with a concentration of 2.5ng/µL (same as the one used in "**a**"). **a,b.** Both experiments were performed separately; n=1 for each point.

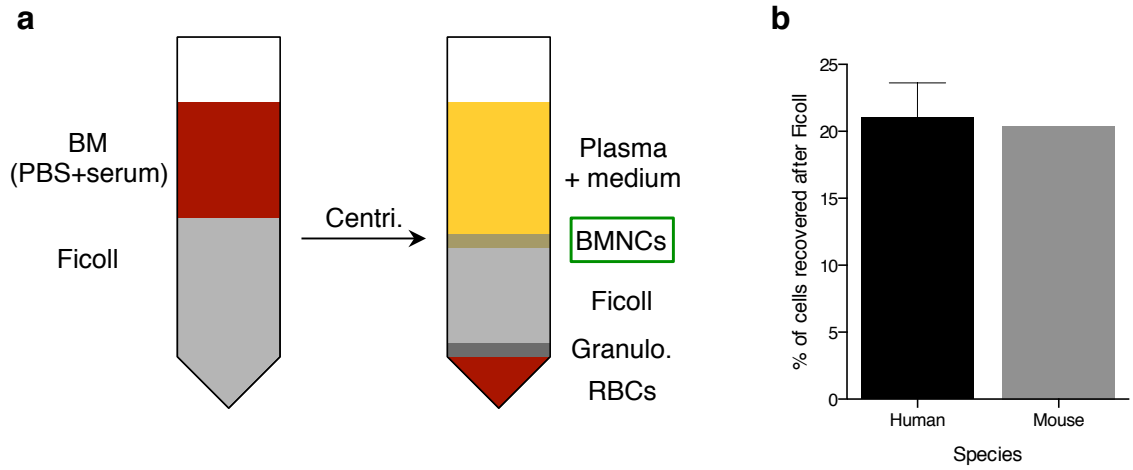

Figure R25. Ficoll density gradient centrifugation

a. Schematic view of the principle of Ficoll density gradient centrifugation to recover bone marrow (BM) mono-nucleated cells (BMNCs). In my experiments, 5mL of human BM sample was diluted by adding 15mL of PBS + 2% serum. The diluted BM was then carefully deposited on 25mL Ficoll solution to avoid mixing; the recipient tube was then centrifuged at 1700rpm for 20min with no acceleration or brake. Thus, I obtained the 5 different phases indicated. I only recovered the BMNCs, which are at the interphase between Plasma and Ficoll. After Ficoll separation, cells were rinsed 3 times using PBS+2% serum, and counted before further analyses. **b.** Percentage of cells recovered after Ficoll centrifugation of human or mouse bone marrow samples (n=3 experiments for human, n=1 for mouse).

a lower concentration than I initially did, but not too low to still be able to detect the FISH signal, and picked a concentration of 0.5ng/µL.

2.4.2 Low yields in the recovery of human hematopoietic cells impede their analysis

In the process of collecting bone marrow cells from donors, an important quantity of red blood cells and plasma is also taken in addition to BM cells and needs to be removed for the analysis of mono-nucleated BM cells. Thus, I had to remove the plasma and enrich these samples for white blood cells using Ficoll density gradient centrifugation (Figure R25.a). Strikingly, this step had an important impact on the yield of cells I recovered in the end: after Ficoll, I recovered only ~20% of the amount of cells I expected based on numeration that was performed by the team of J. Larghero (Figure R25.b). This was very surprising to me, and the elimination of granulocytes by Ficoll seemed unlikely to explain alone this low yield. Thus, I wanted to test my Ficoll protocol on mouse bone marrow cells. Consistent with what I obtained with human BM samples, I also lost ~80% of cells in mouse BM samples after Ficoll (Figure R25.b). It was also consistent with a recent study in rat showing that density gradient centrifugation compromises the yield of bone marrow mononuclear cells (Pösel et al., 2012).

The main issue with the low yield I obtained with Ficoll separation was that I need a large amount of cells for Flow-FISH analyses, whether it is for human or mouse BM analyses. Indeed, the different steps of stainings, rinses, fixation etc. lead to an important loss as well: in average, I lose 80% of cells from the moment I start stainings to the moment I analyze them with the cytometer (data not shown). Furthermore, the population I was most interested in analyzing was HSCs, which are very rare. Thus, I needed a large amount of cells for each Flow-FISH staining, in addition to which I had to prepare several controls to set up the cytometer: Figure R26.a illustrates the optimal conditions I would have required for Flow-FISH analyses on human BM. In mouse experiments, this is not a major problem since I could always use an extra individual to obtain for cells for controls. However, in human BM experiments the low yield of cells after Ficoll separation was a major issue, and I had to find a way to save as many cells as possible for the whole stainings. In the first experiment I performed on immature populations of human BM, where FISH probe concentrations were too high (see part *II-1.5.2*), I did not obtain enough cells for all set up controls, and had to use HeLa cells for controls with FISH probes, and beads that bind to anti-surface marker antibodies to use as set up controls for some of the surface marker stainings (Figure R26.b). Finally, for the last experiment that I will describe in the next part, I obtained only ~15M cells after Ficoll separation, and had to further adapt my protocol (Figure R26.c).

Such adjustments were problematic for the analyses, and obtaining larger human BM samples was not easy. Thus, I wondered if we could use cells from human cord blood samples, which we could also obtain from J. Larghero, for all cytometer setup controls. To this end, I obtained such samples and tested the surface marker antibodies and the Flow-FISH protocol on cells obtained from Ficoll separation of these samples: all stainings worked on these cells. However, obtaining both BM and cord blood samples the same day was another issue. To circumvent this problem, I tested whether I could freeze and store cord blood cells after Ficoll separation, to use them when we would receive new BM samples. There again, I faced an issue in the yield of cells after Ficoll, and

a

BM cells only				BM cells:
	NS	scr	its1h	its2h	4 x 4M
	Lin	CD34	CD38	CD90	4 x 4M
	All, no FISH	All, scr	All, its1h	All, its2h	4 x 6M
					= 56M total

No staining (NS)
FISH probes
Surface markers
Whole stainings

b

HeLa beads / BM				BM cells:
NS	*scr*	*its1h*	*its2h*	0 x 4M
Lin	CD34	**CD38**	**CD90**	2 x 2M
NS	**All, scr**	**All, its1h**	**All, its2h**	4 x 6M
				= 28M total

c

HeLa beads / BM				BM cells:
NS	*scr*	*its1h*	*its2h*	0 x 4M
Lin	CD34	**CD38**	**CD90**	2 x 1,5M
~~NS~~	**All, scr**	~~All, its1h~~	**All, its2h**	2 x 6M
				= 15M total

Figure R26. Preparation of Flow-FISH stainings on human BM samples

To perform Flow-FISH stainings, in addition to whole stainings ("All", purple boxes) I needed to prepare controls for cytometer set-up: non-stained cells ("NS", green), single-stain cells for each FISH probe (beige) and surface marker (blue). **a.** In optimal conditions, I would have used only human BM cells for all points, with 4 million (M) cells for set-up and 6M for whole stainings, requiring a total of 56M BM cells. Whole surface marker staining with no FISH probe (All, no FISH) would have allowed me to verify that FISH stainings do not modify surface markers' signals. **b.** In my first experiments, I recovered only ~30M cells, which was not enough. I used HeLa cells (italicized) for FISH controls, and beads that bind antibodies (underlined) for some surface markers. This meant that I needed a point with non-stained BM cells, and had to give up on the staining with only all surface markers and no FISH probe. **c.** For the last experiment, I obtained only ~15M BM cells and had to also give up on stainings with only surface markers and no probe, and on the control with non-stained BM cells (striked boxes).

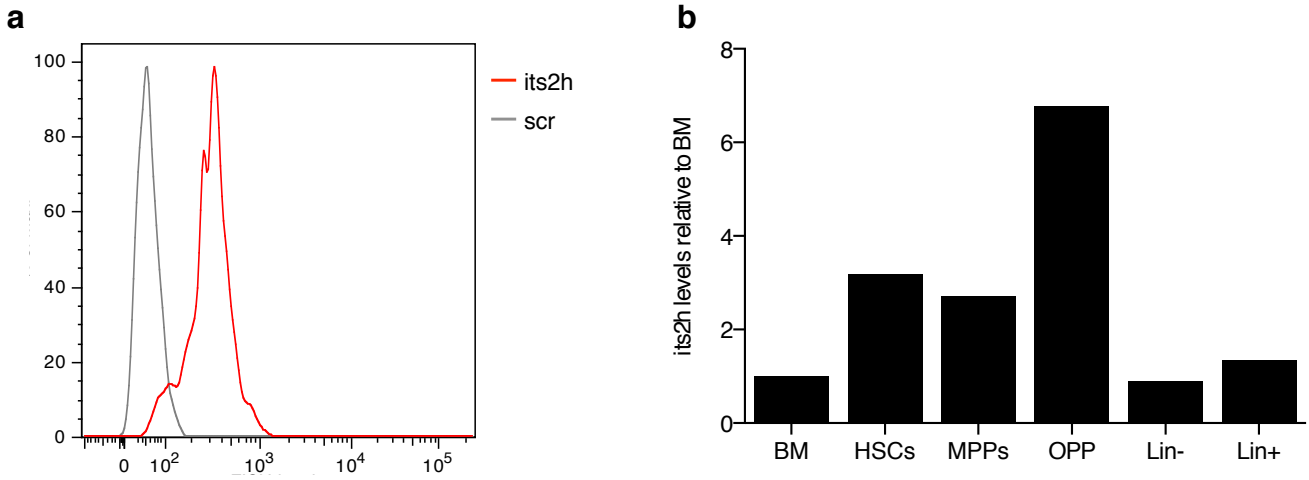

Figure R27. its2 levels in immature hematopoietic populations of human bone marrow

Bone marrow obtained from leftovers of transplantation therapy were enriched in mono-nucleated cells using Ficoll density gradient centrifugation, and were analyzed by Flow-FISH using antibodies directed against surface markers of human immature hematopoietic populations, and FISH probes directed the its2 sequence of human pre-rRNAs (its2h) or a non-targeting probe (scr). **a.** FACS profile of FISH probe levels in cells stained with the scr (grey) or its2h (red) probes. **b.** Quantification of its2h levels in BM (no markers), HSC (Lin^- $CD34^+$ $CD38^-$ $CD90^+$), MPP (Lin^- $CD34^+$ $CD38^-$ $CD90^-$), oligo-potent progenitors (OPP, Lin^- $CD34^+$ $CD38^+$), Lin– and Lin+ populations, relative to levels in BM. For this quantification, scr levels were subtracted from its2h levels to correct for background noise (see article material and methods). n=1 experiment.

also in the number of cells I could recover from stored cord blood cells after thawing them, but still I could recover enough cells that could be used as controls. Unfortunately, I did not have the opportunity to perform further analyses on human samples, but my work has cleared most issues: next experiments should be much easier and give interesting results. Still, I was able to obtain the preliminary results presented in the next paragraph.

2.4.3 Preliminary results of Flow-FISH analysis on human bone marrow samples

Finally, I managed to obtain results regarding the levels of its2h in immature hematopoietic populations of human BM. Similar to what I observed in mouse BM, I observed that oligopotent progenitors (OPP, Lin^- $CD34^+$ $CD38^+$) displayed the highest its2h levels, and that HSCs (Lin^- $CD34^+$ $CD38^-$ $CD90^+$) had similar its2h levels as MPPs (Lin^- $CD34^+$ $CD38^-$ $CD90^-$) (Figure R27 and article Figure 3). Unfortunately, as I discussed above I did not obtain enough cells to analyze its1h levels in these cells. Still, these preliminary results show that in both mouse and human bone marrows, immature hematopoietic populations display similar profiles regarding their pre-rRNA levels.

Discussion

3. How do stem cells respond to *Notchless* inactivation?

During my thesis, one of the main questions I addressed is how stem cells respond to the ribosome biogenesis defects induced by *Nle* loss-of-function. Strikingly, in all systems we have analyzed in the laboratory that require *Nle*, defects in the biogenesis of the large ribosomal subunit are observed as early as 3 days after induction of *Nle* deletion, resulting in the loss of self-renewal capacity of stem cells and their rapid elimination. Is this elimination induced by the activation of similar responses in the different systems, or could tissue- or cell type-specific responses be elicited? Are these general responses to ribosomal stress, or does *Nle* loss-of-function activate specific pathways?

3.1 How are *Nle*-deficient stem cells eliminated?

Using embryonic stem (ES) cells as a model, I have shown that *Nle*-deficient cells very rapidly activate the p53 pathway, leading to subsequent upregulation of pro-apoptotic and cell cycle arrest genes. Consistently, ES cells deficient for *Nle* display a general decrease in proliferation 3 days after induction, accompanied by an increased proportion of G_1 cells and decreased viability. However, it remains unclear whether the increase in G_1 cells is due to cell cycle arrest in this phase, induction of cell death in S and/or G_2/M phases, or both: further analyses will be required to address this point. Interestingly, I also noticed a small yet significant increase in the proportion of G_2/M cells: while I cannot formally exclude that this is due to a preferential elimination of cells during S phase, it may be rather caused by a cell cycle arrest in G_2/M as has been described by Fumagalli *et al.* in response to impaired biogenesis of both ribosome subunits (Fumagalli et al., 2012). Interestingly, the phenotypes induced by *Nle* inactivation in cells of the $p53^{HET}$ Nle^{cKO} vs. Nle^{cKO} ES cell lines seem to differ at least at two levels: the p53 target genes that are upregulated, and the timing of induction of proliferation/survival defects. These differences could be explained by the differences in *p53* zygosity between the two cell lines. An alternative explanation could be the different conditions of derivation and culture of these two cell lines. Indeed, Nle^{cKO} ES cells were derived and cultured using media containing FCS and LIF (serum+LIF), whereas $p53^{HET}$ Nle^{cKO} (and $p53^{HET}$ Nle^{cKO}) cells were derived and cultured using 2i+LIF. In serum+LIF conditions, ES cells are known to be heterogeneous due to oscillations in the expression of pluripotency-associated transcription factors, whereas the use of 2i+LIF has been reported to maintain ES cells in a more "naïve" state (Marks et al., 2012; Toyooka et al., 2008; Wray et al., 2011; Ying et al., 2008). Furthermore, Jérôme Artus observed that in serum+LIF conditions, ES cells also display heterogeneity in basal levels of p53, which he did not observe in ES cultured with 2i+LIF (unpublished). Altogether, this suggests that the use of serum+LIF vs. 2i+LIF conditions could impinge on the basal levels of p53 in ES cells, which may impact on their response to *Nle* inactivation and lead to different outcomes of p53 activation. Therefore, it will be important to compare the phenotypes induced by *Nle* loss-of-function in the different Nle^{cKO} ES cell lines cultured in 2i+LIF vs. serum+LIF conditions. Finally, the presence of pro-pluripotency and/or anti-differentiation factors in the culture medium could also prevent the possible induction of differentiation in *Nle*-deficient ES cells. Indeed, prolonged G_1 phase in ES cells is associated with

their differentiation (Calder et al., 2013; Coronado et al., 2013), and I did observe a general deregulation of genes associated with pluripotency and differentiation in Nle^{cKO} ES cells treated with OHT (data not shown). Therefore, it will also be interesting to test the outcome of *Nle* inactivation in the different ES cell lines when cultured in differentiating conditions.

In the adult mouse, Aline Stedman showed that *Nle* inactivation specifically in the intestinal epithelium also leads to activation of p53 and several of its target genes in intestinal stem and progenitor cells (ISPCs), resulting in their rapid elimination through induction of cell cycle arrest and apoptosis, and biased differentiation of progenitors (*Annex*). In the hematopoietic system, Marie Le Bouteiller also showed a rapid elimination of hematopoietic stem and progenitor cells (HSPCs) following *Nle* loss-of-function; in this system, she did not observe any increase in apoptosis, but rather an exit of HSCs from quiescence (Le Bouteiller et al., 2013). However, how precisely *Nle*-deficient HSCs and downstream progenitors are eliminated remains to be addressed: could they actually undergo apoptosis but concomitantly lose cell surface markers, thereby preventing its detection? Indeed, HSPCs also display activation of p53 and pro-apoptotic target genes upon *Nle* deletion (Le Bouteiller et al., 2013). Could HSCs undergo differentiation? In response to genotoxic stress, it has been shown that HSCs can undergo differentiation mediated by *Batf* or *Gadd45a* (see *Introduction Part 1-II-2.2.2*; (Wang et al., 2012; Wingert and Rieger, 2016)). This hypothesis could be tested using lymphoid differentiation reporters or by analyzing the expression of genes involved in HSC differentiation.

3.2 What are the molecular mechanisms involved in the elimination of *Nle*-deficient stem cells?

3.2.1 p53 plays a major role in the response to RiBi defects induced by *Nle* inactivation

The evolutionary history of the p53 family can be traced back to the appearance of multicellular life, where the primordial role of p53-like genes was to respond to genotoxic stress in order to maintain genome integrity and protect the germline. During evolution, duplications of ancestral p53 family genes have occurred, allowing their diversification and the acquisition of novel functions during the emergence of more complex multicellular organisms, notably expanding the function of p53 to the surveillance of genome integrity and multiple cellular functions in somatic cells (for review, see (Joerger and Fersht, 2016)). In particular, we saw in the introduction that p53 plays a major role in the surveillance of ribosome biogenesis in vertebrates through the RP-MDM2 pathway (for review, see (Bursać et al., 2014)). Consistently, I showed that in ES cells, the activation of p53 in response to *Nle* loss-of-function is mediated at least in part by the interaction of RPL11 with MDM2, indicating that RiBi defects induced by *Nle* deficiency trigger the RP-MDM2-p53 ribosomal stress response. The activation of p53 *in vivo* in adult hematopoietic and intestinal stem cells suggests that this ribosomal stress pathway may also be activated in these cells following *Nle* inactivation. Strikingly, we have shown that the elimination of *Nle*-deficient ES cells, HSPCs and ISPCs is partially rescued in the absence of p53, further supporting the idea that the p53 pathway is a major actor in the response to RiBi defects induced by *Nle* deficiency.

3.2.2 What are the p53-independent mechanisms triggered in response to *Nle* deletion?

Although p53 deficiency partially rescued the phenotype induced by *Nle* inactivation in the different systems we analyzed, *Nle*-deficient ES cells, HSPCs and ISPCs were still eliminated in the absence of p53. This suggests that p53-independent mechanisms can be also be elicited in response to the RiBi defects induced by *Nle* loss-of-function. To date, the nature of such p53-independent mechanisms remains unknown, but different hypotheses can be proposed, which I will develop here.

3.2.2.1 Are translation alterations involved in the elimination of Nle-deficient cells?

There is little information regarding the lifespan of ribosome biogenesis in the cells, especially *in vivo* in mammals. Nonetheless, it is conceivable that the RiBi defects induced by *Nle* inactivation could lead to a decreased quantity of mature, functional ribosomes, which could impact on global protein translation. Indeed, the team of S. Fumagalli showed recently that loss of RPL5 or RPL11 in human normal lung fibroblasts failed to induce upregulation of p53 and cell cycle arrest, but resulted in suppression of cell cycle progression due to reduced mature ribosome content and translational capacity (Teng et al., 2013). In the intestinal epithelium, no significant decrease in protein synthesis was observed in *p53*-deficients ISPCs after *Nle* inactivation at a time when strong apoptosis was observed ref. This observation suggests that, in absence of p53, elimination of *Nle*-deficient ISPCs is not caused by decreased translation. Nevertheless, it will be important to test the translation activity of *Nle*-deficient ES cells and HSCs as well, in both p53-proficient and deficient contexts. Besides global translation, perturbed RiBi upon *Nle* inactivation could also specifically affect the translation of particular subsets of mRNAs, such as IRES-dependent or TOP mRNAs through activation of the ribosomal stress response (Fumagalli et al., 2009; Gismondi et al., 2014; Horos and Lindern, 2012; Marcel et al., 2013). Indeed, stem cells could be particularly sensitive to even small variations in the translation of mRNAs that are important for the maintenance of their properties. For instance, we have seen in the introduction that *c-Myc* expression is regulated by the 5S RNP upon ribosomal stress, and regulation of *Myc* expression is important for the maintenance of HSC properties (Laurenti et al., 2008).

3.2.2.2 Are other MDM2 targets affected by the RiBi defects induced by Nle inactivation?

Besides p53, other MDM2 have been described (Riley and Lozano, 2012). It is therefore likely that the inhibition of MDM2 consecutive to RiBi defects also affects these targets. As I discussed in the introduction, inhibition of MDM2 by RPL11 leads to the degradation of the transcription factor E2F-1 and subsequent down-regulation of its target genes required for the entry and progression through the S phase, resulting in cell cycle arrest (see *Introduction Part2-1.3.3.3* and (Donati et al., 2011b)). Such a response could explain the cell cycle arrest observed in *Nle*-deficient ISPCs, and the potential cell cycle arrest in ES cells: indeed, E2F activity is an important driver of cell division in ES cells, and E2F transcription factors are important regulators of stem cell fate (Julian and Blais, 2015; Stead et al., 2002). MDM2 has also been shown to bind to the p53 paralog p73, which similarly to p53 promotes growth arrest and apoptosis: it would be interesting to see if p73 responses could be elicited following *Nle* deletion in the absence of p53. To test whether p53-independent pathways affected by the 5S RNP-MDM2 interaction are implicated in the

elimination of *Nle*-deficient cells, it would be interesting to analyze the effects of *Nle* inactivation in mice carrying a mutated $Mdm2^{C305F}$ allele preventing binding of MDM2 by the 5S RNP (Lindström et al., 2007; Macias et al., 2010).

3.2.2.3 Nle-specific mechanisms?

Another possibility would be that *Nle* has other functions besides ribosome biogenesis, which could be responsible for the phenotypes observed. However, this does not seem to be the case: treatment of intestinal organoids with the RNA Pol I inhibitor CX-5461 recapitulates the intestinal phenotype induced by *Nle* inactivation, suggesting that at least in this system, the role of *Nle* in ribosome biogenesis is sufficient to explain the phenotype observed (*Annex*).

3.2.3 Conclusions

3.2.3.1 A conserved role for the 5S RNP in the surveillance of ribosome biogenesis?

In which species p53 is involved in the monitoring of RiBi is not entirely clear to date. Nonetheless, while p53 is a major actor of responses to various stresses in vertebrates, it is important to note that this is not the case in all eukaryotes. Thus, RiBi defects are necessarily managed differently in species where p53 does not exist or is not involved in the surveillance of ribosome biogenesis. In yeast, a checkpoint at the end of the G_1 phase, called "restriction point", coordinates cell growth and cell cycle progression in a ribosome-dependent manner, and induces cell cycle arrest in response to RiBi dysfunction. Interestingly, a recent study in yeast showed that perturbed RiBi induces the accumulation of free RPL5, which has a direct impact on the G_1/S transition (Gomez-Herreros et al., 2013). This observation suggests that the role of the 5S RNP (composed of RPL5, RPL11 and the 5S rRNA) in the surveillance of ribosome biogenesis could be conserved throughout eukaryotes. Finally, future studies comparing the responses to RiBi defects elicited in yeast and vertebrates could highlight the existence of more common mechanisms conserved in the eukaryote domain.

3.2.3.2 Implications of ribosomal stress responses in pathological situations

As I discussed in the introduction, ribosomal stress responses, notably the activation of p53, appear to be involved in the physiopathology of ribosomopathies. The identification of additional responses to ribosome biogenesis dysfunctions could provide better understanding of such phenotypes, and help for the development of therapeutic strategies. Interestingly, ribosomopathies are also associated with an increased risk of developing cancers, which could result from the selection of stem cells with impaired p53 responses: the identification of p53-independent responses could also provide new targets for the development of anti-cancer therapies.

4. Alternative *Nle*-independent ribosome biogenesis pathways?

In yeast, *Nle* ortholog Rsa4 plays an essential and unique role in ribosome biogenesis, which our team has shown is conserved in mouse. However, strikingly, it appears that *Nle* is dispensable for some cell types. In the early embryo, in contrast to cells of the inner cell mass (ICM), cells of the trophectoderm (TE) are not affected by *Nle* deficiency: *in vivo*, they are able to implant in the

uterus and can engage the decidual reaction; *ex vivo*, when E3.5 *Nle*$^{null/null}$ embryos are cultured, TE cells do not appear affected while cells of the ICM fail to expand (Cormier et al., 2006). In the ovary, *Nle* inactivation specifically in oocytes does not affect their growth, ovulation or fertilization (Sandrine Vandormael-Pournin, unpublished data). However, interestingly most of fertilized *Nle*-deficient oocytes are not competent for development, indicating that the early steps of embryogenesis are compromised in the absence of maternal stocks of *Nle*. In the hematopoietic system, Marie Le Bouteiller showed that restricted progenitors and differentiated cells of the B lineage are not affected by the loss-of-function of *Nle in vivo* (Le Bouteiller et al., 2013). Finally, my preliminary results in the T lineage indicate that T cell development is only slightly affected by *Nle* inactivation, although this is a preliminary observation that needs to be confirmed. For both the B and T cell lineages, analyses were performed in unperturbed, non-challenging conditions. It will be interesting to test the capacity of *Nle*-deficient B and T cells to respond to stimulation upon infection or treatment with antigens or stimulating signals (such as IL-7 for the T lineage or CpG oligonucleotides for the B lineage). It will also be interesting to test whether *Nle* is equally dispensable for other hematopoietic restricted progenitors and lineages, for instance in the erythroid lineage, which as I showed in the article exhibits very high ribosome biogenesis activity. To this end, the *Gata-1-HRD-iCre* mouse strain could be used, which expresses an constitutively active Cre recombinase during the early stage of erythroid commitment (Yoon et al., 2008).

The observation that *Nle* is dispensable in lymphoid lineages and oocytes is puzzling because B and T progenitor cells are highly proliferative, and mature lymphocytes and oocytes have high protein synthesis activity (oocytes accumulate a large quantity of cellular components and their volume increases ~300-fold during folliculogenesis!), suggesting that they require an important amount of functional ribosomes and thus should have important RiBi activity. Therefore, these observations suggest that alternative ribosome biogenesis pathways may exist in these cells, where NLE is dispensable. Indeed, in the B lineage Marie Le Bouteiller showed that pre-60S processing was not impaired following *Nle* inactivation (this will have to be tested in T cells and oocytes). Functional redundancy could explain such differential requirement for *Nle*, however there are no clear *Nle* homologs in mouse. The closest gene to *Nle* is *Wdr12*, which encodes a WD40-repeats-containing protein with an N-terminal domain resembling that of NLE. However, *Nle* is an ancestral gene that was present in the last common ancestor of all eukaryotes and *Wdr12* is conserved in eukaryotes, and it has been shown in yeast that Ytm1 (WDR12 yeast ortholog) and Rsa4 act successively and non-redundantly during pre-60S maturation (Ahn et al., 2016; Baßler et al., 2010; Gazave et al., 2009; Kressler et al., 2012; Moilanen et al., 2015). It is therefore unlikely that Wdr12 could compensate for Nle. Nevertheless, this should be formally addressed in mouse. In addition, it will be interesting to compare the phenotypes induced by inactivation of *Wdr12* and *Nle* in the different systems to determine whether both genes always act together or if in some cells their activities is differentially required. Finally, besides functional redundancy, alternative ribosome biogenesis pathways could also allow cells to bypass the requirement of NLE for maturation of the 60S pre-particle, which could lead to functionally different ribosomes. Proteomics analyses on pre-60S-associated factors should be considered to compare the composition of the maturating large

subunit between cells that are affected or not by *Nle* loss-of-function: the B lymphoid lineage appears as a good model to address this point.

5. Relationships between ribosome biogenesis and stem cells

Ribosome biogenesis is a fundamental process, essential for all living organisms. Long considered as a process with only a housekeeping function, it is now clear that ribosome biogenesis plays a much more important role in the regulation of cellular functions. However, very little is known today regarding the regulation and proceedings of the ribosome biogenesis pathway in multicellular organisms, especially *in vivo* in mammals.

5.1 Sustained rDNA transcription as a hallmark of (hematopoietic) stem cells?

Motivated by our lack of knowledge on the regulation of ribosome biogenesis in mammals, I set out to analyze the activity of this process *in vivo* in the mouse hematopoietic system at homeostasis. To our knowledge, the work presented in the article provides for the first time information on ribosome biogenesis activity of rare populations *in vivo* in mammals. In particular, I showed that contrary to what could be expected from their mostly quiescent state, HSCs display surprisingly sustained ribosome biogenesis activity similar to that in MPPs, which have very different proliferation status. Furthermore, my preliminary results on human BM cells indicate that human HSCs also have sustained RiBi activity, suggesting that this property of HSCs is conserved in human. These observations raise questions regarding the role of RiBi in HSCs. The RiBi activity in these cells does not seem to correlate with important protein synthesis activity, which is very low in HSCs compared to other populations of the bone marrow, or with their proliferation since they are mostly quiescent. But then, what is the benefit for quiescent cells, with low translational activity, to sustain such an energy-consuming process? Ribosome biogenesis could play an important role in the regulation of other cellular pathways that are particularly important for the maintenance of HSC properties, for instance through the maintenance of nucleolar structure. This could be of particular importance for regulation of the cell cycle and maintenance of self-renewal in HSCs, as well as for their ability to respond to various stress signals. The latter is supported by recent finding that mutations in the *Runx1* gene –a DNA binding transcription factor– lead to reduced ribosome biogenesis activity in HSCs and impede their response to genotoxic and endogenous stresses, providing a selective advantage to pre-leukemia stem cells (Cai et al., 2015). This is particularly interesting, and may have implications in the understanding of hematological pathologies due to genetic defects affecting ribosomes.

In a more general perspective, recent studies in *ex vivo* mammalian models and in Drosophila showed that the downregulation of rRNA synthesis induces differentiation of stem and cancer cells (see *Introduction Part2-3.1.3*; (Hayashi et al., 2014; Watanabe-Susaki et al., 2014; Zhang et al., 2014)). Together with our results, this suggests that sustained rDNA transcription is required for the maintenance of stem cell populations in general. Finally, we saw in the introduction that important ribosome biogenesis is also associated with tumorigenesis, and several new anti-cancer therapeutic treatments consist in the use of rRNA synthesis inhibitors. Although such treatments appear good

alternatives to more aggressive chemotherapeutic treatments, one must keep in mind that they could also interfere with non-cancer cells. Notably, I have shown that megakaryocyte and erythroid progenitors (MEPs) exhibit particularly important RiBi activity, as do pro- and early erythroblasts: these populations could be strongly affected by inhibition of rRNA synthesis. Besides, as we discussed above, sustained ribosome biogenesis appears to be particularly important for the maintenance of stem cell populations. Thus, treatment with rRNA synthesis inhibitors could also have important side effects on stem cell homeostasis, and the example of *Runx1* mutants suggests that reduced RiBi activity may actually not allow the elimination of stem cells that have already acquired tumorigenic mutations, and even favor their accumulation.

5.2 Differential requirement of ribosome biogenesis factors between stem and differentiated cells

As we discussed earlier, our work suggests that *Nle*-dependent ribosome biogenesis pathways are specifically required for the maintenance of hematopoietic and intestinal stem and progenitor cells, whereas alternative *Nle*-independent pathways could be used in more differentiated cells. In addition to our laboratory's work, collaborators have investigated the role of *Nle* in other tissues. In the melanocyte lineage, *Nle* is required for the development and maintenance of melanoblasts (Geneviève Aubin-Houzelstein, unpublished). During embryogenesis, *Nle* inactivation in this lineage leads to increased apoptosis and induces pigmentation defects. Adult mice are subject to accelerated hair whitening, indicative of compromised maintenance of melanocyte stem cells. Premature differentiation of stem cells could explain this phenotype. Finally, preliminary analyses have been performed to investigate the requirement of *Nle* for stem cells of skeletal muscles (satellite cells; Barbara Gayraud-Morel, unpublished). *Nle* inactivation in muscle fibers cultured *ex vivo* induces proliferation defects of activated satellite cells. *In vivo*, deletion of *Nle* in satellite cells does not induce any visible phenotype in unperturbed conditions, but muscle injury experiments showed that *Nle* deficiency impedes regeneration of muscle fibers, indicating that *Nle* is required for the regeneration potential of satellite cells upon activation. Altogether, these observations and our results suggest that *Nle* plays an essential role in stem and immature cells of several lineages.

As I mentioned in the introduction, several studies have shown that RiBi factors are specifically enriched in stem cell populations, such as Drosophila neuroblasts, zebrafish neuroepithelial-like progenitors of the midbrain, or human embryonic stem cells (Huang et al., 2014; Neumüller et al., 2011; Recher et al., 2013). In differentiating mouse ES cells, several small subunit processing factors are downregulated and their knockdown in undifferentiated ES cells impedes the maintenance of their pluripotency (You et al., 2015). Finally, it was recently shown that the Drosophila *mbm* gene encodes a nucleolar protein required for synthesis of the small ribosomal subunit specifically in neuroblasts but not in neurons (Hovhanyan et al., 2014). Altogether, such studies and our work on *Nle* suggest that ribosome biogenesis factors may play specific roles in stem cells, and that they may use ribosome biogenesis pathways different from that of their differentiated progeny. The identification of specificities in the RiBi pathways used in immature and differentiated cells could allow the development of approaches to specifically target

differentiated cells without affecting progenitors and stem cells for the treatment of pathologies associated to ribosome biogenesis dysfunctions.

6. Conclusion

Since the discovery of the concept of stem cells, great efforts have been granted to the identification of the mechanisms underlying the regulation and maintenance of stem cell properties. The work I performed during my thesis supports the emerging idea that specific ribosome biogenesis features distinguish stem cells them from their progenies, and appear to be essential for the maintenance of stem cell properties. In a more general perspective, this is consistent with the observation that stem cells display particular characteristics in fundamental cellular processes compared to progenitors and differentiated cells, such as cell cycle control, management of the energetic metabolism, or the maintenance of genome integrity. In the end, all these processes, including ribosome biogenesis, appear to be intricately linked to one another. Further studies will help better understand the relationships between these processes, and how they act together for the regulation and maintenance of stem cells: the development of tools such as the ones I used for the analysis of RiBi activity in the hematopoietic system will be important to address such questions. Finally, the Flow-FISH approach we have developed in the laboratory could also be useful in a clinical perspective, for instance to identify which hematopoietic populations are affected in ribosomopathies with hematological phenotypes, as well as in *in vivo* models of such diseases.

Annex

(Stedman et al., 2015)

Cell Death and Differentiation (2015) 22, 1865–1876

www.nature.com/cdd

Ribosome biogenesis dysfunction leads to p53-mediated apoptosis and goblet cell differentiation of mouse intestinal stem/progenitor cells

A Stedman[1,2], S Beck-Cormier[1,2,7], M Le Bouteiller[1,2,8], A Raveux[1,2], S Vandormael-Pournin[1,2], S Coqueran[1,2], V Lejour[3,4,5], L Jarzebowski[1,2], F Toledo[3,4,5], S Robine[6] and M Cohen-Tannoudji*[,1,2]

Ribosome biogenesis is an essential cellular process. Its impairment is associated with developmental defects and increased risk of cancer. The *in vivo* cellular responses to defective ribosome biogenesis and the underlying molecular mechanisms are still incompletely understood. In particular, the consequences of impaired ribosome biogenesis within the intestinal epithelium in mammals have not been investigated so far. Here we adopted a genetic approach to investigate the role of Notchless (NLE), an essential actor of ribosome biogenesis, in the adult mouse intestinal lineage. *Nle* deficiency led to defects in the synthesis of large ribosomal subunit in crypts cells and resulted in the rapid elimination of intestinal stem cells and progenitors through distinct types of cellular responses, including apoptosis, cell cycle arrest and biased differentiation toward the goblet cell lineage. Similar observations were made using the rRNA transcription inhibitor CX-5461 on intestinal organoids culture. Importantly, we found that p53 activation was responsible for most of the cellular responses observed, including differentiation toward the goblet cell lineage. Moreover, we identify the goblet cell-specific marker *Muc2* as a direct transcriptional target of p53. *Nle*-deficient ISCs and progenitors disappearance persisted in the absence of p53, underlying the existence of p53-independent cellular responses following defective ribosome biogenesis. Our data indicate that NLE is a crucial factor for intestinal homeostasis and provide new insights into how perturbations of ribosome biogenesis impact on cell fate decisions within the intestinal epithelium.
Cell Death and Differentiation (2015) **22,** 1865–1876; doi:10.1038/cdd.2015.57; published online 12 June 2015

Construction of ribosomes in eukaryotes is a highly complex process. Upon transcription in the nucleolus, the pre-rRNA undergoes a series of cleavages and modifications while being assembled into ribosomal preparticles upon hierarchical addition of ribosomal proteins.[1] In yeast, ≈200 assembly factors and several small nucleolar RNAs have been shown to participate to these processes. In higher eukaryotes, though the core components have been conserved, differences were reported[2–5] suggesting that ribosome biogenesis has become more complex with evolution.

A specific pathway dedicated to the surveillance of ribosome biogenesis was identified originally in mammalian cells. Inhibition of RNA polymerase I activity, or deficiencies in factors required in ribosome biogenesis, was shown to trigger the binding of a 5S rRNA/RPL11/RPL5 inhibitory complex to the MDM2 ubiquitin ligase, thereby preventing MDM2-mediated p53 degradation.[6–8] In human, pathologies caused by ribosome biogenesis dysfunction are called ribosomopathies and represent a set of clinically distinct diseases presenting with tissue-specific developmental defects and increased risk of cancer.[9,10] Studies on cellular and animal models suggest that unscheduled upregulation of p53 may account for many clinical symptoms associated with ribosomopathies.[11–16] There are now evidences that ribosome biogenesis dysfunction also triggers p53-independent mechanisms.[17–19] Because bone marrow defects is a frequent clinical manifestation of ribosomopathies, most studies focused on the hematopoietic tissue and less is known about the impact of ribosome biogenesis dysfunction in other organs.

Notchless (Nle) encodes a WD40 repeats-containing protein highly conserved in eukaryotes. Its ortholog in yeast, *Rsa4*, was shown to be essential for the late step of maturation and subsequent export of the 60S particle.[20–22] We recently showed that *Nle* role in the maturation of the large ribosomal subunit is conserved in mouse and that *Nle* is required for the maintenance of hematopoietic stem cells.[23] During the course of this study, we noticed that the gut was also sensitive to *Nle*

[1]Mouse Functional Genetics, Department of Developmental & Stem Cell Biology, Institut Pasteur, 25 rue du docteur Roux, Paris, France; [2]CNRS URA 2578, Paris, France; [3]Genetics of Tumor Suppression, Equipe Labellisée Ligue Nationale Contre le Cancer, Institut Curie, Centre de recherche, Paris, France; [4]UPMC University Paris 06, Paris, France; [5]CNRS UMR 3244, Paris, France and [6]Unité Mixte de Recherche 144, Centre National de la Recherche Scientifique, Institut Curie, Paris, France
*Corresponding author: M Cohen-Tannoudji, Mouse Functional Genetics, Department of Developmental & Stem Cell Biology, Institut Pasteur, 25 rue du docteur Roux, F-75015 Paris, France. Tel: +33 1 45 68 84 86; Fax: +33 1 45 68 86 34; E-mail: m-cohen@pasteur.fr
[7]Current address: Institut National de la Sante et de la recherche Medicale, U791, LIOAD, STEP group 'Skeletal Tissue Engineering and Physiopathology', Université de Nantes, UFR Odontologie, F-44042 Nantes, France.
[8]Current address: Biotech Research and Innovation Center, University of Copenhagen, DK-2200 Copenhagen N, Denmark.
Abbreviations: BrdU, Bromo-deoxyuridine; CBC, crypt base columnar; cKO, conditionnal Knock-out; GFP, green fluorescent protein; IRES, internal ribosome entry site; Its, internal spacer; Nle, Notchless; PBS, phosphate-buffered saline; PCR, polymerase chain reaction; qPCR, quantitative polymerase chain reaction; PFA, paraformaldehyde; SC, stem cell; ISC, intestinal stem cell; TA, transit-amplifying; RE, response element
Received 28.8.14; revised 31.3.15; accepted 13.4.15; Edited by M Oren; published online 12.6.15

deletion. Here we performed the conditional inactivation of *Nle* in the intestinal epithelium and showed that *Nle*-dependent large ribosomal subunit biogenesis is required for the maintenance of intestinal stem cells (ISCs) and progenitors. Combining *in vivo* analyses with intestinal organoids culture, we demonstrate that defective ribosome biogenesis leads to p53-mediated removal of intestinal SCs and progenitors through several mechanisms including biased differentiation toward the goblet cell lineage. Finally, we show that p53-independent responses are also at play in *Nle* mutant crypt cells.

Results

***Nle* is required in intestinal crypts.** We previously showed that *Nle* is widely expressed in the mouse.[24] To examine more precisely its pattern of expression in the adult small intestine, we performed RT-qPCR and western blot analyses on crypts and villi fractions. We found that both *Nle* mRNA and protein were enriched in crypts compared with villi (Figures 1a and b). To specifically delete *Nle* in the intestinal epithelium, we used the *Villin-CreERT2* transgenic line. Control (*Villin-CreERT2*$^{tg/0}$; *Nle*$^{flox/+}$) and NleVilcKO (*Villin-CreERT2*$^{tg/0}$; *Nle*$^{flox/null}$) littermates were subjected to daily intraperitoneal tamoxifen injection and analyzed at various time points post last tamoxifen injection (p.i.) (Figure 1c). To monitor the conversion of the *Nle*^{flox} allele into the *Nle*^{del} allele, we performed genomic PCR targeting both alleles. We found that Cre-mediated recombination of the *Nle*^{flox} allele was efficient in crypts and villi from both Control and NleVilcKO mice (Figure 1d). Efficiency of deletion was confirmed by the marked decrease of NLE protein levels in NleVilcKO crypts and villi (Figure 1b). A small proportion of nonrecombined cells persisted in the epithelium at the end of the tamoxifen regimen as indicated by the presence of a faint *Nle*^{flox} signal in Control and NleVilcKO samples at day 1 p.i. (Figure 1d). Contrary to Controls that showed limited level of nonrecombined allele up to 60 days p.i. (Figure 1d), the *Nle*^{flox} and *Nle*^{del} alleles were detected at equivalent level in NleVilcKO intestine at day 4 p.i. and the *Nle*^{del} allele was no longer detectable at day 60 p.i. (Figure 1d). This indicates that *Nle*-deficient intestinal epithelium was rapidly and entirely replaced by *Nle*-proficient cells derived from ISCs that have escaped deletion.

Hematoxylin–eosin staining revealed that crypts, but not villi, were clearly affected following *Nle* deletion. At day 1 p.i., apoptotic bodies were present and many crypts exhibited a progressive degeneration phenotype in the following days (Figure 1e, arrowheads and arrows). At day 4 p.i., intestinal regeneration was readily visible, with the presence of abnormally big, hyperplastic crypts (Figure 1e, bracket). Consistent with the reappearance of *Nle*-proficient epithelium, normal histology was observed on sections of NleVilcKo intestines at later time points. Collectively, these data show

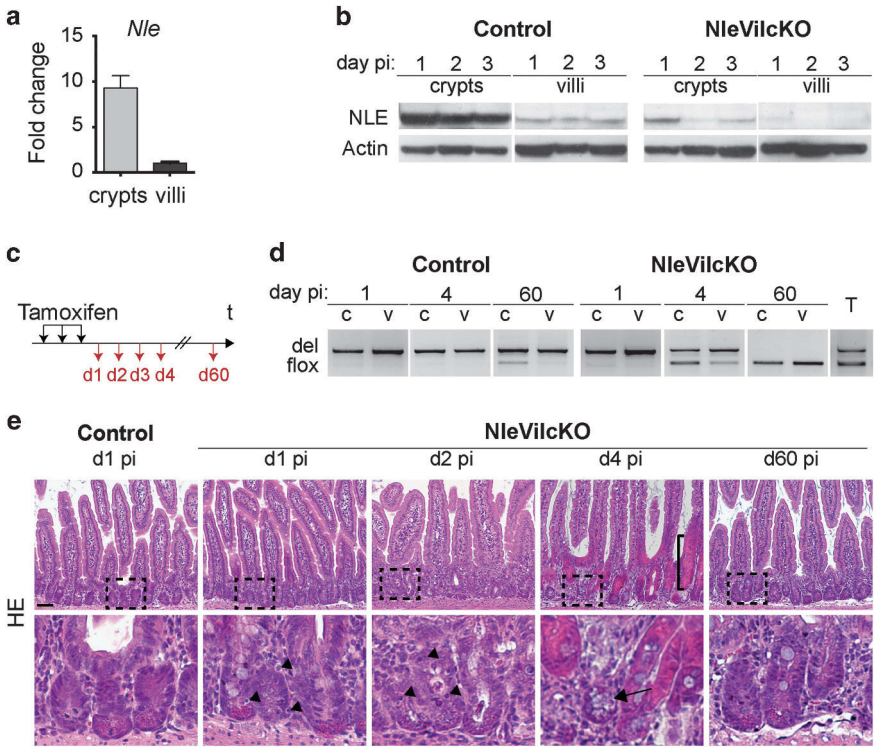

Figure 1 *Nle* is required in intestinal crypts. (**a**) RT-qPCR analysis of *Nle* mRNA levels in crypts and villi. (**b**) Western blot for NLE and α-Actin on crypts or villi enriched extracts from Control and NleVilcKO intestine. All extracts were run on the same gel. (**c**) Scheme of tamoxifen injection and analysis. (**d**) Detection of the nonrecombined (flox) and the recombined (del) *Nle* alleles by PCR performed on crypts (c) or villi (v) enriched DNA extracts from Control and NleVilcKO small intestine. Two bands of similar intensity are amplified from *Nle*$^{flox/del}$ DNA (T). The wild-type *Nle* allele is not amplified in this reaction. (**e**) Hematoxylin–eosin staining of sections from Control and NleVilcKO small intestine. The second line shows magnified views of framed regions. Black arrowheads point to apoptotic bodies. Black bracket indicates a hyperplasic crypt. Black arrow shows a dying crypt. Scale bar, 50 μm

that *Nle* function is required for the maintenance of ISCs and crypt homeostasis.

***Nle* deletion impairs survival and proliferation of intestinal SC and progenitors.** We observed a significant increase in Caspase 3-dependent apoptosis in NleVilcKO crypts at day 2 p.i. (Figures 2a and b). Noticeably, apoptosis seemed to occur preferentially at the crypt base where stem cells and progenitors reside (Figure 2a, data not shown). Increased apoptosis was accompanied by a decrease in the proliferation of intestinal progenitors at day 2 p.i., though some crypts, probably containing recombination escaper cells, retained a normal proliferation profile (Figure 2a, arrow, Figure 2c).

To investigate the early response of ISCs to *Nle* inactivation, we first examined the expression levels of ISCs markers by RT-qPCR. At day 1 p.i., the molecular signature of ISCs was partially deregulated since *Bmi1* expression was increased, and *Olfm4* expression was decreased while *Lgr5* and *Tert* expression was unaffected. One day later, *Olfm4* down-regulation persisted and *Bmi1* expression returned to levels similar to Control mice (Figure 2d). Such uncoupling between *Lgr5* and *Olfm4* expression was puzzling as *Olfm4* was described as a robust marker of *Lgr5*-positive ISCs.[25] To clarify this point, we first looked at *Olfm4* expression by *in situ* hybridization. Most crypt bases were devoid of *Olfm4* expression, and consisted of packed lysozyme-positive paneth cells (Figure 2e) suggesting that crypt base columnar (CBC) stem cells were no longer present at the crypt bases in NleVilcKO mice. Introgression of the *Lgr5*$^{GFP\text{-}IRES\text{-}CreERT2}$ allele into Control and NleVilcKO mice confirmed the absence of GFP-positive CBC cells intermingled with paneth cells at the base of *Nle* mutant crypts (Supplementary Figure S1A, white bracket). In mutant crypts, strong GFP expression was observed in *Olfm4*-negative cells located above paneth cells and at positions normally occupied by progenitors suggesting

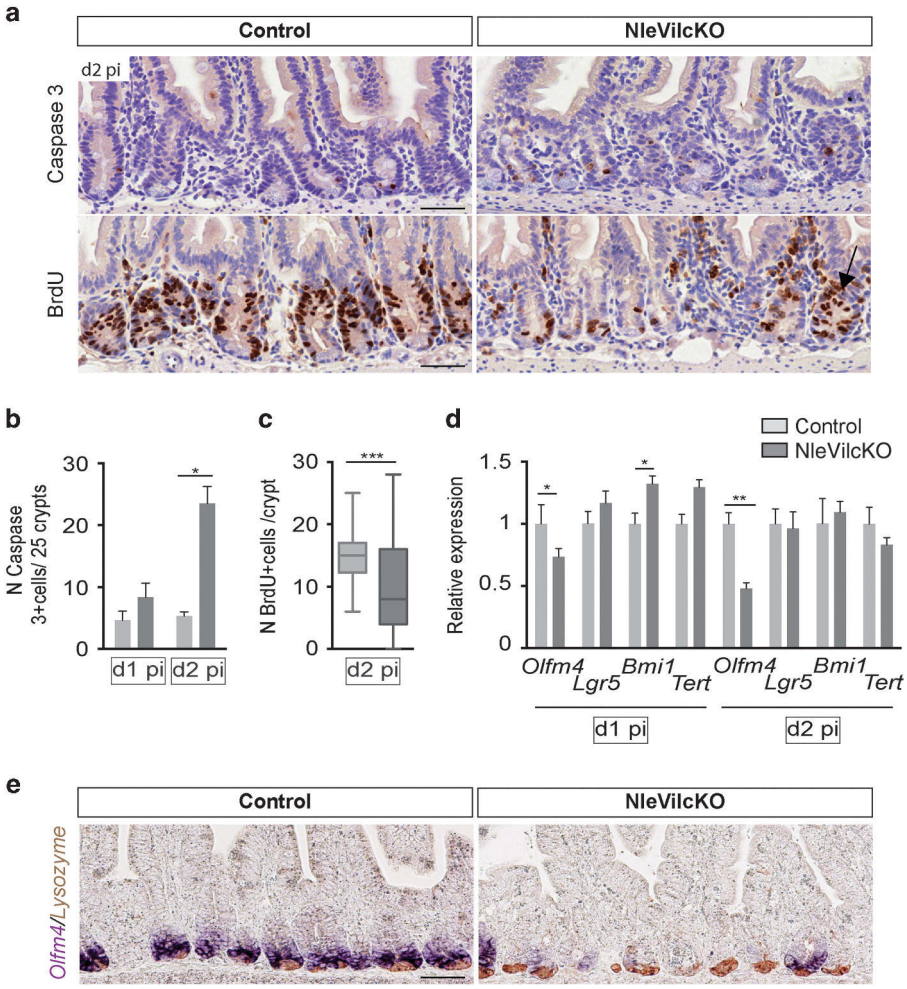

Figure 2 *Nle* deletion is detrimental for ISCs and progenitors. (**a**) Cleaved-Caspase 3 and BrdU immunostaining of intestinal sections from Control and NleVilcKO intestine at day 2 p.i. Rare crypts with normal proliferation profile (arrow) were observed. Scale bars, 50 μm. (**b**) Histogram showing the mean number ($\pm$ S.E.M.) of Caspase 3-positive cells per 25 crypts in Control and NleVilcKO small intestine. Twenty five traverse crypts were scored per mouse, $n=3$ for each genotype. *$P<0.05$, Mann–Whitney Wilcoxon test. (**c**) Box and whiskers plot showing the number of BrdU-positive cells per crypt in Control and mutant NleVilcKO mice. Twenty five traverse crypts were scored per mouse, $n=3$ for each genotype. ***$P<0.001$ *t*-test. (**d**) RT-qPCR performed on mRNA from Control and NleVilcKO intestinal extracts. Graphs represent the mean fold changes $\pm$ S.E.M. for transcripts enriched in ISCs. $n\geq5$ for each genotype. *$P<0.05$ Mann–Whitney Wilcoxon test. (**e**) *In situ* hybridization for *Olfm4* mRNA (blue staining) combined with lysozyme immunostaining (brown staining) on intestinal sections from Control and NleVilcKO intestine. Scale bars, 50 μm

that either CBC stem cells have been displaced from their niche or mutant progenitors maintained high levels of *Lgr5* expression (Supplementary Figure S1A, white bracket, Supplementary Figure S1B, arrow). Altogether, these data suggest that the ISC pool is rapidly compromised following *Nle* deletion.

We next tested the capacity of *Nle*-deficient crypts to form organoids *in vitro*.[26] Cultures were established with crypts from Control and NleVilcKO mice 1 h following the last tamoxifen injection. Control crypts grew into organoids within 3 days of culture, and the vast majority had developed more than 3 buds after 6 days. In contrast, NleVilcKO crypts maintained as small nonbudding units and eventually died (Supplementary Figure S2) confirming that intestinal SC and progenitors are rapidly compromised following *Nle* deletion.

***Nle* deletion increases differentiation toward the goblet cell lineage.** We then analyzed the impact of *Nle* inactivation on the differentiation of the different intestinal cell types. NleVilcKO intestines did not present obvious changes in the size of the villi, suggesting that enterocytic differentiation was not altered. Both alcian blue coloration and MUC2 immunostaining revealed the presence of crypts harboring an excessive number of goblet cells in NleVilcKO intestines at day 3 p.i. (Figure 3a, arrows, Supplementary Figure S3A). In Control mice, crypts with more than five goblet cells were rare (3%) and contained on average six goblet cells. Mutant crypts with numerous goblet cells were more frequent (11%) and contained on average 12 goblet cells (Supplementary Figures S3A and B). Goblet cells were found all along the crypt axis, including at the crypt bottom (Figure 3a, asterisks). Altogether, these results suggest that *Nle*-deficient progenitors underwent premature differentiation. The other secretory cell lineages did not seem affected (Supplementary Figure S3C). Consistent with these results, we measured by RT-qPCR a moderate but significant upregulation of the goblet cell marker *Muc2* in NleVilcKO intestines, whereas *ChromograninA* and *Lysozyme* mRNA levels were unchanged (Figure 3b). We found that the local increase in goblet cell number was preceded by the upregulation of *Atoh1*, a key regulator of secretory cell lineage commitment,[27] and of *Spdef*, which is required downstream of *Atoh1* for goblet cell terminal maturation[28] (Figure 3c). *Hes1* expression was unchanged, confirming that the absorptive lineage was not affected by *Nle* loss of function (Figure 3c).

Altogether, these results demonstrate that *Nle* deficiency rapidly compromises crypts homeostasis by triggering apoptosis, cell cycle exit and premature differentiation into goblet cell lineage of intestinal SCs and progenitors.

Biogenesis of the large ribosomal subunit is affected in *Nle* mutant crypts. To verify that *Nle* deficiency affected biogenesis of the large ribosomal subunit (60S) in the mouse intestine, we first performed fluorescent *in situ* hybridization (FISH) on small intestine sections. *Its1* and *its2* probes were used to evaluate the levels of nucleolar rRNA intermediates of, respectively, the small and large ribosomal subunits (Figure 4a). In Control intestines, although nascent rRNA intermediates were detected in most cells, enriched expression was observed in epithelial cells of the crypts and of the lower part of the villi (Figure 4b). These cells showed a clear upregulation of *its2* signal in NleVilcKO mice at day 1 p.i. (Figure 4b). *Its1* signal was also increased, though to a lesser extent. Increased level of nucleolar rRNA intermediates was also evidenced when performing FISH with a 28S probe (Supplementary Figure S4), and was further confirmed by RT-qPCR on total intestine RNA extracts (Figure 4c). We next monitored the effect of *Nle* deletion on the processing of the different rRNAs intermediates by performing a northern blot experiment on RNAs extracted from Control and NleVilcKO crypts at day 1 p.i. (Figure 4d). Consistent with the role of *Nle* in large subunit maturation, specific accumulation of rRNA precursors of the large subunit was observed in NleVilcKO crypts (Figure 4d, arrows).

Levels of 18S and 28S mature rRNAs were not altered in NleVilcKO crypts at day 1 p.i. (Figure 4c and Supplementary Figure S4) suggesting that large subunit biogenesis defects in *Nle*-deficient progenitors did not cause a rapid reduction in ribosome content. To verify this point, crypt protein extracts were prepared from Control and NleVilcKO mice 10 min after puromycin injection and analyzed by immunoblotting using anti-puromycin monoclonal antibody. Puromycin enters cells and is covalently incorporated into nascent polypeptides allowing the quantification of actively translating ribosomes.[29] At day 2 p.i., when the phenotype is the most severe, no significant change in the quantity of puromycylated nascent chains was detected in NleVilcKO crypts compared with Control (Figure 4e), suggesting that protein translation was not altered at this early time point after *Nle* deletion.

Defects in ribosome biogenesis trigger p53 activation in ISCs and progenitors. A dedicated surveillance pathway tightly links the activity of ribosome biogenesis to p53 levels. We therefore analyzed p53 protein levels in *Nle*-deficient intestine by immunostaining and western blot analysis. We found that p53 was stabilized in NleVilcKO crypts as early as day 1 p.i. (Figures 5a and c). At this time point, nuclear p53 protein could be detected in CBC stem cells, recognizable by their shape and location at the crypt base (Figure 5b). Noticeably, p53 activation was detected neither in villi nor in paneth cells. Consistent with p53 activation, we measured a significant increased expression of several p53 direct transcriptional targets such as the cell cycle inhibitor p21 (Figures 5c and d), and the proapoptotic genes *Bax, Pidd* and *Noxa* (Figure 5d).

To test whether p53 pathway activation was a general feature of ISCs and progenitors response to ribosome biogenesis defects, we treated intestinal organoids with CX-5461, a selective inhibitor of RNA polymerase I-driven rRNA transcription.[30] Incubation of organoids with 1 μM CX-5461 resulted in a rapid reduction in rRNA precursors levels (Figure 6a). After 1 day of treatment, buds size appeared reduced compared with vehicle-treated control organoids (Figure 6b), and after 2 days most treated organoids started to degenerate (not shown). At day 1, CX-5461 treatment resulted in increased mRNA levels of several p53 target genes (Figure 6c) as well as variations in expression of markers of SCs, progenitors and differentiated cells (Figures 6d–f) suggesting that inhibition of rRNA transcription causes p53 activation and affects survival and differentiation

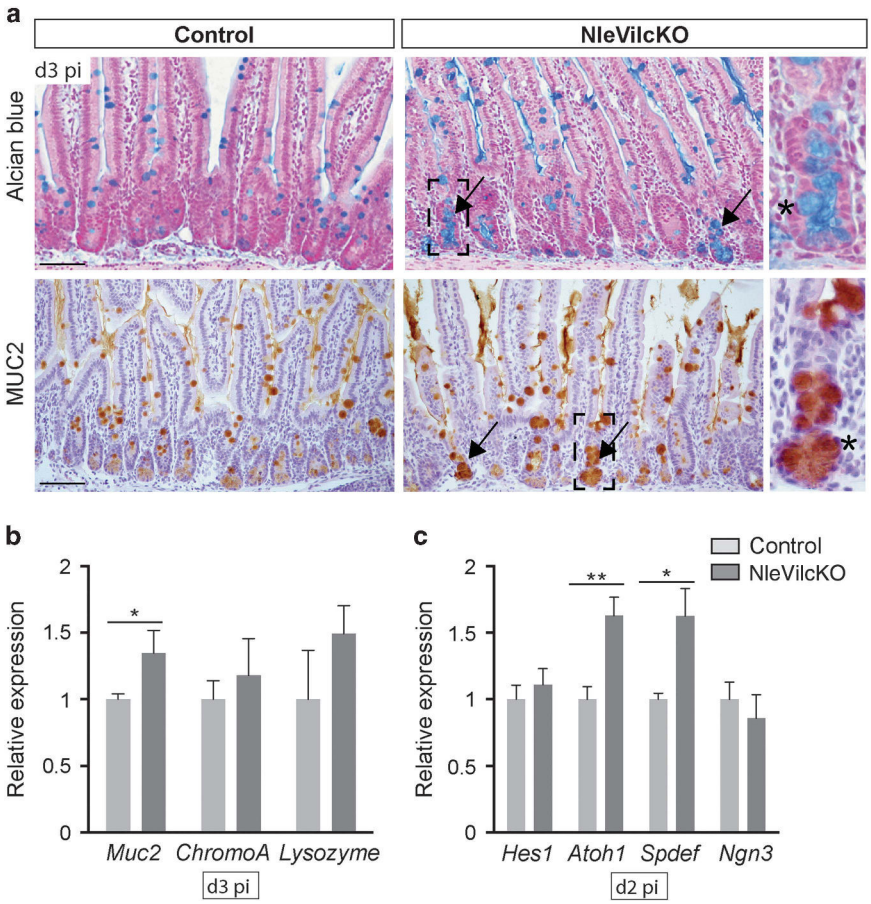

Figure 3 *Nle* deletion leads to biased differentiation toward the goblet lineage. (**a**) Alcian blue staining and MUC2 immunostaining on intestinal sections from Control and NleVilcKO intestine. Black arrows show crypts with elevated number of goblet cells. Third row shows magnified views of framed regions. Asterisks indicate goblet cells ectopically located in the stem cell zone. Scale bars, 50 μm. (**b** and **c**) RT-qPCR performed on mRNA from Control and NleVilcKO intestinal extracts. Graphs represent the mean fold changes $\pm$ S.E.M. for transcripts representative of cells from the different secretory lineages (**b**) or intestinal progenitors (**c**). $n \geq 4$ for each genotype. $^*P < 0.05$ Mann–Whitney Wilcoxon test

of intestinal SC and progenitors *ex vivo*. Although the experimental conditions differed, CX-5461-treated organoids and intestinal epithelium of NleVilcKO mice shared striking similarities including uncoupling in the expression of *Olfm4* and *Lgr5* SC markers and upregulation of *Muc2* goblet cell marker. Interestingly, such variations were not observed when *p53*-deficient organoids were treated with CX-5461 (Figures 6g and k).

Altogether, these results strongly suggest that defects in large ribosomal subunit biogenesis caused by *Nle* deficiency activate a potent p53 response in intestinal SCs and progenitors.

p53 drives the elimination of intestinal SCs and progenitors by cell cycle arrest, apoptosis and directed differentiation toward the goblet cell lineage. To evaluate the contribution of *p53* in the phenotype of *Nle* mutant crypts, we crossed NleVilcKO mice with $p53^{-/-}$ mice. NleVilcKO; p53KO double mutants (*VilCreERT2*$^{tg/0}$; *Nle*$^{flox/null}$; $p53^{-/-}$) were compared with NleVilcKO; p53+/– (*Villin-CreERT2*$^{tg/0}$; *Nle*$^{flox/null}$; $p53^{+/-}$) and Control; p53KO (*Villin-CreERT2*$^{tg/0}$; *Nle*$^{flox/+}$; $p53^{-/-}$) littermates, as well as to wild-type p53 Controls from the previous cross (*Villin-CreERT2*$^{tg/0}$; *Nle*$^{flox/+}$; $p53^{+/+}$). Intestinal phenotype of NleVilcKO; p53+/– mice was similar to that of NleVilcKO mice, including decreased *Olfm4* expression, reduced proliferation and local increase in goblet cell number in the crypts (Figure 7a). Strikingly, both the expression of *Olfm4* at the crypt base and proliferation in the transit-amplifying compartment were restored in NleVilcKO; p53KO crypts, showing that *Nle*-deficient ISCs and progenitors were elimimated via a p53-dependent mechanism (Figures 7a and c). In addition, NleVilcKO; p53KO crypts exhibited a rescued pattern of goblet cell differentiation (Figure 7a). Consistently, *Muc2* expression was significantly reduced in NleVilcKO; p53KO mice compared with NleVilcKO; p53+/– (Figure 7d). We next used *in silico* analysis[31] to identify putative p53 response elements (REs) associated with goblet cell-specific genes. Interestingly, two partially overlapping p53 REs with high scores were found within an intronic sequence of the *Muc2* gene (Figures 7e and f). When this intronic sequence was cloned upstream of a luciferase reporter gene, a strong induction was observed upon cotransfection with a p53 expression vector into *p53*-deficient fibroblasts (Figure 7g). Either deletion of the two REs or use of an expression vector encoding a p53 variant lacking transactivation activity (p53R270H) abolished luciferase reporter induction (Figure 7g).

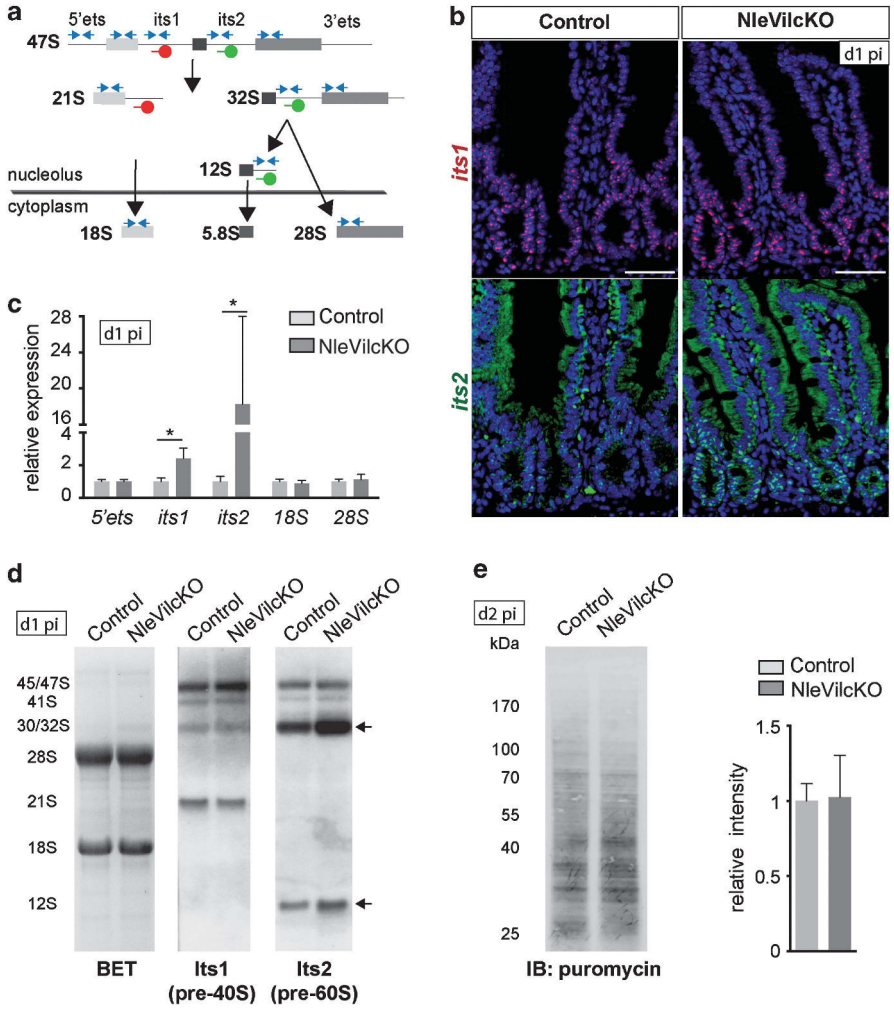

Figure 4 Ribosome biogenesis is impaired in *Nle* mutant crypts. (**a**) Simplified diagram illustrating the main steps of ribosome biogenesis in eukaryotic cells. Blue arrows represent the primers used to measure the levels of ribosomal RNAs by RT-qPCR. FISH probes used to detect its1 (red) and its2 (green) sequences from precursors of the small and large ribosomal subunits, respectively, are indicated. (**b**) FISH for its1 (red) or its2 (green) on intestinal sections from Control and NleVilcKO intestine. Scale bars, 20 μm. (**c**) RT-qPCR performed on mRNA from Control and NleVilcKO intestinal extracts. Graphs represent the mean fold changes $\pm$ S.E.M. for the different amplicons. $n=3$ for each genotype. *$P<0.05$ Mann–Whitney Wilcoxon test. (**d**) Northern blot of RNAs from Control and NleVilcKO crypts at day 1. In the left panel, BET coloration shows the 28S and 18S rRNAs mature species Control and NleVilcKO crypts. Hybridization with probes against the its1 (central panel) or its2 (right panel) shows precursors of the small and large ribosomal subunit, respectively. Black arrows indicate the accumulation of the 32 and 12S precursors of the large ribosomal subunit in NleVilcKO crypts. (**e**) Anti-puromycin immunoblotting of protein extracts for identical number of crypts cells from Control and NleVilcKO intestine at day 2 p.i. Results obtained from two independent experiments are shown. Graphs represent the mean normalized intensity $\pm$ S.E.M. $n=4$ for each genotype. $P>0.05$ Mann–Whitney Wilcoxon test

These data strongly suggest that *Muc2* is a direct p53 target gene and provide insights into the contribution of p53 to the goblet cell differentiation phenotype.

Removal of *Nle*-deficient ISCs persists independently of p53. Presence of the *Nle* recombined allele was monitored by genomic PCR on NleVilcKO; p53KO crypts at different times after tamoxifen injection (Figure 8a). This analysis revealed that the replacement of *Nle*-deficient intestinal epithelium by *Nle*-proficient cells occurred between days 4 and 10 p.i. in a *p53*-deficient background. Therefore, *Nle* mutant ISCs were not maintained even in the absence of p53. We next analyzed cell death in NleVilcKO; p53KO intestine. Interestingly, increased apoptosis was observed in NleVilcKO; p53KO crypts at day 2 p.i. (Figures 8b and c), even though the expression of proapoptotic genes was not induced (Supplementary Figure S5). Contrary to NleVilcKO; p53+/– crypts, Caspase 3-positive cells were found more rarely at the crypt base and more frequently in the upper third of the crypt where progenitors normally exit cell cycle (Figure 8d). In the absence of *p53*, *Nle*-deficient intestinal progenitors seem therefore to progress further along the differentiation pathway before possibly being eliminated through *p53*-independent apoptosis. As *Nle* deficiency does not affect protein synthesis at day 2 p.i. (Figure 4e), defects in protein translation are unlikely to be the primary cause of p53-independent cell death at that time. At day 4 p.i., a diminution, although nonsignificant, in protein synthesis was observed in NleVilcKO; p53KO crypts compared with Control; p53KO (Figure 8e) suggesting that deregulated protein

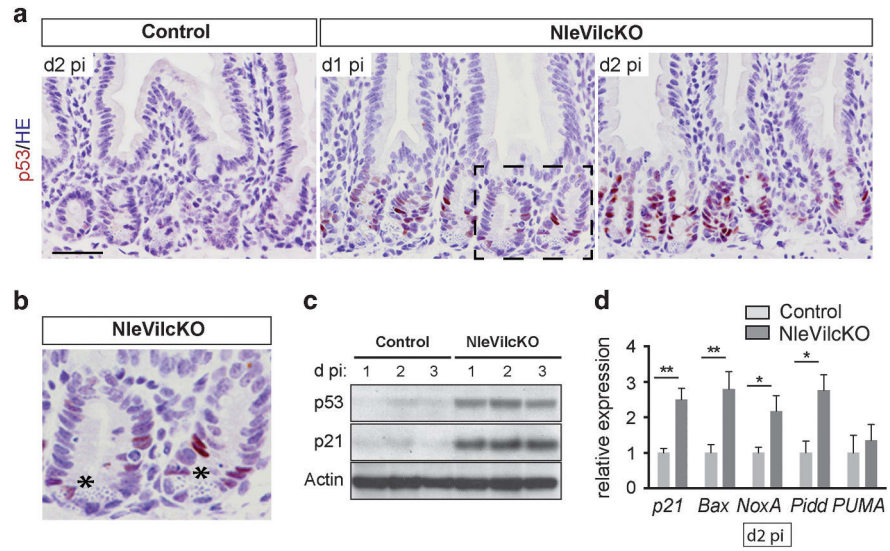

Figure 5 p53 is activated in ISCs and progenitors following *Nle* deletion. (**a** and **b**) p53 immunostaining on intestinal sections from Control and NleVilcKO intestine. Asterisks indicate ISCs with nuclear accumulation of p53. Scale bar, 50 μm. (**b**) Magnified view of the framed region in **a**. (**c**) Western blot for p53, p21 and α-Actin performed on crypts enriched protein extracts from Control and NleVilcKO intestines. (**d**) RT-qPCR performed on mRNA from Control (gray bars) and NleVilcKO (red bars) intestinal extracts. Graphs represent the mean fold changes $\pm$ S.E.M. of the indicated p53 transcriptionnal targets. $n \geq 5$ for each genotype. $^{*}P<0.05$; $^{**}P<0.001$ Mann–Whitney Wilcoxon test

synthesis might also contribute to the elimination of *Nle*-deficient ISCs and progenitors in absence of p53.

Altogether these data show that p53-independent mechanisms also participate in the elimination of mutant ISCs and progenitors.

Discussion

Our data reveal the crucial role of *Nle* in maintaining adult intestinal homeostasis and stem cells. Higher levels of *Nle* and nascent rRNA expression are found in crypts compared with villi, and accordingly, ribosome biogenesis dysfunction consecutive to NLE depletion is restricted to the crypt compartment. In response to ribosome biogenesis defects, p53 is activated in ISCs and progenitors, causing their rapid elimination through cell cycle arrest and apoptosis. In addition to these well-described stress responses, we found that p53 also triggers the premature differentiation of progenitors into goblet cells. Although premature differentiation may represent an efficient way to remove damaged or unfit stem/progenitor cells from active pools, few examples have been documented so far. In response to DNA damage in embryonic stem cells, p53 induces differentiation through direct repression and activation of pluripotency- and differentiation-associated genes respectively.[32] In adult melanocyte and hematopoietic stem cells, premature differentiation in response to genotoxic stress occurs independently of p53.[33,34] *Muc2* expression was upregulated both in NleVilcKO crypts and in CX-5641-treated organoids. Together with the identification of functional p53 response elements within the *Muc2* gene, this indicates that p53 has a direct transcriptional control on the differentiation of intestinal cells toward the goblet cell lineage in response to ribosome biogenesis defects. Interestingly, a previous study reported the transcriptional activation of *MUC2* by p53 in human colon cancer cell lines,[35] suggesting that such mechanism could also be operating in humans. Whether p53 transcriptionally regulates the expression of other genes associated with the goblet cell differentiation program would require further studies. It would also be interesting to determine if p53-dependent differentiation responses are elicited in other organs following ribosome biogenesis defects.

Nle acts in large ribosomal subunit in yeasts,[20,21] fungi,[36] plants[37] and mammals.[23] Contrary to *Drosophila*,[38] *Nle* loss of function does not seem to interfere with the Notch pathway in the mouse hematopoietic[23] and intestinal (this study) lineages. Indeed, although increasing or decreasing Notch activity systematically results in strong variations of *Hes1* expression levels in the intestinal crypt cells,[39–43] *Hes1* mRNA levels were unchanged following *Nle* inactivation in the intestinal epithelium (Figure 3c and data not shown). Interestingly, premature differentiation toward the goblet cell lineage of intestinal stem/progenitor cells is observed when Notch activity is inhibited.[39,41–43] In view of our results, it would therefore be important to determine whether p53 participates in the hypersecretory phenotype of Notch-defective intestinal epithelium.

This work also unravels the existence of p53-independent responses to ribosomal stress in the intestine including progenitors apoptosis and ISCs disappearance. In human cancer cell lines, p53-independent mechanisms linking ribosome biogenesis defects to cell cycle arrest have been reported.[44,45] Interestingly, binding of RPL11 to MDM2 was shown to inhibit its E2F1-stabilizing activity, thereby hindering cell cycle progression.[44] Increased binding of RPL11 to MDM2 consecutive to ribosome biogenesis dysfunction could therefore potentially interfere with other p53-independent functions of MDM2 such as inhibition of apoptosis.[46–48] So far, such functions has been described in cell lines and it will be interesting in future studies to evaluate their contribution to the phenotype of NleVilcKO; p53KO mice.

Besides the activation of p53-dependent and independent checkpoints, defective ribosome biogenesis is likely to confer Nle-deficient ISCs/progenitors with a cell proliferation

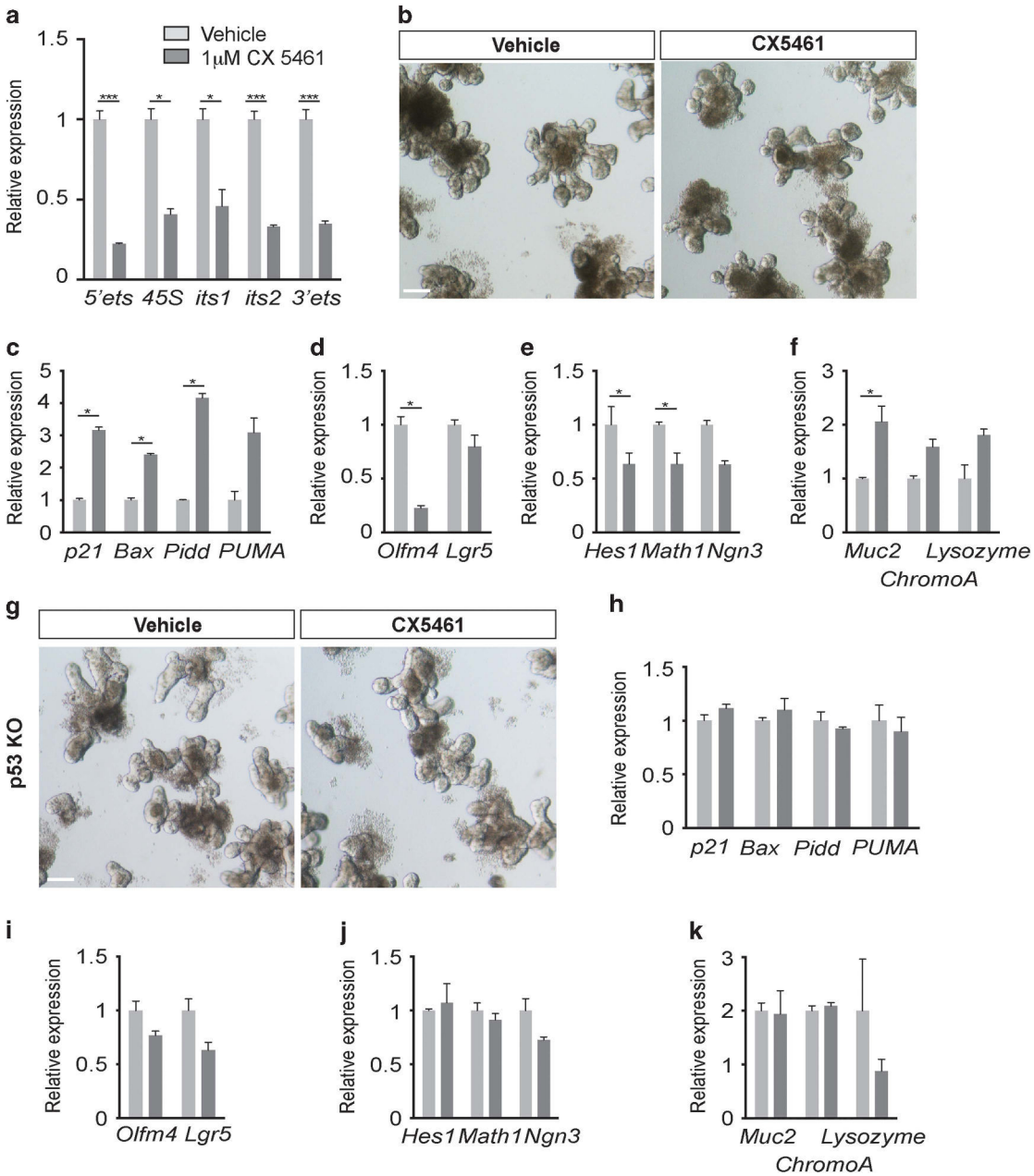

Figure 6 Incubation of intestinal organoids with the rRNA polymerase I inhibitor CX-5461 recapitulates the NleVilcKO phenotypes. (**a**) RT-qPCR performed on mRNA from vehicle or CX-5461 treated organoids after 1 h incubation. Graphs represent the mean fold changes ± S.E.M. for rRNA precursors. $n = 3$ for each condition. $^{*}P < 0.05$; $^{***}P < 0.0001$ multiple Student test with the Holm–Sidak correction method. (**b** and **g**) Pictures of organoids obtained from WT (**b**) or *P53* KO mice (**g**), after 1 day incubation with vehicle or CX-5461. Scale bars, 20 μm. (**c**–**f**) and (**h**–**j**), RT-qPCR performed on mRNA from vehicle or CX-5461 treated organoids 1 day after addition of vehicle or CX-5461. Expression levels of p53 effectors, and markers of CBCs, progenitors and differentiated intestinal cells are shown. Graphs represent the mean fold changes ± S.E.M. $n \geq 3$ for each condition. $^{*}P < 0.05$ Mann–Whitney Wilcoxon test

disadvantage due to decreased ribosome content and reduced rate of translation. Indeed, the reduced levels of RPL5 or RPL11 in human lung fibroblasts was recently shown to reduce their translational capacity and impede their proliferation.[49] A similar mechanism was proposed to account for the delayed larval development and reduced body size of *Drosophila* minute mutants harboring hypomorphic mutations in ribosomal proteins.[50] When surrounded by wild-type cells, minute clones are outcompeted and disappear (for review, see Amoyel and Bach[51]). Thus, such cell competition phenomena might also contribute to the replacement of *Nle*-deficient crypt cells by cells that have escaped recombination. Another possibility is that reduced ribosome biogenesis would alter the self-renewal of *Nle*-deficient ISCs. Support from this hypothesis comes from the recent demonstration that modulation of ribosome DNA transcription and ribosome biogenesis is directly influencing the self-renewal properties of *Drosophila* germ stem cells.[52]

Ribosome production is increased in cancer cells and deregulation of ribosome biogenesis is associated with increased risks of developing cancer.[53,54] In human colorectal

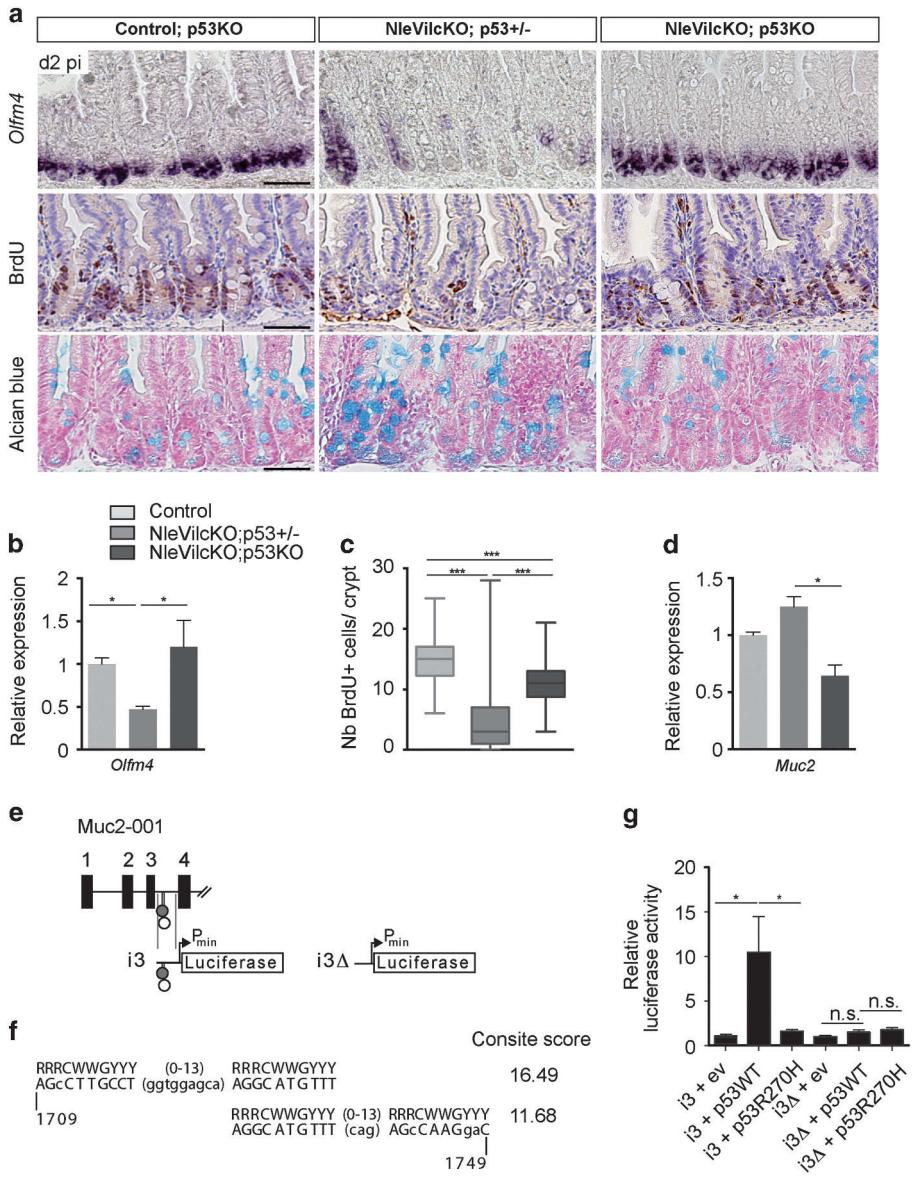

Figure 7 Cell cycle exit and differentiation of intestinal SCs and progenitors toward the goblet cell lineage depend on p53. (**a**) *Olfm4 in situ* hybridization, BrdU immunostaining and alcian blue staining on sections of Control; p53KO, NleVilcKO; p53+/− and NleVilcKO; p53KO intestines. (**b** and **c**) Histogram showing *Olfm4* mRNA levels and mean number ± S.E.M. of BrdU-positive cells per crypt in Control; p53KO, NleVilcKO; p53+/− and NleVilcKO; p53KO small intestine. $n = 4$ for each genotype. (**d**) RT-qPCR performed on mRNA from Control, NleVilcKO; p53+/− and NleVilcKO; p53KO intestines at day 2 p.i. showing the level of *Muc2* expression. Graphs represent the mean fold changes ± S.E.M. $n \geq 3$ for each genotype. (**e**) Partial map of the *Muc2* gene corresponding to the 5' region of the *Muc2-001* Ensembl transcript and showing the putative p53 REs (lollipops) within intron 3. The maps of Luciferase reporter plasmids are shown, with plasmid i3 containing WT sequences from *Muc2* intron 3, plasmid i3 Δ containing the intron 3 deleted for both p53 REs. (**f**) DNA sequences of the partially overlapping p53 REs identified within *Muc2* intron 3. On top, the consensus sequence for a p53 RE is shown, with two p53-binding half-sites separated by 0–13 nucleotides. The p53 REs are shown, with putative half-sites having 0–3 mismatches with the consensus (matches in capital letters and mismatches in lowercase). Numbers are relative to the transcription start site. (**g**) Luciferase reporter assay. The i3 or i3Δ plasmid were transfected in $p53^{-/-}$ MEFs together with an empty vector (ev), an expression vector encoding WT p53 (p53WT) or mutant p53 (p53R270H). The graph shows luciferase activity normalized to the control renilla luciferase. Three independent experiments were plotted. *$P < 0.05$ Student's *t*-test

cancer, increase in the levels of many ribosomal proteins was reported and the expression patterns of specific RPs were associated with tumor differentiation, progression or metastasis status.[55] Furthermore, a germline mutation in the *Rps20* gene was recently shown to cause hereditary nonpolyposis colorectal carcinoma predisposition.[53] Finally, in patients with ulcerative colitis, IL-6-mediated stimulation of ribosome biogenesis and subsequent decrease in p53 levels were recently proposed as a possible mechanism favoring cancer progression in colonic mucosa exposed to chronic inflammation.[56] Future investigations using the NleVilcKO model will help to obtain a deeper understanding on the mechanisms that link ribosomes biogenesis to intestinal cancer.

Materials and methods

Mice. Experiments on mice were conducted according to the French and European regulations on care and protection of laboratory animals (EC Directive 86/609, French Law 2001-486 issued on 6 June 2001) and the National Institutes of

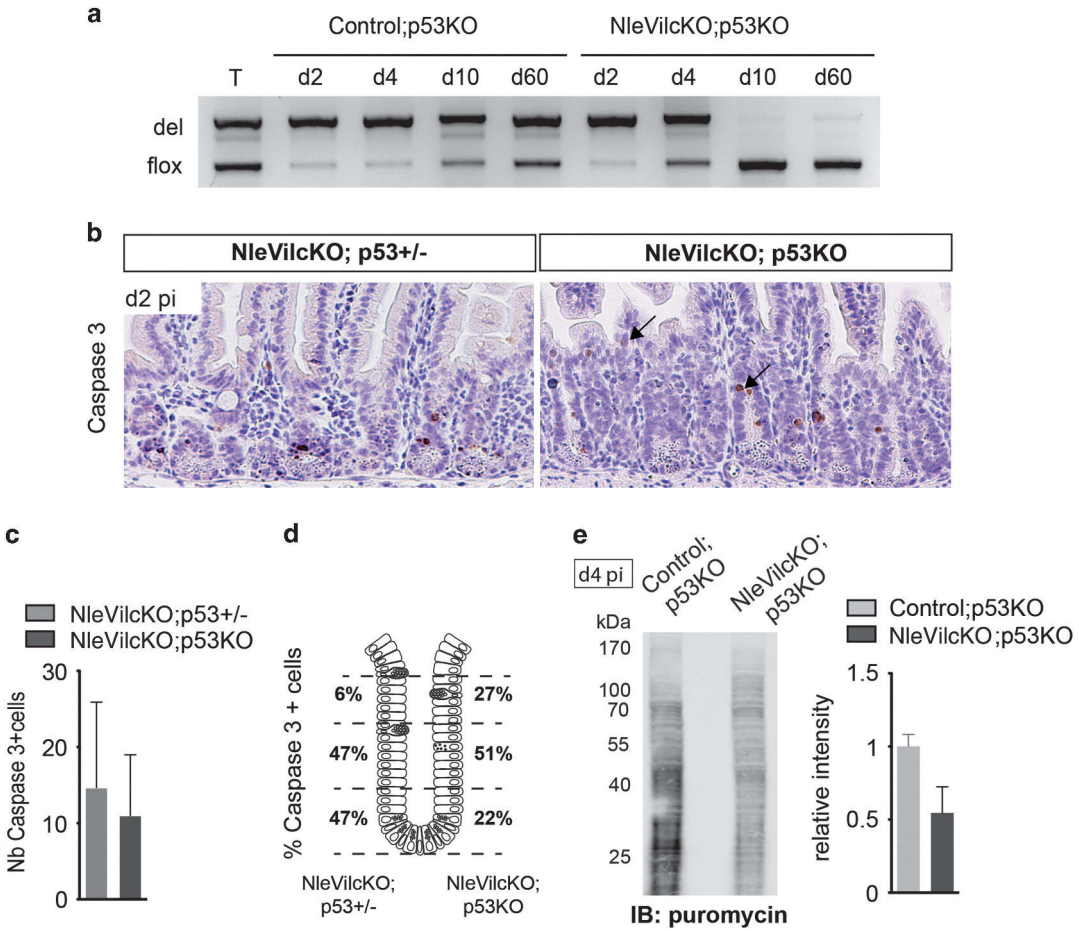

Figure 8 p53-independent elimination of *Nle* mutant intestinal SCs and progenitors. (**a**) Detection of the nonrecombined (flox) and recombined (del) *Nle* alleles by genomic PCR performed on crypts (c) or villi (v) enriched DNA extracts from Control; p53KO and NleVilcKO; p53KO intestines. (**b**) Caspase 3 immunostaining on sections of NleVilcKO; p53+/ − and NleVilcKO; p53KO intestines. Arrows show apoptotic cells located in the upper crypt region. Scale bars, 50 μm. (**c**) Histogram showing the mean number (± S.E.M.) of Caspase 3-positive cells per crypt in NleVilcKO; p53+/ − and NleVilcKO; p53KO small intestine. $n = 3$ for each genotype. (**d**) Diagram representing the percentage of Caspase 3-positive cells found in the lower, middle and upper thirds of the crypts in NleVilcKO; p53+/ − and NleVilcKO; p53KO small intestine. (**e**) Anti-puromycin immunoblotting of protein extracts for identical number of crypts cells from Control; p53KO and NleVilcKO; p53KO intestine at day 4 p.i. Graphs represent the mean normalized intensity ± S.E.M. $n = 3$ for each genotype

Health Animal Welfare (Insurance #A5476-01 issued on 02/07/2007). The alleles used were as follows: *Nle*^{flox},[23] *Nle*^{null},[24] *Villin-CreERT2*,[57] *Lgr5*$^{GFP\text{-}IRES\text{-}CreERT2}$,[58] *p53*$^{-}$.[59] To generate Control and NleVilcKO mice, *Villin-CreERT2*$^{tg/tg}$; *Nle*$^{flox/flox}$ mice were crossed to *Nle*$^{null/+}$ mice. Mice at 5 to 6 weeks of age were injected intraperitoneally with 75 mg/kg tamoxifen for three consecutive days. For proliferation assays, mice were injected with BrdU (100 mg/kg) 2.5 h before killing.

Tissue extracts. For paraffin sections, the intestinal tract was dissected, flushed twice with ice-cold PBS to remove any fecal content and perfused with ice-cold 4% paraformaldehyde (PFA). The small intestine was rolled up from the proximal to the distal end in concentric circles, fixed in 4% PFA at 4 °C overnight, dehydrated, and embedded in paraffin wax. For RT-qPCR on total intestine, 1 cm of duodenum was harvested in 1 ml Trizol (Invitrogen, Carlsbad, CA, USA). For crypts and villi isolation, 5–10 cm of jejunum were collected, opened longitudinally and processed as previously described.[60]

Histology and immunostaining. Histology and immunostaining were performed as described previously.[61] Specific antibodies binding was detected using either biotinylated secondary antibodies and Streptavidin/HRP complexes (Dako, Glostrup, Denmark), or ImmPRESS-HRP (Vector Laboratories, Burlingame, CA, USA). Bright field microscopy was performed using a Zeiss Axiophot microscope, or a MiraxScan device (Carl Zeiss microImaging, Goettingen, Germany) equipped with a 20× objective lens. The system was set to run in automated batch mode with automated focus and tissue finding. For immunofluorescence staining, sections were mounted in vectashield and images were acquired with an upright microscope Zeiss Axiovert 200 M with a Zeiss apotome system controlled by the Zeiss axiovision 4.4 software. Primary and secondary antibodies used in this study are listed in Supplementary material Supplementary Table S2.

***In situ* hybridization.** Digoxigenin-labeled *Olfm4* antisense probe was synthesized from a plasmid containing *Olfm4* cDNA (Gift from B Romagnolo, Cochin Institute, Paris) using T7 RNA polymerase and Dig labeling kit (Roche Diagnostics, Basel, Switzerland). Paraffin sections (8 μm) were rehydrated and treated with 15 μg/ml Proteinase K for 15 min. Proteinase K was inactivated with a 1 min wash in 0.2% Glycin in PBS-Tween. Sections were postfixed in 4% PFA for 10 min and washed several times in PBS-0.1% tween. Prehybridization was carried out for 1 h at 65 °C in 50% deionized formamide, 2× sodium saline citrate (SSC), 50 µg/ml yeast tRNA and 50 μg/ml Heparin. Hybridization was performed overnight at 65 °C with the riboprobe diluted in prehybridization mix, and was followed by washes in 50% formamide/2× SSC at 65 °C for 1 h. Sections were washed for an additional hour in maleate buffer (100 mM maleic acid, 150 mM NaCl, 0,1% tween) at room temperature, and incubated for 1.5 h with the anti-digoxigenin alkaline phosphatase-conjugated antibody (dilution, 1 : 500, in Blocking Buffer, Roche Diagnostics). Sections were then washed in maleate buffer before incubation with the chromogenic substrates of alkaline phosphatase, 5-bromo-4-chloro-3-indolyl-

phosphate (0.175 mg/ml) and NBT (0.337 mg/ml) (Roche Diagnostics), in 100 mM Tris (pH 9.5), 100 mM NaCl, and 50 mM $MgCl_2$ at room temperature.

For fluorescent *in situ* hybridization, the hybridization step was performed as previously described.[62] Conjugated FISH probes were purchased from Eurogentec: its1-Cy5: tagacacggaagagccggacgggaaaga; its2-Cy3: gcgattgatcgtcaaccgacgctc; 28S-Alexa488: cccgttcccttggctgtggtttcgctggata; 18S-Cy5: tttacttcctctagatagtcaagttc gacc and validated in a previous study.[23]

Crypts culture. Isolated crypts were cultured as previously described.[26] In brief, 450 crypts were embedded in growth factor reduced matrigel (Corning LifeSciences, Tewksbury, MA, USA) and plated in 24-wells plates with culture medium (Advanced DMEM/F12; Invitrogen) containing EGF (Peprotech, Rocky Hill, NJ, USA); R-spondin 1 (R&D Systems, Minneapolis, MN, USA); and noggin (Peprotech); and supplemented with N2 and B27 (Invitrogen). The medium was exchanged every 4 days. For CX-5461 treatment, organoids were cultured for 4 days, and new culture medium containing 1 μM CX-5461 (Axon Medchem, Groningen, The Netherlands) diluted in 0,1M citrate. 0,1 M citrate only was added as a vehicle control.

RT-qPCR. For total RNAs extraction, intestinal samples were homogenized in Trizol containing 0.4 g of glass beads (212–300 µm ø, Sigma, St. Louis, MO, USA) for 40 s in a FastPrep Instrument (MP Biochemicals, Illkirch, France). To extract their RNAs, organoids were recovered from Matrigel and processed following the mRNeasy mini kit procedure (Qiagen Sciences, Germantown, MD, USA). Reverse-transcription was performed using the Superscript II kit (Invitrogen) according to the manufacturers' instructions. Real-time PCR was carried on using custom-designed primers (Supplementary Table S1) and SYBR green PCR master mix (Applied Biosystem, Foster city, CA, USA) on a StepOne instrument (StepOne software version 2.2; Applied Biosystems). Expression levels were normalized using *TBP*, *Aldolase* and/or *Rrm2* as reference genes.

Western blot. Proteins were extracted in a urea buffer supplemented with antiproteases (Roche Diagnostics) and 1 mM DTT. Extracts were sonicated 5 min and treated with Benzonase (Sigma) to get rid of DNA contaminants. The protein content was determined using a Bradford assay. Proteins were denatured in Laemmli buffer at 95 °C for 10 min before being loaded on a 10% polyacrylamide gel. After migration, proteins were transferred onto a nitrocellulose membrane (Biorad, Hercules, CA, USA) and incubated overnight at 4 °C with the primary antibodies. Membranes were incubated with peroxidase labeled secondary antibodies at RT for 45 min, rinsed in PBS. Signals were visualized using ECl (Pierce Biotechnology, Rockford, IL, USA) and quantified on a Typhoon Instrument. Primary and secondary antibodies used in these experiments are listed in supplementary material Supplementary Table S2.

Quantification of protein synthesis. Mice were injected intraperitoneally with 1 mg of puromycin in PBS, 10 min before killing. Intestines were rapidly harvested in ice-cold PBS containing emetine to block puromycin incorporation during the procedure. Crypts were isolated as described previously, and dissociated into single cells. Single cells were counted on a hemocytometer before being lysed in protein extraction buffer. Puromycilated peptide chains were quantified on a western blot against puromycin by measuring the pixel intensity through the whole length of each lane using typhoon instrument.

Northern blot. Total RNA from crypts cells was prepared with TRIzol reagent following the supplier's instructions (Sigma). Migration and hybridization were performed as previously described.[63] The probes used in this study were Its1-1a (5′-ACGCCGCCGCTCCTCCACAGTCTCCCGTT-3′) and Its2-2 (5′-ACTGGTGAGG CAGCGGTCCGGGAGGCGCCGACG-3′).

***In silico* search for putative p53 response elements.** To identify putative p53 REs, we used the Consite software (http://consite.genereg.net/) with a positional frequency matrix for p53 response elements modified to take varying spacer lengths (0–13 bp) into account. With this method, p53 REs from known p53 target genes were previously found to have a mean value (M) of 11.7, with a S.D. of 1.2. Putative REs were plotted against the map as lollipops, with greytones according to their score: white for scores between 10.5 and 12.9 (M ± S.D.) and black for scores > 15.3 (M+3S.D.).

Luciferase expression assays. To construct the p53 RE reporter plasmids, we cloned intronic sequences upstream of a SV40 minimal promoter before the firefly luciferase gene. For each experiment, 10^6 exponentially growing $p53^{-/-}$ mouse embryonic fibroblasts were nucleofected using the Lonza MEF2 nucleofector kit with 3 μg of a p53 RE-firefly luciferase reporter plasmid (i3 or i3Δ) and 3 μg of an empty expression plasmid, 3 μg of the same reporter plasmid and 3 μg of a WT p53 expression plasmid or 3 μg of the same reporter plasmid and 3 μg of a $p53^{R270H}$ expression plasmid. For all points, data were normalized by adding 30 ng of renilla luciferase expression plasmid (pGL4.73, Promega, San Luis Obispo, CA, USA). Nucleofected cells were allowed to grow for 24 h, then trypsinized, resuspended in 75 μl culture medium and transferred into a well of an optical 96 well plate (Nunc, ThermoFisherScientific, Rugby, UK). The dual-glo luciferase assay system (Promega) was used according to the manufacturer's protocol to lyse the cells and read firefly and renilla luciferase signals.

Statistical analysis. Graphs were performed using Prism5 software (GraphPad Software, La Jolla, CA, USA). For mean comparisons, all bar graphs with pooled data show means ± S.E.M. Statistical analyses were performed using the Mann–Whitney Wilcoxon test or the Student's *t*-test. $P < 0.05$ was considered significant.

Conflict of Interest

The authors declare no conflict of interest.

Acknowledgements. We are grateful to the members of the histopathology unit and of B Romagnolo's team and to A David and S El Messaoudi-Aubert for technical help and advices. We thank P Sansonetti for the *Lgr5*$^{CreERT2\text{-}IRES\text{-}Gfp}$ mouse line, B Romagnolo for the *Olfm4 in situ* probe and B Gayraud-Morel, L Le Cam, JC Marine for providing reagents. We thank B Romagnolo, P Jay and J Artus for critical reading of the manuscript, and all members of the GIstem consortium, S Tajbakhsh's lab and the Mouse Functional Genetics unit for helpful discussions. Imaging was performed at the Imagopole and the histopathology Unit from Institut Pasteur. This work was supported by the Institut National du Cancer (INCa 2007-1-COL-6-IC-1 and PLBIO09-070), the Institut Pasteur, the Centre National de la Recherche Scientifique, the Agence Nationale de la Recherche (ANR-10-LABX-73-01 REVIVE) and the Fondation ARC (Programme labellisé 2014). AS received support from the Fondation des Treilles.

1. Fromont-Racine M, Senger B, Saveanu C, Fasiolo F. Ribosome assembly in eukaryotes. *Gene* 2003; **313**: 17–42.
2. Wild T, Horvath P, Wyler E, Widmann B, Badertscher L, Zemp I *et al.* A protein inventory of human ribosome biogenesis reveals an essential function of exportin 5 in 60S subunit export. *PLoS Biol* 2010; **8**: e1000522.
3. Sloan KE, Mattijssen S, Lebaron S, Tollervey D, Pruijn GJM, Watkins NJ. Both endonucleolytic and exonucleolytic cleavage mediate ITS1 removal during human ribosomal RNA processing. *J Cell Biol* 2013; **200**: 577–588.
4. Carron C, O'Donohue M-F, Choesmel V, Faubladier M, Gleizes P-E. Analysis of two human pre-ribosomal factors, bystin and hTsr1, highlights differences in evolution of ribosome biogenesis between yeast and mammals. *Nucleic Acids Res* 2011; **39**: 280–291.
5. Tafforeau L, Zorbas C, Langhendries J-L, Mullineux S-T, Stamatopoulou V, Mullier R *et al.* The complexity of human ribosome biogenesis revealed by systematic nucleolar screening of Pre-rRNA processing factors. *Mol Cell* 2013; **51**: 539–551.
6. Donati G, Peddigari S, Mercer CA, Thomas G. 5S ribosomal RNA is an essential component of a nascent ribosomal precursor complex that regulates the Hdm2-p53 checkpoint. *Cell Rep* 2013; **4**: 87–98.
7. Zhang Y, Wolf GW, Bhat K, Jin A, Allio T, Burkhart WA *et al.* Ribosomal protein L11 negatively regulates oncoprotein MDM2 and mediates a p53-dependent ribosomal-stress checkpoint pathway. *Mol Cell Biol* 2003; **23**: 8902–8912.
8. Fumagalli S, Ivanenkov VV, Teng T, Thomas G. Suprainduction of p53 by disruption of 40S and 60S ribosome biogenesis leads to the activation of a novel G2/M checkpoint. *Genes Dev* 2012; **26**: 1028–1040.
9. Armistead J, Triggs-Raine B. Diverse diseases from a ubiquitous process: the ribosomopathy paradox. *FEBS Lett* 2014; **588**: 1491–1500.
10. Narla A, Ebert BL. Ribosomopathies: human disorders of ribosome dysfunction. *Blood* 2010; **115**: 3196–3205.
11. McGowan KA, Li JZ, Park CY, Beaudry V, Tabor HK, Sabnis AJ *et al.* Ribosomal mutations cause p53-mediated dark skin and pleiotropic effects. *Nat Genet* 2008; **40**: 963–970.
12. Dutt S, Narla A, Lin K, Mullally A, Abayasekara N, Megerdichian C *et al.* Haploinsufficiency for ribosomal protein genes causes selective activation of p53 in human erythroid progenitor cells. *Blood* 2011; **117**: 2567–2576.

13. Stadanlick JE, Zhang Z, Lee S-Y, Hemann M, Biery M, Carleton MO *et al.* Developmental arrest of T cells in Rpl22-deficient mice is dependent upon multiple p53 effectors. *J Immunol* 2011; **187**: 664–675.
14. McGowan KA, Pang WW, Bhardwaj R, Perez MG, Pluvinage JV, Glader BE *et al.* Reduced ribosomal protein gene dosage and p53 activation in low-risk myelodysplastic syndrome. *Blood* 2011; **118**: 3622–3633.
15. Pereboom TC, van Weele LJ, Bondt A, MacInnes AW. A zebrafish model of dyskeratosis congenita reveals hematopoietic stem cell formation failure resulting from ribosomal protein-mediated p53 stabilization. *Blood* 2011; **118**: 5458–5465.
16. Jaako P, Flygare J, Olsson K, Quere R, Ehinger M, Henson A *et al.* Mice with ribosomal protein S19 deficiency develop bone marrow failure and symptoms like patients with Diamond-Blackfan anemia. *Blood* 2011; **118**: 6087–6096.
17. Torihara H, Uechi T, Chakraborty A, Shinya M, Sakai N, Kenmochi N. Erythropoiesis failure due to RPS19 deficiency is independent of an activated Tp53 response in a zebrafish model of Diamond-Blackfan anaemia. *Br J Haematol* 2011; **152**: 648–654.
18. Provost E, Wehner KA, Zhong X, Ashar F, Nguyen E, Green R *et al.* Ribosomal biogenesis genes play an essential and p53-independent role in zebrafish pancreas development. *Development* 2012; **139**: 3232–3241.
19. Yadav GV, Chakraborty A, Uechi T, Kenmochi N. Ribosomal protein deficiency causes Tp53-independent erythropoiesis failure in zebrafish. *Int J Biochem Cell Biol* 2014; **49**: 1–7.
20. la Cruz de J, Sanz-Martínez E, Remacha M. The essential WD-repeat protein Rsa4p is required for rRNA processing and intra-nuclear transport of 60S ribosomal subunits. *Nucleic Acids Res* 2005; **33**: 5728–5739.
21. Ulbrich C, Diepholz M, Baszligler J, Kressler D, Pertschy B, Galani K *et al.* Mechanochemical Removal of Ribosome Biogenesis Factors from Nascent 60S Ribosomal Subunits. *Cell* 2009; **138**: 911–922.
22. Matsuo Y, Granneman S, Thoms M, Manikas R-G, Tollervey D, Hurt E. Coupled GTPase and remodelling ATPase activities form a checkpoint for ribosome export. *Nature* 2014; **505**: 112–116.
23. Le Bouteiller M, Souilhol C, Cormier S, Stedman A, Burlen-Defranoux O, Vandormael-Pournin S *et al.* Notchless-dependent ribosome synthesis is required for the maintenance of adult hematopoietic stem cells. *J Exp Med* 2013; **210**: 2351–2369.
24. Cormier S, Le Bras S, Souilhol C, Vandormael-Pournin S, Durand B, Babinet C *et al.* The murine ortholog of notchless, a direct regulator of the notch pathway in Drosophila melanogaster, is essential for survival of inner cell mass cells. *Mol Cell Biol* 2006; **26**: 3541–3549.
25. van der Flier LG, van Gijn ME, Hatzis P, Kujala P, Haegebarth A, Stange DE *et al.* Transcription factor achaete scute-like 2 controls intestinal stem cell fate. *Cell* 2009; **136**: 903–912.
26. Sato T, Vries RG, Snippert HJ, van de Wetering M, Barker N, Stange DE *et al.* Single Lgr5 stem cells build crypt-villus structures *in vitro* without a mesenchymal niche. *Nature* 2009; **459**: 262–265.
27. Yang Q, Bermingham NA, Finegold MJ, Zoghbi HY. Requirement of Math1 for secretory cell lineage commitment in the mouse intestine. *Science* 2001; **294**: 2155–2158.
28. Noah TK, Donahue B, Shroyer NF. Intestinal development and differentiation. *Exp Cell Res* 2011; **317**: 2702–2710.
29. David A, Dolan BP, Hickman HD, Knowlton JJ, Clavarino G, Pierre P *et al.* Nuclear translation visualized by ribosome-bound nascent chain puromycylation. *J Cell Biol* 2012; **197**: 45–57.
30. Drygin D, Lin A, Bliesath J, Ho CB, O'Brien SE, Proffitt C *et al.* Targeting RNA polymerase I with an oral small molecule CX-5461 inhibits ribosomal RNA synthesis and solid tumor growth. *Cancer Res* 2011; **71**: 1418–1430.
31. Simeonova I, Lejour V, Bardot B, Bouarich-Bourimi R, Morin A, Fang M *et al.* Fuzzy tandem repeats containing p53 response elements may define species-specific p53 target genes. *PLoS Genet* 2012; **8**: e1002731.
32. Li M, He Y, Dubois W, Wu X, Shi J, Huang J. Distinct regulatory mechanisms and functions for p53-activated and p53-repressed DNA damage response genes in embryonic stem cells. *Mol Cell* 2012; **46**: 30–42.
33. Inomata K, Aoto T, Binh NT, Okamoto N, Tanimura S, Wakayama T *et al.* Genotoxic stress abrogates renewal of melanocyte stem cells by triggering their differentiation. *Cell* 2009; **137**: 1088–1099.
34. Wang J, Sun Q, Morita Y, Jiang H, Groß A, Lechel A *et al.* A differentiation checkpoint limits hematopoietic stem cell self-renewal in response to DNA damage. *Cell* 2012; **148**: 1001–1014.
35. Ookawa K, Kudo T, Aizawa S, Saito H, Tsuchida S. Transcriptional activation of the *MUC2* gene by p53. *J Biol Chem* 2002; **277**: 48270–48275.
36. Baßler J, Paternoga H, Holdermann I, Thoms M, Granneman S, Barrio-Garcia C *et al.* A network of assembly factors is involved in remodeling rRNA elements during preribosome maturation. *J Cell Biol* 2014; **207**: 481–498.
37. Chantha S-C, Matton DP. Underexpression of the plant NOTCHLESS gene, encoding a WD-repeat protein, causes pleitropic phenotype during plant development. *Planta* 2007; **225**: 1107–1120.
38. Royet J, Bouwmeester T, Cohen SM. Notchless encodes a novel WD40-repeat-containing protein that modulates Notch signaling activity. *EMBO J* 1998; **17**: 7351–7360.
39. van Es JH, van Gijn ME, Riccio O, van den Born M, Vooijs M, Begthel H *et al.* Notch/gamma-secretase inhibition turns proliferative cells in intestinal crypts and adenomas into goblet cells. *Nature* 2005; **435**: 959–963.
40. Fre S, Huyghe M, Mourikis P, Robine S, Louvard D, Artavanis-Tsakonas S. Notch signals control the fate of immature progenitor cells in the intestine. *Nature* 2005; **435**: 964–968.
41. Riccio O, van Gijn ME, Bezdek AC, Pellegrinet L, van Es JH, Zimber-Strobl U *et al.* Loss of intestinal crypt progenitor cells owing to inactivation of both Notch1 and Notch2 is accompanied by derepression of CDK inhibitors p27Kip1 and p57Kip2. *EMBO Rep* 2008; **9**: 377–383.
42. Guilmeau S, Flandez M, Bancroft L, Sellers RS, Tear B, Stanley P *et al.* Intestinal deletion of Pofut1 in the mouse inactivates notch signaling and causes enterocolitis. *Gastroenterology* 2008; **135**: 849–860 : 860.e1–6.
43. Pellegrinet L, Rodilla V, Liu Z, Chen S, Koch U, Espinosa L *et al.* Dll1- and dll4-mediated notch signaling are required for homeostasis of intestinal stem cells. *Gastroenterology* 2011; **140**: 1230–1240.e1–7.
44. Donati G, Brighenti E, Vici M, Mazzini G, Treré D, Montanaro L *et al.* Selective inhibition of rRNA transcription downregulates E2F-1: a new p53-independent mechanism linking cell growth to cell proliferation. *J Cell Sci.* 2011; **124**: 3017–3028.
45. Iadevaia V, Caldarola S, Biondini L, Gismondi A, Karlsson S, Dianzani I *et al.* PIM1 kinase is destabilized by ribosomal stress causing inhibition of cell cycle progression. *Oncogene* 2010; **29**: 5490–5499.
46. Kurokawa M, Kim J, Geradts J, Matsuura K, Liu L, Ran X *et al.* A network of substrates of the E3 ubiquitin ligases MDM2 and HUWE1 control apoptosis independently of p53. *Sci Signal* 2013; **6**: ra32.
47. Gu L, Zhu N, Zhang H, Durden DL, Feng Y, Zhou M. Regulation of XIAP translation and induction by MDM2 following irradiation. *Cancer Cell* 2009; **15**: 363–375.
48. Yang J-Y, Zong CS, Xia W, Yamaguchi H, Ding Q, Xie X *et al.* ERK promotes tumorigenesis by inhibiting FOXO3a via MDM2-mediated degradation. *Nat Cell Biol* 2008; **10**: 138–148.
49. Teng T, Mercer CA, Hexley P, Thomas G, Fumagalli S. Loss of tumor suppressor RPL5/RPL11 does not induce cell cycle arrest but impedes proliferation due to reduced ribosome content and translation capacity. *Mol Cell Biol* 2013; **33**: 4660–4671.
50. Morata G, Ripoll P. Minutes: mutants of drosophila autonomously affecting cell division rate. *Dev Biol* 1975; **42**: 211–221.
51. Amoyel M, Bach EA. Cell competition: how to eliminate your neighbours. *Development* 2014; **141**: 988–1000.
52. Zhang Q, Shalaby NA, Buszczak M. Changes in rRNA transcription influence proliferation and cell fate within a stem cell lineage. *Science* 2014; **343**: 298–301.
53. Lai M-D, Xu J. Ribosomal proteins and colorectal cancer. *Curr Genomics* 2007; **8**: 43–49.
54. Stumpf CR, Ruggero D. The cancerous translation apparatus. *Curr Opin Genet Dev* 2011; **21**: 474–483.
55. Nieminen TT, O'Donohue M-F, Wu Y, Lohi H, Scherer SW, Paterson AD *et al.* Germline mutation of RPS20, encoding a ribosomal protein, causes predisposition to hereditary nonpolyposis colorectal carcinoma without DNA mismatch repair deficiency. *Gastroenterology* 2014; **147**: 595–598.e5.
56. Brighenti E, Calabrese C, Liguori G, Giannone FA, Treré D, Montanaro L *et al.* Interleukin 6 downregulates p53 expression and activity by stimulating ribosome biogenesis: a new pathway connecting inflammation to cancer. *Oncogene* 2014; **33**: 4396–4406.
57. El Marjou F, Janssen KP, Chang BH, Li M, Hindie V, Chan L *et al.* Tissue-specific and inducible Cre-mediated recombination in the gut epithelium. *Genesis* 2004; **39**: 186–193.
58. Barker N, van Es JH, Kuipers J, Kujala P, van den Born M, Cozijnsen M *et al.* Identification of stem cells in small intestine and colon by marker gene *Lgr5. Nature* 2007; **449**: 1003–1007.
59. Jacks T, Remington L, Williams BO, Schmitt EM, Halachmi S, Bronson RT *et al.* Tumor spectrum analysis in p53-mutant mice. *Curr Biol* 1994; **4**: 1–7.
60. Guo J, Longshore S, Nair R, Warner BW. Retinoblastoma protein (pRb), but not p107 or p130, is required for maintenance of enterocyte quiescence and differentiation in small intestine. *J Biol Chem* 2009; **284**: 134–140.
61. Léguillier T, Vandormael-Pournin S, Artus J, Houlard M, Picard C, Bernex F *et al.* Omcg1 is critically required for mitosis in rapidly dividing mouse intestinal progenitors and embryonic stem cells. *Biol Open* 2012; **1**: 648–657.
62. O'Donohue M-F, Choesmel V, Faubladier M, Fichant G, Gleizes P-E. Functional dichotomy of ribosomal proteins during the synthesis of mammalian 40S ribosomal subunits. *J Cell Biol* 2010; **190**: 853–866.
63. Fichelson P, Moch C, Ivanovitch K, Martin C, Sidor CM, Lepesant J-A *et al.* Live-imaging of single stem cells within their niche reveals that a U3snoRNP component segregates asymmetrically and is required for self-renewal in Drosophila. *Nat Cell Biol* 2009; **11**: 685–693.

Supplementary Information accompanies this paper on Cell Death and Differentiation website (http://www.nature.com/cdd)

– Annex –

References

A

Abbas, H.A., Maccio, D.R., Coskun, S., Jackson, J.G., Hazen, A.L., Sills, T.M., You, M.J., Hirschi, K.K., and Lozano, G. (2010). Mdm2 is required for survival of hematopoietic stem cells/progenitors via dampening of ROS-induced p53 activity. Cell Stem Cell *7*, 606–617.

Abujarour, R., Efe, J., and Ding, S. (2010). Genome-wide gain-of-function screen identifies novel regulators of pluripotency. Stem Cells *28*, 1487–1497.

Ahn, C.S., Cho, H.K., Lee, D.-H., Sim, H.-J., Kim, S.-G., and Pai, H.-S. (2016). Functional characterization of the ribosome biogenesis factors PES, BOP1, and WDR12 (PeBoW), and mechanisms of defective cell growth and proliferation caused by PeBoW deficiency in Arabidopsis. J. Exp. Bot. erw288.

Akala, O.O., Park, I.-K., Qian, D., Pihalja, M., Becker, M.W., and Clarke, M.F. (2008). Long-term haematopoietic reconstitution by Trp53-/-p16Ink4a-/-p19Arf-/- multipotent progenitors. Nature *453*, 228–232.

Allsopp, R.C., Morin, G.B., DePinho, R., Harley, C.B., and Weissman, I.L. (2003). Telomerase is required to slow telomere shortening and extend replicative lifespan of HSCs during serial transplantation. Blood *102*, 517–520.

Alter, B.P., Baerlocher, G.M., Savage, S.A., Chanock, S.J., Weksler, B.B., Willner, J.P., Peters, J.A., Giri, N., and Lansdorp, P.M. (2007). Very short telomere length by flow fluorescence in situ hybridization identifies patients with dyskeratosis congenita. Blood *110*, 1439–1447.

Amsterdam, A., Sadler, K.C., Lai, K., Farrington, S., Bronson, R.T., Lees, J.A., and Hopkins, N. (2004). Many ribosomal protein genes are cancer genes in zebrafish. Plos Biol *2*, E139.

Anderson, S.J., Lauritsen, J.P.H., Hartman, M.G., Foushee, A.M.D., Lefebvre, J.M., Shinton, S.A., Gerhardt, B., Hardy, R.R., Oravecz, T., and Wiest, D.L. (2007). Ablation of ribosomal protein L22 selectively impairs alphabeta T cell development by activation of a p53-dependent checkpoint. Immunity *26*, 759–772.

Ayrault, O., Andrique, L., Fauvin, D., Eymin, B., Gazzeri, S., and Séité, P. (2006). Human tumor suppressor p14ARF negatively regulates rRNA transcription and inhibits UBF1 transcription factor phosphorylation. Oncogene *25*, 7577–7586.

B

Ball, S. (2011). Diamond blackfan anemia. Hematology Am Soc Hematol Educ Program *2011*, 487–491.

Bar-Peled, L., and Sabatini, D.M. (2014). Regulation of mTORC1 by amino acids. Trends Cell Biol. *24*, 400–406.

Barlow, J.L., Drynan, L.F., Hewett, D.R., Holmes, L.R., Lorenzo-Abalde, S., Lane, A.L., Jolin, H.E., Pannell, R., Middleton, A.J., Wong, S.H., et al. (2010). A p53-dependent mechanism underlies macrocytic anemia in a mouse model of human 5q- syndrome. Nat. Med. *16*, 59–66.

Barroca, V., Mouthon, M.A., Lewandowski, D., Brunet de la Grange, P., Gauthier, L.R., Pflumio, F., Boussin, F.D., Arwert, F., Riou, L., Allemand, I., et al. (2012). Impaired functionality and

homing of Fancg-deficient hematopoietic stem cells. Hum. Mol. Genet. *21*, 121–135.

Baßler, J., Kallas, M., Pertschy, B., Ulbrich, C., Thoms, M., and Hurt, E. (2010). The AAA-ATPase Rea1 drives removal of biogenesis factors during multiple stages of 60S ribosome assembly. Molecular Cell *38*, 712–721.

Baßler, J., Paternoga, H., Holdermann, I., Thoms, M., Granneman, S., Barrio-Garcia, C., Nyarko, A., Stier, G., Clark, S.A., Schraivogel, D., et al. (2014). A network of assembly factors is involved in remodeling rRNA elements during preribosome maturation. The Journal of Cell Biology.

Beck-Cormier, S., Escande, M., Souilhol, C., Vandormael-Pournin, S., Sourice, S., Pilet, P., Babinet, C., and Cohen-Tannoudji, M. (2014). Notchless is required for axial skeleton formation in mice. PLoS ONE *9*, e98507.

Beerman, I., Seita, J., Inlay, M.A., Weissman, I.L., and Rossi, D.J. (2014). Quiescent Hematopoietic Stem Cells Accumulate DNA Damage during Aging that Is Repaired upon Entry into Cell Cycle. Cell Stem Cell.

Bender, C.F., Sikes, M.L., Sullivan, R., Huye, L.E., Le Beau, M.M., Roth, D.B., Mirzoeva, O.K., Oltz, E.M., and Petrini, J.H.J. (2002). Cancer predisposition and hematopoietic failure in Rad50(S/S) mice. Genes & Development *16*, 2237–2251.

Benveniste, P., Frelin, C., Janmohamed, S., Barbara, M., Herrington, R., Hyam, D., and Iscove, N.N. (2010). Intermediate-term hematopoietic stem cells with extended but time-limited reconstitution potential. Cell Stem Cell *6*, 48–58.

Benz, C., Copley, M.R., Kent, D.G., Wohrer, S., Cortes, A., Aghaeepour, N., Ma, E., Mader, H., Rowe, K., Day, C., et al. (2012). Hematopoietic Stem Cell Subtypes Expand Differentially during Development and Display Distinct Lymphopoietic Programs. Cell Stem Cell *10*, 273–283.

Bernardes de Jesus, B., Vera, E., Schneeberger, K., Tejera, A.M., Ayuso, E., Bosch, F., and Blasco, M.A. (2012). Telomerase gene therapy in adult and old mice delays aging and increases longevity without increasing cancer. EMBO Molecular Medicine *4*, 691–704.

Bertwistle, D., Sugimoto, M., and Sherr, C.J. (2004). Physical and functional interactions of the Arf tumor suppressor protein with nucleophosmin/B23. Molecular and Cellular Biology *24*, 985–996.

Bondar, T., and Medzhitov, R. (2010). p53-mediated hematopoietic stem and progenitor cell competition. Cell Stem Cell *6*, 309–322.

Bonnet, D., and Dick, J.E. (1997). Human acute myeloid leukemia is organized as a hierarchy that originates from a primitive hematopoietic cell. Nat. Med. *3*, 730–737.

Brack, A.S., and Rando, T.A. (2012). Tissue-specific stem cells: lessons from the skeletal muscle satellite cell. Cell Stem Cell *10*, 504–514.

Bretones, G., Delgado, M.D., and León, J. (2015). Myc and cell cycle control. Biochimica Et Biophysica Acta (BBA) - Gene Regulatory Mechanisms *1849*, 506–516.

Bryder, D., Rossi, D.J., and Weissman, I.L. (2006). Hematopoietic stem cells: the paradigmatic tissue-specific stem cell. Am. J. Pathol. *169*, 338–346.

Bursać, S., Brdovčak, M.C., Donati, G., and Volarevic, S. (2014). Activation of the tumor suppressor p53 upon impairment of ribosome biogenesis. Biochim. Biophys. Acta *1842*, 817–830.

Bursać, S., Brdovčak, M.C., Pfannkuchen, M., Orsolić, I., Golomb, L., Zhu, Y., Katz, C., Daftuar, L., Grabusic, K., Vukelić, I., et al. (2012). Mutual protection of ribosomal proteins L5 and L11 from degradation is essential for p53 activation upon ribosomal biogenesis stress. Proc. Natl. Acad. Sci. U.S.a. *109*, 20467–20472.

Busch, K., Klapproth, K., Barile, M., Flossdorf, M., Holland-Letz, T., Schlenner, S.M., Reth, M., Höfer, T., and Rodewald, H.-R. (2015). Fundamental properties of unperturbed haematopoiesis from stem cells in vivo. Nature *518*, 542–546.

Buszczak, M., Signer, R.A.J., and Morrison, S.J. (2014). Cellular Differences in Protein Synthesis Regulate Tissue Homeostasis. Cell *159*, 242–251.

Byrne, M.E. (2009). A role for the ribosome in development. Trends Plant Sci. *14*, 512–519.

C

Cabezas-Wallscheid, N., Klimmeck, D., Hansson, J., Lipka, D.B., Reyes, A., Wang, Q., Weichenhan, D., Lier, A., Paleske, von, L., Renders, S., et al. (2014). Identification of Regulatory Networks in HSCs and Their Immediate Progeny via Integrated Proteome, Transcriptome, and DNA Methylome Analysis. Cell Stem Cell *15*, 507–522.

Cai, X., Gao, L., Teng, L., Ge, J., Oo, Z.M., Kumar, A.R., Gilliland, D.G., Mason, P.J., Tan, K., and Speck, N.A. (2015). Runx1 Deficiency Decreases Ribosome Biogenesis and Confers Stress Resistance to Hematopoietic Stem and Progenitor Cells. - PubMed - NCBI. Cell Stem Cell *17*, 165–177.

Calder, A., Roth-Albin, I., Bhatia, S., Pilquil, C., Lee, J.H., Bhatia, M., Levadoux-Martin, M., McNicol, J., Russell, J., Collins, T., et al. (2013). Lengthened G1 phase indicates differentiation status in human embryonic stem cells. Stem Cells Dev. *22*, 279–295.

Calés, C., Román-Trufero, M., Pavón, L., Serrano, I., Melgar, T., Endoh, M., Pérez, C., Koseki, H., and Vidal, M. (2008). Inactivation of the polycomb group protein Ring1B unveils an antiproliferative role in hematopoietic cell expansion and cooperation with tumorigenesis associated with Ink4a deletion. Molecular and Cellular Biology *28*, 1018–1028.

Carlone, D.L., and Breault, D.T. (2012). Tales from the crypt: the expanding role of slow cycling intestinal stem cells. Cell Stem Cell *10*, 2–4.

Carroll, A.J., Heazlewood, J.L., Ito, J., and Millar, A.H. (2008). Analysis of the Arabidopsis cytosolic ribosome proteome provides detailed insights into its components and their post-translational modification. Mol. Cell Proteomics *7*, 347–369.

Chakraborty, A., Uechi, T., and Kenmochi, N. (2011). Guarding the “translation apparatus”: defective ribosome biogenesis and the p53 signaling pathway. Wiley Interdiscip Rev RNA *2*, 507–522.

Challagundla, K.B., Sun, X.-X., Zhang, X., DeVine, T., Zhang, Q., Sears, R.C., and Dai, M.-S. (2011). Ribosomal protein L11 recruits miR-24/miRISC to repress c-Myc expression in response to

ribosomal stress. Molecular and Cellular Biology *31*, 4007–4021.

Challen, G.A., and Little, M.H. (2006). A side order of stem cells: the SP phenotype. Stem Cells *24*, 3–12.

Chan, J.C., Hannan, K.M., Riddell, K., Ng, P.Y., Peck, A., Lee, R.S., Hung, S., Astle, M.V., Bywater, M., Wall, M., et al. (2011). AKT promotes rRNA synthesis and cooperates with c-MYC to stimulate ribosome biogenesis in cancer. Sci Signal *4*, ra56–ra56.

Charitou, P., and Burgering, B.M.T. (2013). Forkhead box(O) in control of reactive oxygen species and genomic stability to ensure healthy lifespan. Antioxid Redox Signal *19*, 1400–1419.

Chauvin, C., Koka, V., Nouschi, A., Mieulet, V., Hoareau-Aveilla, C., Dreazen, A., Cagnard, N., Carpentier, W., Kiss, T., Meyuhas, O., et al. (2014). Ribosomal protein S6 kinase activity controls the ribosome biogenesis transcriptional program. Oncogene *33*, 474–483.

Chen, C., Liu, Y., Liu, R., Ikenoue, T., Guan, K.-L., Liu, Y., and Zheng, P. (2008a). TSC-mTOR maintains quiescence and function of hematopoietic stem cells by repressing mitochondrial biogenesis and reactive oxygen species. J. Exp. Med. *205*, 2397–2408.

Chen, J., Ellison, F.M., Keyvanfar, K., Omokaro, S.O., Desierto, M.J., Eckhaus, M.A., and Young, N.S. (2008b). Enrichment of hematopoietic stem cells with SLAM and LSK markers for the detection of hematopoietic stem cell function in normal and Trp53 null mice. Exp. Hematol. *36*, 1236–1243.

Cheng, T., Rodrigues, N., Shen, H., Yang, Y., Dombkowski, D., Sykes, M., and Scadden, D.T. (2000). Hematopoietic stem cell quiescence maintained by p21cip1/waf1. Science *287*, 1804–1808.

Cheshier, S.P., Morrison, S.J., Liao, X.S., and Weissman, I.L. (1999). In vivo proliferation and cell cycle kinetics of long-term self-renewing hematopoietic stem cells. Proceedings of the National Academy of Sciences *96*, 3120–3125.

Chow, D.C., Wenning, L.A., Miller, W.M., and Papoutsakis, E.T. (2001). Modeling pO(2) distributions in the bone marrow hematopoietic compartment. II. Modified Kroghian models. Biophysical Journal *81*, 685–696.

Cicalese, A., Bonizzi, G., Pasi, C.E., Faretta, M., Ronzoni, S., Giulini, B., Brisken, C., Minucci, S., Di Fiore, P.P., and Pelicci, P.G. (2009). The tumor suppressor p53 regulates polarity of self-renewing divisions in mammary stem cells. Cell *138*, 1083–1095.

Cormier, S., Le Bras, S., Souilhol, C., Vandormael-Pournin, S., Durand, B., Babinet, C., Baldacci, P., and Cohen-Tannoudji, M. (2006). The murine ortholog of notchless, a direct regulator of the notch pathway in Drosophila melanogaster, is essential for survival of inner cell mass cells. Molecular and Cellular Biology *26*, 3541–3549.

Coronado, D., Godet, M., Bourillot, P.-Y., Tapponnier, Y., Bernat, A., Petit, M., Afanassieff, M., Markossian, S., Malashicheva, A., Iacone, R., et al. (2013). A short G1 phase is an intrinsic determinant of naïve embryonic stem cell pluripotency. Stem Cell Res *10*, 118–131.

Csibi, A., Lee, G., Yoon, S.-O., Tong, H., Ilter, D., Elia, I., Fendt, S.-M., Roberts, T.M., and Blenis, J.

(2014). The mTORC1/S6K1 pathway regulates glutamine metabolism through the eIF4B-dependent control of c-Myc translation. Curr. Biol. *24*, 2274–2280.

D

Dai, M.-S., Arnold, H., Sun, X.-X., Sears, R., and Lu, H. (2007). Inhibition of c-Myc activity by ribosomal protein L11. Embo J. *26*, 3332–3345.

Dang, C.V. (2013). MYC, metabolism, cell growth, and tumorigenesis. Cold Spring Harb Perspect Med *3*.

Danilova, N., and Gazda, H.T. (2015). Ribosomopathies: how a common root can cause a tree of pathologies. - PubMed - NCBI. Dis Model Mech *8*, 1013–1026.

Danilova, N., Bibikova, E., Covey, T.M., Nathanson, D., Dimitrova, E., Konto, Y., Lindgren, A., Glader, B., Radu, C.G., Sakamoto, K.M., et al. (2014). The role of DNA damage response in zebrafish and cellular models of Diamond Blackfan Anemia. Dis Model Mech.

Danilova, N., Sakamoto, K.M., and Lin, S. (2008). Ribosomal protein S19 deficiency in zebrafish leads to developmental abnormalities and defective erythropoiesis through activation of p53 protein family. Blood *112*, 5228–5237.

Danilova, N., Sakamoto, K.M., and Lin, S. (2011). Ribosomal protein L11 mutation in zebrafish leads to haematopoietic and metabolic defects. Br. J. Haematol. *152*, 217–228.

David, A., Bennink, J.R., and Yewdell, J.W. (2013). Emetine optimally facilitates nascent chain puromycylation and potentiates the ribopuromycylation method (RPM) applied to inert cells. Histochem. Cell Biol. *139*, 501–504.

David, A., Dolan, B.P., Hickman, H.D., Knowlton, J.J., Clavarino, G., Pierre, P., Bennink, J.R., and Yewdell, J.W. (2012). Nuclear translation visualized by ribosome-bound nascent chain puromycylation. The Journal of Cell Biology *197*, 45–57.

De Keersmaecker, K., Sulima, S.O., and Dinman, J.D. (2015). Ribosomopathies and the paradox of cellular hypo- to hyperproliferation. Blood *125*, 1377–1382.

Deisenroth, C., and Zhang, Y. (2010). Ribosome biogenesis surveillance: probing the ribosomal protein-Mdm2-p53 pathway. Oncogene *29*, 4253–4260.

Donati, G., Bertoni, S., Brighenti, E., Vici, M., Treré, D., Volarevic, S., Montanaro, L., and Derenzini, M. (2011a). The balance between rRNA and ribosomal protein synthesis up- and downregulates the tumour suppressor p53 in mammalian cells. Oncogene *30*, 3274–3288.

Donati, G., Brighenti, E., Vici, M., Mazzini, G., Treré, D., Montanaro, L., and Derenzini, M. (2011b). Selective inhibition of rRNA transcription downregulates E2F-1: a new p53-independent mechanism linking cell growth to cell proliferation. Journal of Cell Science *124*, 3017–3028.

Donati, G., Peddigari, S., Mercer, C.A., and Thomas, G. (2013). 5S Ribosomal RNA Is an Essential Component of a Nascent Ribosomal Precursor Complex that Regulates the Hdm2-p53 Checkpoint. Cell Rep *4*, 87–98.

Doulatov, S., Notta, F., Laurenti, E., and Dick, J.E. (2012). Hematopoiesis: a human perspective. Cell Stem Cell *10*, 120–136.

Draptchinskaia, N., Gustavsson, P., Andersson, B., Pettersson, M., Willig, T.N., Dianzani, I., Ball, S., Tchernia, G., Klar, J., Matsson, H., et al. (1999). The gene encoding ribosomal protein S19 is mutated in Diamond-Blackfan anaemia. Nat Genet *21*, 169–175.

Drygin, D., O'Brien, S.E., Hannan, R.D., McArthur, G.A., and Hoff, Von, D.D. (2013). Targeting the nucleolus for cancer-specific activation of p53. Drug Discov. Today.

Drygin, D., Rice, W.G., and Grummt, I. (2010). The RNA polymerase I transcription machinery: an emerging target for the treatment of cancer. Annu. Rev. Pharmacol. Toxicol. *50*, 131–156.

Durut, N., and Sáez-Vásquez, J. (2015). Nucleolin: dual roles in rDNA chromatin transcription. Gene *556*, 7–12.

Dutt, S., Narla, A., Lin, K., Mullally, A., Abayasekara, N., Megerdichian, C., Wilson, F.H., Currie, T., Khanna-Gupta, A., Berliner, N., et al. (2011). Haploinsufficiency for ribosomal protein genes causes selective activation of p53 in human erythroid progenitor cells. Blood *117*, 2567–2576.

Dykstra, B., Kent, D., Bowie, M., McCaffrey, L., Hamilton, M., Lyons, K., Lee, S.-J., Brinkman, R., and Eaves, C. (2007). Long-term propagation of distinct hematopoietic differentiation programs in vivo. Cell Stem Cell *1*, 218–229.

E-F

Ema, H., Sudo, K., Seita, J., Matsubara, A., and Morita, Y. (2005). Quantification of self-renewal capacity in single hematopoietic stem cells from normal and Lnk-deficient mice. Developmental Cell.

Ema, H., Morita, Y., and Suda, T. (2014). Heterogeneity and hierarchy of hematopoietic stem cells. Exp. Hematol. *42*, 74–e2.

Enver, T., Heyworth, C.M., and Dexter, T.M. (1998). Do stem cells play dice? Blood *92*, 348–51–discussion352.

Felton-Edkins, Z.A., Fairley, J.A., Graham, E.L., Johnston, I.M., White, R.J., and Scott, P.H. (2003). The mitogen-activated protein (MAP) kinase ERK induces tRNA synthesis by phosphorylating TFIIIB. Embo J. *22*, 2422–2432.

Fichelson, P., Moch, C., Ivanovitch, K., Martin, C., Sidor, C.M., Lepesant, J.-A., Bellaiche, Y., and Huynh, J.-R. (2009). Live-imaging of single stem cells within their niche reveals that a U3snoRNP component segregates asymmetrically and is required for self-renewal in Drosophila. Nat Cell Biol *11*, 685–693.

Fischer, A., Hacein-Bey-Abina, S., and Cavazzana-Calvo, M. (2010). 20 years of gene therapy for SCID. Nat Immunol *11*, 457–460.

Flach, J., Bakker, S.T., Mohrin, M., Conroy, P.C., Pietras, E.M., Reynaud, D., Alvarez, S., Diolaiti, M.E., Ugarte, F., Forsberg, E.C., et al. (2014). Replication stress is a potent driver of functional decline in ageing haematopoietic stem cells. Nature *512*, 198–202.

Flores, I., Canela, A., Vera, E., Tejera, A., Cotsarelis, G., and Blasco, M.A. (2008). The longest telomeres: a general signature of adult stem cell compartments. Genes & Development *22*, 654–667.

Fonseca, B.D., Zakaria, C., Jia, J.-J., Graber, T.E., Svitkin, Y., Tahmasebi, S., Healy, D., Hoang, H.-D., Jensen, J.M., Diao, I.T., et al. (2015). La-related Protein 1 (LARP1) Represses Terminal Oligopyrimidine (TOP) mRNA Translation Downstream of mTOR Complex 1 (mTORC1). J. Biol. Chem. *290*, 15996–16020.

Forsberg, E.C., Passegue, E., Prohaska, S.S., Wagers, A.J., Koeva, M., Stuart, J.M., and Weissman, I.L. (2010). Molecular signatures of quiescent, mobilized and leukemia-initiating hematopoietic stem cells. PLoS ONE *5*, e8785.

Foudi, A., Hochedlinger, K., Van Buren, D., Schindler, J.W., Jaenisch, R., Carey, V., and Hock, H. (2008). Analysis of histone 2B-GFP retention reveals slowly cycling hematopoietic stem cells. Nat Biotechnol *27*, 84–90.

Fumagalli, S., Di Cara, A., Neb-Gulati, A., Natt, F., Schwemberger, S., Hall, J., Babcock, G.F., Bernardi, R., Pandolfi, P.P., and Thomas, G. (2009). Absence of nucleolar disruption after impairment of 40S ribosome biogenesis reveals an rpL11-translation-dependent mechanism of p53 induction. Nat Cell Biol *11*, 501–508.

Fumagalli, S., Ivanenkov, V.V., Teng, T., and Thomas, G. (2012). Suprainduction of p53 by disruption of 40S and 60S ribosome biogenesis leads to the activation of a novel G2/M checkpoint. Genes & Development *26*, 1028–1040.

G

Gan, B., Sahin, E., Jiang, S., Sánchez-Aguilera, A., Scott, K.L., Chin, L., Williams, D.A., Kwiatkowski, D.J., and DePinho, R.A. (2008). mTORC1-dependent and -independent regulation of stem cell renewal, differentiation, and mobilization. Proc. Natl. Acad. Sci. U.S.a. *105*, 19384–19389.

Gartner, S., and Kaplan, H.S. (1980). Long-term culture of human bone marrow cells. Proceedings of the National Academy of Sciences *77*, 4756–4759.

Gazave, E., Lapébie, P., Richards, G.S., Brunet, F., Ereskovsky, A.V., Degnan, B.M., Borchiellini, C., Vervoort, M., and Renard, E. (2009). Origin and evolution of the Notch signalling pathway: an overview from eukaryotic genomes. BMC Evol. Biol. *9*, 249.

Geyer, P.K., Meyuhas, O., Perry, R.P., and Johnson, L.F. (1982). Regulation of ribosomal protein mRNA content and translation in growth-stimulated mouse fibroblasts. Molecular and Cellular Biology *2*, 685–693.

Gismondi, A., Caldarola, S., Lisi, G., Juli, G., Chellini, L., Iadevaia, V., Proud, C.G., and Loreni, F. (2014). Ribosomal stress activates eEF2K-eEF2 pathway causing translation elongation inhibition and recruitment of Terminal Oligopyrimidine (TOP) mRNAs on polysomes. Nucleic Acids Research.

Golomb, L., Volarevic, S., and Oren, M. (2014). p53 and ribosome biogenesis stress: The essentials. FEBS Lett.

Gomez-Herreros, F., Rodriguez-Galan, O., Morillo-Huesca, M., Maya, D., Arista-Romero, M., la Cruz, de, J., Chavez, S., and Munoz-Centeno, M.-C. (2013). Balanced production of ribosome components is required for proper G1/S transition in Saccharomyces cerevisiae. Journal of Biological Chemistry.

Gomez-Roman, N., Felton-Edkins, Z.A., Kenneth, N.S., Goodfellow, S.J., Athineos, D., Zhang, J., Ramsbottom, B.A., Innes, F., Kantidakis, T., Kerr, E.R., et al. (2006). Activation by c-Myc of transcription by RNA polymerases I, II and III. Biochem. Soc. Symp. 141–154.

Goodell, M.A., Brose, K., Paradis, G., Conner, A.S., and Mulligan, R.C. (1996). Isolation and functional properties of murine hematopoietic stem cells that are replicating in vivo. J. Exp. Med. *183*, 1797–1806.

Greer, S.N., Metcalf, J.L., Wang, Y., and Ohh, M. (2012). The updated biology of hypoxia-inducible factor. Embo J. *31*, 2448–2460.

Gunderson, J.H., Sogin, M.L., Wollett, G., Hollingdale, M., la Cruz, de, V.F., Waters, A.P., and McCutchan, T.F. (1987). Structurally distinct, stage-specific ribosomes occur in Plasmodium. Science *238*, 933–937.

Gwinn, D.M., Shackelford, D.B., Egan, D.F., Mihaylova, M.M., Mery, A., Vasquez, D.S., Turk, B.E., and Shaw, R.J. (2008). AMPK phosphorylation of raptor mediates a metabolic checkpoint. Molecular Cell *30*, 214–226.

H

Hammoud, M., Vlaski, M., Duchez, P., Chevaleyre, J., Lafarge, X., Boiron, J.-M., Praloran, V., la Grange, de, P.B., and Ivanovic, Z. (2012). Combination of low O(2) concentration and mesenchymal stromal cells during culture of cord blood CD34(+) cells improves the maintenance and proliferative capacity of hematopoietic stem cells. J. Cell. Physiol. *227*, 2750–2758.

Haneline, L.S., White, H., Yang, F.-C., Chen, S., Orschell, C., Kapur, R., and Ingram, D.A. (2006). Genetic reduction of class IA PI-3 kinase activity alters fetal hematopoiesis and competitive repopulating ability of hematopoietic stem cells in vivo. Blood *107*, 1375–1382.

Hannan, K.M., Brandenburger, Y., Jenkins, A., Sharkey, K., Cavanaugh, A., Rothblum, L., Moss, T., Poortinga, G., McArthur, G.A., Pearson, R.B., et al. (2003). mTOR-dependent regulation of ribosomal gene transcription requires S6K1 and is mediated by phosphorylation of the carboxy-terminal activation domain of the nucleolar transcription factor UBF. Molecular and Cellular Biology *23*, 8862–8877.

Hannan, K.M., Sanij, E., Hein, N., Hannan, R.D., and Pearson, R.B. (2011). Signaling to the ribosome in cancer--It is more than just mTORC1. IUBMB Life *63*, 79–85.

Hannan, R.D., Drygin, D., and Pearson, R.B. (2013). Targeting RNA polymerase I transcription and the nucleolus for cancer therapy. Expert Opin Ther Targets *17*, 873–878.

Hayashi, Y., Kuroda, T., Kishimoto, H., Wang, C., Iwama, A., and Kimura, K. (2014). Downregulation of rRNA Transcription Triggers Cell Differentiation. PLoS ONE *9*, e98586.

Hermitte, F., Brunet de la Grange, P., Belloc, F., Praloran, V., and Ivanovic, Z. (2006). Very low

O2 concentration (0.1%) favors G0 return of dividing CD34+ cells. Stem Cells *24*, 65–73.

Hock, H., Hamblen, M.J., Rooke, H.M., Schindler, J.W., Saleque, S., Fujiwara, Y., and Orkin, S.H. (2004). Gfi-1 restricts proliferation and preserves functional integrity of haematopoietic stem cells. Nature *431*, 1002–1007.

Hoppe, S., Bierhoff, H., Cado, I., Weber, A., Tiebe, M., Grummt, I., and Voit, R. (2009). AMP-activated protein kinase adapts rRNA synthesis to cellular energy supply. Proc. Natl. Acad. Sci. U.S.a. *106*, 17781–17786.

Horiguchi, G., Van Lijsebettens, M., Candela, H., Micol, J.L., and Tsukaya, H. (2012). Ribosomes and translation in plant developmental control. Plant Sci. *191-192*, 24–34.

Horos, R., and Lindern, von, M. (2012). Molecular mechanisms of pathology and treatment in Diamond Blackfan Anaemia. Br. J. Haematol.

Hovhanyan, A., Herter, E.K., Pfannstiel, J., Gallant, P., and Raabe, T. (2014). Drosophila mbm is a nucleolar myc and casein kinase 2 target required for ribosome biogenesis and cell growth of central brain neuroblasts. Molecular and Cellular Biology *34*, 1878–1891.

Hölzel, M., Burger, K., Mühl, B., Orban, M., Kellner, M., and Eick, D. (2010). The tumor suppressor p53 connects ribosome biogenesis to cell cycle control: a double-edged sword. Oncotarget *1*, 43–47.

Hölzel, M., Rohrmoser, M., Schlee, M., Grimm, T., Harasim, T., Malamoussi, A., Gruber-Eber, A., Kremmer, E., Hiddemann, W., Bornkamm, G.W., et al. (2005). Mammalian WDR12 is a novel member of the Pes1-Bop1 complex and is required for ribosome biogenesis and cell proliferation. The Journal of Cell Biology *170*, 367–378.

Hsieh, A.C., Liu, Y., Edlind, M.P., Ingolia, N.T., Janes, M.R., Sher, A., Shi, E.Y., Stumpf, C.R., Christensen, C., Bonham, M.J., et al. (2012). The translational landscape of mTOR signalling steers cancer initiation and metastasis. Nature *485*, 55–61.

Huang, K., Maruyama, T., and Fan, G. (2014). The naive state of human pluripotent stem cells: a synthesis of stem cell and preimplantation embryo transcriptome analyses. Cell Stem Cell *15*, 410–415.

Huo, Y., Iadevaia, V., Yao, Z., Kelly, I., Cosulich, S., Guichard, S., Foster, L.J., and Proud, C.G. (2012). Stable isotope-labelling analysis of the impact of inhibition of the mammalian target of rapamycin on protein synthesis. Biochem J *444*, 141–151.

I

Iadevaia, V., Liu, R., and Proud, C.G. (2014). mTORC1 signaling controls multiple steps in ribosome biogenesis. *36*, 113–120.

Inoki, K., Li, Y., Xu, T., and Guan, K.-L. (2003a). Rheb GTPase is a direct target of TSC2 GAP activity and regulates mTOR signaling. Genes & Development *17*, 1829–1834.

Inoki, K., Zhu, T., and Guan, K.-L. (2003b). TSC2 mediates cellular energy response to control cell growth and survival. Cell *115*, 577–590.

Inomata, K., Aoto, T., Binh, N.T., Okamoto, N., Tanimura, S., Wakayama, T., Iseki, S., Hara, E., Masunaga, T., Shimizu, H., et al. (2009). Genotoxic stress abrogates renewal of melanocyte stem cells by triggering their differentiation. Cell *137*, 1088–1099.

Itahana, K., Bhat, K.P., Jin, A., Itahana, Y., Hawke, D., Kobayashi, R., and Zhang, Y. (2003). Tumor suppressor ARF degrades B23, a nucleolar protein involved in ribosome biogenesis and cell proliferation. Molecular Cell *12*, 1151–1164.

Ito, K., Hirao, A., Arai, F., Matsuoka, S., Takubo, K., Hamaguchi, I., Nomiyama, K., Hosokawa, K., Sakurada, K., Nakagata, N., et al. (2004). Regulation of oxidative stress by ATM is required for self-renewal of haematopoietic stem cells. Nature *431*, 997–1002.

Ito, K., Hirao, A., Arai, F., Takubo, K., Matsuoka, S., Miyamoto, K., Ohmura, M., Naka, K., Hosokawa, K., Ikeda, Y., et al. (2006). Reactive oxygen species act through p38 MAPK to limit the lifespan of hematopoietic stem cells. Nat. Med. *12*, 446–451.

Ito, K., Takubo, K., Arai, F., Satoh, H., Matsuoka, S., Ohmura, M., Naka, K., Azuma, M., Miyamoto, K., Hosokawa, K., et al. (2007). Regulation of reactive oxygen species by Atm is essential for proper response to DNA double-strand breaks in lymphocytes. J. Immunol. *178*, 103–110.

J

Jaako, P., Debnath, S., Olsson, K., Zhang, Y., Flygare, J., Lindström, M.S., Bryder, D., and Karlsson, S. (2015). Disruption of the 5S RNP-Mdm2 interaction significantly improves the erythroid defect in a mouse model for Diamond-Blackfan anemia. Leukemia.

Jaako, P., Flygare, J., Olsson, K., Quere, R., Ehinger, M., Henson, A., Ellis, S., Schambach, A., Baum, C., Richter, J., et al. (2011). Mice with ribosomal protein S19 deficiency develop bone marrow failure and symptoms like patients with Diamond-Blackfan anemia. Blood *118*, 6087–6096.

Jang, Y.-Y., and Sharkis, S.J. (2007). A low level of reactive oxygen species selects for primitive hematopoietic stem cells that may reside in the low-oxygenic niche. Blood *110*, 3056–3063.

Jefferies, H.B., Fumagalli, S., Dennis, P.B., Reinhard, C., Pearson, R.B., and Thomas, G. (1997). Rapamycin suppresses 5'TOP mRNA translation through inhibition of p70s6k. Embo J. *16*, 3693–3704.

Jefferies, H.B., Reinhard, C., Kozma, S.C., and Thomas, G. (1994). Rapamycin selectively represses translation of the “polypyrimidine tract” mRNA family. Proceedings of the National Academy of Sciences *91*, 4441–4445.

Joerger, A.C., and Fersht, A.R. (2016). The p53 Pathway: Origins, Inactivation in Cancer, and Emerging Therapeutic Approaches. Biochemistry *85*, 375–404.

Jones, M., Osawa, G., Regal, J.A., Weinberg, D.N., Taggart, J., Kocak, H., Friedman, A., Ferguson, D.O., Keegan, C.E., and Maillard, I. (2013). Hematopoietic stem cells are acutely sensitive to Acd shelterin gene inactivation. J Clin Invest *124*, 353–366.

Jorgensen, P., Nishikawa, J.L., Breitkreutz, B.-J., and Tyers, M. (2002). Systematic identification of pathways that couple cell growth and division in yeast. Science *297*, 395–400.

Julian, L.M., and Blais, A. (2015). Transcriptional control of stem cell fate by E2Fs and pocket

proteins. Front Genet *6*, 161.

Juntilla, M.M., Patil, V.D., Calamito, M., Joshi, R.P., Birnbaum, M.J., and Koretzky, G.A. (2010). AKT1 and AKT2 maintain hematopoietic stem cell function by regulating reactive oxygen species. Blood *115*, 4030–4038.

K

Kajiume, T., Ninomiya, Y., Ishihara, H., Kanno, R., and Kanno, M. (2004). Polycomb group gene mel-18 modulates the self-renewal activity and cell cycle status of hematopoietic stem cells. Exp. Hematol. *32*, 571–578.

Kamer, I., Sarig, R., Zaltsman, Y., Niv, H., Oberkovitz, G., Regev, L., Haimovich, G., Lerenthal, Y., Marcellus, R.C., and Gross, A. (2005). Proapoptotic BID is an ATM effector in the DNA-damage response. Cell *122*, 593–603.

Kantidakis, T., Ramsbottom, B.A., Birch, J.L., Dowding, S.N., and White, R.J. (2010). mTOR associates with TFIIIC, is found at tRNA and 5S rRNA genes, and targets their repressor Maf1. Proc. Natl. Acad. Sci. U.S.a. *107*, 11823–11828.

Kharas, M.G., Okabe, R., Ganis, J.J., Gozo, M., Khandan, T., Paktinat, M., Gilliland, D.G., and Gritsman, K. (2010). Constitutively active AKT depletes hematopoietic stem cells and induces leukemia in mice. Blood *115*, 1406–1415.

Kharde, S., Calviño, F.R., Gumiero, A., Wild, K., and Sinning, I. (2015). The structure of Rpf2-Rrs1 explains its role in ribosome biogenesis. Nucleic Acids Research *43*, 7083–7095.

Kiel, M.J., Yilmaz, O.H., Iwashita, T., Terhorst, C., and Morrison, S.J. (2005). SLAM family receptors distinguish hematopoietic stem and progenitor cells and reveal endothelial niches for stem cells. Cell *121*, 1109–1121.

Kiel, M.J., He, S., Ashkenazi, R., Gentry, S.N., Teta, M., Kushner, J.A., Jackson, T.L., and Morrison, S.J. (2007). Haematopoietic stem cells do not asymmetrically segregate chromosomes or retain BrdU. Nature *449*, 238–242.

Kim, C.G., Lee, J.J., Jung, D.Y., Jeon, J., Heo, H.S., Kang, H.C., Shin, J.H., Cho, Y.S., Cha, K.J., Kim, C.G., et al. (2006). Profiling of differentially expressed genes in human stem cells by cDNA microarray. Mol. Cells *21*, 343–355.

Kim, J.Y., Sawada, A., Tokimasa, S., Endo, H., Ozono, K., Hara, J., and Takihara, Y. (2004). Defective long-term repopulating ability in hematopoietic stem cells lacking the Polycomb-group gene rae28. Eur. J. Haematol. *73*, 75–84.

Klauke, K., Radulović, V., Broekhuis, M., Weersing, E., Zwart, E., Olthof, S., Ritsema, M., Bruggeman, S., Wu, X., Helin, K., et al. (2013). Polycomb Cbx family members mediate the balance between haematopoietic stem cell self-renewal and differentiation. Nat Cell Biol *15*, 353–362.

Kocabas, F., Zheng, J., Thet, S., Copeland, N.G., Jenkins, N.A., Deberardinis, R.J., Zhang, C., and Sadek, H.A. (2012). Meis1 regulates the metabolic phenotype and oxidant defense of hematopoietic stem cells. Blood *120*, 4963–4972.

Kressler, D., Hurt, E., and Baßler, J. (2010). Driving ribosome assembly. Biochim. Biophys. Acta *1803*, 673–683.

Kressler, D., Hurt, E., Bergler, H., and Baßler, J. (2012). The power of AAA-ATPases on the road of pre-60S ribosome maturation--molecular machines that strip pre-ribosomal particles. Biochim. Biophys. Acta *1823*, 92–100.

Krishnamurthy, P., Ross, D.D., Nakanishi, T., Bailey-Dell, K., Zhou, S., Mercer, K.E., Sarkadi, B., Sorrentino, B.P., and Schuetz, J.D. (2004). The stem cell marker Bcrp/ABCG2 enhances hypoxic cell survival through interactions with heme. J. Biol. Chem. *279*, 24218–24225.

Kubota, Y., Takubo, K., and Suda, T. (2008). Bone marrow long label-retaining cells reside in the sinusoidal hypoxic niche. Biochem. Biophys. Res. Commun. *366*, 335–339.

Kusnadi, E.P., Hannan, K.M., Hicks, R.J., Hannan, R.D., Pearson, R.B., and Kang, J. (2015). Regulation of rDNA transcription in response to growth factors, nutrients and energy. Gene *556*, 27–34.

L

la Cruz, de, J., Sanz-Martínez, E., and Remacha, M. (2005). The essential WD-repeat protein Rsa4p is required for rRNA processing and intra-nuclear transport of 60S ribosomal subunits. Nucleic Acids Research *33*, 5728–5739.

Lacorazza, H.D., Yamada, T., Liu, Y., Miyata, Y., Sivina, M., Nunes, J., and Nimer, S.D. (2005). The transcription factor MEF/ELF4 regulates the quiescence of primitive hematopoietic cells. Cancer Cell *9*, 175–187.

Laferté, A., Favry, E., Sentenac, A., Riva, M., Carles, C., and Chédin, S. (2006). The transcriptional activity of RNA polymerase I is a key determinant for the level of all ribosome components. Genes & Development *20*, 2030–2040.

Lai, K., Amsterdam, A., Farrington, S., Bronson, R.T., Hopkins, N., and Lees, J.A. (2009). Many ribosomal protein mutations are associated with growth impairment and tumor predisposition in zebrafish. Dev. Dyn. *238*, 76–85.

Lambertsson, A. (1998). The minute genes in Drosophila and their molecular functions. Adv. Genet. *38*, 69–134.

Laurenti, E., Varnum-Finney, B., Wilson, A., Ferrero, I., Blanco-Bose, W.E., Ehninger, A., Knoepfler, P.S., Cheng, P.-F., MacDonald, H.R., Eisenman, R.N., et al. (2008). Hematopoietic stem cell function and survival depend on c-Myc and N-Myc activity. Cell Stem Cell *3*, 611–624.

Le Bouteiller, M., Souilhol, C., Beck-Cormier, S., Stedman, A., Burlen-Defranoux, O., Vandormael-Pournin, S., Bernex, F., Cumano, A., and Cohen-Tannoudji, M. (2013). Notchless-dependent ribosome synthesis is required for the maintenance of adult hematopoietic stem cells. J. Exp. Med. *210*, 2351–2369.

Le Bras, S., Cohen-Tannoudji, M., Guyot, V., Vandormael-Pournin, S., Coumailleau, F., Babinet, C., and Baldacci, P. (2002). Transcript map of the Ovum mutant (Om) locus: isolation by exon trapping of new candidate genes for the DDK syndrome. Gene *296*, 75–86.

Lee, S.-W., Berger, S.J., Martinović, S., Pasa-Tolić, L., Anderson, G.A., Shen, Y., Zhao, R., and Smith, R.D. (2002). Direct mass spectrometric analysis of intact proteins of the yeast large ribosomal subunit using capillary LC/FTICR. Proceedings of the National Academy of Sciences *99*, 5942–5947.

Lee, S.C.W., Miller, S., Hyland, C., Kauppi, M., Lebois, M., Di Rago, L., Metcalf, D., Kinkel, S.A., Josefsson, E.C., Blewitt, M.E., et al. (2015). Polycomb repressive complex 2 component Suz12 is required for hematopoietic stem cell function and lymphopoiesis. Blood *126*, 167–175.

Leidig, C., Thoms, M., Holdermann, I., Bradatsch, B., Berninghausen, O., Bange, G., Sinning, I., Hurt, E., and Beckmann, R. (2014). 60S ribosome biogenesis requires rotation of the 5S ribonucleoprotein particle. Nature Communications *5*, 3491.

Lessard, F., Morin, F., Ivanchuk, S., Langlois, F., Stefanovsky, V., Rutka, J., and Moss, T. (2010). The ARF tumor suppressor controls ribosome biogenesis by regulating the RNA polymerase I transcription factor TTF-I. Molecular Cell *38*, 539–550.

Li, J. (2011). Quiescence regulators for hematopoietic stem cell. Exp. Hematol. *39*, 511–520.

Li, L., and Clevers, H. (2010). Coexistence of quiescent and active adult stem cells in mammals. Science *327*, 542–545.

Li, M., He, Y., Dubois, W., Wu, X., Shi, J., and Huang, J. (2012). Distinct regulatory mechanisms and functions for p53-activated and p53-repressed DNA damage response genes in embryonic stem cells. Molecular Cell *46*, 30–42.

Li, Y., Challagundla, K.B., Sun, X.-X., Zhang, Q., and Dai, M.-S. (2015). MicroRNA-130a associates with ribosomal protein L11 to suppress c-Myc expression in response to UV irradiation. Oncotarget *6*, 1101–1114.

Liao, J.-M., Zhou, X., Gatignol, A., and Lu, H. (2013). Ribosomal proteins L5 and L11 co-operatively inactivate c-Myc via RNA-induced silencing complex. Oncogene.

Lindström, M.S. (2011). NPM1/B23: A Multifunctional Chaperone in Ribosome Biogenesis and Chromatin Remodeling. Biochem Res Int *2011*, 195209–195216.

Lindström, M.S., Jin, A., Deisenroth, C., White Wolf, G., and Zhang, Y. (2007). Cancer-associated mutations in the MDM2 zinc finger domain disrupt ribosomal protein interaction and attenuate MDM2-induced p53 degradation. Molecular and Cellular Biology *27*, 1056–1068.

Liu, D., Ou, L., Clemenson, G.D., Chao, C., Lutske, M.E., Zambetti, G.P., Gage, F.H., and Xu, Y. (2010). Puma is required for p53-induced depletion of adult stem cells. Nat Cell Biol *12*, 993–998.

Liu, J., Cao, L., Chen, J., Song, S., Lee, I.H., Quijano, C., Liu, H., Keyvanfar, K., Chen, H., Cao, L.-Y., et al. (2009a). Bmi1 regulates mitochondrial function and the DNA damage response pathway. Nature *459*, 387–392.

Liu, Y., Elf, S.E., Asai, T., Miyata, Y., Liu, Y., Sashida, G., Huang, G., Di Giandomenico, S., Koff, A., and Nimer, S.D. (2009b). The p53 tumor suppressor protein is a critical regulator of hematopoietic stem cell behavior. Cell Cycle *8*, 3120–3124.

Liu, Y., Elf, S.E., Miyata, Y., Sashida, G., Liu, Y., Huang, G., Di Giandomenico, S., Lee, J.M., Deblasio, A., Menendez, S., et al. (2009c). p53 regulates hematopoietic stem cell quiescence. Cell Stem Cell *4*, 37–48.

Lopes, A.M., Miguel, R.N., Sargent, C.A., Ellis, P.J., Amorim, A., and Affara, N.A. (2010). The human RPS4 paralogue on Yq11.223 encodes a structurally conserved ribosomal protein and is preferentially expressed during spermatogenesis. BMC Mol. Biol. *11*, 33.

Lord, B.I., Testa, N.G., and Hendry, J.H. (1975). The relative spatial distributions of CFUs and CFUc in the normal mouse femur. Blood *46*, 65–72.

Lossie, A.C., Lo, C.-L., Baumgarner, K.M., Cramer, M.J., Garner, J.P., and Justice, M.J. (2012). ENU mutagenesis reveals that Notchless homolog 1 (Drosophila) affects Cdkn1a and several members of the Wnt pathway during murine pre-implantation development. BMC Genet. *13*, 106.

M

Macias, E., Jin, A., Deisenroth, C., Bhat, K., Mao, H., Lindström, M.S., and Zhang, Y. (2010). An ARF-independent c-MYC-activated tumor suppression pathway mediated by ribosomal protein-Mdm2 Interaction. Cancer Cell *18*, 231–243.

Maggi, L.B., Winkeler, C.L., Miceli, A.P., Apicelli, A.J., Brady, S.N., Kuchenreuther, M.J., and Weber, J.D. (2014). ARF tumor suppression in the nucleolus. Biochimica Et Biophysica Acta (BBA) - Molecular Basis of Disease *1842*, 831–839.

Manesia, J.K., Xu, Z., Broekaert, D., Boon, R., van Vliet, A., Eelen, G., Vanwelden, T., Stegen, S., Van Gastel, N., Pascual-Montano, A., et al. (2015). Highly proliferative primitive fetal liver hematopoietic stem cells are fueled by oxidative metabolic pathways. Stem Cell Res *15*, 715–721.

Marcel, V., Ghayad, S.E., Belin, S., Thérizols, G., Morel, A.-P., Solano-Gonzàlez, E., Vendrell, J.A., Hacot, S., Mertani, H.C., Albaret, M.A., et al. (2013). p53 Acts as a Safeguard of Translational Control by Regulating Fibrillarin and rRNA Methylation in Cancer. Cancer Cell *24*, 318–330.

Marks, H., Kalkan, T., Menafra, R., Denissov, S., Jones, K., Hofemeister, H., Nichols, J., Kranz, A., Stewart, A.F., Smith, A., et al. (2012). The transcriptional and epigenomic foundations of ground state pluripotency. Cell *149*, 590–604.

Marusyk, A., Porter, C.C., Zaberezhnyy, V., and DeGregori, J. (2010). Irradiation selects for p53-deficient hematopoietic progenitors. Plos Biol *8*, e1000324.

Maryanovich, M., Oberkovitz, G., Niv, H., Vorobiyov, L., Zaltsman, Y., Brenner, O., Lapidot, T., Jung, S., and Gross, A. (2012). The ATM–BID pathway regulates quiescence and survival of haematopoietic stem cells. Nat Cell Biol *14*, 535–541.

Marygold, S.J., Roote, J., Reuter, G., Lambertsson, A., Ashburner, M., Millburn, G.H., Harrison, P.M., Yu, Z., Kenmochi, N., Kaufman, T.C., et al. (2007). The ribosomal protein genes and Minute loci of Drosophila melanogaster. Genome Biol. *8*, R216.

Matsumoto, A., and Nakayama, K.I. (2013). Role of key regulators of the cell cycle in maintenance of hematopoietic stem cells. Biochim. Biophys. Acta *1830*, 2335–2344.

Matsumoto, A., Takeishi, S., Kanie, T., Susaki, E., Onoyama, I., Tateishi, Y., Nakayama, K., and Nakayama, K.I. (2011). p57 is required for quiescence and maintenance of adult hematopoietic stem cells. Cell Stem Cell *9*, 262–271.

Mauro, V.P., and Edelman, G.M. (2007). The ribosome filter redux. Cell Cycle *6*, 2246–2251.

Mayer, C., and Grummt, I. (2006). Ribosome biogenesis and cell growth: mTOR coordinates transcription by all three classes of nuclear RNA polymerases. Oncogene *25*, 6384–6391.

Mayer, C., Zhao, J., Yuan, X., and Grummt, I. (2004). mTOR-dependent activation of the transcription factor TIF-IA links rRNA synthesis to nutrient availability. Genes & Development *18*, 423–434.

McConkey, E.H., and Hauber, E.J. (1975). Evidence for heterogeneity of ribosomes within the HeLa cell. J. Biol. Chem. *250*, 1311–1318.

McCune, J.M., Namikawa, R., Kaneshima, H., Shultz, L.D., Lieberman, M., and Weissman, I.L. (1988). The SCID-hu mouse: murine model for the analysis of human hematolymphoid differentiation and function. Science *241*, 1632–1639.

Meletis, K., Wirta, V., Hede, S.-M., Nistér, M., Lundeberg, J., and Frisén, J. (2006). p53 suppresses the self-renewal of adult neural stem cells. Development *133*, 363–369.

Miharada, K., Karlsson, G., Rehn, M., Rörby, E., Siva, K., Cammenga, J., and Karlsson, S. (2011). Cripto regulates hematopoietic stem cells as a hypoxic-niche-related factor through cell surface receptor GRP78. Cell Stem Cell *9*, 330–344.

Miller, C.L., Dykstra, B., and Eaves, C.J. (2008). Characterization of mouse hematopoietic stem and progenitor cells. Curr Protoc Immunol *Chapter 22*, Unit–Uni2.

Miloslavski, R., Cohen, E., Avraham, A., Iluz, Y., Hayouka, Z., Kasir, J., Mudhasani, R., Jones, S.N., Cybulski, N., Rüegg, M.A., et al. (2014). Oxygen sufficiency controls TOP mRNA translation via the TSC-Rheb-mTOR pathway in a 4E-BP-independent manner. J Mol Cell Biol *6*, 255–266.

Milyavsky, M., Gan, O.I., Trottier, M., Komosa, M., Tabach, O., Notta, F., Lechman, E., Hermans, K.G., Eppert, K., Konovalova, Z., et al. (2010). A distinctive DNA damage response in human hematopoietic stem cells reveals an apoptosis-independent role for p53 in self-renewal. Cell Stem Cell *7*, 186–197.

Min, I.M., Pietramaggiori, G., Kim, F.S., Passegue, E., Stevenson, K.E., and Wagers, A.J. (2008). The transcription factor EGR1 controls both the proliferation and localization of hematopoietic stem cells. Cell Stem Cell *2*, 380–391.

Miyamoto, K., Araki, K.Y., Naka, K., Arai, F., Takubo, K., Yamazaki, S., Matsuoka, S., Miyamoto, T., Ito, K., Ohmura, M., et al. (2007). Foxo3a is essential for maintenance of the hematopoietic stem cell pool. Cell Stem Cell *1*, 101–112.

Mohrin, M., Bourke, E., Alexander, D., Warr, M.R., Barry-Holson, K., Le Beau, M.M., Morrison, C.G., and Passegue, E. (2010). Hematopoietic stem cell quiescence promotes error-prone DNA repair and mutagenesis. Cell Stem Cell *7*, 174–185.

Mohyeldin, A., Garzón-Muvdi, T., and Quiñones-Hinojosa, A. (2010). Oxygen in stem cell

biology: a critical component of the stem cell niche. Cell Stem Cell *7*, 150–161.

Moilanen, A.-M., Rysä, J., Kaikkonen, L., Karvonen, T., Mustonen, E., Serpi, R., Szabó, Z., Tenhunen, O., Bagyura, Z., Näpänkangas, J., et al. (2015). WDR12, a Member of Nucleolar PeBoW-Complex, Is Up-Regulated in Failing Hearts and Causes Deterioration of Cardiac Function. PLoS ONE *10*, e0124907.

Morales, M., Theunissen, J.-W.F., Kim, C.F.B., Kitagawa, R., Kastan, M.B., and Petrini, J.H.J. (2005). The Rad50S allele promotes ATM-dependent DNA damage responses and suppresses ATM deficiency: implications for the Mre11 complex as a DNA damage sensor. Genes & Development *19*, 3043–3054.

Morgado-Palacin, L., Llanos, S., and Serrano, M. (2012). Ribosomal stress induces L11- and p53-dependent apoptosis in mouse pluripotent stem cells. Cell Cycle *11*, 503–510.

Morita, Y., Ema, H., and Nakauchi, H. (2010). Heterogeneity and hierarchy within the most primitive hematopoietic stem cell compartment. J. Exp. Med. *207*, 1173–1182.

Morrison, S.J., Prowse, K.R., Ho, P., and Weissman, I.L. (1996). Telomerase activity in hematopoietic cells is associated with self-renewal potential. Immunity *5*, 207–216.

Muller-Sieburg, C.E., Cho, R.H., Thoman, M., Adkins, B., and Sieburg, H.B. (2002). Deterministic regulation of hematopoietic stem cell self-renewal and differentiation. Blood *100*, 1302–1309.

Müller-Sieburg, C.E., Cho, R.H., Karlsson, L., Huang, J.-F., and Sieburg, H.B. (2004). Myeloid-biased hematopoietic stem cells have extensive self-renewal capacity but generate diminished lymphoid progeny with impaired IL-7 responsiveness. Blood *103*, 4111–4118.

N

Naka, K., and Hirao, A. (2011). Maintenance of genomic integrity in hematopoietic stem cells. Int. J. Hematol. *93*, 434–439.

Nakamura-Ishizu, A., Takizawa, H., and Suda, T. (2014). The analysis, roles and regulation of quiescence in hematopoietic stem cells. Development *141*, 4656–4666.

Narla, A., and Ebert, B.L. (2010). Ribosomopathies: human disorders of ribosome dysfunction. Blood *115*, 3196–3205.

Nerurkar, P., Altvater, M., Gerhardy, S., Schütz, S., Fischer, U., Weirich, C., and Panse, V.G. (2015). Eukaryotic Ribosome Assembly and Nuclear Export. Int Rev Cell Mol Biol *319*, 107–140.

Neumüller, R.A., Betschinger, J., Fischer, A., Bushati, N., Poernbacher, I., Mechtler, K., Cohen, S.M., and Knoblich, J.A. (2008). Mei-P26 regulates microRNAs and cell growth in the Drosophila ovarian stem cell lineage. Nature *454*, 241–245.

Neumüller, R.A., Richter, C., Fischer, A., Novatchkova, M., Neumüller, K.G., and Knoblich, J.A. (2011). Genome-wide analysis of self-renewal in Drosophila neural stem cells by transgenic RNAi. Cell Stem Cell *8*, 580–593.

Nijnik, A., Woodbine, L., Marchetti, C., Dawson, S., Lambe, T., Liu, C., Rodrigues, N.P., Crockford,

T.L., Cabuy, E., Vindigni, A., et al. (2007). DNA repair is limiting for haematopoietic stem cells during ageing. Nature *447*, 686–690.

O

Oguro, H., Ding, L., and Morrison, S.J. (2013). SLAM Family Markers Resolve Functionally Distinct Subpopulations of Hematopoietic Stem Cells and Multipotent Progenitors. Cell Stem Cell *13*, 102–116.

Oh, E., Becker, A.H., Sandikci, A., Huber, D., Chaba, R., Gloge, F., Nichols, R.J., Typas, A., Gross, C.A., Kramer, G., et al. (2011). Selective ribosome profiling reveals the cotranslational chaperone action of trigger factor in vivo. Cell *147*, 1295–1308.

Oh, W.J., Wu, C.-C., Kim, S.J., Facchinetti, V., Julien, L.-A., Finlan, M., Roux, P.P., Su, B., and Jacinto, E. (2010). mTORC2 can associate with ribosomes to promote cotranslational phosphorylation and stability of nascent Akt polypeptide. Embo J. *29*, 3939–3951.

Osawa, M., Hanada, K., Hamada, H., and Nakauchi, H. (1996). Long-term lymphohematopoietic reconstitution by a single CD34-low/negative hematopoietic stem cell. Science *273*, 242–245.

Oskarsson, T., and Trumpp, A. (2005). The Myc trilogy: lord of RNA polymerases. Nat Cell Biol *7*, 215–217.

Ozenne, P., Eymin, B., Brambilla, E., and Gazzeri, S. (2010). The ARF tumor suppressor: structure, functions and status in cancer. Int. J. Cancer *127*, 2239–2247.

P

Paik, J.-H., Kollipara, R., Chu, G., Ji, H., Xiao, Y., Ding, Z., Miao, L., Tothova, Z., Horner, J.W., Carrasco, D.R., et al. (2007). FoxOs are lineage-restricted redundant tumor suppressors and regulate endothelial cell homeostasis. Cell *128*, 309–323.

Paiva, R.M.A., and Calado, R.T. (2013). Telomere dysfunction and hematologic disorders. Prog Mol Biol Transl Sci *125*, 133–157.

Panic, L., Tamarut, S., Sticker-Jantscheff, M., Barkic, M., Solter, D., Uzelac, M., Grabusic, K., and Volarevic, S. (2006). Ribosomal protein S6 gene haploinsufficiency is associated with activation of a p53-dependent checkpoint during gastrulation. Molecular and Cellular Biology *26*, 8880–8891.

Park, C.H., Bergsagel, D.E., and McCulloch, E.A. (1971). Mouse myeloma tumor stem cells: a primary cell culture assay. J. Natl. Cancer Inst. *46*, 411–422.

Park, I.-K., Qian, D., Kiel, M., Becker, M.W., Pihalja, M., Weissman, I.L., Morrison, S.J., and Clarke, M.F. (2003). Bmi-1 is required for maintenance of adult self-renewing haematopoietic stem cells. Nature *423*, 302–305.

Parmar, K., Kim, J., Sykes, S.M., Shimamura, A., Stuckert, P., Zhu, K., Hamilton, A., Deloach, M.K., Kutok, J.L., Akashi, K., et al. (2010). Hematopoietic stem cell defects in mice with deficiency of Fancd2 or Usp1. Stem Cells *28*, 1186–1195.

Parmar, K., Mauch, P., Vergilio, J.-A., Sackstein, R., and Down, J.D. (2007). Distribution of

hematopoietic stem cells in the bone marrow according to regional hypoxia. Proceedings of the National Academy of Sciences *104*, 5431–5436.

Passegue, E., Wagers, A.J., Giuriato, S., Anderson, W.C., and Weissman, I.L. (2005). Global analysis of proliferation and cell cycle gene expression in the regulation of hematopoietic stem and progenitor cell fates. J. Exp. Med. *202*, 1599–1611.

Pellagatti, A., and Boultwood, J. (2015). The molecular pathogenesis of the myelodysplastic syndromes. Scand J Haematol *95*, 3–15.

Pellagatti, A., Hellström-Lindberg, E., Giagounidis, A., Perry, J., Malcovati, L., Porta, Della, M.G., Jädersten, M., Killick, S., Fidler, C., Cazzola, M., et al. (2008). Haploinsufficiency of RPS14 in 5q- syndrome is associated with deregulation of ribosomal- and translation-related genes. Br. J. Haematol. *142*, 57–64.

Pellagatti, A., Marafioti, T., Paterson, J.C., Barlow, J.L., Drynan, L.F., Giagounidis, A., Pileri, S.A., Cazzola, M., McKenzie, A.N.J., Wainscoat, J.S., et al. (2010). Induction of p53 and up-regulation of the p53 pathway in the human 5q- syndrome. Blood *115*, 2721–2723.

Pende, M., Um, S.H., Mieulet, V., Sticker, M., Goss, V.L., Mestan, J., Mueller, M., Fumagalli, S., Kozma, S.C., and Thomas, G. (2004). S6K1(-/-)/S6K2(-/-) mice exhibit perinatal lethality and rapamycin-sensitive 5'-terminal oligopyrimidine mRNA translation and reveal a mitogen-activated protein kinase-dependent S6 kinase pathway. Molecular and Cellular Biology *24*, 3112–3124.

Pestov, D.G.D., Strezoska, Z.Z., and Lau, L.F.L. (2001). Evidence of p53-dependent cross-talk between ribosome biogenesis and the cell cycle: effects of nucleolar protein Bop1 on G(1)/S transition. Molecular and Cellular Biology *21*, 4246–4255.

Pietras, E.M., Warr, M.R., and Passegue, E. (2011). Cell cycle regulation in hematopoietic stem cells. The Journal of Cell Biology *195*, 709–720.

Poortinga, G., Quinn, L.M., and Hannan, R.D. (2014). Targeting RNA polymerase I to treat MYC-driven cancer. Oncogene.

Pösel, C., Möller, K., Fröhlich, W., Schulz, I., Boltze, J., and Wagner, D.-C. (2012). Density gradient centrifugation compromises bone marrow mononuclear cell yield. PLoS ONE *7*, e50293.

R

Rathinam, C., Thien, C.B.F., Langdon, W.Y., Gu, H., and Flavell, R.A. (2008). The E3 ubiquitin ligase c-Cbl restricts development and functions of hematopoietic stem cells. Genes & Development *22*, 992–997.

Recher, G., Jouralet, J., Brombin, A., Heuzé, A., Mugniery, E., Hermel, J.-M., Desnoulez, S., Savy, T., Herbomel, P., Bourrat, F., et al. (2013). Zebrafish midbrain slow-amplifying progenitors exhibit high levels of transcripts for nucleotide and ribosome biogenesis. Development *140*, 4860–4869.

Riley, M.F., and Lozano, G. (2012). The Many Faces of MDM2 Binding Partners. Genes & Cancer *3*, 226–239.

Romanova, L., Grand, A., Zhang, L., Rayner, S., Katoku-Kikyo, N., Kellner, S., and Kikyo, N. (2009). Critical role of nucleostemin in pre-rRNA processing. J. Biol. Chem. *284*, 4968–4977.

Rossi, D.J., Bryder, D., Seita, J., Nussenzweig, A., Hoeijmakers, J., and Weissman, I.L. (2007). Deficiencies in DNA damage repair limit the function of haematopoietic stem cells with age. Nature *447*, 725–729.

Rossi, L., Lin, K.K., Boles, N.C., Yang, L., King, K.Y., Jeong, M., Mayle, A., and Goodell, M.A. (2012). Less is more: unveiling the functional core of hematopoietic stem cells through knockout mice. Cell Stem Cell *11*, 302–317.

Roy, S., Tripathy, M., Mathur, N., Jain, A., and Mukhopadhyay, A. (2012). Hypoxia improves expansion potential of human cord blood-derived hematopoietic stem cells and marrow repopulation efficiency. Eur. J. Haematol. *88*, 396–405.

Royet, J., Bouwmeester, T., and Cohen, S.M. (1998). Notchless encodes a novel WD40-repeat-containing protein that modulates Notch signaling activity. Embo J. *17*, 7351–7360.

Rudolph, K.L., Chang, S., Lee, H.W., Blasco, M., Gottlieb, G.J., Greider, C., and DePinho, R.A. (1999). Longevity, stress response, and cancer in aging telomerase-deficient mice. Cell *96*, 701–712.

Ruggero, D., Grisendi, S., Piazza, F., Rego, E., Mari, F., Rao, P.H., Cordon-Cardo, C., and Pandolfi, P.P. (2003). Dyskeratosis congenita and cancer in mice deficient in ribosomal RNA modification. Science *299*, 259–262.

Ruvinsky, I., Sharon, N., Lerer, T., Cohen, H., Stolovich-Rain, M., Nir, T., Dor, Y., Zisman, P., and Meyuhas, O. (2005). Ribosomal protein S6 phosphorylation is a determinant of cell size and glucose homeostasis. Genes & Development *19*, 2199–2211.

Rübe, C.E., Fricke, A., Widmann, T.A., Fürst, T., Madry, H., Pfreundschuh, M., and Rübe, C. (2011). Accumulation of DNA damage in hematopoietic stem and progenitor cells during human aging. PLoS ONE *6*, e17487.

S

Sablina, A.A., Budanov, A.V., Ilyinskaya, G.V., Agapova, L.S., Kravchenko, J.E., and Chumakov, P.M. (2005). The antioxidant function of the p53 tumor suppressor. Nat. Med. *11*, 1306–1313.

Sancar, A., Lindsey-Boltz, L.A., Unsal-Kaçmaz, K., and Linn, S. (2004). Molecular mechanisms of mammalian DNA repair and the DNA damage checkpoints. Annu. Rev. Biochem. *73*, 39–85.

Saporita, A.J., Chang, H.-C., Winkeler, C.L., Apicelli, A.J., Kladney, R.D., Wang, J., Townsend, R.R., Michel, L.S., and Weber, J.D. (2011). RNA helicase DDX5 is a p53-independent target of ARF that participates in ribosome biogenesis. Cancer Research *71*, 6708–6717.

Sarbassov, D.D., Ali, S.M., Sengupta, S., Sheen, J.-H., Hsu, P.P., Bagley, A.F., Markhard, A.L., and Sabatini, D.M. (2006). Prolonged rapamycin treatment inhibits mTORC2 assembly and Akt/PKB. Molecular Cell *22*, 159–168.

Sasaki, M., Kawahara, K., Nishio, M., Mimori, K., Kogo, R., Hamada, K., Itoh, B., Wang, J., Komatsu, Y., Yang, Y.R., et al. (2011). Regulation of the MDM2-P53 pathway and tumor growth

by PICT1 via nucleolar RPL11. Nat. Med. *17*, 944–951.

Scandura, J.M., Boccuni, P., Massagué, J., and Nimer, S.D. (2004). Transforming growth factor beta-induced cell cycle arrest of human hematopoietic cells requires p57KIP2 up-regulation. Proceedings of the National Academy of Sciences *101*, 15231–15236.

Schalm, S.S., Fingar, D.C., Sabatini, D.M., and Blenis, J. (2003). TOS motif-mediated raptor binding regulates 4E-BP1 multisite phosphorylation and function. Curr. Biol. *13*, 797–806.

Schneider, R.K., Schenone, M., Ferreira, M.V., Kramann, R., Joyce, C.E., Hartigan, C., Beier, F., Brümmendorf, T.H., Germing, U., Platzbecker, U., et al. (2016). Rps14 haploinsufficiency causes a block in erythroid differentiation mediated by S100A8 and S100A9. Nat. Med.

Schofield, R. (1978). The relationship between the spleen colony-forming cell and the haemopoietic stem cell. Blood Cells *4*, 7–25.

Sears, R., Nuckolls, F., Haura, E., Taya, Y., Tamai, K., and Nevins, J.R. (2000). Multiple Ras-dependent phosphorylation pathways regulate Myc protein stability. Genes & Development *14*, 2501–2514.

Sedelnikova, O.A., Horikawa, I., Zimonjic, D.B., Popescu, N.C., Bonner, W.M., and Barrett, J.C. (2004). Senescing human cells and ageing mice accumulate DNA lesions with unrepairable double-strand breaks. Nat Cell Biol *6*, 168–170.

Seedhom, M.O., Hickman, H.D., Wei, J., David, A., and Yewdell, J.W. (2016). Protein Translation Activity: A New Measure of Host Immune Cell Activation. J. Immunol. *197*, 1498–1506.

Seita, J., and Weissman, I.L. (2010). Hematopoietic stem cell: self-renewal versus differentiation. Wiley Interdiscip Rev Syst Biol Med *2*, 640–653.

Semenza, G.L. (2007). Life with oxygen. Science *318*, 62–64.

Shay, J.W., and Wright, W.E. (2010). Telomeres and telomerase in normal and cancer stem cells. FEBS Lett. *584*, 3819–3825.

Sherr, C.J. (2006). Divorcing ARF and p53: an unsettled case. Nat. Rev. Cancer *6*, 663–673.

Shiue, C.-N., Berkson, R.G., and Wright, A.P.H. (2009). c-Myc induces changes in higher order rDNA structure on stimulation of quiescent cells. Oncogene *28*, 1833–1842.

Shor, B., Wu, J., Shakey, Q., Toral-Barza, L., Shi, C., Follettie, M., and Yu, K. (2010). Requirement of the mTOR kinase for the regulation of Maf1 phosphorylation and control of RNA polymerase III-dependent transcription in cancer cells. Journal of Biological Chemistry *285*, 15380–15392.

Sieburg, H.B., Cho, R.H., and Müller-Sieburg, C.E. (2002). Limiting dilution analysis for estimating the frequency of hematopoietic stem cells: uncertainty and significance. Exp. Hematol. *30*, 1436–1443.

Sieburg, H.B., Cho, R.H., Dykstra, B., Uchida, N., Eaves, C.J., and Müller-Sieburg, C.E. (2006). The hematopoietic stem compartment consists of a limited number of discrete stem cell subsets. Blood *107*, 2311–2316.

Signer, R.A.J., Magee, J.A., Salic, A., and Morrison, S.J. (2014). Haematopoietic stem cells require a highly regulated protein synthesis rate. Nature *509*, 49–54.

Simon, M.C., and Keith, B. (2008). The role of oxygen availability in embryonic development and stem cell function. Nat. Rev. Mol. Cell Biol. *9*, 285–296.

Simsek, T., Kocabas, F., Zheng, J., Deberardinis, R.J., Mahmoud, A.I., Olson, E.N., Schneider, J.W., Zhang, C.C., and Sadek, H.A. (2010). The distinct metabolic profile of hematopoietic stem cells reflects their location in a hypoxic niche. Cell Stem Cell *7*, 380–390.

Sloan, K.E., Bohnsack, M.T., and Watkins, N.J. (2013). The 5S RNP couples p53 homeostasis to ribosome biogenesis and nucleolar stress. Cell Rep *5*, 237–247.

Song, X., Yuan, Y., Shen, H., Yu, H., Xu, F., Huang, P., Shields, D., Wang, J., and Cheng, T. (2006). Long-term engraftment of p18 INK4C-deficient hematopoietic stem cells is enhanced in the sublethally-irradiated recipients. Science in China Series C: Life Sciences *49*, 390–394.

Sotiropoulou, P.A., Candi, A., Mascré, G., De Clercq, S., Youssef, K.K., Lapouge, G., Dahl, E., Semeraro, C., Denecker, G., Marine, J.-C., et al. (2010). Bcl-2 and accelerated DNA repair mediates resistance of hair follicle bulge stem cells to DNA-damage-induced cell death. Nat Cell Biol *12*, 572–582.

Souilhol, C., Cormier, S., Tanigaki, K., Babinet, C., and Cohen-Tannoudji, M. (2006). RBP-Jkappa-dependent notch signaling is dispensable for mouse early embryonic development. Molecular and Cellular Biology *26*, 4769–4774.

Soulier, J. (2011). Fanconi anemia. Hematology Am Soc Hematol Educ Program *2011*, 492–497.

Spangrude, G.J., Heimfeld, S., and Weissman, I.L. (1988). Purification and Characterization of Mouse Hematopoietic Stem-Cells. Science *241*, 58–62.

Stadanlick, J.E., Zhang, Z., Lee, S.-Y., Hemann, M., Biery, M., Carleton, M.O., Zambetti, G.P., Anderson, S.J., Oravecz, T., and Wiest, D.L. (2011). Developmental arrest of T cells in Rpl22-deficient mice is dependent upon multiple p53 effectors. J. Immunol. *187*, 664–675.

Stead, E., White, J., Faast, R., Conn, S., Goldstone, S., Rathjen, J., Dhingra, U., Rathjen, P., Walker, D., and Dalton, S. (2002). Pluripotent cell division cycles are driven by ectopic Cdk2, cyclin A/E and E2F activities. Oncogene *21*, 8320–8333.

Stedman, A., Beck-Cormier, S., Le Bouteiller, M., Raveux, A., Vandormael-Pournin, S., Coqueran, S., Lejour, V., Jarzebowski, L., Toledo, F., Robine, S., et al. (2015). Ribosome biogenesis dysfunction leads to p53-mediated apoptosis and goblet cell differentiation of mouse intestinal stem/progenitor cells. Cell Death Differ *22*, 1865–1876.

Stefanovsky, V.Y., Pelletier, G., Hannan, R., Gagnon-Kugler, T., Rothblum, L.I., and Moss, T. (2001). An immediate response of ribosomal transcription to growth factor stimulation in mammals is mediated by ERK phosphorylation of UBF. Molecular Cell *8*, 1063–1073.

Stępiński, D. (2016). Nucleolus-derived mediators in oncogenic stress response and activation of p53-dependent pathways. Histochem. Cell Biol. *146*, 119–139.

Strezoska, Z., Pestov, D.G., and Lau, L.F. (2002). Functional inactivation of the mouse nucleolar protein Bop1 inhibits multiple steps in pre-rRNA processing and blocks cell cycle progression. J. Biol. Chem. *277*, 29617–29625.

Suda, T., Takubo, K., and Semenza, G.L. (2011). Metabolic regulation of hematopoietic stem cells in the hypoxic niche. Cell Stem Cell *9*, 298–310.

Sugihara, Y., Honda, H., Iida, T., Morinaga, T., Hino, S., Okajima, T., Matsuda, T., and Nadano, D. (2010). Proteomic analysis of rodent ribosomes revealed heterogeneity including ribosomal proteins L10-like, L22-like 1, and L39-like. J. Proteome Res. *9*, 1351–1366.

Sugiyama, T., Kohara, H., Noda, M., and Nagasawa, T. (2006). Maintenance of the hematopoietic stem cell pool by CXCL12-CXCR4 chemokine signaling in bone marrow stromal cell niches. Immunity *25*, 977–988.

Sulic, S., Panic, L., Barkic, M., Mercep, M., Uzelac, M., and Volarevic, S. (2005). Inactivation of S6 ribosomal protein gene in T lymphocytes activates a p53-dependent checkpoint response. Genes & Development *19*, 3070–3082.

Sun, J., Ramos, A., Chapman, B., Johnnidis, J.B., Le, L., Ho, Y.-J., Klein, A., Hofmann, O., and Camargo, F.D. (2014). Clonal dynamics of native haematopoiesis. Nature *514*, 322–327.

Sun, X.-X., Wang, Y.-G., Xirodimas, D.P., and Dai, M.-S. (2010). Perturbation of 60 S ribosomal biogenesis results in ribosomal protein L5- and L11-dependent p53 activation. Journal of Biological Chemistry *285*, 25812–25821.

T

Taichman, R.S., Reilly, M.J., and Emerson, S.G. (1996). Human osteoblasts support human hematopoietic progenitor cells in vitro bone marrow cultures. Blood *87*, 518–524.

Takahashi, K., and Nakayama, K. (2000). Mice lacking a CDK inhibitor, p57Kip2, exhibit skeletal abnormalities and growth retardation. J. Biochem. *127*, 73–83.

Takubo, K., Goda, N., Yamada, W., Iriuchishima, H., Ikeda, E., Kubota, Y., Shima, H., Johnson, R.S., Hirao, A., Suematsu, M., et al. (2010). Regulation of the HIF-1alpha level is essential for hematopoietic stem cells. Cell Stem Cell *7*, 391–402.

Tang, H., Hornstein, E., Stolovich, M., Levy, G., Livingstone, M., Templeton, D., Avruch, J., and Meyuhas, O. (2001). Amino acid-induced translation of TOP mRNAs is fully dependent on phosphatidylinositol 3-kinase-mediated signaling, is partially inhibited by rapamycin, and is independent of S6K1 and rpS6 phosphorylation. Molecular and Cellular Biology *21*, 8671–8683.

Taylor, A.M., Humphries, J.M., White, R.M., Murphey, R.D., Burns, C.E., and Zon, L.I. (2012). Hematopoietic defects in rps29 mutant zebrafish depend upon p53 activation. Exp. Hematol. *40*, 228–237.e5.

TeKippe, M., Harrison, D.E., and Chen, J. (2003). Expansion of hematopoietic stem cell phenotype and activity in Trp53-null mice. Exp. Hematol.

Teng, T., Mercer, C.A., Hexley, P., Thomas, G., and Fumagalli, S. (2013). Loss of tumor

suppressor RPL5/RPL11 does not induce cell cycle arrest but impedes proliferation due to reduced ribosome content and translation capacity. Molecular and Cellular Biology *33*, 4660–4671.

Tesio, M., Golan, K., Corso, S., Giordano, S., Schajnovitz, A., Vagima, Y., Shivtiel, S., Kalinkovich, A., Caione, L., Gammaitoni, L., et al. (2011). Enhanced c-Met activity promotes G-CSF-induced mobilization of hematopoietic progenitor cells via ROS signaling. Blood *117*, 419–428.

Thomson, E., Ferreira-Cerca, S., and Hurt, E. (2013). Eukaryotic ribosome biogenesis at a glance. Journal of Cell Science *126*, 4815–4821.

Thoreen, C.C., Chantranupong, L., Keys, H.R., Wang, T., Gray, N.S., and Sabatini, D.M. (2012). A unifying model for mTORC1-mediated regulation of mRNA translation. Nature *485*, 109–113.

Till, J.E., and McCulloch, E.A. (1961). A direct measurement of the radiation sensitivity of normal mouse bone marrow cells. Radiat. Res. *14*, 213–222.

Tothova, Z., and Gilliland, D.G. (2007). FoxO transcription factors and stem cell homeostasis: insights from the hematopoietic system. Cell Stem Cell *1*, 140–152.

Tothova, Z., Kollipara, R., Huntly, B.J., Lee, B.H., Castrillon, D.H., Cullen, D.E., McDowell, E.P., Lazo-Kallanian, S., Williams, I.R., Sears, C., et al. (2007). FoxOs are critical mediators of hematopoietic stem cell resistance to physiologic oxidative stress. Cell *128*, 325–339.

Toyooka, Y., Shimosato, D., Murakami, K., Takahashi, K., and Niwa, H. (2008). Identification and characterization of subpopulations in undifferentiated ES cell culture. Development *135*, 909–918.

Tsai, R.Y.L., and McKay, R.D.G. (2002). A nucleolar mechanism controlling cell proliferation in stem cells and cancer cells. Genes & Development *16*, 2991–3003.

Tsai, W.-B., Aiba, I., Long, Y., Lin, H.-K., Feun, L., Savaraj, N., and Kuo, M.T. (2012). Activation of Ras/PI3K/ERK pathway induces c-Myc stabilization to upregulate argininosuccinate synthetase, leading to arginine deiminase resistance in melanoma cells. Cancer Research *72*, 2622–2633.

U-V

Ulbrich, C., Diepholz, M., Baßler, J., Kressler, D., Pertschy, B., Galani, K., BOttcher, B., and Hurt, E. (2009). Mechanochemical removal of ribosome biogenesis factors from nascent 60S ribosomal subunits. Cell *138*, 911–922.

Urao, N., and Ushio-Fukai, M. (2013). Redox regulation of stem/progenitor cells and bone marrow niche. Free Radic. Biol. Med. *54*, 26–39.

van der Wath, R.C., Wilson, A., Laurenti, E., Trumpp, A., and Liò, P. (2009). Estimating dormant and active hematopoietic stem cell kinetics through extensive modeling of bromodeoxyuridine label-retaining cell dynamics. PLoS ONE *4*, e6972.

Varela, E., Muñoz-Lorente, M.A., Tejera, A.M., Ortega, S., and Blasco, M.A. (2016). Generation of mice with longer and better preserved telomeres in the absence of genetic manipulations. Nature Communications *7*, 11739.

Varela, E., Schneider, R.P., Ortega, S., and Blasco, M.A. (2011). Different telomere-length dynamics at the inner cell mass versus established embryonic stem (ES) cells. Proc. Natl. Acad. Sci. U.S.a. *108*, 15207–15212.

Vaziri, H., Dragowska, W., Allsopp, R.C., Thomas, T.E., Harley, C.B., and Lansdorp, P.M. (1994). Evidence for a mitotic clock in human hematopoietic stem cells: loss of telomeric DNA with age. Proceedings of the National Academy of Sciences *91*, 9857–9860.

Vesper, O., Amitai, S., Belitsky, M., Byrgazov, K., Kaberdina, A.C., Engelberg-Kulka, H., and Moll, I. (2011). Selective translation of leaderless mRNAs by specialized ribosomes generated by MazF in Escherichia coli. Cell *147*, 147–157.

Viatour, P., Somervaille, T.C., Venkatasubrahmanyam, S., Kogan, S., McLaughlin, M.E., Weissman, I.L., Butte, A.J., Passegue, E., and Sage, J. (2008). Hematopoietic stem cell quiescence is maintained by compound contributions of the retinoblastoma gene family. Cell Stem Cell *3*, 416–428.

W

Wagers, A.J., Sherwood, R.I., Christensen, J.L., and Weissman, I.L. (2002). Little evidence for developmental plasticity of adult hematopoietic stem cells. Science *297*, 2256–2259.

Walasek, M.A., van Os, R., and de Haan, G. (2012). Hematopoietic stem cell expansion: challenges and opportunities. Annals of the Lyceum of Natural History of New York *1266*, 138–150.

Wang, J., Sun, Q., Morita, Y., Jiang, H., Gross, A., Lechel, A., Hildner, K., Guachalla, L.M., Gompf, A., Hartmann, D., et al. (2012). A differentiation checkpoint limits hematopoietic stem cell self-renewal in response to DNA damage. Cell *148*, 1001–1014.

Wang, L., Benedito, R., Bixel, M.G., Zeuschner, D., Stehling, M., Sävendahl, L., Haigh, J.J., Snippert, H., Clevers, H., Breier, G., et al. (2013). Identification of a clonally expanding haematopoietic compartment in bone marrow. Embo J. *32*, 219–230.

Wang, X., Li, W., Williams, M., Terada, N., Alessi, D.R., and Proud, C.G. (2001). Regulation of elongation factor 2 kinase by p90(RSK1) and p70 S6 kinase. Embo J. *20*, 4370–4379.

Wang, Y.V., Leblanc, M., Fox, N., Mao, J.-H., Tinkum, K.L., Krummel, K., Engle, D., Piwnica-Worms, D., Piwnica-Worms, H., Balmain, A., et al. (2011). Fine-tuning p53 activity through C-terminal modification significantly contributes to HSC homeostasis and mouse radiosensitivity. Genes & Development *25*, 1426–1438.

Wang, Z., Du, Z., Cai, H., Ye, Z., Fan, J., and Tan, W.-S. (2016). Low oxygen tension favored expansion and hematopoietic reconstitution of CD34(+) CD38(-) cells expanded from human cord blood-derived CD34(+) Cells. Biotechnol J *11*, 945–953.

Warner, J.R. (1999). The economics of ribosome biosynthesis in yeast. Trends Biochem. Sci. *24*, 437–440.

Warner, J.R., and McIntosh, K.B. (2009). How common are extraribosomal functions of ribosomal proteins? Molecular Cell *34*, 3–11.

Watanabe-Susaki, K., Takada, H., Enomoto, K., Miwata, K., Ishimine, H., Intoh, A., Ohtaka, M., Nakanishi, M., Sugino, H., Asashima, M., et al. (2014). Biosynthesis of Ribosomal RNA in Nucleoli Regulates Pluripotency and Differentiation Ability of Pluripotent Stem Cells. Stem Cells *32*, 3099–3111.

Weber, J.D., Jeffers, J.R., Rehg, J.E., Randle, D.H., Lozano, G., Roussel, M.F., Sherr, C.J., and Zambetti, G.P. (2000). p53-independent functions of the p19(ARF) tumor suppressor. Genes & Development *14*, 2358–2365.

Wilson, A., Laurenti, E., Oser, G., van der Wath, R.C., Blanco-Bose, W., Jaworski, M., Offner, S., Dunant, C., Eshkind, L., Bockamp, E., et al. (2008). Hematopoietic Stem Cells Reversibly Switch from Dormancy to Self-Renewal during Homeostasis and Repair. Cell *138*, 209–209.

Wingert, S., and Rieger, M.A. (2016). Terminal differentiation induction as DNA damage response in hematopoietic stem cells by GADD45A. Exp. Hematol. *44*, 561–566.

Wingert, S., Thalheimer, F.B., Haetscher, N., Rehage, M., Schroeder, T., and Rieger, M.A. (2016). DNA-damage response gene GADD45A induces differentiation in hematopoietic stem cells without inhibiting cell cycle or survival. Stem Cells *34*, 699–710.

Woolford, J.L., and Baserga, S.J. (2013). Ribosome Biogenesis in the Yeast Saccharomyces cerevisiae. Genetics *195*, 643–681.

Wray, J., Kalkan, T., Gomez-Lopez, S., Eckardt, D., Cook, A., Kemler, R., and Smith, A. (2011). Inhibition of glycogen synthase kinase-3 alleviates Tcf3 repression of the pluripotency network and increases embryonic stem cell resistance to differentiation. Nat Cell Biol *13*, 838–845.

Wu, A.M., Siminovitch, L., Till, J.E., and McCulloch, E.A. (1968). Evidence for a relationship between mouse hemopoietic stem cells and cells forming colonies in culture. Proceedings of the National Academy of Sciences *59*, 1209–1215.

X-Y

Xu, X., Xiong, X., and Sun, Y. (2016). The role of ribosomal proteins in the regulation of cell proliferation, tumorigenesis, and genomic integrity. Sci. China Life Sci. *59*, 656–672.

Xue, S., and Barna, M. (2012). Specialized ribosomes: a new frontier in gene regulation and organismal biology. Nat. Rev. Mol. Cell Biol. *13*, 355–369.

Yahata, T., Takanashi, T., Muguruma, Y., Ibrahim, A.A., Matsuzawa, H., Uno, T., Sheng, Y., Onizuka, M., Ito, M., Kato, S., et al. (2011). Accumulation of oxidative DNA damage restricts the self-renewal capacity of human hematopoietic stem cells. Blood *118*, 2941–2950.

Yalcin, S., Zhang, X., Luciano, J.P., Mungamuri, S.K., Marinkovic, D., Vercherat, C., Sarkar, A., Grisotto, M., Taneja, R., and Ghaffari, S. (2008). Foxo3 is essential for the regulation of ataxia telangiectasia mutated and oxidative stress-mediated homeostasis of hematopoietic stem cells. J. Biol. Chem. *283*, 25692–25705.

Yamada, T., Park, C.S., and Lacorazza, H.D. (2013). Genetic control of quiescence in hematopoietic stem cells. Cell Cycle *12*, 2376–2383.

Yamashita, M., Nitta, E., and Suda, T. (2015). Aspp1 Preserves Hematopoietic Stem Cell Pool Integrity and Prevents Malignant Transformation. Cell Stem Cell *17*, 23–34.

Yamazaki, S., Iwama, A., Takayanagi, S.-I., Eto, K., Ema, H., and Nakauchi, H. (2009). TGF-beta as a candidate bone marrow niche signal to induce hematopoietic stem cell hibernation. Blood *113*, 1250–1256.

Yan, Y., Frisen, J., Lee, M.H., Massague, J., and Barbacid, M. (1997). Ablation of the CDK inhibitor p57Kip2 results in increased apoptosis and delayed differentiation during mouse development. Genes & Development *11*, 973–983.

Yang, A., Shi, G., Zhou, C., Lu, R., Li, H., Sun, L., and Jin, Y. (2011). Nucleolin maintains embryonic stem cell self-renewal by suppression of p53 protein-dependent pathway. Journal of Biological Chemistry *286*, 43370–43382.

Yasunaga, S., Ohno, Y., Shirasu, N., Zhang, B., Suzuki-Takedachi, K., Ohtsubo, M., and Takihara, Y. (2016). Role of Geminin in cell fate determination of hematopoietic stem cells (HSCs). Int. J. Hematol.

Yilmaz, O.H., Valdez, R., Theisen, B.K., Guo, W., Ferguson, D.O., Wu, H., and Morrison, S.J. (2006). Pten dependence distinguishes haematopoietic stem cells from leukaemia-initiating cells. Nature *441*, 475–482.

Ying, Q.-L., Wray, J., Nichols, J., Batlle-Morera, L., Doble, B., Woodgett, J., Cohen, P., and Smith, A. (2008). The ground state of embryonic stem cell self-renewal. Nature *453*, 519–523.

Yoon, A., Peng, G., Brandenburger, Y., Brandenburg, Y., Zollo, O., Xu, W., Rego, E., and Ruggero, D. (2006). Impaired control of IRES-mediated translation in X-linked dyskeratosis congenita. Science *312*, 902–906.

Yoon, D., Kim, B., and Prchal, J.T. (2008). Cre recombinase expression controlled by the hematopoietic regulatory domain of Gata-1 is erythroid-specific. Blood Cells Mol. Dis. *40*, 381–387.

Yoshihara, H., Arai, F., Hosokawa, K., Hagiwara, T., Takubo, K., Nakamura, Y., Gomei, Y., Iwasaki, H., Matsuoka, S., Miyamoto, K., et al. (2007). Thrombopoietin/MPL signaling regulates hematopoietic stem cell quiescence and interaction with the osteoblastic niche. Cell Stem Cell *1*, 685–697.

You, K.T., Park, J., and Kim, V.N. (2015). Role of the small subunit processome in the maintenance of pluripotent stem cells. Genes & Development *29*, 2004–2009.

Yu, H., Yuan, Y., Shen, H., and Cheng, T. (2006). Hematopoietic stem cell exhaustion impacted by p18 INK4C and p21 Cip1/Waf1 in opposite manners. Blood *107*, 1200–1206.

Yu, Y., Ji, H., Doudna, J.A., and Leary, J.A. (2005). Mass spectrometric analysis of the human 40S ribosomal subunit: native and HCV IRES-bound complexes. Protein Sci. *14*, 1438–1446.

Yuan, X., Zhou, Y., Casanova, E., Chai, M., Kiss, E., Gröne, H.-J., Schütz, G., and Grummt, I. (2005). Genetic inactivation of the transcription factor TIF-IA leads to nucleolar disruption, cell cycle arrest, and p53-mediated apoptosis. Molecular Cell *19*, 77–87.

Yuan, Y., Shen, H., Franklin, D.S., Scadden, D.T., and Cheng, T. (2004). In vivo self-renewing divisions of haematopoietic stem cells are increased in the absence of the early G1-phase inhibitor, p18INK4C. Nat Cell Biol *6*, 436–442.

Z

Zeng, Z., Sarbassov, D.D., Samudio, I.J., Yee, K.W.L., Munsell, M.F., Ellen Jackson, C., Giles, F.J., Sabatini, D.M., Andreeff, M., and Konopleva, M. (2007). Rapamycin derivatives reduce mTORC2 signaling and inhibit AKT activation in AML. Blood *109*, 3509–3512.

Zhang, C.C., and Sadek, H.A. (2014). Hypoxia and metabolic properties of hematopoietic stem cells. Antioxid Redox Signal *20*, 1891–1901.

Zhang, J., Grindley, J.C., Yin, T., Jayasinghe, S., He, X.C., Ross, J.T., Haug, J.S., Rupp, D., Porter-Westpfahl, K.S., Wiedemann, L.M., et al. (2006). PTEN maintains haematopoietic stem cells and acts in lineage choice and leukaemia prevention. Nature *441*, 518–522.

Zhang, J., Niu, C., Ye, L., Huang, H., He, X., Tong, W.-G., Ross, J., Haug, J., Johnson, T., Feng, J.Q., et al. (2003). Identification of the haematopoietic stem cell niche and control of the niche size. Nature *425*, 836–841.

Zhang, P., Liégeois, N.J., Wong, C., Finegold, M., Hou, H., Thompson, J.C., Silverman, A., Harper, J.W., DePinho, R.A., and Elledge, S.J. (1997). Altered cell differentiation and proliferation in mice lacking p57KIP2 indicates a role in Beckwith-Wiedemann syndrome. Nature *387*, 151–158.

Zhang, Q., Shalaby, N.A., and Buszczak, M. (2014). Changes in rRNA transcription influence proliferation and cell fate within a stem cell lineage. Science *343*, 298–301.

Zhang, Q.-S., Marquez-Loza, L., Eaton, L., Duncan, A.W., Goldman, D.C., Anur, P., Watanabe-Smith, K., Rathbun, R.K., Fleming, W.H., Bagby, G.C., et al. (2010). Fancd2-/- mice have hematopoietic defects that can be partially corrected by resveratrol. Blood *116*, 5140–5148.

Zhang, Y., and Lu, H. (2009). Signaling to p53: ribosomal proteins find their way. Cancer Cell *16*, 369–377.

Zhao, J., Yuan, X., Frödin, M., and Grummt, I. (2003). ERK-dependent phosphorylation of the transcription initiation factor TIF-IA is required for RNA polymerase I transcription and cell growth. Molecular Cell *11*, 405–413.

Zhou, X., Liao, W.-J., Liao, J.-M., Liao, P., and Lu, H. (2015). Ribosomal proteins: functions beyond the ribosome. J Mol Cell Biol *7*, 92–104.

Zinzalla, V., Stracka, D., Oppliger, W., and Hall, M.N. (2011). Activation of mTORC2 by association with the ribosome. Cell *144*, 757–768.

Zou, P., Yoshihara, H., Hosokawa, K., Tai, I., Shinmyozu, K., Tsukahara, F., Maru, Y., Nakayama, K., Nakayama, K.I., and Suda, T. (2011). p57(Kip2) and p27(Kip1) cooperate to maintain hematopoietic stem cell quiescence through interactions with Hsc70. Cell Stem Cell *9*, 247–261.